

UNIVERSITY OF SOUTHAMPTON

ANALYTIC THEORY OF  
LIQUID CRYSTALLINE PHENOMENA

Timothy Howard Payne

A dissertation submitted in partial fulfilment of the requirements for the degree of  
Doctor of Philosophy at the University of Southampton.

Department of Chemistry

November 2000

UNIVERSITY OF SOUTHAMPTON

ABSTRACT

FACULTY OF SCIENCE

CHEMISTRY

Doctor of Philosophy

ANALYTIC THEORY OF LIQUID CRYSTALLINE PHENOMENA

by Timothy Howard Payne

This Thesis is concerned with the application of analytic theory to the calculation of the properties of thermotropic nematic liquid crystals based on their molecular structure. For these studies we employ the molecular field approximation, which has been shown to give a good qualitative and semi-quantitative understanding of liquid crystalline properties. In the first chapter we give an introduction to liquid crystals and their properties as it pertains to the theoretical studies of later chapters. In the next chapter we lay the necessary foundations in statistical mechanics and introduce the molecular field approximation as a theoretical framework within which we develop the molecular field theories which we employ subsequently. We begin our studies by considering the application of an electric field to a nematic monodomain, a procedure that has potential applications in the production of non-linear optical devices. The idea is that by polarising a nematic rather than an ordinary liquid, the polarisation is augmented. Thus we seek to probe the theoretical basis of this by estimating the response of the order parameters to the field using molecular field theory. In the next chapter we move on to consider the composition dependence of order parameters in binary mixtures where the solute is less anisotropic than the solvent. This is to investigate the validity of extrapolation procedures commonly used in experiment to obtain values for properties of non-mesogenic compounds intrinsic to the compound in question, in a hypothetical pure nematic state. In the final chapter we undertake to predict the properties of liquid crystal dendrimers, a fascinating new class of highly flexible mesogenic molecule. Here the problem of the very great conformational flexibility is addressed and a solution is presented involving a hybrid methodology that draws on both molecular field theory and Monte Carlo computer simulation techniques.

## Acknowledgements

I would like to thank Professor Geoffrey Luckhurst for all his help, understanding and patience throughout the duration of my PhD studies here in Southampton. I would also like to thank Dr Steve Roskilly for his help initially when I first arrived and the many members of the department, both past and present, who have helped me in many ways both great and small, during my time here.

Special thanks have to go to my family, without whose unflagging support it would never have been possible and also to Francesca Castiglione and Marina Carravetta for the strength of their friendship through thick and thin.

I would like to thank all the people of computing services for their assistance, in particular Ian Hardy, for bearing the dubious privilege of managing iris02, almost, it seems, just for me, with such grace.

I am also grateful to the Engineering and Physical Sciences Research Council for funding through a studentship.

To My Family

<b>Chapter 1</b>	<b>Liquid Crystals</b>	<b>1</b>
1.1	Introduction . . . . .	1
1.2	States of Matter . . . . .	2
1.3	Definition of Mesophases and Liquid Crystals . . . . .	4
1.4	Thermotropic and Lyotropic Mesophases . . . . .	5
1.5	Classification of Thermotropic Mesophases . . . . .	7
1.5.1	The Nematic Phase ( $N$ ) . . . . .	8
1.5.2	Chiral Nematic (Cholesteric) Phases ( $N^*$ ) . . . . .	10
1.5.3	Smectic Phases ( $Sm : SmA, SmB, \dots, SmL$ ) . . . . .	11
1.6	The Molecules That Form Liquid Crystals . . . . .	11
1.7	Phase Transitions . . . . .	15
1.8	Orientational Order in the Nematic Phase . . . . .	19
1.8.1	Defining the orientation of a molecule in a monodomain . . . . .	19
1.8.2	Uniaxial Phase of Uniaxial Molecules . . . . .	20
1.8.3	Uniaxial Phase of Biaxial Molecules . . . . .	29
1.9	Molecular Models of Liquid Crystallinity . . . . .	30
1.10	Liquid Crystal Properties and Theoretical Modelling . . . . .	32
1.11	Summary of Contents . . . . .	35
1A	Appendix 1A: Definition of the Euler Angles . . . . .	36

1B	Appendix 1B: Legendre polynomials and spherical harmonics . . . . .	39
<b>Chapter 2</b>	<b>The Statistical Mechanics and Molecular Field Theory of Nematics Composed of Rigid Molecules</b>	<b>43</b>
2.1	Introduction . . . . .	43
2.2	Introduction to Statistical Mechanics . . . . .	43
2.3	The Equilibrium Free Energy . . . . .	46
2.4	The Molecular Field Approximation . . . . .	47
2.5	Distribution Functions and the Molecular Field Approximation . . . . .	51
2.6	Helmholtz Free Energy within the Molecular Field Approximation . . . . .	53
2.7	An Alternative Development of the Helmholtz Free Energy . . . . .	54
2.8	Molecular Field Theories—Uniaxial Phase Composed of Uniaxial Rigid Particles . . . . .	58
2.8.1	Maier-Saupe Theory . . . . .	58
2.8.2	Expansion of $U(\beta)$ in a basis set of Legendre polynomials . . . . .	60
2.8.3	Variational Derivation of the Maier-Saupe Theory . . . . .	62
2.8.4	Predictions of the Maier-Saupe Theory . . . . .	65
2.8.5	Numerical Methodologies in Molecular Field Theory . . . . .	75
2.9	Uniaxial Phase of Rigid Biaxial Particles . . . . .	77
2.9.1	Variational Derivation of the Distribution Function and the Potential of Mean Torque . . . . .	77

2.9.2	Predictions of the Theory . . . . .	82
2A	Appendix 2A: The Calculus of Variations . . . . .	88
2A.1	Introduction . . . . .	88
2A.2	The Problem . . . . .	89
2A.3	Variational Notation . . . . .	93
2A.4	Application to Multivariate Problems . . . . .	97
2A.5	Application to Distribution Functions in Statistical Mechanics . . . . .	101
<b>Chapter 3</b>	<b>Electric Field Polarisation of Nematic Liquid Crystals: A</b>	
	<b>Molecular Field Theory</b>	<b>114</b>
3.1	Aims and Rationale . . . . .	114
3.2	Formal Development of the Theory . . . . .	115
3.3	Methodological Application . . . . .	117
3.4	The Free Energy . . . . .	120
3.5	Evaluating the Orientational Order Parameters . . . . .	121
3.6	Results and Discussion . . . . .	121
3.7	The Problem of an Inhomogeneous Ground State . . . . .	131
3.8	The Theory . . . . .	134
3.9	Introduction to the Humphries-James-Luckhurst Theory of Binary Nematic Mixtures . . . . .	135

3.10	Adaptation of the HJL Theory to Model Nematics with Predominantly Antiferroelectric Coupling . . . . .	138
3.11	Methodology . . . . .	140
3.11.1	Minimisation of the Free Energy . . . . .	140
3.11.2	Solution of the Self-Consistency Equations . . . . .	143
3.12	Results and Discussion . . . . .	143
3.13	Conclusions . . . . .	150
3A	Appendix 3A: Proofs and Derivations . . . . .	152
 <b>Chapter 4 A Molecular Field Theoretic Study of Order Parameters in Binary Nematic Mixtures</b>		<b>159</b>
4.1	Introduction . . . . .	159
4.2	Variational Derivation of the HJL Theory of Binary Nematic Mixtures	161
4.3	Application . . . . .	165
4.4	Methodology for Solving the Molecular Field Equations . . . . .	169
4.5	Results and Discussion . . . . .	172
4.5.1	Analysis of the meaning of the extrapolated value for the order parameter of the dopant in the pure phase . . . . .	183
 <b>Chapter 5 Liquid Crystals Formed from Highly Flexible Molecules</b>		<b>191</b>
5.1	Introduction . . . . .	191
5.2	Theoretical Background and Methodology . . . . .	198



5.2.1	General introduction to the problem . . . . .	198
5.2.2	Formal Aspects of the Molecular Field Calculation . . . . .	201
5.2.3	Details of the Molecular Field Calculation . . . . .	207
5.3	Computational Technique . . . . .	214
5.4	Results and Discussion . . . . .	225
5.4.1	Determination of the Transitional Properties . . . . .	225
5.4.2	Statistical Errors . . . . .	233
5.4.3	The Transitional Properties . . . . .	236

# Chapter 1: Liquid Crystals

## 1.1 Introduction

For centuries scientists have classified matter into three different states, namely solid, liquid and gas. At sufficiently low temperatures and high densities, all substances exist as solids, at somewhat higher temperatures and lower densities as liquids and at higher temperatures and lower densities still as gases. In the case of liquids and gases we are assuming that chemical decomposition does not occur before these states of the original substance are realised. Thus, with this caveat in place, liquids are generally obtained upon heating solids, and gases upon heating liquids. In more modern times we also have the notion of the plasma as another state of matter, where at even higher temperatures a gas may become ionised and exist as a mixture of gaseous ions and electrons. There will be a variety of transitions to plasmas consisting of particles that have been multiply ionised to an increasing extent co-existing alongside an increasing amount of electron gas. In addition to such esoteric states as plasmas at high temperatures, we have also had the concept of a class of states of matter collectively known as mesophases, which were initially discovered as intermediate states of matter that seemed to occur between the solid and the liquid on the temperature axis of the phase diagram of some substances, *meso* meaning *between*. Liquid crystals are the most common type of mesophase and their discovery is normally attributed to the Austrian botanist Reinitzer [1] who, in 1888, observed colour changes and turbidity upon cooling molten cholesteryl benzoate or acetate. His observations and line of enquiry paved the way for further investigation by Lehmann [2] using a polarising microscope who coined the term *liquid crystals* to refer to the fluid mesophases he

observed, because they appeared to be liquids but with optical properties reminiscent of crystals. We now discuss in general, but more physical, terms the relationship of mesophases to the more familiar states of matter.

## 1.2 States of Matter

Consider a solid of a pure substance at equilibrium, that is, a crystal. At a given temperature the constituent particles librate about fixed equilibrium positions and (if the particles are not single atoms) orientations, in space. Thus, there is long range order in every degree of freedom at the molecular (or atomic) level. There are three of these for translations involving the centre of mass positions (for instance, cartesian  $x$ ,  $y$  and  $z$  coordinates) and three for the particle orientations (for instance, the Euler angles—see section 1.8), giving six in all. If we consider a flawless crystal, we see that this ordering can persist over essentially infinite distances. It is this ordering that results in the characteristic feature of crystals of possessing anisotropic properties. That is, any property that is a non-scalar quantity and is measured with respect to certain directions will be found in general to exhibit different values depending on the direction chosen. This obtains because the structure of the crystal confers on it its own internal directionality and so different directions are physically non-equivalent. From a theoretical standpoint, the crystal is best viewed as an example of a system exhibiting a broken symmetry [3]. That is, compared to a higher temperature state of matter, the symmetry is lower since the ordering in one or more degrees of freedom has to some extent destroyed, or broken, the symmetry in the less ordered state. This imposes on the system certain special direction(s), such as exist in a crystal for instance. We also note that it is the long range persistence of the lattice (ie, the translational order) that results in the rigidity of the structure. In other words, it is solid—meaning it can maintain itself indefinitely against a shear stress, provided that it is not above some finite threshold (above which the crystal is destroyed).

As the temperature is increased, the molecular librations become progressively more vigorous, with the excursions from the equilibrium coordinates at that temperature becoming more extreme. At some temperature, the long range order in one or more degrees of freedom is completely destroyed and we observe a change of state to one of higher symmetry and with less overall order. Usually, this temperature corresponds to one at which it is no longer possible for the system to maintain the lattice structure and the whole structure breaks down abruptly, destroying all long range positional and orientational order completely. The resulting state of isotropy (complete long range disorder in all degrees of freedom) is the normal or isotropic liquid; every direction is equivalent and, in the language of symmetry, there is full translational and rotational symmetry, at least at the macroscopic level. On passing through the phase transition, the thermal energy has overcome that associated with maintaining specific particles in specific locations and orientations. The victory is not, however, a total one, since the thermal energy of the system is still competing with the attractive interaction energies that persist at short range. Thus the density of the liquid is of roughly the same order of magnitude as that of the solid.

With further increase in temperature, however, the kinetic energy eventually predominates over the intermolecular potential energy. At this temperature the particles of the fluid become widely separated so that on average this separation is essentially infinite (by comparison with atomic or molecular dimensions), particles interacting only weakly, except during brief collisions. This is the gaseous state, and the transition to it from the liquid is marked by a sudden decrease in density of several orders of magnitude.

It is clear that the crystal and the isotropic liquid represent extremes as measured on the scale of increasing symmetry and decreasing numbers of degrees of freedom with long range order. It should be pointed out, however, that this scale is not a sliding, continuous one. A particular symmetry element is either present or absent (or equivalently, on a molecular scale, there is either long range ordering in a particular

degree of freedom or there is not); there can be no intermediate case [4]. However, within a particular phase, we may wish to characterise the degree of order distinguishing the phase, this being the measure of how the ordering within the degree(s) of freedom involved changes as the transition to the state of next highest symmetry is approached. In quantifying the degree of order of a certain kind that distinguishes one phase from another, we would like to have a measure that vanishes if the symmetry feature to which it is related (ie, the ordering in the degree of freedom involved) also vanishes. A quantity that has this property, whether it be defined or measured at the molecular or macroscopic level, is termed an *order parameter*. [Incidentally, the case of the transition from liquid to gas then presents something of a problem, in the sense that the normal liquid already has maximal symmetry at long range. What then, is to be the parameter that serves as the indicator of the transition to the gaseous state ? Clearly we might try to construct the analogue of an order parameter, identifying the density as the basic measure. To be sure, it would not be the same kind of symmetry-related tensor order parameter of which we have been speaking earlier; in particular, it would be a scalar. To conform to the requirement of vanishing at the phase transition, we would take the difference between the density of the liquid at the temperature in question at some given pressure and the density of the gas at the transition temperature at this same pressure.] We should also make the point that experiment cannot always distinguish a small non-zero order parameter from zero, whereas by definition a symmetry element is either present or absent.

### 1.3 Definition of Mesophases and Liquid Crystals

Having said all this, the normal process of melting a solid to yield a liquid involves a transition from a system with complete long range order in all degrees of freedom to one in which there is none in any. Therefore there is much scope in principle (ie, there are enough degrees of freedom) for there to exist a whole variety of states of matter which, in terms of symmetry and long range ordering, are intermediate to the

normal solid and the normal liquid. Transitions could then occur to such a state from (say) the crystal, as a function of some thermodynamic state variable, for instance the temperature. We usually use the term *state* (as we have just done here) to refer to the thermodynamic variables that together define the bulk properties of a system at equilibrium. Therefore, to avoid ambiguity, we refer to the various forms of matter with their characteristic symmetries as *phases* rather than states of matter. Phases, then, that are intermediate in terms of their long range ordering characteristics and symmetry are referred to as *mesophases*. Substances which are able to form mesophases are called *mesogens* and are often referred to as *mesogenic*. If the disordering transition from the solid is to a phase in which the disorder is in one or more orientational degrees of freedom, but full positional order is retained, then the phase will still be solid (in the sense defined earlier). It is, therefore, still regarded as a crystal of some sort, albeit a rather special kind, and is referred to as a plastic crystal. Usually, however, mesophases do not possess full long range translational order (although they may retain ordering in some translational degrees of freedom), but are fluid. That is, like a normal liquid, they cannot withstand shear stresses no matter how small, but flow in response to them. This confers on such mesophases the unique combination of properties that accounts for their importance in materials applications, namely, their anisotropic properties—a characteristic normally associated with crystals—while at the same time retaining fluidity like a liquid. This combination has then given rise to the (somewhat oxymoronic) term of reference *liquid crystal*. A liquid crystal, then, is a fluid mesophase. The characteristic feature that all liquid crystals have in common at the molecular level is long range orientational order; they may or may not possess one or two degrees of translational order.

## 1.4 Thermotropic and Lyotropic Mesophases

For the moment, we have been considering simply heating a crystal through to the isotropic liquid (that is, the changes in symmetry as a function of temperature), with

there being the possibility of other kinds of phases, namely mesophases, to occur in between. Since the thermodynamic state variable being used to change the phase behaviour is the temperature and the mesophases are generated thermally with respect to the crystal, they are referred to as thermotropic mesophases, or most often simply as thermotropics. Phases of such intermediate symmetries do not arise only in systems composed of a single pure compound as a function of temperature, however. They can also occur in certain multicomponent systems (solutions, mixtures), where the transitions to and between such phases may be observed at a given temperature as a function of the composition of the system. Since in this case the state variable governing the observed thermodynamic phase is now not only the temperature, but the mole fraction of solvent, such mesophases are referred to as lyotropic mesophases, or simply lyotropics.

There are also systems which are lyotropic in the sense just defined, but the nature of the mesophase behaviour is quite different from a mixture of two different low molar mass components one or both of which is a thermotropic mesogen. These systems are composed of a solution of amphiphilic molecules, usually in water. Here the solvent is actively involved in causing the mesophase structure in the sense that it induces aggregation of the amphiphiles into micelles, which are themselves then capable of aggregating into other structures with long range order. Thus the role of the solvent is not simply to dissolve the solute, and so disperse the mesogenic molecules. This solvent-driven self-organising behaviour is sufficiently different to low molar mass mixtures or solutions that it seems appropriate to regard these amphiphilic systems as a separate class of mesophases.

In addition to thermotropic, lyotropic and amphiphilic systems there is yet another way in which mesophases can manifest, namely colloidal suspensions of anisometric particles, such as certain virus particles [5] and minerals [6]. These systems, due to the macroscopic nature of the colloidal particles, behave in many ways as systems of hard particles. That is, the long range ordering results essentially entirely from excluded

volume effects without the subtlety of attractive forces. Thus they potentially provide real-world models of the hard particle systems studied as conceptual and theoretical points of reference in statistical mechanical theories [7] and computer simulations [8]. It is to be noted, however, that such systems are relatively rare in nature.

In this Thesis we shall be concerned solely with thermotropic systems, including mixtures of particles which are themselves all considered potentially thermotropic at both the theoretical and pragmatic levels. Therefore we shall not pursue any further the topic of other kinds of mesophases such as those formed by amphiphilic or colloidal systems.

## 1.5 Classification of Thermotropic Mesophases

As far as thermotropic liquid crystalline phases are concerned, various schemes have been suggested for their classification. It is clear that for a single compound there are six degrees of freedom in which there can be long range order, and so there should be a definite number of possible phases with characteristic symmetries, depending on the possible combinations of long range ordering. Herrman [9] argued, on purely geometrical grounds, that there should be 18 possible phases of differing symmetry between the crystal and the isotropic liquid. Later, Boccara [10] applied group theoretical arguments to this problem and came to similar conclusions. In practise, however, the most widely used classification is that of Friedel [11], who, incidentally, introduced *mesophases* as a more general term to replace *liquid crystals* (although this change did not find favour), and it is his scheme, based on their properties, that we shall follow. He identified three major subgroups of thermotropic mesophase (besides plastic crystals): nematic, cholesteric and smectic. In this Thesis we shall be almost entirely concerned with nematic liquid crystals.



### 1.5.1 The Nematic Phase ( $N$ )

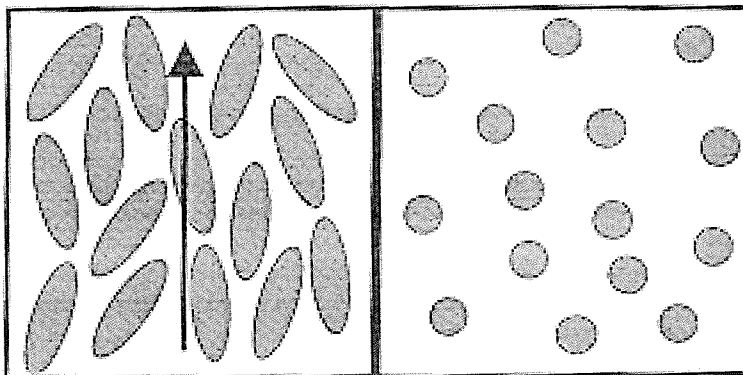
The simplest and least ordered thermotropic liquid crystalline phases are the nematic phases. They possess long range orientational order only, having full translational symmetry (ie, they are macroscopically translationally isotropic). In the simplest kind of nematic, the phase is optically uniaxial, meaning that there is one direction in which plane polarised light may be directed through it, without its plane of orientation being rotated. If the refractive index is measured along this direction it has one value, and if measured orthogonal to this direction it has another, the latter being independent of which orthogonal direction is chosen. Materials such as nematics that have two different refractive principal indices are known as birefringent.

The phase would appear to have, then, cylindrical (or *uniaxial*) symmetry, and is the normal, or uniaxial, nematic. In addition, the phase is not polar with respect to the symmetry axis (or any other axis) of the phase, and thus has a mirror plane of symmetry orthogonal to the symmetry axis. The nematic phase would appear from optical characterisation, then, to have  $D_{\infty h}$  symmetry. Strictly speaking all we can say, however, is that the phase has  $D_{nh}$  symmetry with  $n \geq 3$ . This is because the refractive index, which we have used to characterise the symmetry, is related to the dielectric anisotropy, which is a tensorial quantity of rank 2. In other words the phase symmetry is  $D_{3h}$  or higher; in practise, however, nematics are normally assumed to have full  $D_{\infty h}$  symmetry.

The symmetry axis of the phase is known as the director and is commonly denoted as the direction (ie, the unit vector)  $\hat{\mathbf{n}}$ . We note that since the phase is non-polar, the sense of the unit vector is unimportant, so that while the director is commonly represented as a unit vector, in apolar phases it is in reality the pseudovector  $\hat{\mathbf{n}} \equiv -\hat{\mathbf{n}}$ . The molecules in a nematic phase are usually calamitic (elongated or rod-like), but are sometimes also flattened, or disc-like. Thus, the molecules can be approximated to rods or discs and in either case will have a near-symmetry axis, that is, an approximate

axis of cylindrical symmetry. It is normally assumed that the symmetry axes of the molecules tend to align with the director with a distribution such that the density of probability is greatest in that direction. This is an assumption, however, since the probability density could be peaked at an angle away from the director, but be uniform around the cone corresponding to this constant angle in three dimensions, and still yield the same phase symmetry. However, it is common informally to think of the director as being the direction along which the near symmetry axes of the molecules preferentially align. This is illustrated in figure 1.1. Thus we regard the system as having one degree of long range orientational order. In the most common case of prolate or rod-like molecules we have the normal, calamitic nematic. In the case of oblate or disc-like molecules, again the symmetry axes tend to align with the director to give what is known as a discotic nematic ( $N_D$ ). From the point of view of macroscopic symmetry, however, there is no distinction between  $N$  and  $N_D$  phases.

Figure 1.1: Schematic representation of molecular ordering in the nematic phase showing a view perpendicular and parallel to the director [12].



In reality, however, most molecules deviate somewhat from cylindrical symmetry, that is, they are *biaxial*. In principle then, it is possible for more than one molecular axis to align to give long range orientational order in more than one degree of freedom, at least at some temperature where the corresponding interaction energies can assert themselves. Such phases would be referred to as biaxial nematics, and have been observed,

but only in amphiphilic systems [13]. A number of claims have been made to have discovered biaxial thermotropic nematics [14, 15], but have not been proven [16, 17]. In the limit of long range order in all orientational degrees of freedom, there will be three directors,  $\hat{\mathbf{l}}$ ,  $\hat{\mathbf{m}}$  and  $\hat{\mathbf{n}}$ , orthogonal to each other. The major director  $\hat{\mathbf{n}}$  corresponds to the preferred direction of alignment of the major molecular symmetry axis (as in the uniaxial nematic) and two minor directors correspond to the directions of alignment of the minor axes. We note that in practise it may be difficult to define major and minor axes unless the size of principal values of some property are used, but even then, there is the possibility of ambiguity, since this may depend on the property chosen.

Strictly, as with the uniaxial nematic, the term biaxial comes from its optical characterisation in the sense that there will be two directions, orthogonal to each other, in which plane polarised light can pass through the phase without having its plane of polarisation rotated. (Although neither of these, it turns out, correspond to any of the symmetry axes of the phase.) We are not interested in biaxial phases in this Thesis and so we shall not pursue the topic any further.

### 1.5.2 Chiral Nematic (Cholesteric) Phases ( $N^*$ )

The chiral nematic phase, as its name suggests, is really a kind of nematic, at least locally. We define a nematic as a mesophase with long range orientational order, but no translational order (or simply a liquid crystal with no long range translational order), and this is true of the chiral nematic phase. As the term suggests, it is a nematic phase in which there is macroscopic (or *phase* or *form*) chirality resulting ultimately from the chirality of the molecules whose interactions somehow propagate over long range. It is thus consistent with the general (von Neumann) principle that a phase should reflect the symmetry of the constituent molecules (in its most ordered form) and so has lower symmetry than the normal nematic. The term *cholesteric* originates from the fact these phases were first observed in cholesterol derivatives such as those studied by Reinitzer. Since then these phases have been observed in other types of compounds

and the common feature is that the molecules are chiral, so it is preferable to use the more accurate (and informative) name *chiral nematic*. We have included it simply for completeness, since in this Thesis we do not have any need to focus on chiral nematics, and so we shall say no more about them.

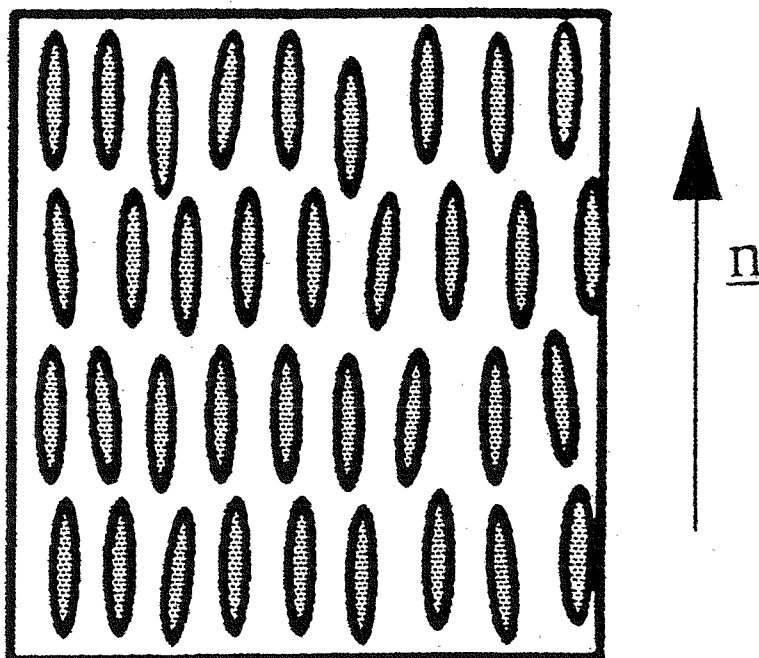
### 1.5.3 Smectic Phases ( $Sm : SmA, SmB, \dots, SmL$ )

In the smectic phases ( $Sm$ ), not only is there long range orientational order, but also some long range order in one or more of the translational degrees of freedom. There are a variety of smectic phases, only one of which we are interested in here, and that is the smectic A phase ( $SmA$ ), so named because it was the first smectic phase discovered. It is the simplest form of smectic phase, with ordering in the least number of translational degrees of freedom. The molecules in smectic phases tend, not only to align parallel to each other and to a common direction, but also form layers. In the case of the smectic A, the phase is optically uniaxial, and the directors of the layers are parallel to the layer normal and to its axis of assumed cylindrical symmetry, as illustrated in figure 1.2.

## 1.6 The Molecules That Form Liquid Crystals

From the variety of mesogenic molecules it should be possible to identify and distinguish those features of molecular structure that are necessary for liquid crystal formation, those that are simply desirable and those which are largely irrelevant. Gray [18, 19] has given a number of empirical rules describing the influence of various aspects of the molecular structure upon thermotropic phase behaviour. The most basic requirement is one or more rigid moieties which should be either prolate (elongated or rod-like) or oblate (flattened or disc-like). In addition, they may have flexible alkyl chains, as terminal substituents of the mesogenic groups, as interconnecting bridges between them or as lateral substituents (or possibly some combination of these).

Figure 1.2: Schematic representation of molecular ordering in the smectic A phase (view perpendicular to the director).



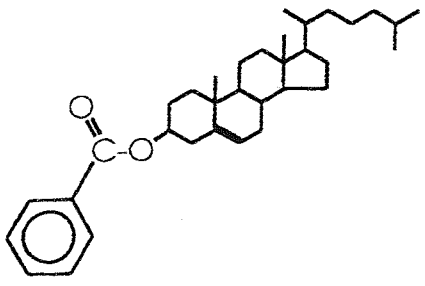
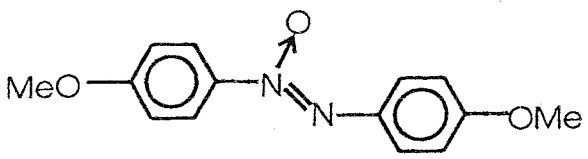
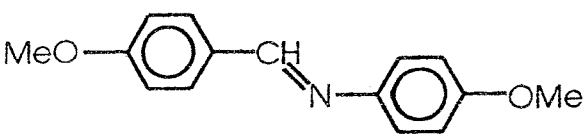
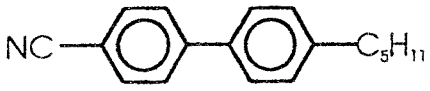
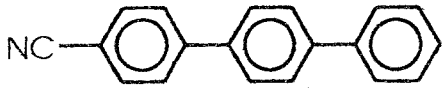
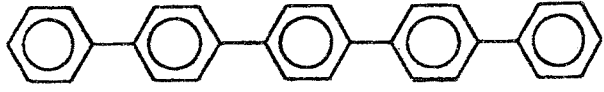
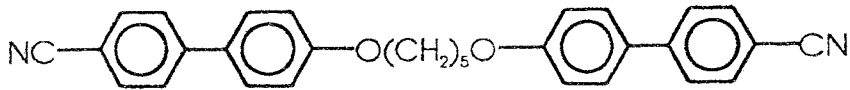
The alkyl chains may be connected to the mesogenic groups via any of various linkage groups. The rigid moieties generally consist of aromatic or saturated cyclic rings, which may be connected via a linkage group. These rigid groups are usually made up of phenyl rings. Also, the molecules often in practise possess polar groups. This is thought to help stabilise liquid crystalline phases, although as in the case of flexible chains, this is not a requirement for liquid crystalline phase behaviour, as evidenced by, for instance, quinquephenyl which has a high  $T_{NI}$ . Some examples of mesogenic molecules are shown in figure 1.3.

It would appear that the main factor driving the formation of liquid crystalline phases is the anisometric shape of the molecules. In other words, the molecules forming liquid crystals are ones that deviate significantly from spherical symmetry. It is the

anisotropy in the properties of the molecules which consequently propagates over long range to give rise to liquid crystalline order and hence macroscopically anisotropic fluids of various forms. In the light of this it might seem surprising that there are not more mesogenic compounds than there are, since the number of molecules that are spherically symmetric must surely be in the minority. It is thought that the reason for this is that the compound typically crystallises at a temperature above that at which it would otherwise exhibit a transition to a liquid crystalline phase. The liquid crystal transition temperature of such a compound is thus said to be *virtual*. If the molecule is made more anisometric, however, the transition temperature is raised, and is thus more likely to be exceeded than that of crystallisation, all other things being equal. To have a good chance of designing a mesogenic molecule then, we should first make sure it has a high anisometry and also try to include modifications (such as adding or lengthening flexible chains) which lower the melting point.

To a first approximation, mesogenic molecules can be thought of as rigid, cylindrically symmetric rods (or possibly discs, depending on the molecule). Indeed some of the theoretical studies in the earlier chapters work within this assumption. In reality, however, most molecules deviate to some extent from cylindrical symmetry, most mesogenic molecules being lath-like. It is possible to take this into account by constructing measures, based on second rank properties (say), to describe this deviation, giving the notion of molecular biaxiality (as opposed to uniaxiality). When built into theories the molecular biaxiality can in principle result not only in a uniaxial phase, but also a biaxial nematic phase. This could be a phase with with no orientational preference of one minor molecular axis, or a biaxial phase with order in all orientational degrees of freedom, although we shall not be interested in such possibilities here.

Figure 1.3: Examples of the chemical structures of some typical mesogens and their nematic-isotropic transition temperatures [12].

	$T_{NI}/^{\circ}\text{C}$
<p>Cholesteryl benzoate</p> 	182
<p>4-4'-dimethoxyazoxybenzene(PAA)</p> 	136
<p>4-methoxybenzylidene-4'-n-butylaniline(MBBA)</p> 	47
<p>4-n-pentyl-4'-cyanobiphenyl(5CB)</p> 	35
<p>4-cyano-p-terphenyl</p> 	275
<p>p-quinquephenyl</p> 	445
<p><math>\alpha</math>-<math>\omega</math>-bis(4,4-cyanobiphenyloxy)pentane</p> 	186

In addition to allowing for molecular biaxiality, we should note that, even though a rigid, anisometric region of the molecule is a prerequisite for liquid crystal formation, in practise in most cases there are also flexible components. Treating the molecule as rigid then is also an approximation. Moreover, it is also common to deliberately incorporate flexible chains as well as the required rigid (mesogenic) group(s) into molecules. This enhances the liquid crystallinity of the compound in that it lowers the melting point, thus extending the liquid crystalline temperature range. Clearly then, it is desirable not only to include the effects of deviation from cylindrical symmetry, but also those due to flexibility of, for instance, alkyl chains (which also cause the molecule to deviate from cylindrical symmetry). To this end various workers have attempted to allow for molecular flexibility in developing theories of liquid crystals [20, 21]. We shall apply some of these ideas in the last chapter where we describe a methodology for modelling nematic phases consisting of molecules which may exhibit an extremely high degree of flexibility.

## 1.7 Phase Transitions

A thermotropic mesogen may exhibit one or a more mesophases. As the temperature is increased the translational and orientational order generally decreases, with the system potentially passing from the crystal through a variety of smectic phases to the smectic A, then the nematic and finally the isotropic. These phases may not always occur, however, and some compounds in addition exhibit re-entrant phase behaviour in which, a higher symmetry phase recurs as a transition from a lower symmetry one. The transitions between these phases are traditionally characterised using the Ehrenfest scheme. In this scheme a transition is said to be  $n$ th order if the first  $n - 1$  temperature derivatives of the free energy are analytic across the transition, but the  $n$ th is non-analytic. In this context, *analytic* and *non-analytic* are conventionally taken to mean *continuous* and *discontinuous*, although it strictly refers to whether or not the form can be expanded as a Taylor series. The first derivative of the free energy with respect to temperature is essentially the entropy of the system, in this case the entropy



either side of the transition. That is,

$$\left(\frac{\partial A}{\partial T}\right)_V = \left(\frac{\partial G}{\partial T}\right)_p = -S, \quad (1.1)$$

so that if the transition is first order, the entropy changes abruptly from one side of the transition to the other, giving rise to a non-zero transitional entropy change. If, on the other hand, the first derivative is continuous (that is, the transitional entropy change is zero), we should investigate the second derivative, which is essentially the specific heat capacity. That is, given that we are considering systems at constant volume,

$$C_V = \left(\frac{dq}{dT}\right)_V = \left(\frac{\partial U}{\partial T}\right)_V, \quad (1.2)$$

and

$$\begin{aligned} dU &= dq - pdV \quad (\text{no additional work}) \\ &= TdS - pdV \quad (\text{at equilibrium}). \end{aligned} \quad (1.3)$$

Therefore,

$$C_V = \left(\frac{TdS - pdV}{dT}\right)_V = T\left(\frac{\partial S}{\partial T}\right)_V. \quad (1.4)$$

Now as we have already seen

$$S = -\left(\frac{\partial A}{\partial T}\right)_V. \quad (1.5)$$

Hence,

$$C_V = T\left(\frac{\partial}{\partial T}\left(-\frac{\partial A}{\partial T}\right)_V\right)_V = -T\left(\frac{\partial^2 A}{\partial T^2}\right)_V. \quad (1.6)$$

A similar analysis follows using the Gibbs free energy for the specific heat capacity at constant pressure. That is,

$$C_p = \left(\frac{dq}{dT}\right)_p = \left(\frac{\partial H}{\partial T}\right)_p, \quad (1.7)$$

and

$$dH = d(U + pV) = dU + pdV + Vdp$$

$$= TdS + Vdp \quad (\text{equilibrium, no additional work}), \quad (1.8)$$

giving

$$C_p = \left( \frac{TdS + Vdp}{dT} \right)_p = T \left( \frac{\partial S}{\partial T} \right)_p. \quad (1.9)$$

But

$$S = - \left( \frac{\partial G}{\partial T} \right)_p, \quad (1.10)$$

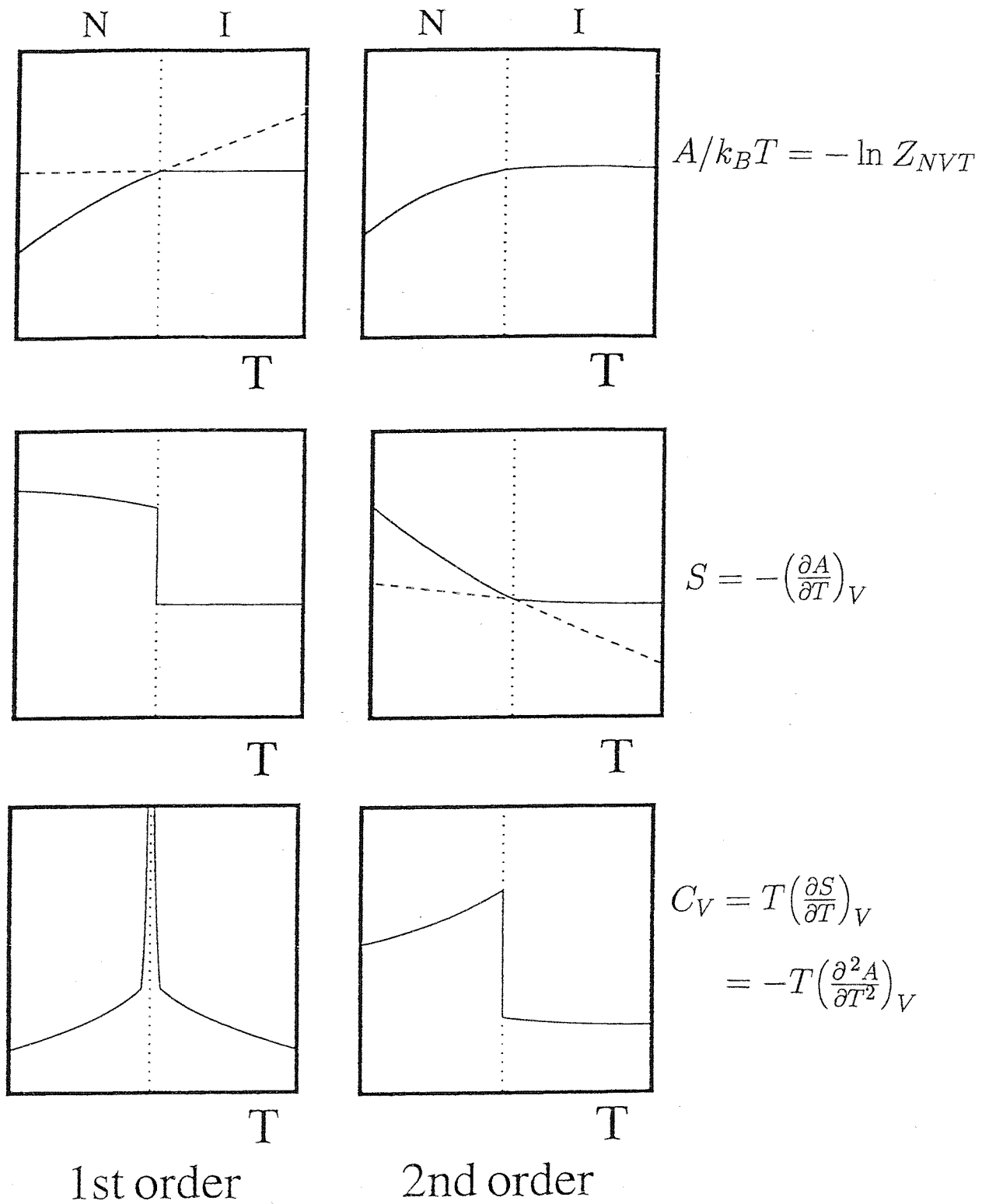
so that

$$C_p = -T \left( \frac{\partial}{\partial T} \left( \frac{\partial G}{\partial T} \right)_p \right)_p = -T \left( \frac{\partial^2 G}{\partial T^2} \right)_p. \quad (1.11)$$

In the case of a first order transition, we might ask what is the variation of the specific heat capacity through the transition. Since the first derivative is discontinuous, it is theoretically an infinitely sharp spike going to infinity. The free energy and its temperature derivatives through first and second order transitions are illustrated in figure 1.4.

It is found that the melting transitions from crystal to isotropic liquid and liquid crystal are first order, as are the clearing transitions (liquid crystal to isotropic liquid). [We note, however, that the theoretical biaxial nematic-isotropic transition is exceptional in that it is predicted to be second order.] Since the predominant contribution to the entropy of a fluid is that associated with disorder in translational degrees of freedom, the entropy change (or equivalently at constant volume the latent heat) is much larger ( $\Delta S/R \sim 10$ ) at the melting transitions than at the clearing transitions ( $\Delta S/R \sim 0.1$ ). The former are correspondingly referred to as strongly first order and the latter as weakly first order. Transitions between different liquid crystalline phases, such as between different kinds of smectic phase or from smectic to nematic (or even hypothetically between different nematic phases) are generally even weaker, or second order.

Figure 1.4: The Ehrenfest classification of how the free energy, entropy and heat capacity change with temperature in the neighbourhood of first and second order phase transitions for a constant volume system.



As an addendum we note that when this concept of order in relation to the free energy through a transition was first introduced by Ehrenfest, it was thought that it would prove to be of fundamental significance. It turns out that this is not the case, however. While third order and higher transitions do occur, it is now accepted that transitions are most usefully characterised as either *phase transitions of the first kind* or *phase transitions of the second kind*. Phase transitions of the first kind are those in which the entropy is discontinuous across the transition, and so are also called *discontinuous* transitions; they correspond to first order transitions in the Ehrenfest scheme. Phase transitions of the second kind are those in which the entropy is continuous across the transition; they are also called *continuous* transitions and correspond to second order and higher transitions in the traditional scheme [3].

## 1.8 Orientational Order in the Nematic Phase

### 1.8.1 Defining the orientation of a molecule in a monodomain

The orientation of a rigid molecule is described with respect to a cartesian coordinate system set in an external laboratory frame of reference via the three Euler angles  $\alpha$ ,  $\beta$  and  $\gamma$ . A simple (although formally incomplete) illustration of the Euler angles is given in figures 1.5c and 1.6c. It is then customary and convenient for uniaxial liquid crystals to define the laboratory  $z$  axis as coincident with the director. This picture is incomplete because strictly the angle  $\gamma$  is not formally defined. We can, however, define  $\gamma$  precisely by means of a reference frame set in the molecule. That is, if the angles  $\alpha$  and  $\beta$  are as in the figures, then the angle between the  $z$ -axis of the molecular frame and that of the laboratory frame is obviously  $\beta$ . However, the azimuthal angle of the laboratory  $z$ -axis in the molecular frame is then  $(\pi - \gamma)$ . This gives an intuitive (although still not complete) understanding of the Euler angles sufficient for our purposes. A full, formal definition of the Euler angles is given in Appendix 1A.

There is also an alternative way of representing the orientation of a molecule and that is by using direction cosines. Whilst the use of direction cosines is in many cases cumbersome, they lead to particularly simple, physically understandable transformations in the case of uniaxial phases of biaxial particles involving the Saupe ordering matrix.

## 1.8.2 Uniaxial Phase of Uniaxial Molecules

For a cylindrically symmetric molecule all angles  $\gamma$  are energetically equivalent and for a cylindrically symmetric phase all angles  $\alpha$  are energetically equivalent (see figure 1.5c) so that the distribution does not depend on them. The orientation of a given molecule is then specified by a single angle,  $\beta$ , the angle between the molecular symmetry axis and the director. In the nematic phase the molecules prefer, on average, to lie parallel to the director with  $\beta = 0, \pi$ . At finite temperatures, however, thermal motion prevents perfect alignment with respect to the director and the molecules are thus distributed over the continuum of possible angles  $\beta$  with  $\beta = 0, \pi$  being assumed to have identically the highest probability density. This probability density is that pertaining to the orientations of individual molecules, rather than of simultaneous orientations of more than one molecule; it is a single molecule (singlet) property. Strictly, it is the singlet orientational probability density distribution function, but is usually referred to simply as the singlet orientational distribution function, denoted  $f(\Omega)$  ( $\Omega \equiv \alpha, \beta, \gamma$ ). It is conventional then in the case of uniaxial phases of assumed uniaxial molecules to remove the redundant variables  $\alpha$  and  $\gamma$ , and so the distribution is denoted  $f(\beta)$ . We also note that in this case it is by convention  $f(\beta)$  that is assumed to be normalised, rather than  $f(\Omega)$  itself. In other words,

$$\int_0^\pi f(\beta) \sin \beta \, d\beta = 1 \quad (1.12)$$

so that the distribution in  $\beta$  space alone may be interpreted probabilistically in the sense that it integrates to unity.

Figure 1.5: Cylindrically symmetric molecule in a uniaxial phase [12]. Schematic representation of the molecular alignment a) perpendicular to the director and b) parallel to the director. Diagram c) illustrates that only one Euler angle  $\beta$  is required to define the orientation of the molecule with respect to the director.

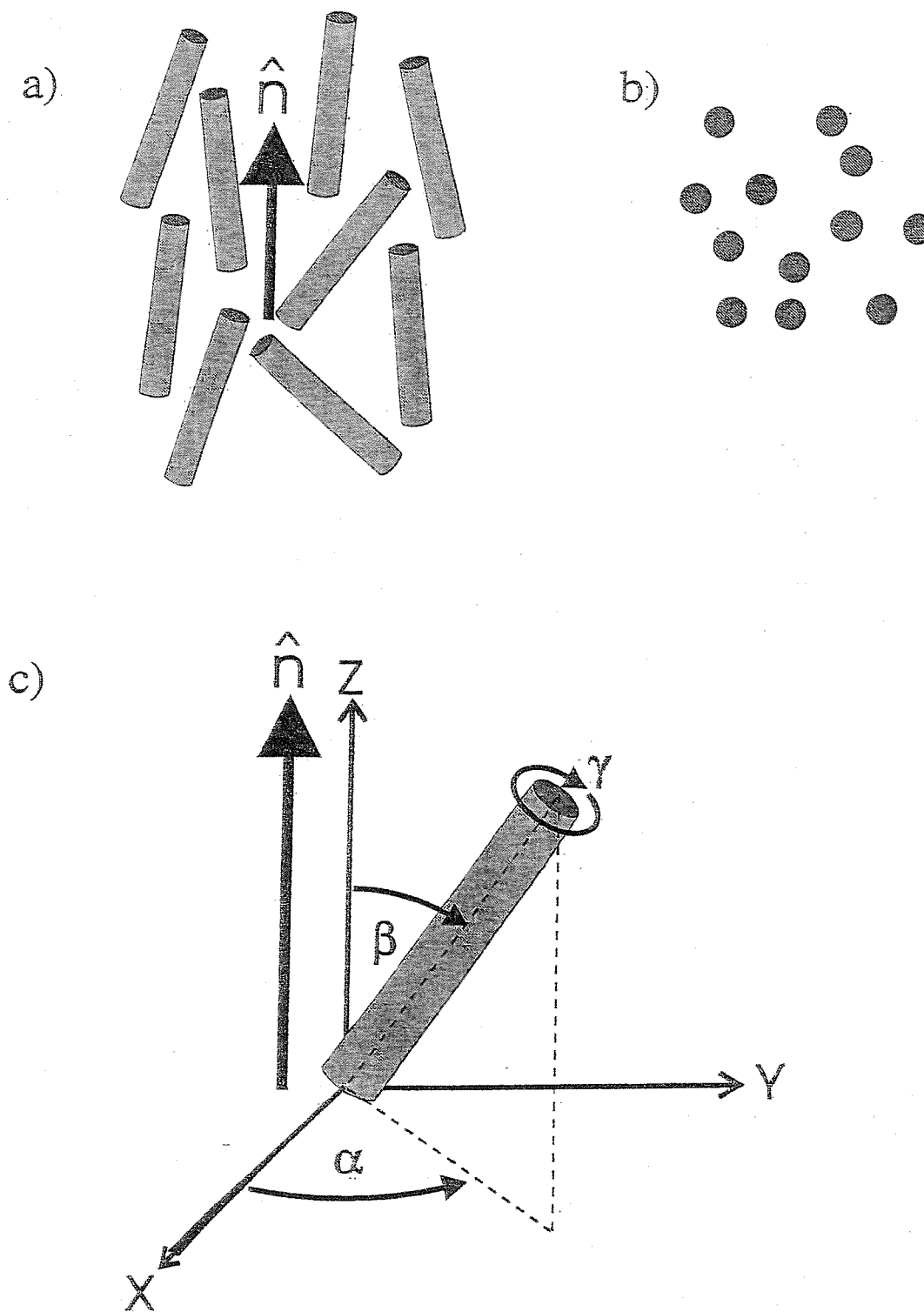
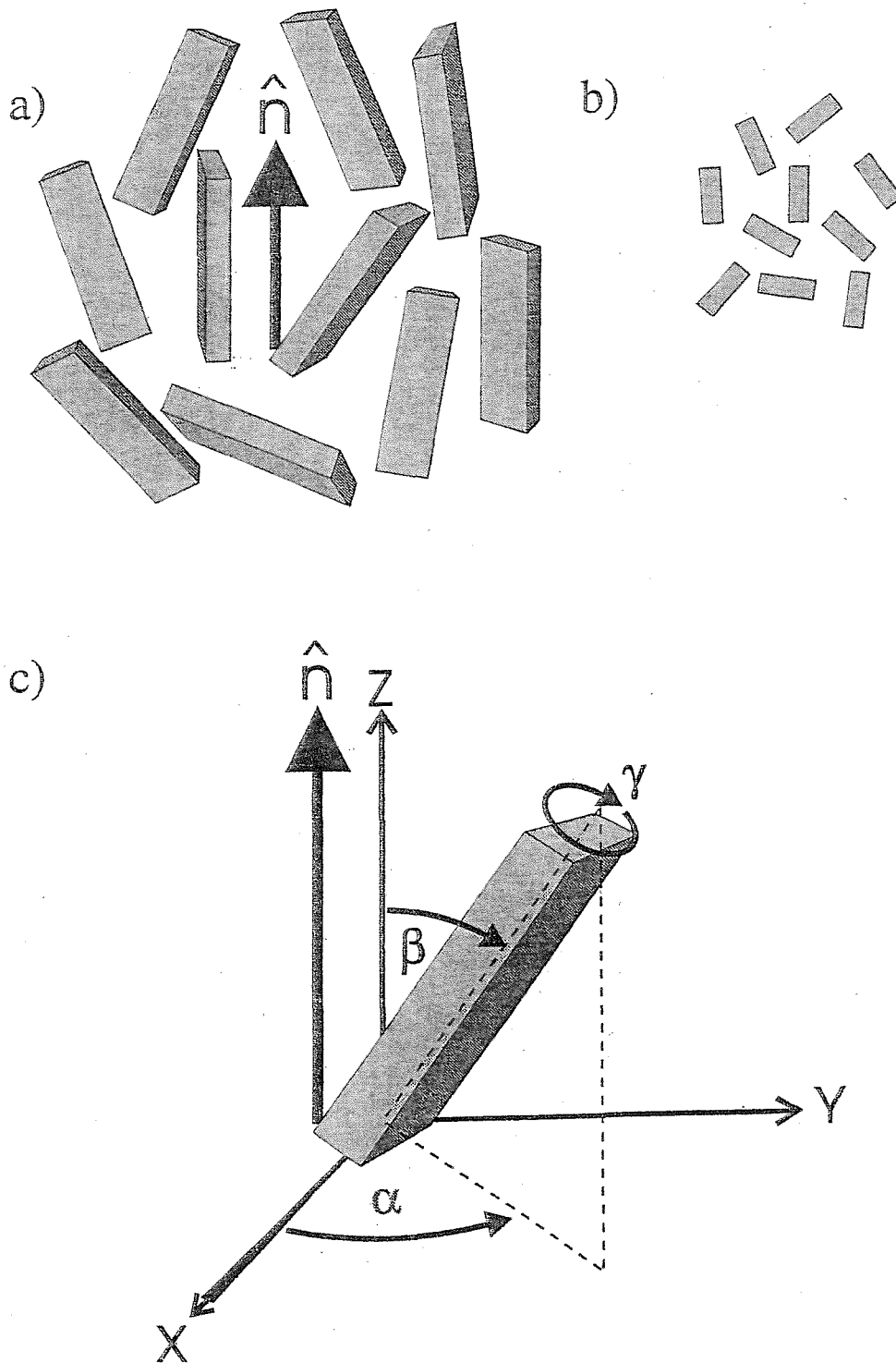


Figure 1.6: Biaxial molecule in a uniaxial phase [12]. Schematic representation of the molecular alignment a) perpendicular to the director and b) parallel to the director. Diagram c) illustrates that two Euler angles  $\beta$  and  $\alpha$  are required to define the orientation of the molecule with respect to the director.



This function,  $f(\beta)$  [22], provides the most complete description of the single molecule orientational order available. We note that since the phase is non-polar, it has a plane of symmetry orthogonal to the director, which imposes the constraint that the single molecule orientational probability density at  $\beta$  must be the same as that at  $\pi - \beta$  so that  $f(\beta) = f(\pi - \beta)$ . For polar phases, however, such as those produced by application of an electric field (see later), the symmetry of the phase is lowered to  $C_{\infty V}$ , and then, due to the lack of symmetry orthogonal to the director,  $f(\beta)$  is no longer equal to  $f(\pi - \beta)$ .

It is clearly important to be able to write down some expression to attempt to encapsulate the singlet orientational distribution function. This may be achieved by means of a series expansion in a basis of continuous well-behaved functions, which in the case of a non-polar phase must have the same apolar character, that is be even about  $\pi/2$  (this constraint is relaxed for polar phases) and span the space. A good mathematical choice of basis functions is the Legendre polynomials (see Appendix 1B). One reason for this is that, for any arbitrary curve, they provide the best least squares fit of any power series up to any given desired order [23]. When Legendre's equation is solved by the Frobenius series method, the solutions, the Legendre polynomials,  $P_L(x)$  are obtained as two fundamentally different series—the even order and the odd order series. Even order  $P_L(x)$  are polynomials containing terms in all even powers of  $x$  from a term in  $x^L$  down to a zeroth term. Odd order  $P_L(x)$  contain all odd order terms from a  $x^L$  term down to a linear term. Thus  $P_L(x)$  is an even function for  $L$  even and an odd function for  $L$  odd. For a nematic we require a function that is even about  $\beta = \pi/2$  and periodic in  $\pi$  and we note that  $x$  must be bounded and periodic on  $(-1, 1)$ . We may then employ the even rank  $P_L(x)$  by careful choice of the functional dependence of the argument,  $x$ , on the polar angle. We require the argument,  $x$ , of the Legendre polynomials to be a circular function which is zero at  $\beta = \pi/2$  (since  $P_L(x)$  ( $L$  even) is even about about  $x = 0$ ) and such that the magnitude of the circular function is also even about  $\beta = \pi/2$ , a maximum at  $0, \pi$  and periodic in  $\pi$ . Such a function is provided



by the cosine of the polar angle. The Legendre series for  $f(\beta)$  is then written

$$f(\beta) = \sum_{L(\text{even})=0}^{\infty} f_L P_L(\cos \beta). \quad (1.13)$$

Now  $\cos \beta$  is the projection of the molecule, treated as a vector, onto the director and normalised with respect to the molecular length (i.e. it is the projection of a unit vector along the molecular axis onto  $\hat{n}$ ). Thus  $\cos^n \beta$  (where  $n = 1, 2, \dots$ ) is a measure of the extent to which a given molecule is aligned with the director; this measure is apolar for  $n$  even, polar for  $n$  odd. The observation that the  $P_{L(\text{odd})}$  are linear combinations of  $\cos^n \beta$  ( $n$  odd) suggests that one can allow for the situation where the nematic phase becomes polarised by removing from (1.13) the constraint upon  $L$  to take only even values. Furthermore, it might be thought that quantities of the form  $\cos^n \beta$  averaged over all molecules would provide various measures of the extent of the single molecule orientational order, that is, serve as some kind of order parameters. It is convenient and conventional, however, to define an order parameter such that it is unity in the limit of perfect ordering of the type described by it and to vanish when there is no such order. This is not in general the case for the ensemble averages of all  $\cos^n \beta$ , so an alternative is required. Now the  $P_{L(\text{even})}(\cos \beta)$  are linear combinations of  $\cos^n \beta$  ( $n$  even) and the  $P_{L(\text{odd})}(\cos \beta)$  are linear combinations of  $\cos^n \beta$  ( $n$  odd). The solutions obtained from the Frobenius method are normalised such that the value of a  $P_L(x)$  is unity when its argument,  $x$ , is unity. Hence in the limit of perfect non-polar order  $P_{L(\text{even})}(\cos \beta)$  is unity for all molecules and so its ensemble average is also unity. Similarly in the limit of perfect polar order  $\overline{P}_{L(\text{odd})}$  is also unity. In the limit of complete isotropy (non-polar/polar) the  $\overline{P}_{L(\text{even/odd})}$  are zero. Thus, another useful feature of the Legendre polynomials is that the ensemble averages of the  $P_L(\cos \beta)$ , denoted by  $\overline{P}_L$ , furnish a convenient set of order parameters. These are defined as averages of the  $P_L(\cos \beta)$  over the distribution function,

$$\overline{P}_L = \int_0^\pi P_L(\cos \beta) f(\beta) \sin \beta d\beta, \quad (1.14)$$

thus giving a measure of the single molecule orientational order. A further useful feature of the Legendre polynomials is that, in addition to forming a *complete* set of

basis functions (which ensures that in principle the function being expanded may be completely encapsulated), they are also an *orthogonal* set. Thus

$$\int_{-1}^1 P_L(x) P_{L'}(x) dx = 0 \quad (1.15)$$

for all  $L \neq L'$ . This enables us to find the expansion coefficients  $f_L$  in equation (1.13) and hence to obtain the set of order parameters in a more formal, sophisticated manner, as we shall now demonstrate. To find a particular coefficient  $f_{L'}$  we multiply (1.13) by  $P_{L'}(\cos \beta)$  and integrate over the whole range of the argument  $\cos \beta$

$$\int_{-1}^1 f(\beta) P_{L'}(\cos \beta) d \cos \beta = \int_{-1}^1 \left( P_{L'}(\cos \beta) \sum_{L \text{ even}} f_L P_L(\cos \beta) \right) d \cos \beta. \quad (1.16)$$

All the terms in the summation over  $L$  of integrals vanish except for the term where  $L = L'$ . The left hand side of (1.16) is by definition  $\bar{P}_{L'}$  and so

$$\bar{P}_{L'} = f_{L'} \int_{-1}^1 P_{L'}(\cos \beta)^2 d \cos \beta. \quad (1.17)$$

Now using the fact that

$$\int_{-1}^1 P_L(\cos \beta) P_{L'}(\cos \beta) d \cos \beta = \frac{2}{2L+1} \delta_{LL'} \quad (1.18)$$

we have

$$\bar{P}_{L'} = \frac{2}{2L'+1} f_{L'}. \quad (1.19)$$

Hence for any given value of  $L$ ,

$$f_L = \frac{2L+1}{2} \bar{P}_L. \quad (1.20)$$

Equation (1.13) then becomes

$$f(\beta) = \sum_{L(\text{even})=0}^{\infty} \frac{2L+1}{2} \bar{P}_L P_L(\cos \beta). \quad (1.21)$$

The order parameters are thus seen to be essentially the coefficients of the different moments of the expansion of  $f(\beta)$ , and to form a complete, orthogonal set. Knowledge of the entire set of order parameters thus completely defines the singlet orientational

distribution function. A complete set of order parameters is not available for real mesogens, however. Only  $\overline{P}_2$  and  $\overline{P}_4$  are routinely measurable and even then measuring  $\overline{P}_4$  is difficult, although, in principle, neutron scattering can give the complete set. The expansion (1.13,1.21) turns out to be slow to converge in general, at least for single component or other systems with relatively high orientational order. That is, it is generally found that systems have a Maier-Saupe-like distribution function (see Chapter 2) and for such a distribution its Legendre polynomial expansion is slow to converge when the largest orientational order parameter,  $\overline{P}_2 \geq \text{ca. } 0.2$ . Hence it is usually a poor approximation when truncated at the second or fourth rank term.

A better expansion in such cases may be obtained as follows. Assuming  $f(\beta)$  is well-behaved we may write it as the exponential of a different function  $g(\beta)$ ,

$$f(\beta) = \exp(g(\beta)). \quad (1.22)$$

We may then proceed to expand this new function  $g(\beta)$  in the same manner as we expanded  $f(\beta)$ . This is clearly consistent with the expected Boltzmann distribution, so long as the expansion of  $g(\beta)$  contains a zeroth term leading to a constant multiplier the reciprocal of which is analogous to a partition function. Therefore we write

$$g(\beta) = \sum_{L=0}^{\infty} a_L P_L(\cos \beta), \quad (1.23)$$

where for a non-polar phase  $L$  is restricted to even values only. The distribution function  $f(\beta)$  is then

$$f(\beta) = \exp\left(\sum_{L=0}^{\infty} a_L P_L(\cos \beta)\right), \quad (1.24)$$

which we can also write, by factoring out a zeroth term, as

$$f(\beta) = \exp(a_0) \exp(g'(\beta)), \quad (1.25)$$

where  $\exp(a_0) \equiv Z^{-1}$  ( $Z$  being a partition function) and

$$g'(\beta) = \sum_{L \neq 0}^{\infty} a_L P_L(\cos \beta). \quad (1.26)$$

The distribution function is then

$$f(\beta) = Z^{-1} \exp \left( \sum_{L \neq 0}^{\infty} a_L P_L(\cos \beta) \right),$$

$$Z = \int \exp \left( \sum_{L \neq 0}^{\infty} a_L P_L(\cos \beta) \right) \sin \beta d\beta. \quad (1.27)$$

The justification for this procedure is ultimately pragmatic. We know that the distribution, when represented by the exponential of a Legendre series expansion, generally converges much more rapidly, as evidence by, for instance,  $f(\beta)$  as determined from computer simulations. That is, in the Maier-Saupe theory (see Chapter 2),  $f(\beta)$  is Boltzmann-like and the exponent has the form of the expansion (1.26) truncated at the first term. Moreover, we find that the singlet orientational distribution function from computer simulation (using, for instance, the Gay-Berne potential [24]) is indeed well-represented (ie, almost quantitatively) by an exponential function with a single term in  $P_2(\cos \beta)$  in the exponent. Furthermore, upon inclusion of an extra term in  $P_4(\cos \beta)$  with a relatively small coefficient ( $a_4/a_2 \sim 0.1$ ), the functional form then does become quantitative.

We know from the physics that if we have a single molecule orientational density distribution  $f(\beta)$  then we can define a corresponding single molecule orientational potential energy function  $U(\beta)$  over which the system is distributed in accordance with the Boltzmann distribution. Thus we should have

$$f(\beta) = Z^{-1} \exp \left( -U(\beta)/k_B T \right),$$

$$Z = \int \exp \left( -U(\beta)/k_B T \right) \sin \beta d\beta. \quad (1.28)$$

The quantity  $U(\beta)$  is formally referred to as the *potential of mean torque* and has a central importance in molecular field theories (of which the Maier-Saupe theory is a prototype) as we shall see in Chapter 2. Equation (1.28) is then strictly the defining

equation for the potential of mean torque. We are also able to make the identification

$$U(\beta) = -k_B T g'(\beta). \quad (1.29)$$

Whilst for many distributions the exponential of a Legendre series expansion is more rapid to converge, we note that the coefficients of the Legendre series no longer have any physical significance (unlike the Legendre series for  $f(\beta)$  itself where they are the order parameters,  $\overline{P}_L$ ). They do, however, determine the order parameters, albeit indirectly.

In addition to these formal ways of obtaining general expansions for  $f(\beta)$  there is another, more pragmatic, way of obtaining the distribution in specific instances where, for some system, certain order parameters have been determined by experiment. This is by appeal to information theory [25] and the maximum entropy principle [26]. The general approach is as follows. For some arbitrary system we assume a probability density distribution function,  $\rho = \rho\{X\}$ , where  $\{X\}$  represents all the variables (degrees of freedom of the system) on which  $\rho$  depends. We then proceed to obtain the least biased distribution consistent with the information we have about the system. This involves maximising the Boltmann entropy

$$S = -k_B \int \rho\{X\} \ln \rho\{X\} d\{X\} \quad (1.30)$$

of the system, subject to certain constraints, these being the specific information we have about the system. In many theories,  $S$  is a measure of the information content of a system and in this present context, where we focus on single particle orientational quantities, becomes the expression for the single particle orientational entropy. The constraints are the measured values of the order parameters obtained from experiment. Thus, if we have measured values for one or more order parameters  $\overline{P}_L$ , then the constraints are that the order parameters take their measured values. Maximising  $S$  with respect to the distribution  $\rho\{X\} \equiv f(\beta)$  subject to these constraints gives the singlet orientational distribution function as [27, 28]

$$f(\beta) = Z^{-1} \exp \left( \sum_L a_L P_L(\cos \beta) \right),$$

$$Z = \int_0^\pi \exp\left(\sum_L a_L P_L(\cos \beta)\right) \sin \beta d\beta. \quad (1.31)$$

We note the similarity of this expression to that obtained earlier by expansion of  $g(\beta)$  (equation (1.27)).

### 1.8.3 Uniaxial Phase of Biaxial Molecules

The molecules forming liquid crystalline phases and the conformations of alkyl chains will not in reality possess cylindrical symmetry and will tend to be more lath-like. If the phase is uniaxial, then a biaxial molecule will require specification of the two angles  $\beta$  and  $\alpha$  to define its orientation with respect to the director of the phase (see figure 1.6c). For uniaxial phases, however, it is more convenient to define the orientation of the director in a molecular frame, that is in terms of the Euler angles  $\beta$  and  $\gamma$  (see Appendix 1A). The singlet orientational distribution function is now a function of these two angles  $\beta$  ( $0 \leq \beta \leq \pi$ ) and  $\gamma$  ( $0 \leq \gamma \leq 2\pi$ ). Thus we need to generalise the approach of section 1.8.2. We require a set of functions with similar properties to the Legendre polynomials, but which are functions now of two angles and which span the required space. Both the spherical harmonics and the modified spherical harmonics (which are simply related to each other) provide such a set. They are defined on the surface of a sphere and span the space of any function of two angles where one has a range of  $0 - \pi$  and the other  $0 - 2\pi$ . Each set of functions is complete in this space. The functions are also orthogonal so that the integral of the product of two with differing rank over the entire angular space vanishes, thus analogously furnishing a method of determining the expansion coefficients, and thence a complete, independent set of order parameters. For convenience, we choose the modified (or Racah) spherical harmonics,  $C_{L,m}(\beta, \gamma)$  [22](see Appendix IB), as the basis for the expansion of  $f(\beta, \gamma)$ . We write

$$f(\beta, \gamma) = \sum_{L(\text{even}), m} f_{L,m} C_{L,m}^*(\beta, \gamma), \quad (1.32)$$

where the coefficients  $f_{L,m}$  are related to the orientational order parameters by

$$f_{L,m} = \frac{2L+1}{4\pi} \bar{C}_{L,m}. \quad (1.33)$$

Again this expansion may be slow to converge and under these circumstances a better one can be obtained by assuming an exponential function for  $f(\beta, \gamma)$  and expanding the exponent, as before. This yields

$$f(\beta, \gamma) = Z^{-1} \exp \left( \sum_{L,m} a_{L,m} C_{L,m}^*(\beta, \gamma) \right), \quad (1.34)$$

where the normalisation factor is now

$$Z = \int_{\gamma=0}^{2\pi} \int_{\beta=0}^{\pi} \exp \left( \sum_{L,m} a_{L,m} C_{L,m}^*(\beta, \gamma) \right) \sin \beta \, d\beta \, d\gamma, \quad (1.35)$$

which is analogous to a partition function. Here,  $m$  takes values  $-L, -L+1, \dots, L$ , hence there are  $2L+1$  values for each  $L$ . Thus, if we truncate the expansion at second order we have  $L=2$  and so there are five second rank order parameters corresponding to  $m=0, \pm 1, \pm 2$ . In a principal axis system this simplifies so that only two order parameters,  $\bar{C}_{20}$  and  $\bar{C}_{22}$ , are required. As before, information theory and the principle of maximum entropy may be brought to bear on a particular system for which some of the order parameters are known. This yields an expression for the distribution function of that system which is of a similar form.

In addition to forming a uniaxial phase, it is possible in principle for a phase of biaxial molecules to exhibit a correspondingly biaxial phase, in which the molecules orient preferentially with respect to a second minor director. In this case all three Euler angles are required to define the orientation of the molecule with respect to the phase.

## 1.9 Molecular Models of Liquid Crystallinity

The long range orientational order characteristic of liquid crystal phases indicates that it is the anisotropy in the intermolecular potential which is essential for their existence.

As to the nature of these forces it has long been held that in simple liquids it is predominantly the repulsive forces that are responsible for determining their structure with the attractive forces serving to maintain a high density. It also seems reasonable to assert that this is true for orientationally ordered fluids. Such a view was first developed by Onsager who believed that it is the short range repulsive forces between anisometric particles that result in their orientational order [7]. On the other hand there is the model proposed by Maier and Saupe [29, 30, 31] which assumed, at least in its original derivation, that the long range anisotropic attractive forces are responsible for the formation of the nematic phase. There have also been attempts at a compromise and to bring the two approaches together [32], which appears reasonable as both anisotropic repulsive and attractive forces should play a role in stabilising the liquid crystal phase. Indeed, the attractive forces must be important because the transitions are thermally driven. (We should note, however, that at constant pressure the density also changes as a function of temperature so that the phase behaviour is at least in part still density driven.)

In fact it turns out that in modern derivations of the Maier-Saupe theory based on the pair potential or variational approaches (see Chapter 2) it is not necessary to make any assumptions about the relative importance of the roles of attractive and repulsive forces; both are implicitly included. Computer simulations have made it possible to concentrate on the essential features of the model rather than the statistical mechanical approximations and thus to explore the role of repulsive and attractive forces in determining liquid crystal phase behaviour. For example, simulations of hard ellipsoidal shaped molecules have shown that nematic-isotropic transitions do occur on changing the density provided the length : breadth ratio is greater than about 3 : 1 [33]. From these results it seems, therefore, that anisotropic repulsive forces could play a role in the creation of the nematic phase. Such ellipsoidal systems can, however, only form a nematic phase (and in addition the transitions are only driven by a change in the density of the system). No smectic A phase is formed. To develop a model which exhibits other phases such as smectic phases it is necessary to change the shape of the particles or



introduce attractive forces. So, for instance, hard spherocylinders are found to exhibit a smectic A phase and the phase transition is density driven. To develop a model that shows thermally-driven phase behaviour it is necessary to introduce attractive forces. An example is the Gay-Berne potential [24], which is a single-site potential with both attractive and repulsive anisotropic forces. This potential is found to give thermally driven phase behaviour and to result in smectic phases and columnar phases (for discs), as well as the nematic phase. Simulations of the nematic phase formed by the Gay-Berne mesogen show that the form of the singlet orientational distribution function is essentially identical to that predicted by the Maier-Saupe theory. It seems clear, therefore, that the Maier-Saupe theory, although originally derived assuming purely attractive anisotropic forces, also describes the liquid crystal behaviour for mesogens where both shape and attractive anisotropies are important.

## 1.10 Liquid Crystal Properties and Theoretical Modelling

In attempting to construct theories of liquid crystalline behaviour, it is clearly germane to give some attention to the properties we would like the theories to predict. That is, some properties are clearly better indicators than others of the liquid crystalline state of the system. Properties such as the heat capacity and the isothermal compressibility are not significantly different in the liquid crystal to the isotropic liquid and as such are relatively poor candidates for any serious attempts at modelling the distinctive features of, say, the nematic phase. On the other hand, there are readily measureable properties that are distinctive features of liquid crystalline phases. For instance, the defining feature of a liquid crystal is the non-zero values of the order parameters that characterise its order and distinguish it from less ordered phases. For example, for a nematic phase this could be taken to be the second rank orientational order parameter characterising its long range orientational order. The point at which the order parameter becomes non-zero then reflects the transition temperature on the phase diagram, and given that it also defines the difference between the ordered and disordered phases, most interest

attaches to this transitional region. A distinctive feature that would provide a fairly crude test of any theory would then be the nature of the second rank orientational order parameter profile around the transition. To begin with the theory should be correct in its qualitative predictions. That is, it should predict the  $N - I$  transition and its order. If the theory succeeds at this first hurdle, and the  $N - I$  transition is correctly predicted to be first order, the next test is to predict the  $N - I$  transitional value of the second rank orientational order parameter,  $\overline{P}_2$ .

Some theories clearly fare better than others in these matters. For instance the Onsager theory of nematics we have alluded to in section 1.9 predicts (correctly) that there should be a first order  $N - I$  transition, but the predicted transitional second rank orientational order parameter (0.8) is far in excess of that found experimentally (ca. 0.35). The transition is predicted to be very much stronger than is found in reality, to the extent that order parameters of this magnitude are not normally found in nematics—the system would have long since undergone transition to a smectic phase or simply crystallised. The Maier-Saupe theory, on the other hand, predicts a weak first order transition, with roughly the correct transitional orientational order parameter, although we note that the transitional entropy (the measure of the “strength” of the transition), albeit small, is still significantly too high.

Having said this, however, it is found, to a reasonable approximation that the order parameter is a universal function of the reduced temperature for a wide variety of mesogens. Thus, once a theory has passed the first distinctive test by predicting the approximate value of the orientational order parameter at the  $N - I$  transition, and by predicting universality in broadly correct terms, the orientational order parameter then becomes a somewhat blunter tool for probing the success of a theory, since in a sense there is nothing more to test. However, the temperature dependence of  $\overline{P}_2$  does differ between real mesogens, particularly in the neighbourhood of the  $N - I$  transition (eg, strong or weak) so it still could does provide a testing ground theories.

From the point of view of the theory, to predict strict universality there will necessarily

be just one parameter related to the structure. (This could be used to scale the temperature and would then cancel upon constructing a reduced temperature scale.) However, the behaviour of real mesogens is not absolutely universal, and so predicting the temperature variation would really be concerned with distinguishing between them on the basis of their structure. Indeed, no one-parameter theory could predict anything other than strict universality, so to go beyond this and distinguish between real mesogens would require further parameters relating to aspects of molecular structure. However, for such theories, there is then scope for testing their validity by comparison with the different ways in which the orientational order parameter varies with temperature for mesogens of different structure.

A much more severe test of the theory would be provided by other readily measurable properties that are related to the transition between the phases, and that are found, in practise, to be strongly related to the molecular structure. An good example would be the  $N-I$  transition temperature, which depends exquisitely on the molecular structure. However, the Maier-Saupe theory does not give the scaling parameter required to convert the scaled transition temperature to an absolute temperature. It is therefore the orientational order parameter (primarily  $\overline{P}_2$ ) and the  $N-I$  entropy change,  $\Delta S_{NI}/R$ , which do not depend on the scaling parameter which provide the best contact with experiment.

## 1.11 Summary of Contents

We begin, in the following chapter, by sketching the essential background in statistical mechanics for the theoretical treatments and applications that follow. We then apply this to the electric field polarisation of nematics, where, for the purposes of producing non-linear optical materials, there has been interest in the induced polarisation that can be attained with a given field strength. This is then followed by application of the Humphries-James-Luckhurst theory of binary nematic mixtures to probe order parameters beyond the limits of miscibility of the mesogen since the solutes in real systems do not form liquid crystals. This is to investigate the validity of the linear extrapolations commonly performed by experimentalists to the pure compound to produce comparative measures of their properties. Finally, we combine the Marcelja-Luckhurst theory with Monte Carlo simulation to provide a hybrid methodology for modelling nematics composed of molecules of arbitrary flexibility with continuous torsional potentials.

## Appendix 1A: Definition of the Euler angles

In defining the Euler angles we are in effect addressing the problem of how to relate the orientation of one cartesian axis system (say, a laboratory frame) to that of another (say, a molecular frame). In other words, we need to define the rotation that takes one frame of reference into coincidence with the other. The Euler angles,  $\alpha, \beta$  and  $\gamma$  are defined by performing the rotation of the cartesian frame of reference in three steps (ie, three successive rotations). Let  $XYZ$  denote the fixed laboratory frame and  $UVW$  the rotated (ie, molecular) frame. A positive rotation about an axis is taken to be one such that a right handed screw would advance in the positive direction of that axis. The three successive rotations are as follows (see figure 1A.1):

1. rotate positively by an angle  $\alpha$  ( $0 \leq \alpha \leq 2\pi$ ) about the  $Z$ -axis, thereby bringing  $XYZ$  into position  $X'Y'Z'$ ;
2. rotate by an angle  $\beta$  ( $0 \leq \beta \leq \pi$ ) about the new  $Y$  axis  $Y'$ , thereby bringing  $X'Y'Z'$  into position  $X''Y''Z''$ ;

[It can now be seen that these angles clearly correspond precisely to those similarly denoted in figures 1.5 and 1.6.]

3. rotate by an angle  $\gamma$  ( $0 \leq \gamma \leq 2\pi$ ) about the new  $Z$ -axis  $Z''$ , thereby bringing the  $X''Y''Z''$  system into the final position  $X'''Y'''Z''' \equiv UVW$ .

The polar coordinates of  $W$  (the molecular  $Z$ -axis) in the  $XYZ$  (laboratory) system are  $(\beta, \alpha)$  and the polar coordinates of  $Z$  (the laboratory  $Z$ -axis) in  $UVW$  (molecular) system are  $(\beta, \pi - \gamma)$ . We note that for the special case of a cylindrically symmetric molecule with the  $W$  axis along the line of molecular symmetry, only the two angles  $(\beta, \alpha)$  are necessary; in this case the third Euler angle  $\gamma$  is redundant and can be put equal to zero.

Figure 1A.1: The Euler angles  $\alpha, \beta, \gamma$  and the three Euler rotations that carry the initial  $x, y, z$  axis system into the final  $x''', y''', z'''$  system [35, 36].

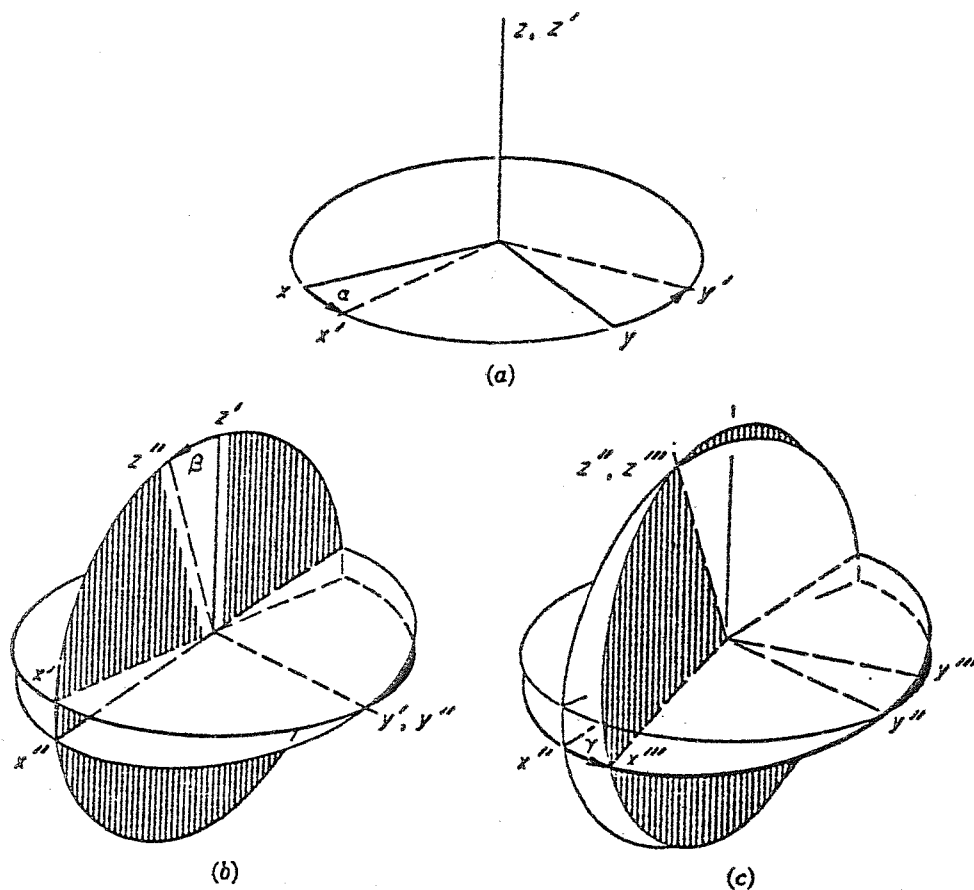
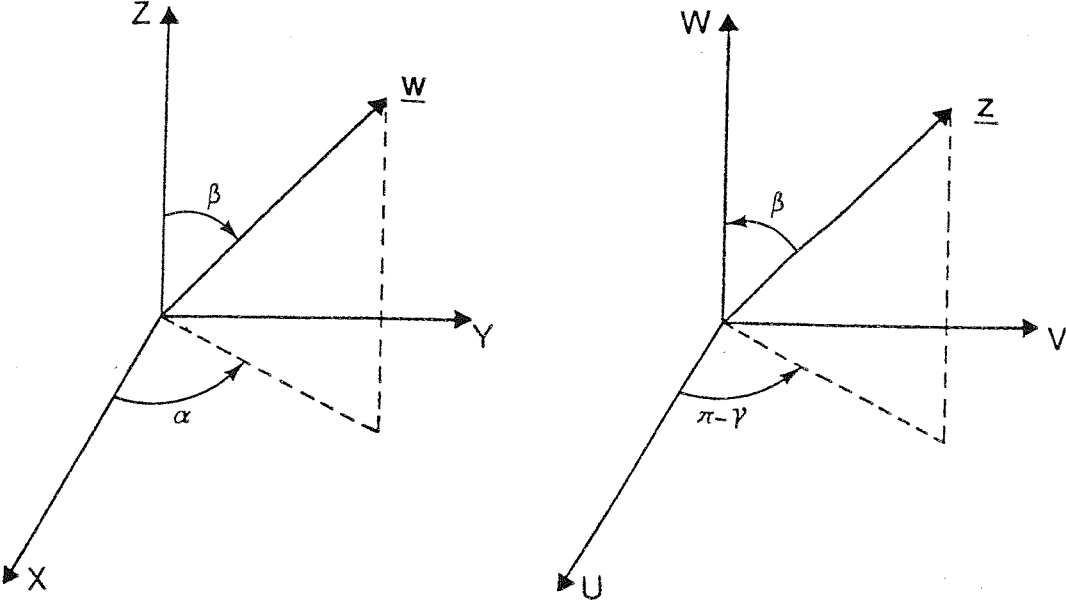


Figure 1A.2: The polar coordinates of  $W$  in the  $XYZ$  axis system and the polar coordinates of  $Z$  in the  $UVW$  system [36].



## Appendix 1B: Legendre polynomials and spherical harmonics

Here we give explicit expressions for the first six Legendre polynomials  $P_L(\cos \beta)$  and for the modified (Racah) spherical harmonics of second degree  $C_{2m}(\omega)$  where  $m = -2, -1, \dots, 2$ .

### 1. Legendre polynomials.

$$P_0(\cos \beta) = 1 \quad (1B.1)$$

$$P_1(\cos \beta) = \cos \beta \quad (1B.2)$$

$$P_2(\cos \beta) = \frac{1}{2}(3 \cos^2 \beta - 1) \quad (1B.3)$$

$$P_3(\cos \beta) = \frac{1}{2}(5 \cos^3 \beta - 3 \cos \beta) \quad (1B.4)$$

$$P_4(\cos \beta) = \frac{1}{8}(35 \cos^4 \beta - 30 \cos^2 \beta + 3) \quad (1B.5)$$

$$P_5(\cos \beta) = \frac{1}{8}(63 \cos^5 \beta - 70 \cos^3 \beta + 15 \cos \beta) \quad (1B.6)$$

$$P_6(\cos \beta) = \frac{1}{48}(693 \cos^6 \beta - 945 \cos^4 \beta + 315 \cos^2 \beta - 15). \quad (1B.7)$$

### 2. Modified spherical harmonics.

$$C_{2-2}(\beta, \gamma) = \sqrt{\frac{3}{8}} \sin^2 \beta e^{-2i\gamma} \quad (1B.8)$$

$$C_{2-1}(\beta, \gamma) = \sqrt{\frac{3}{2}} \sin \beta \cos \beta e^{-i\gamma} \quad (1B.9)$$

$$C_{20}(\beta, \gamma) = P_2(\cos \beta) \quad (1B.10)$$

$$C_{21}(\beta, \gamma) = -\sqrt{\frac{3}{2}} \sin \beta \cos \beta e^{i\gamma} \quad (1B.11)$$

$$C_{22}(\beta, \gamma) = \sqrt{\frac{3}{8}} \sin^2 \beta e^{2i\gamma}. \quad (1B.12)$$



## References

- [1] F. Reinitzer, *Mh. Chem.*, **9**, 421 (1888).
- [2] O. Z. Lehmann, *Phys. Chem.*, **4**, 462 (1889).
- [3] L. D. Landau and E. M. Lifshitz, *Statistical Physics*, Second Edition, Pergamon Press, London and Paris (1968).
- [4] L. D. Landau, *Collected Papers of L. D. Landau*, edited by D. ter Haar, Gordon and Breach, New York (1965).
- [5] S. Fraden, in *Observation, Prediction and Simulation of Phase Transitions in Complex Fluids*, edited by M. Baus, L. F. Rull and J.-P. Ryckaert, Kluwer Academic Publishers, Dordrecht (1995).
- [6] H. N. W. Lekkerkerker, P. Buining, J. Buitenhuis, G. J. Vroegea and A. Stroobants in *Observation, Prediction and Simulation of Phase Transitions in Complex Fluids*, edited by M. Baus, L. F. Rull and J.-P. Ryckaert, Kluwer Academic Publishers, Dordrecht (1995).
- [7] L. Onsager, *Ann. N. Y. Acad. Sci.*, **51**, 627 (1949).
- [8] D. Frenkel, H. N. W. Lekkerkerker and A. Stroobants, *Nature*, **332**, 822 (1988).
- [9] K. Herrman, *Z. Krist.*, **92**, 49 (1935).
- [10] N. Boccara, *Annals. Phys.*, **76**, 72 (1973).
- [11] G. Friedel, *Annals. Phys.*, **18**, 273 (1972).
- [12] S. J. Roskilly, PhD Thesis, University of Southampton (1994).
- [13] L. J. Yu and A. Saupe, *Phys. Rev. Lett.*, **45**, 1000 (1980).
- [14] S. Chandrasekhar, B. K. Sadashiva, S. Ramesha and B. S. Srikanta, *Pramana J. Phys.*, **27**, L713 (1986).

- [15] K. Praefcke, B. Kohne, D. Singer, D. Demus, G. Pelzl and S. Diele, *Liq. Cryst.* **7**, 589 (1990).
- [16] S. M. Fan, I. D. Fletcher, B. Gundogan, N. J. Heaton, G. Kothe, G. R. Luckhurst and K. Praefcke, *Chem. Phys. Lett.* **204**, 517 (1993).
- [17] J. R. Hughes, G. Kothe, G. R. Luckhurst, J. Malthete, M. E. Neubert, I. Shenouda, B. A. Timimi and M. Tittlebach, *J. Chem. Phys.* **107**, 9252 (1997).
- [18] G. W. Gray, *Molecular Structure and the Properties of Liquid Crystals*, Academic Press, London (1962).
- [19] G. W. Gray, in *The Molecular Physics of Liquid Crystals*, edited by G. R. Luckhurst and G. W. Gray, Chapter 1, Academic Press, London (1979).
- [20] S. Marcelja, *J. Chem. Phys.*, **60**, 3599 (1974).
- [21] G. R. Luckhurst *Mol. Phys.* **82**, 1063 (1994).
- [22] C. Zannoni, in *The Molecular Physics of Liquid Crystals*, edited by G. R. Luckhurst and G. W. Gray, Chapter 3, Academic Press, London (1979).
- [23] M. Boas, *Mathematical Methods in the Physical Sciences*, Wiley, New York (1983).
- [24] See, for example, M. A. Bates and G. R. Luckhurst, *Structure and Bonding*, **94**, 65 (1999).
- [25] E. T. Jaynes, *Phys. Rev.*, **106**, 620 (1957).
- [26] R. D. Levine and M. Tribus, *The Maximum Entropy Formalism*, M.I.T. Press, Cambridge, Massachusetts (1979).
- [27] D. I. Bower, *J. Polymer Sc.*, **19**, 93 (1981).
- [28] C. Zannoni, *J. Chem. Phys.*, **84**, 424 (1986).
- [29] W. Maier and A. Saupe, *Z. Naturforsch.*, **13a**, 564 (1958).

- [30] W. Maier and A. Saupe, *Z. Naturforsch.*, **14a**, 882 (1959).
- [31] W. Maier and A. Saupe, *Z. Naturforsch.*, **15a**, 287 (1960).
- [32] R. Alben, *Mol. Cryst. Liq. Cryst.*, **13**, 193 (1971).
- [33] D. Frenkel, *Mol. Phys.*, **60**, 1 (1987).
- [34] C. G. Gray and K. E. Gubbins, *Theory of Molecular Fluids Volume I: Fundamentals*, Clarendon Press, Oxford (1984).
- [35] M. E. Rose, *Elementary Theory of Angular Momentum*, Wiley, New York (1957).
- [36] H. B. Zewdie, PhD Thesis, University of Southampton (1986).

# Chapter 2: The Statistical Mechanics and Molecular Field Theory of Nematics Composed of Rigid Molecules

## 2.1 Introduction

In this chapter we lay the foundations of the necessary background in statistical mechanics from which to describe one of the most successful classes of molecular theories of liquid crystals, namely *molecular field theories*. These are the theories that we shall employ subsequently in later chapters. We then describe the molecular field approximation from which these theories arise and its relationship to the single particle distribution function and Helmholtz free energy. We then discuss the application of molecular field theory to uniaxial phases composed of uniaxial particles, including the seminal Maier-Saupe theory, its derivation, some necessary generalisations of it in preparation for later studies and its predictions. Finally, we turn our attention to uniaxial phases composed of biaxial particles, deriving the theory and discussing its implications.

## 2.2 Introduction to Statistical Mechanics

Within the framework of classical statistical mechanics it is possible, in principle, to describe a system completely at any given time by specifying the momenta and positional coordinates associated with each of its constituent molecules. Thus the state of a system of  $N$  particles is defined by specifying  $(\mathbf{p}_1, \mathbf{p}_2, \dots, \mathbf{p}_N) \equiv \mathbf{p}^{(N)}$  and  $(\mathbf{X}_1, \mathbf{X}_2, \dots, \mathbf{X}_N) \equiv \mathbf{X}^{(N)}$ , where  $\mathbf{p}_i$  is the momentum vector of particle  $i$ ,  $\mathbf{X}_i$  is

the set of positional coordinates associated with particle  $i$  and  $i = 1, 2, \dots, N$ . If the molecules concerned are considered to be rigid then we may write  $\mathbf{X}_i$  as  $\mathbf{X}_i(\mathbf{r}_i, \Omega)$  where  $\mathbf{r}_i$  is the position vector of some physically convenient point in the molecule (e.g. the centre of mass) and  $\Omega$  stands for the Euler angles  $(\alpha, \beta, \gamma)$  of a frame set in molecule  $i$  with respect to an external laboratory frame of reference.

The discipline of statistical mechanics makes the transition from an unwieldy number of microscopic variables ( $N$  may be of the order  $10^{23}$  for an experimental sample) to a small number of macroscopic properties, namely the bulk thermodynamic properties of the system. A straightforward approach to this discipline is to develop the concept of a many- dimensional phase space, each dimension representing the value of a component of the momentum, or centre of mass position, vector of a molecule or the value of one of its Euler angles. Thus for a system of  $N$  rigid molecules the phase space is  $9N$  dimensional and the entire system at any instant in time is represented by a single point in this space. Over time the system will trace out a trajectory in phase space and the value of any bulk thermodynamic property of the system will be the time average,  $\langle A \rangle_t$ , of its instantaneous value,  $A(t)$ . That is, the average over the phase space trajectory which may be written

$$A_{obs} = \langle A \rangle_t = \lim_{t \rightarrow \infty} \left( \frac{1}{t} \int_0^t A(\mathbf{p}^{(N)}, \mathbf{X}^{(N)}, s) ds \right), \quad (2.1)$$

where  $s$  is the particular instant in time in question in the range  $0-t$ . It was argued by the founders of statistical mechanics that the straightforward time averaging approach to the discipline would be utterly impossible. An alternative approach was, therefore, put forward by Gibbs: rather than average the properties of one system over time, we imagine that we have a huge number of replicas of the system, identical in their bulk properties; we then average the property of interest over the *ensemble* of replicas at *one instant* in time. This alternative gains us nothing unless we know the distribution of states (hence the instantaneous values of the property) in the ensemble. It is this at which Gibbs guessed and which forms the fundamental axiom of statistical mechanics—the so-called principle of equal a priori probabilities. It asserts that the probability of

occurrence of a given state of the system depends only on the energy of the state (ie, all states of the same energy are equally probable).

Using this principle we can define, for any given ensemble, a phase space density, which is in fact a probability density distribution function for possible states of the system in phase space. The normalisation factor that appears as the proportionality coefficient in the expression for this probability density is the *partition function* for that ensemble. This partition function is a multidimensional integral over all phase space of the expression to which the probability density (the distribution function) is proportional. Such a definition of the distribution function manifestly depends on the principle of equal a priori probabilities in terms of the proportionality and its normalisation. In this development of statistical mechanics it turns out that the partition function is a crucial quantity, the evaluation of which enables calculation of all the averages that determine the bulk thermodynamic properties of systems. A convenient and conventional ensemble in the statistical mechanics of the nematic phase is that under conditions of constant volume ( $V$ ), temperature ( $T$ ) and number of particles ( $N$ ), that is, the *canonical ensemble*. For a system of  $N$  indistinguishable particles the corresponding (ie, canonical) partition function is written as

$$Q_{NVT} = \frac{1}{h^{3N}N!} \int \exp(-E(\mathbf{p}^{(N)}, \mathbf{X}^{(N)})/k_B T) d\{\mathbf{p}^{(N)}\} d\{\mathbf{X}^{(N)}\}, \quad (2.2)$$

where  $E$  is the total internal energy,  $k_B$  is the Boltzmann constant and  $h$  is the Planck constant. This is the classical analogue of the sum over discrete states representation

$$Q_{NVT} = \sum_{\text{states}} \exp(-E(\mathbf{p}^{(N)}, \mathbf{X}^{(N)})/k_B T). \quad (2.3)$$

The factor of  $1/(h^{3N})$  in (2.2) preserves the fundamental quantum mechanical nature of the phase space seen in (2.3) and makes the partition function dimensionless so that a logarithm may be obtained. The factor of  $1/N!$  is a correction factor to take account of the overcounting of the potential energy in the integration over positional coordinates, and is a good approximation at all but very low temperatures. Within classical statistical mechanics the positions and momenta of the rigid molecules are

uncorrelated. The Hamiltonian for the system ( $E$ ) is then the sum of the kinetic and potential energies, the kinetic energy,  $K(\mathbf{p}^{(N)})$ , being a function of momenta only (both translational and orientational) and the potential energy,  $U(\mathbf{X}^{(N)})$ , being a function of positions only. Hence

$$Q_{NVT} = \frac{1}{h^{3N} N!} \int \exp(-(K(\mathbf{p}^{(N)}) + U(\mathbf{X}^{(N)}))/k_B T) d\{\mathbf{p}^{(N)}\} d\{\mathbf{X}^{(N)}\} \quad (2.4)$$

which after integration over the momenta gives

$$\begin{aligned} Q_{NVT} &= \Lambda_{\text{rot}} \frac{\Lambda^{-3N}}{N!} \int \exp(-U(\mathbf{X}^{(N)})/k_B T) d\mathbf{X}^{(N)} \\ &= \Lambda_{\text{rot}} \frac{\Lambda^{-3N}}{N!} Z_{NVT}, \end{aligned} \quad (2.5)$$

where  $\Lambda = (h^2/2\pi m k_B T)^{1/2}$  is the thermal de Broglie wavelength,  $m$  being the particle mass, and  $Z_{NVT}$  is known as the configurational partition function. (Note: some workers include the factor  $1/N!$  in the definition of  $Z_{NVT}$ .) The quantity  $\Lambda_{\text{rot}}$  is the kinetic rotational partition function resulting from integration over the angular momenta and is given by

$$\Lambda_{\text{rot}} = \frac{1}{\sigma} \left[ \frac{2I_a k_B T}{\hbar^2} \frac{2I_b k_B T}{\hbar^2} \frac{2I_c k_B T}{\hbar^2} \right]^{1/2}, \quad (2.6)$$

where  $\sigma$  is the symmetry number of the particle and  $I_a, I_b, I_c$  are the principal components of its inertial tensor. For a system of rigid particles equation (2.5) becomes

$$Q_{NVT} = \Lambda_{\text{rot}} \frac{\Lambda^{-3N}}{N!} \int \exp(-U(\mathbf{r}^{(N)}, \Omega^{(N)})/k_B T) d\mathbf{r}^{(N)} d\Omega^{(N)}, \quad (2.7)$$

where  $d\Omega^{(N)} \equiv d\Omega_1 d\Omega_2 \dots d\Omega_N$  and  $d\Omega_i \equiv \sin \beta_i d\beta_i d\alpha_i d\gamma_i$  [ $i = 1, 2, \dots, N$ ].

## 2.3 The Equilibrium Free Energy

An important quantity to be able to calculate is the free energy since it defines the position of equilibrium of the system at finite temperatures. For a generalised ensemble,

the thermodynamic driving force,  $D$ , to the equilibrium position is related to the relevant partition function via the relation

$$D = -k_B T \ln Q. \quad (2.8)$$

Thus we may obtain the equilibrium Helmholtz free energy from the canonical partition function as

$$A = -k_B T \ln Q_{NVT}. \quad (2.9)$$

$Q_{NVT}$  may be decomposed as in (2.5) so that

$$\begin{aligned} A &= -k_B T \{ \ln(\Lambda^{-3N}/N!) + \ln Z_{NVT} \} \\ &= (-k_B T \ln Q_K) + (-k_B T \ln Z_{NVT}). \end{aligned} \quad (2.10)$$

Thus the total free energy associated with the total Hamiltonian may be considered the sum of a part associated with the kinetic energy (momenta) and a part associated with the potential energy (configuration):

$$A = A_K + A_U. \quad (2.11)$$

We may then write the free energy associated with the thermodynamic potential energy as

$$A_U = -k_B T \ln Z_{NVT}. \quad (2.12)$$

## 2.4 The Molecular Field Approximation

It is not possible to evaluate the partition function (2.5) from which we obtain the thermodynamic properties exactly analytically, at least for any system of interest. Therefore we need some kind of approximation to render the integral  $Z_{NVT}$  more mathematically tractable (or something equivalent). Therefore we introduce an approximation,



known as the molecular field approximation, to enable the calculation of the thermodynamic properties. There are various ways of introducing this approximation [1]. One procedure involves the more or less intuitive averaging of the anisotropic pair potential over the coordinates of one particle [2] while a more rigorous approach starts with the partition function which is then factored into positional and orientational contributions [3, 4]. This latter approach is the one we shall take in this section. Later (section 2.8.3) we shall also give the variational derivation due to de Gennes [5] in which the many body distribution function is assumed to be factored into a product of single body distributions to give a generic single body distribution (as the geometric mean). This is then the foundation for constructing the entropy contribution to the free energy, the internal energy contribution being constructed from other single-body quantities, namely the order parameters. The free energy is then made stationary by application of the calculus of variations (see Appendix 2A) to obtain the singlet orientational distribution function and then the corresponding potential energy function, which is the central feature of theories based on the molecular field approximation. There are a couple of alternative derivations that are worth mentioning in passing. One is based on a solution of the Kirkwood integral equations for the spatial and orientational distribution functions [6]. Another approach, advocated by Woo and co-workers [7] develops the Bogoliubov-Born-Green-Kirkwood-Yvon hierarchy of equations for the distribution functions [8].

Here, however, as we have stated, we shall proceed to decompose the partition function. We suppose that the total potential energy may be approximately represented by a sum of effective single particle energies. That is, we invoke a rescaling of the single body potential energy contribution to the infinite series expansion for  $U(\mathbf{r}^{(N)}, \Omega^{(N)})$ ,

$$U(\mathbf{r}^{(N)}, \Omega^{(N)}) = U_1(\mathbf{r}^{(N)}, \Omega^{(N)}) + U_2(\mathbf{r}^{(N)}, \Omega^{(N)}) + U_3(\mathbf{r}^{(N)}, \Omega^{(N)}) + \dots, \quad (2.13)$$

to attempt to encapsulate the total potential energy  $U(\mathbf{r}^{(N)}, \Omega^{(N)})$ . Here,  $U_n(\mathbf{r}^{(N)}, \Omega^{(N)})$  is the total potential energy arising from  $n$ -body interactions and is a sum of  $n$ -body interaction terms. We note that the energy arising from two body (pair) interactions

is dominant, the three-body (triplet) energy is small (but not insignificant) and the single body energy in real systems normally vanishes. We write the single body term  $U_1(\mathbf{r}^{(N)}, \Omega^{(N)})$  as

$$U(\mathbf{r}^{(N)}, \Omega^{(N)}) = \sum_i U(\mathbf{r}_i, \Omega_i), \quad (2.14)$$

where from now on we suppress the subscript 1 for simplicity. The approximation we have made in effect envisages any single molecule interacting independently with the projected out positional coordinates of all the other molecules; the molecule thus experiences an overall *mean* or *molecular field* due to all the others. The approximation will be good only if the strength of the field experienced by any particular molecule is insensitive to the coordinates of every molecule except that being considered. Or strictly, if it is insensitive to the detailed structure as opposed to the global structure as represented by the director. It thus ignores all short range correlations since it assumes that the pair correlation can be written as the product of two single particle distributions. Given that the essential feature of nematics we are trying to describe is their long range orientational order, however, it is expected that the approach will nevertheless provide a reasonable description of the essential features of the nematic phase. The justification, however, is ultimately *a posteriori* by comparison with experiment or simulation. We may now write the configuration integral as

$$\begin{aligned} Z_{NVT} &= \int \exp\left(-\sum_i U_i(\mathbf{r}_i, \Omega_i)/k_B T\right) d\mathbf{r}^{(N)} d\Omega^{(N)} \\ &= \int \exp\left(-\sum_i U_i(\mathbf{r}_i, \Omega_i)/k_B T\right) d\mathbf{r}_1 d\mathbf{r}_2 \dots d\mathbf{r}_N d\Omega_1 d\Omega_2 \dots d\Omega_N. \end{aligned} \quad (2.15)$$

The integration over  $d\mathbf{r}_i d\Omega_i$  is now uniquely associated with particle  $i$  and its potential energy  $U_i$  (which is a function only of  $\mathbf{r}_i$  and  $\Omega_i$ ) and hence

$$Z_{NVT} = \prod_i^N \int \exp(-U_i(\mathbf{r}_i, \Omega_i)/k_B T) d\mathbf{r}_i d\Omega_i. \quad (2.16)$$

Within the foregoing approximation each integral of the product is identical and so the sum of  $N$  single particle energies may be written as  $N$  times one representative single

particle energy. We write

$$Z_{NVT} = \left\{ \int \exp(-U(\mathbf{r}, \Omega)/k_B T) d\mathbf{r} d\Omega \right\}^N = Z_{1VT}^N, \quad (2.17)$$

where  $Z_{1VT}$  is the single molecule partition function. The assumption that the total configurational energy may be approximated as a sum of single particle energies, thus allowing decomposition of the total partition function in (2.5) or (2.7) into the product of  $N$  single particle partition functions, is known within statistical mechanics generally as the *mean field approximation*. Within liquid crystal theory, however, we refer to it as the *molecular field approximation* to retain contact with the terminology of Maier-Saupe type theories which focus explicitly on the molecular interactions. The configurational partition function may be further decomposed by noting that the single molecule potential energy is composed of an isotropic and an anisotropic part:

$$U_{1VT} = U_{\text{iso}}(\mathbf{r}) + U_{\text{aniso}}(\mathbf{r}, \Omega). \quad (2.18)$$

$U_{\text{iso}}$  is a function only of the centre of mass position,  $\mathbf{r}$ , of the test molecule whereas  $U_{\text{aniso}}$  is a function of both the position and the Euler angles. Hence

$$Z_{1VT} = \int \exp(-U_{\text{iso}}(\mathbf{r})/k_B T) d\mathbf{r} \int \exp(-U_{\text{aniso}}(\mathbf{r}, \Omega)/k_B T) d\Omega = Z_{\text{iso}} Z_{\text{aniso}}. \quad (2.19)$$

$Z_{\text{aniso}}$ , usually denoted simply by  $Z$ , may be simplified in the case of nematic phases, since then the anisotropic part of the thermodynamic potential energy is no longer a function of  $\mathbf{r}$ . A further simplification arises in the case of uniaxial particles comprising a uniaxial phase. For uniaxial particles  $U_{\text{aniso}}$  can have no dependence on the angle of rotation about the molecular symmetry axis. Furthermore, if we define the  $z$  axis of the laboratory frame of reference as the nematic director then making the usual assumption that the phase has  $D_{\infty h}$  symmetry rules out any azimuthal angle ( $\alpha$ ) dependence. Thus

$$Z = \int_{\gamma=0}^{2\pi} \int_{\alpha=0}^{2\pi} \int_{\beta=0}^{\pi} \exp(-U_{\text{aniso}}(\alpha, \beta, \gamma)/k_B T) \sin \beta d\beta d\alpha d\gamma \quad (2.20)$$

becomes, upon performing the integration,

$$Z = 4\pi^2 \int_0^{\pi} \exp(-U_{\text{aniso}}(\beta)/k_B T) \sin \beta d\beta, \quad (2.21)$$

where  $U_{\text{aniso}}(\beta)$  is the anisotropic (orientational) part of the single molecule potential energy, the so-called potential of mean torque, and is usually denoted  $U(\beta)$ .

## 2.5 Distribution Functions and the Molecular Field Approximation

We can clearly invoke the molecular field approximation to decompose the total many particle distribution function

$$\rho(\mathbf{p}^{(N)}, \mathbf{X}^{(N)}) = \frac{\exp(-E(\mathbf{p}^{(N)}, \mathbf{X}^{(N)})/k_B T)}{Q_{NVT}} \quad (2.22)$$

in a manner analogous to that applied to the partition function itself. Within classical statistical mechanics the  $\mathbf{p}^{(N)}$  and the  $\mathbf{X}^{(N)}$  are decoupled and hence

$$\rho(\mathbf{p}^{(N)}, \mathbf{X}^{(N)}) = \frac{\exp(-(K + U)/k_B T)}{\frac{\Lambda^{-3N}}{N!} \int d\mathbf{p}^{(N)} \exp(-K/k_B T) \int d\mathbf{X}^{(N)} \exp(-U/k_B T)}$$

where  $Q_U = Z_{NVT}$ . Now

$$\exp\{-K/k_B T\}/Q_K = \rho(\mathbf{p}^{(N)}) \quad (2.23)$$

and

$$\exp\{-U/k_B T\}/Z_{NVT} = \rho(\mathbf{X}^{(N)}). \quad (2.24)$$

Hence

$$\rho(\mathbf{p}^{(N)}, \mathbf{X}^{(N)}) = \rho(\mathbf{p}^{(N)}) \rho(\mathbf{X}^{(N)}). \quad (2.25)$$

Within liquid crystal theory it is customary to denote  $\rho(\mathbf{X}^{(N)})$ , the many body configurational distribution function, as  $P(\mathbf{X}^{(N)})$ . Invoking the molecular field approximation we have

$$\begin{aligned} P(\mathbf{X}^{(N)}) &= \frac{\exp(-\sum_i U_i/k_B T)}{\int d\mathbf{X}^{(N)} \exp(-\sum_i U_i/k_B T)}, \\ &= \prod_i^N \frac{\exp(-U_i(\mathbf{X}_i)/k_B T)}{\int d\mathbf{X}^{(N)} \exp(-U_i(\mathbf{X}_i)/k_B T)}, \\ &= \prod_i^N f_i(\mathbf{X}_i), \end{aligned}$$

$$\begin{aligned}
&= \left( \frac{\exp(-U(\mathbf{X})/k_B T)}{\int d\mathbf{X} \exp(-U(\mathbf{X})/k_B T)} \right)^N, \\
&= \{f(\mathbf{X})\}^N,
\end{aligned} \tag{2.26}$$

where  $f(\mathbf{X})$  is the single particle (configurational) distribution function. Again, in an exactly analogous manner to the decomposition of  $Z_{1VT}$ , within the molecular field approximation, we may write the single molecule distribution function as

$$\begin{aligned}
f(\mathbf{X}) &= \frac{\exp(-(U_{\text{iso}}(\mathbf{r}) + U_{\text{aniso}}(\mathbf{r}, \Omega))/k_B T)}{\int \exp(-(U_{\text{iso}}(\mathbf{r}) + U_{\text{aniso}}(\mathbf{r}, \Omega))/k_B T) d\mathbf{r} d\Omega}, \\
&= \frac{\exp(-U_{\text{iso}}(\mathbf{r})/k_B T) \exp(-U_{\text{aniso}}(\mathbf{r}, \Omega)/k_B T)}{\int \exp(-U_{\text{iso}}(\mathbf{r})/k_B T) d\mathbf{r} \int \exp(U_{\text{aniso}}(\mathbf{r}, \Omega)/k_B T) d\mathbf{r} d\Omega}, \\
&= \frac{\exp(-U_{\text{iso}}(\mathbf{r})/k_B T) \exp(-U_{\text{aniso}}(\mathbf{r}, \Omega)/k_B T)}{Z_{\text{iso}} Z_{\text{aniso}}}, \\
&= f_{\text{iso}}(\mathbf{r}) f_{\text{aniso}}(\mathbf{r}, \Omega).
\end{aligned} \tag{2.27}$$

In the case of a nematic  $f_{\text{aniso}}(\mathbf{r}, \Omega)$  becomes  $f_{\text{aniso}}(\Omega)$ , which then defines a single molecule orientational distribution function  $f(\Omega)$ , more commonly known as a singlet orientational distribution function. For a uniaxial phase of uniaxial particles  $f(\Omega)$  is independent of  $\alpha$  and  $\gamma$  so that

$$f(\Omega) = \frac{\exp(-U(\alpha, \beta, \gamma)/k_B T)}{\int_{\gamma=0}^{2\pi} \int_{\alpha=0}^{2\pi} \int_{\beta=0}^{\pi} \exp(-U(\alpha, \beta, \gamma)/k_B T) \sin \beta d\beta d\alpha d\gamma} \tag{2.28}$$

becomes, on removal of the redundant variables,

$$f(\beta) = \frac{\exp(-U(\beta)/k_B T)}{\int_0^{\pi} \exp(-U(\beta)/k_B T) \sin \beta d\beta} = Z^{-1} \exp(-U(\beta)/k_B T). \tag{2.29}$$

The function  $f(\beta)$  is then the singlet orientational distribution function for the nematic. Equation (2.29) is strictly the defining equation for the potential of mean torque, at least in the sense that  $f(\beta)$  is in principle a measurable quantity or one that may be obtained from computer simulation.

## 2.6 Helmholtz Free Energy within the Molecular Field Approximation

From (2.12) it is tempting to write the molar free energy as

$$A = -k_B T \ln(Z_{1VT}^{N_A}) = -N_A k_B T \ln Z_{1VT}. \quad (2.30)$$

Equation (2.30) is incorrect within the molecular field approximation, however, since the potential energy,  $U$ , in  $A = U - TS$  is counted twice due to the fact that each molecule can be considered to be both experiencing and generating the molecular field (this is intuitive reasoning based upon the implicit assumption that the energy is a sum of effective pair energies). Note that we cannot simply introduce a factor of  $1/2$  into the exponent of (2.15), (2.16) and (2.17) giving  $Z_{NVT} = Z_{1VT}^{N/2} \Rightarrow A_U = -(N/2)k_B T \ln Z_{1VT}$ , since the entropy given by (2.30) is correct as it stands; such a manipulation would only contain half the entropy. Hence we retain (2.30) to yield the correct entropy and subtract from this expression the potential energy:

$$A_U = -N_A \bar{U} - N_A k_B T \ln Z_{1VT}, \quad (2.31)$$

where  $\bar{U}$  is the average potential energy per molecule (so that  $N_A \bar{U} = U$  is the molar thermodynamic potential energy). Using (2.18),(2.19) we obtain

$$\begin{aligned} A_U &= -N_A (\bar{U}_{\text{iso}} + \bar{U}_{\text{aniso}}) - N_A k_B T \ln(Z_{\text{iso}} Z_{\text{aniso}}) \\ &= (-N_A \bar{U}_{\text{iso}} - N_A k_B T \ln Z_{\text{iso}}) + (-N_A \bar{U}_{\text{aniso}} - N_A k_B T \ln Z_{\text{aniso}}), \\ A_U &= A_{U,\text{iso}} + A_{U,\text{aniso}}. \end{aligned} \quad (2.32)$$

The free energy associated with the anisotropic part of the thermodynamic potential energy is then written as

$$A = -N_A \bar{U} - N_A k_B T \ln Z, \quad (2.33)$$

where the subscripts  $U$  and  $\text{aniso}$  are now suppressed for simplicity. From here on then (with the exception of the next section) the notations used for the properties should be taken to have their normal meanings, except that we shall be implicitly referring to the orientational configurational analogues only.

## 2.7 An Alternative Development of the Helmholtz Free Energy

We may also develop the free energy within the molecular field approximation from the singlet orientational distribution function as follows. The Boltzmann definition of the entropy is

$$S = -k_B \int \rho(\mathbf{p}^{(N)}, \mathbf{X}^{(N)}) \ln \rho(\mathbf{p}^{(N)}, \mathbf{X}^{(N)}) d\mathbf{p}^{(N)} d\mathbf{X}^{(N)} \quad (2.34)$$

so that within classical statistical mechanics we may write

$$\begin{aligned} S_T &= -k_B \left( \int \rho(\mathbf{p}^{(N)}) \rho(\mathbf{X}^{(N)}) \ln(\rho(\mathbf{p}^{(N)}) \rho(\mathbf{X}^{(N)})) d\mathbf{p}^{(N)} d\mathbf{X}^{(N)} \right), \\ &= -k_B \left( \int \rho(\mathbf{p}^{(N)}) \rho(\mathbf{X}^{(N)}) \ln(\rho(\mathbf{p}^{(N)})) d\mathbf{p}^{(N)} d\mathbf{X}^{(N)} \right. \\ &\quad \left. + \int \rho(\mathbf{p}^{(N)}) \rho(\mathbf{X}^{(N)}) \ln(\rho(\mathbf{X}^{(N)})) d\mathbf{p}^{(N)} d\mathbf{X}^{(N)} \right), \\ &= -k_B \left( \int \rho(\mathbf{p}^{(N)}) \ln(\rho(\mathbf{p}^{(N)})) d\mathbf{p}^{(N)} \int \rho(\mathbf{X}^{(N)}) d\mathbf{X}^{(N)} \right. \\ &\quad \left. + \int \rho(\mathbf{X}^{(N)}) \ln(\rho(\mathbf{X}^{(N)})) d\mathbf{X}^{(N)} \int \rho(\mathbf{p}^{(N)}) d\mathbf{p}^{(N)} \right), \end{aligned} \quad (2.35)$$

where  $S_T$  is the total entropy. Now  $\rho(\mathbf{X}^{(N)})$  and  $\rho(\mathbf{p}^{(N)})$  are normalised probability density distribution functions and so

$$S_T = S(\mathbf{p}^{(N)}) + S(\mathbf{X}^{(N)}). \quad (2.36)$$

Hence the total entropy is separable into a sum of kinetic and configurational parts. The configurational entropy is then

$$S_{\text{conf}} = -k_B \int P(\mathbf{X}^{(N)}) \ln P(\mathbf{X}^{(N)}) d\mathbf{X}^{(N)}, \quad (2.37)$$

where  $\rho(\mathbf{X}^{(N)})$  is now denoted by  $P(\mathbf{X}^{(N)})$ . Within the molecular field approximation (2.37) becomes

$$S_{\text{conf}} = -k_B \left( \int \dots \int f_1 f_2 \dots f_N \ln(f_1 f_2 \dots f_N) d\mathbf{X}_1 d\mathbf{X}_2 \dots d\mathbf{X}_N \right),$$

$$\begin{aligned}
&= -k_B \left( \int f_1 f_2 \dots f_N \ln f_1 d\mathbf{X}_1 d\mathbf{X}_2 \dots d\mathbf{X}_N + \int f_1 f_2 \dots f_N \ln f_2 d\mathbf{X}_1 d\mathbf{X}_2 \dots d\mathbf{X}_N + \dots \right. \\
&\quad \left. + \int f_1 f_2 \dots f_N \ln f_N d\mathbf{X}_1 d\mathbf{X}_2 \dots d\mathbf{X}_N \right), \\
&= -k_B \left( \int f_1 \ln f_1 d\mathbf{X}_1 \int f_2 d\mathbf{X}_2 \dots \int f_N d\mathbf{X}_N + \int f_2 \ln f_2 d\mathbf{X}_2 \int f_3 d\mathbf{X}_3 \dots \int f_N d\mathbf{X}_N + \dots \right. \\
&\quad \left. + \int f_N \ln f_N d\mathbf{X}_N \int f_{N-1} d\mathbf{X}_{N-1} \right). \tag{2.38}
\end{aligned}$$

Each of these integrals is identical and so

$$S_{\text{conf}} = -N_A k_B \left( \int f(\mathbf{X}) \ln f(\mathbf{X}) d\mathbf{X} \right), \tag{2.39}$$

where

$$S = -k_B \int f(\mathbf{X}) \ln f(\mathbf{X}) d\mathbf{X} \tag{2.40}$$

is the configurational entropy per molecule. The configurational free energy is then written

$$\begin{aligned}
A_U &= N\bar{U} - TS_{\text{config}} \\
&= N\bar{U} + Nk_B T \int f(\mathbf{X}) \ln f(\mathbf{X}) d\mathbf{X} \tag{2.41}
\end{aligned}$$

and  $\bar{U}$  may now be defined as

$$\begin{aligned}
\bar{U} &= \frac{1}{2} \langle U(\mathbf{X}) \rangle_{f(\mathbf{X})} \\
&= \frac{1}{2} \int U(\mathbf{X}) f(\mathbf{X}) d\mathbf{X}, \tag{2.42}
\end{aligned}$$

where  $U(\mathbf{X}) \equiv U(\beta)$  and  $\langle \rangle_{f(\mathbf{X})}$  indicates averaging over the distribution function  $f(\mathbf{X})$ . The factor of 1/2 is included to take account of the double counting of the contributions to the potential energy due to the molecular field approximation. Hence

$$A_U = N\bar{U} + Nk_B T \int Z_{1VT}^{-1} \exp(U(\mathbf{X})/k_B T) \ln(Z_{1VT}^{-1} \exp(-U(\mathbf{X})/k_B T)) d\mathbf{X},$$



$$\begin{aligned}
&= N\bar{U} + Nk_B T \langle \ln(Z_{1VT}^{-1} \exp(-U(\mathbf{X})/k_B T)) \rangle_{f(\mathbf{X})}, \\
&= N\bar{U} + Nk_B T \langle \ln(Z_{1VT}^{-1} - U(\mathbf{X})/k_B T) \rangle_{f(\mathbf{X})}, \\
&= N\bar{U} + Nk_B T (\ln Z_{1VT}^{-1} - \langle U(\mathbf{X})/k_B T \rangle_{f(\mathbf{X})}). \tag{2.43}
\end{aligned}$$

But  $\langle U(\mathbf{X})/k_B T \rangle_{f(\mathbf{X})} = 2\bar{U}/k_B T$  and so

$$\begin{aligned}
A_U &= N\bar{U} + Nk_B T \ln(Z_{1VT}^{-1}) - 2N\bar{U}, \\
&= -N\bar{U} - Nk_B T \ln Z_{1VT}, \tag{2.44}
\end{aligned}$$

which is just (2.31) as we had derived previously. Now the general distribution function  $f(\mathbf{X}) = f(\mathbf{r}, \Omega)$  simplifies in the case of a nematic, since it is no longer a function of position but of orientation only, so  $f(\mathbf{X}) \propto f(\Omega)$ . That is,

$$f(\mathbf{X}) = cf(\Omega), \tag{2.45}$$

where  $c$  is a constant. The configurational entropy is then

$$\begin{aligned}
S_{\text{conf}} &= -Nk_B \int cf(\Omega) \ln(cf(\Omega)) d\mathbf{r} d\Omega, \\
&= -Nk_B \left( \int cf(\Omega) \ln c d\mathbf{r} d\Omega + \int cf(\Omega) \ln f(\Omega) d\mathbf{r} d\Omega \right), \\
&= -Nk_B \left( \int c \ln c d\mathbf{r} \int f(\Omega) d\Omega + \int f(\Omega) \ln f(\Omega) d\Omega \int c d\mathbf{r} \right), \\
&= \left( -Nk_B \int c \ln c d\mathbf{r} \right) + \left( -Nk_B \int f(\Omega) \ln f(\Omega) d\Omega \right). \tag{2.46}
\end{aligned}$$

Hence

$$S_{\text{conf}} = S'_{\text{trans}} + S'_{\text{orien}}, \tag{2.47}$$

where  $f(\Omega)$  is for a uniaxial phase of uniaxial particles  $f(\beta)$ . The configurational entropy per particle is then

$$S = S_{\text{conf}}/N = S_{\text{trans}} + S_{\text{orien}}, \quad (2.48)$$

where  $S_{\text{trans}}$  is the configurational translational entropy per particle and  $S_{\text{orien}}$  is the configurational orientational entropy per particle. The latter is of interest to us here and, written explicitly, is

$$S_{\text{orien}} = -k_B \int f(\beta) \ln f(\beta) \sin \beta d\beta. \quad (2.49)$$

$A_U$  is then

$$\begin{aligned} A_U &= N_A \bar{U} - TS_{\text{conf}}, \\ &= N_A \{ (\bar{U}_{\text{iso}} + \bar{U}_{\text{aniso}}) - T(S_{\text{trans}} + S_{\text{orien}}) \}, \end{aligned} \quad (2.50)$$

where

$$\begin{aligned} \bar{U}_{\text{aniso}} &= \frac{1}{2} \langle U(\beta) \rangle_{f(\beta)}, \\ &= \frac{1}{2} \int_0^\pi U(\beta) f(\beta) \sin \beta d\beta, \end{aligned} \quad (2.51)$$

the factor of 1/2 again taking account of the overcounting of the contributions to the energy. Therefore,

$$A_U = (N_A (\bar{U}_{\text{iso}} - TS_{\text{trans}})) + (N_A (\bar{U}_{\text{aniso}} - TS_{\text{orien}})), \quad (2.52)$$

and so

$$\begin{aligned} A_{U,\text{aniso}} &= N_A \bar{U}_{\text{aniso}} + N_A k_B T \int_0^\pi f(\beta) \ln f(\beta) \sin \beta d\beta, \\ &= N_A \bar{U}_{\text{aniso}} + N_A k_B T \int_0^\pi f(\beta) \ln (Z^{-1} \exp(-U(\beta)/k_B T)) \sin \beta d\beta, \\ &= N_A \bar{U}_{\text{aniso}} + N_A k_B T \langle \ln (Z^{-1} \exp(-U(\beta)/k_B T)) \rangle_{f(\beta)}, \\ &= N_A \bar{U}_{\text{aniso}} + N_A k_B T \ln Z - 2N_A \bar{U}_{\text{aniso}}, \\ &= -N_A \bar{U}_{\text{aniso}} - N_A k_B T \ln Z, \end{aligned} \quad (2.53)$$

which is just equation (2.33) that we developed intuitively from the partition function.

## 2.8 Molecular Field Theories—Uniaxial Phase Composed of Uniaxial Rigid Particles

### 2.8.1 Maier-Saupe Theory

The pioneering theory of Maier and Saupe for nematics [9, 10, 11] was originally derived by analogy with the mean field theory of ferro(/antiferro)magnetism [12, 13]. In a solid state system of magnetic spins an individual lattice spin site is treated as if acted upon by a mean magnetic field (“mean field”) resulting from all of the other spins. In an infinite system all sites are equivalent and so a mean field at a generalised spin site is obtained by evaluating the net magnetisation at a single central site in the limit of infinite extent. Similarly in a nematic we have a tightly coupled many body problem (due to the fact that the density is high—about that of a typical liquid) and rather than attempting to evaluate all the molecular interactions explicitly Maier and Saupe introduced the concept of a generalised representative molecule experiencing an analogous mean field. This mean field is now not the net combined effect of all the surrounding magnetic spins, but of the surrounding molecules. The mean field is no longer a magnetic field but a so-called molecular field. It turns out that we do not need to pursue too deeply the precise nature of this field; we need only the concept of the field. Using this concept then, Maier and Saupe were able to write down a generalised single particle orientational potential energy function,  $U(\beta)$ , which forms the basis of their theory. This  $U(\beta)$  is the potential of mean torque and is related to the singlet orientational distribution function encountered in the previous section by

$$f(\beta) = Z^{-1} \exp(-U(\beta)/k_B T). \quad (2.54)$$

Here we derive  $U(\beta)$  in an intuitive, semi-formal manner; it can also be derived in a more formal way via the variational analysis of de Gennes [5] (see also section 2.8.3).

From the symmetry of the phase and hence  $f(\beta)$  we require that  $U(\beta) = U(\pi - \beta)$  and that  $U(\beta)$  will be a minimum at  $\beta = 0, \pi$ , a maximum at  $\beta = \pi/2$  and periodic in  $\pi$ .

We require an angular dependence with such properties.

All of the even order polynomials have this property. Noting the similarity between the required properties of the angular dependence to those of  $f(\beta)$  it is clear that  $U(\beta)$  may be similarly expanded in a basis set of Legendre polynomials in  $\cos\beta$ . For a non-polar phase the summation must be restricted to even order polynomials due to the symmetry of the phase. A polar phase, however, will require terms which are both odd and even in rank and, in addition, if the phase is being polarised by an external field, terms relating to the direct effect of the field on the energy of the test molecule. Systems capable of forming polar phases and those polarised by electric fields are not part of the Maier-Saupe theory per se, however, and so we postpone full discussion of these sophistications until section 2.8.2 and Chapter 3.

Here, in the Maier-Saupe theory we consider just the first term of the expansion in even polynomials in a non-polar phase. Thus we can write

$$U(\beta) = -XP_2(\cos\beta), \quad (2.55)$$

where  $X$  is essentially just a proportionality coefficient, and is referred to as a strength parameter. The coefficient of  $P_2(\cos\beta)$  is expected to be overall negative so that the orientations  $\beta = 0, \pi$  are global minima; hence  $X$  is defined to be positive. In addition it is required that  $X$  vanish in the isotropic phase. It seems reasonable, then, that the strength of the molecular field should be related to the orientational ordering present in the system; we assume the simplest case  $X \propto \overline{P}_2$  (see 2.8.2 and 2.8.3 for further discussion). Then  $X = \epsilon\overline{P}_2$  where  $\epsilon$  is an intrinsic coefficient that is expected to vary between materials; it is a measure of the molecular anisotropy and has the dimensions of energy. The potential of mean torque is then

$$U(\beta) = -\epsilon\overline{P}_2P_2(\cos\beta), \quad (2.56)$$

which is the central feature of the Maier-Saupe theory of nematics.

## 2.8.2 Expansion of $U(\beta)$ in a basis set of Legendre polynomials

The anisotropic potential energy of a molecule in a liquid crystal may be represented as an infinite series expansion in some appropriate basis function. For reasons already explained in Chapter 1 in relation to expanding  $f(\beta)$ , the functions of choice are Legendre polynomials in the cosine of the polar angle. For a non-polar phase we write

$$U(\beta) = - \sum_{L(\text{even})} u'_L P_L(\cos \beta) \quad [L \neq 0] \quad (2.57)$$

where the restriction to  $L$  even is due to the plane of symmetry orthogonal to the director as already explained in relation to  $f(\beta)$  and the  $-$  sign appears so that the leading coefficient is positive. If we wish to develop a molecular field theory for systems capable of forming a polar phase (as we shall in Chapter 3 on the electric field polarisation of nematics), then we must include the odd rank (polar molecular field) terms so that (2.57) becomes, in the absence of external fields,

$$U(\beta) = - \sum_L u'_L P_L(\cos \beta) \quad [L \neq 0]. \quad (2.58)$$

Since a polar nematic has never been observed these terms are usually ignored in mean field theory of nematics in the absence of external electrical fields. We certainly cannot ignore the influence of polar molecular fields when an external polarising field is applied, however, as we shall require in Chapter 3. Indeed, the object of applying the field is to induce a high polar order, that is, non-zero values of the polar (odd rank) order parameters. For the case where an electric field is polarising a nematic, however, equation (2.58) is incomplete and requires further terms relating to the direct interaction between the electric field and the test molecule; we shall discuss this in Chapter 3. The expansion coefficients in (2.57) can be made more explicit by separating the non-angular functions in the terms (strength parameters) into the product of an order parameter and an intrinsic coefficient (the latter having dimensions of energy):

$$U(\beta) = - \sum_{L \text{ even}} u_L \bar{P}_L P_L(\cos \beta). \quad (2.59)$$

This may be understood intuitively in that one would expect the strength of the molecular field to be related to the degree of ordering already present in the system; a simple case scenario is a proportional relationship. That which is not so readily understood in this manner is the concept that the total coefficient of each term should contain the orientationally-averaged Legendre function of the same rank as the Legendre polynomial describing the angular dependence. The formal justification of equation (2.59) is either by the pair potential approach of the Humphries-James-Luckhurst theory [2] or by the variational analysis of de Gennes [5] extended to higher rank order parameters (see 2.8.3). In an exactly analogous manner we can re-express (2.58) as

$$U(\beta) = - \sum_{L \text{ even}} u_L \bar{P}_L P_L(\cos \beta) - \sum_{L \text{ odd}} u_L \bar{P}_L P_L(\cos \beta). \quad (2.60)$$

It should be noted at this point, however, that in the pair potential approach, the averaging over the intermolecular vector orientation dependence of the potential would imply that all permanent electrostatic terms should vanish identically. Thus, strictly, if we were to use a pair potential derivation of molecular field theory, any term in the potential of mean torque which is representing a permanent electrostatic interaction should vanish, that is, its coefficient should be zero. Given that these terms are in general non-zero we are forced to conclude that there is a problem with this averaging. This is related to the assumed spherical distribution of the intermolecular vector, whereas for uniaxial particles it is in reality highly anisotropic, at least for neighbouring molecules. Strictly, then, we ought to use a variational derivation which includes polar order parameters.

Inclusion of *polar* molecular fields in practice means that their coefficients must be sufficiently small as to only give rise to “virtual” polar phases, that is, polar phases at temperatures below which a real nematogen would certainly have crystallised. Thus the non- existence of an observed polar nematic–non-polar nematic transition, at least to date, means that we cannot obtain the specific values of the odd rank coefficients but are able only to place upper values on them. This is an important point which we take up further in Chapter 3.

The expansion (2.57) is generally believed to be quite rapidly convergent since, except in the high order limit,  $\bar{P}_2 \gg \bar{P}_4 \gg \bar{P}_6 \dots$  and hence may be truncated at the second or fourth rank term to a good approximation. It is thus seen that  $U(\beta)$  in the Maier-Saupe theory is simply the first term in this expansion; taking it to the fourth rank term gives some improvement in the quantitative results predicted by the theory as compared with experiment but it may be that the extra term is compensating for errors introduced by the molecular field approximation [16]. There is little improvement beyond the second term in (2.57).

### 2.8.3 Variational Derivation of the Maier-Saupe Theory

We now proceed to give the formal, variational derivation of the Maier-Saupe theory of nematic liquid crystals [5]. This derivation involves, as one component, the calculus of variations and the concept of functional differentiation. An explanation of these concepts and their relationship to molecular field theories is given in Appendix 2A.

First, we identify the dominant order parameter of the system, which here we take as  $\bar{P}_2$  in accord with the experimental values for the order parameters near the nematic-isotropic transition. We then construct the anisotropic internal potential energy per molecule from the order parameter. We assume that the internal energy is quadratic in the order parameter since, strictly, liquid crystal order parameters are second rank tensors and the energy is a scalar. That is, the internal energy can only contain scalar invariants of the tensor order parameter, which must be formed from it by using, rather than negating, its tensorial nature. The lowest order scalar invariant that can be formed from a second rank tensor is the quadratic. In addition the internal energy is predominated by pair energies, and since the order parameter is a single molecule property, this suggests that the energy should be quadratic in the order parameter. Hence we write

$$\bar{U} \propto \bar{P}_2^2.$$

Inserting an arbitrary coefficient,  $\epsilon$ , we have

$$\bar{U} = -\frac{1}{2} \epsilon \bar{P}_2^2, \quad (2.61)$$

where  $\epsilon$  is defined to be positive so that  $\bar{U}$  is overall negative and the factor of 1/2 is included to preserve the connection with the Maier-Saupe theory. The orientational entropy per molecule is, within the molecular field approximation

$$S = -k_B \int f(\beta) \ln f(\beta) \sin \beta d\beta. \quad (2.62)$$

The orientational Helmholtz free energy per molecule is then

$$\begin{aligned} A &= \bar{U} - TS, \\ &= -\frac{\epsilon \bar{P}_2^2}{2} + k_B T \int f(\beta) \ln f(\beta) \sin \beta d\beta. \end{aligned} \quad (2.63)$$

We now minimise the free energy with respect to fluctuations  $\delta f(\beta)$  in  $f(\beta)$  (see Appendix 2A on the calculus of variations) to obtain the equilibrium distribution:

$$\begin{aligned} \delta A &= \frac{-\epsilon \delta(\bar{P}_2^2)}{2} + k_B T \int \delta [f(\beta) \ln f(\beta)] \sin \beta d\beta = 0, \\ &= -\epsilon \bar{P}_2 \delta \bar{P}_2 + k_B T \int [\delta f(\beta) \ln f(\beta) + \delta f(\beta)] \sin \beta d\beta, \\ &= -\epsilon \bar{P}_2 \delta \bar{P}_2 + k_B T \int \delta f(\beta) [\ln f(\beta) + 1] \sin \beta d\beta. \end{aligned} \quad (2.64)$$

We must take into account the constraint that prevents us from taking any arbitrary distribution function, namely

$$\int f(\beta) \sin \beta d\beta = 1, \quad (2.65)$$

and in terms of the fluctuations

$$\int \delta f(\beta) \sin \beta d\beta = 0. \quad (2.66)$$



The constraint equation (2.66) is now added to the main variation equation, having first been multiplied by a Lagrange undetermined multiplier, to obtain

$$-\epsilon\bar{P}_2\delta\bar{P}_2 + k_B T \int \delta f(\beta) [\ln f(\beta) + 1] \sin \beta d\beta + \lambda \int \delta f(\beta) \sin \beta d\beta = 0. \quad (2.67)$$

Now

$$\delta\bar{P}_2 = \int P_2(\cos \beta) \delta f(\beta) \sin \beta d\beta. \quad (2.68)$$

Hence, combining the integrals and factoring out  $\delta f(\beta)$ ,

$$\int \delta f(\beta) \left( -\epsilon\bar{P}_2 P_2(\cos \beta) + k_B T [\ln f(\beta) + 1] + \lambda \right) \sin \beta d\beta = 0. \quad (2.69)$$

Now (2.69) must hold for any arbitrary fluctuation  $\delta f(\beta)$ . To see what this means we consider the generalised integral

$$I = \int_{x_1}^{x_2} f(x)g(x) dx = 0, \quad (2.70)$$

where  $g(x)$  is a given unknown function and  $f(x)$  is completely arbitrary. For (2.70) to hold for *any*  $f(x)$ ,  $g(x)$  *must* vanish. Otherwise we could pick  $f(x)$  to be positive where  $g(x)$  is positive and negative where  $g(x)$  is negative giving  $I \neq 0$ ; thus we have proof by contradiction. Hence from (2.69)

$$-\epsilon\bar{P}_2 P_2(\cos \beta) + k_B T [\ln f(\beta) + 1] + \lambda = 0, \quad (2.71)$$

from which we obtain

$$\ln f(\beta) = (1/k_B T)(\epsilon\bar{P}_2 P_2(\cos \beta) - \lambda) - 1,$$

$$f(\beta) = \exp(\epsilon\bar{P}_2 P_2(\cos \beta)/k_B T - \lambda/k_B T - 1),$$

$$f(\beta) = \exp(\epsilon\bar{P}_2 P_2(\cos \beta)/k_B T) \exp(-\lambda/k_B T - 1). \quad (2.72)$$

We know from the Boltzmann distribution and its normalisation that the distribution is proportional to the Boltzmann factor  $\exp(-U(\beta)/k_B T)$  in the energy, with the

coefficient of proportionality being the inverse partition function (see equation (2.29)). So then, from

$$f(\beta) \propto \exp(-U(\beta)/k_B T) \quad (2.73)$$

we may write the singlet orientational distribution as

$$f(\beta) = Z^{-1} \exp(\epsilon \bar{P}_2 P_2(\cos \beta)/k_B T) \quad (2.74)$$

if we identify the inverse partition function as

$$Z^{-1} = \exp(-\lambda/k_B T - 1) \quad (2.75)$$

and the angular dependent exponent in (2.72) as the angular dependent exponent  $-U(\beta)/k_B T$  in (2.73) and (2.29). By inspection then,

$$U(\beta) = -\epsilon \bar{P}_2 P_2(\cos \beta), \quad (2.76)$$

which is just the standard Maier-Saupe result. The factor  $\exp(-1 - \lambda/k_B T)$  is therefore identified as  $Z^{-1}$ ; we do not then need to find  $\lambda$  since  $Z$  is defined via the normalisation condition. If we identify all the order parameters  $\bar{P}_L$  as important (noting the restriction on  $L$  to be even in some cases, as already discussed in (2.8.2)) then we obtain

$$U(\beta) = - \sum_L \epsilon_L \bar{P}_L P_L(\cos \beta). \quad (2.77)$$

#### 2.8.4 Predictions of the Maier-Saupe Theory

The order parameter  $\bar{P}_2$  appearing in the potential of mean torque is defined as an average over the singlet orientational distribution function

$$\bar{P}_2 = \int P_2(\cos \beta) f(\beta) \sin \beta d\beta. \quad (2.78)$$

The distribution function is obtained from the variational analysis in terms of the order parameter itself

$$f(\beta) = Z^{-1} \exp(\epsilon \bar{P}_2 P_2(\cos \beta)/k_B T),$$

$$Z = \int \exp(\epsilon \bar{P}_2 P_2(\cos \beta) / k_B T) \sin \beta d\beta. \quad (2.79)$$

It is clear that substitution of the singlet distribution (2.79) into the expression for the order parameter (2.78) results in an expression in which the order parameter occurs self-consistently on the left and right of the equation. Thus, in the case of the Maier-Saupe theory, we have a single self-consistency equation. We can solve this numerically fairly simply by defining a quantity which we shall refer to as the scaled strength parameter

$$X^* = \frac{\epsilon \bar{P}_2}{k_B T}, \quad (2.80)$$

which upon substitution into the self-consistency equation gives

$$\bar{P}_2 = Z^{-1} \int P_2(\cos \beta) \exp(X^* P_2(\cos \beta)) \sin \beta d\beta. \quad (2.81)$$

We note that this relationship strictly results from minimising the free energy with respect to the order parameter, so that it is guaranteed to be an equilibrium expression. We can then calculate the order parameter, using numerical integration, for a range of scaled strength parameters  $X^*$  corresponding to non-trivial solutions (ie,  $X^* \neq 0$ ). The ratio of each value of the order parameter calculated to the corresponding scaled strength parameter then gives a corresponding scaled temperature  $T^* = k_B T / \epsilon$ , since by rearranging equation (2.80) for  $X^*$  we obtain

$$\frac{k_B T}{\epsilon} = \frac{\bar{P}_2}{X^*}. \quad (2.82)$$

The nematic-isotropic phase transition occurs where the free energy difference between isotropic and nematic phases is zero. That is, the vanishing of  $\Delta A$  yields a value for  $X_{NI}^*$  from which  $\bar{P}_2^{NI}$  and hence  $T_{NI}^*$  can be determined. The molar Helmholtz free energy is given by

$$A = \frac{N_A \epsilon \bar{P}_2^2}{2} - N_A k_B T \ln Z. \quad (2.83)$$

In the isotropic phase  $\bar{P}_2$  is zero so the first term vanishes and the second term becomes  $-N_A k_B T \ln 2$ . The difference in free energy between the nematic and isotropic phases is then given by

$$\Delta A_{IN} = \frac{N_A \epsilon \bar{P}_2^2}{2} - N_A k_B T \ln \frac{Z_N}{2}, \quad (2.84)$$

where  $Z_N$  is the rotational partition function in the nematic phase and  $Z_I = 2$  is that in the isotropic phase. It is not necessary to specify the order parameter dependence of the scaled strength parameter (as given in equation (2.80)) to determine the transitional values of the properties, since (2.84) can be written in terms of  $X^*$  as

$$\frac{\Delta A_{IN}}{N_A k_B T} = \frac{X^* \bar{P}_2}{2} - \ln \frac{Z_N}{2}. \quad (2.85)$$

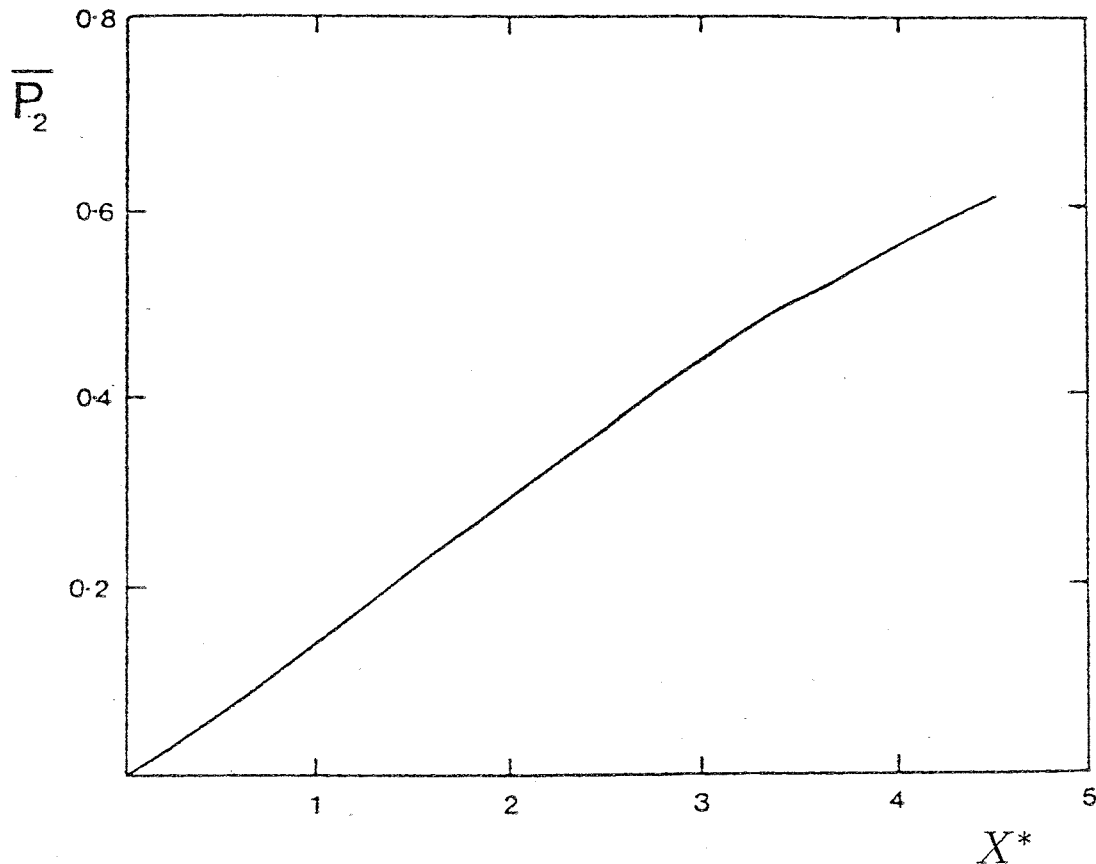
This must vanish at the  $N - I$  transition and so the transitional values of  $X^*$  and  $\bar{P}_2$  can be obtained from a plot of  $\Delta A_{IN}/N_A k_B T$  against  $X^*$  where the graph cuts the line  $\Delta A_{IN}/N_A k_B T = 0$ . The entropy change,  $\Delta S_{NI} = S_N - S_I$ , can be found from the value of  $X_{NI}^*$  and the corresponding value of  $\bar{P}_2^{NI}$  since

$$\begin{aligned} \frac{\Delta S_{NI}}{k_B} &= \frac{\Delta U_{NI}}{k_B T} \\ &= X_{NI}^* \bar{P}_2^{NI} / 2. \end{aligned} \quad (2.86)$$

We now give the results of the Maier-Saupe theory calculations. Figures 2.1 and 2.2 show the order parameter and the scaled  $I - N$  free energy difference  $\Delta A_{IN}/N_A k_B T$  respectively as a function of  $X^*$ . The graph of  $\bar{P}_2(X^*)$  is a sigmoidal curve starting at the origin, taking a limiting value of unity. We note that  $\bar{P}_2$  is defined for all values of  $X^*$ , whether or not these values for the order parameter represent thermodynamically stable states (see below). The graph of  $\Delta A_{IN}(X^*)/N_A k_B T$  begins at the origin, increases with increase in  $X^*$ , passes through a maximum, decreases and then passes through zero to become negative. The point where  $\Delta A_{IN}$  is zero defines the transitional value of the scaled strength parameter,  $X_{NI}^*$ , from which other transitional properties may be found. At lower values of  $X^*$  the isotropic phase is more stable and  $\Delta A_{IN}$  is positive whereas at higher values  $\Delta A_{IN}$  is negative and the nematic phase is more stable.

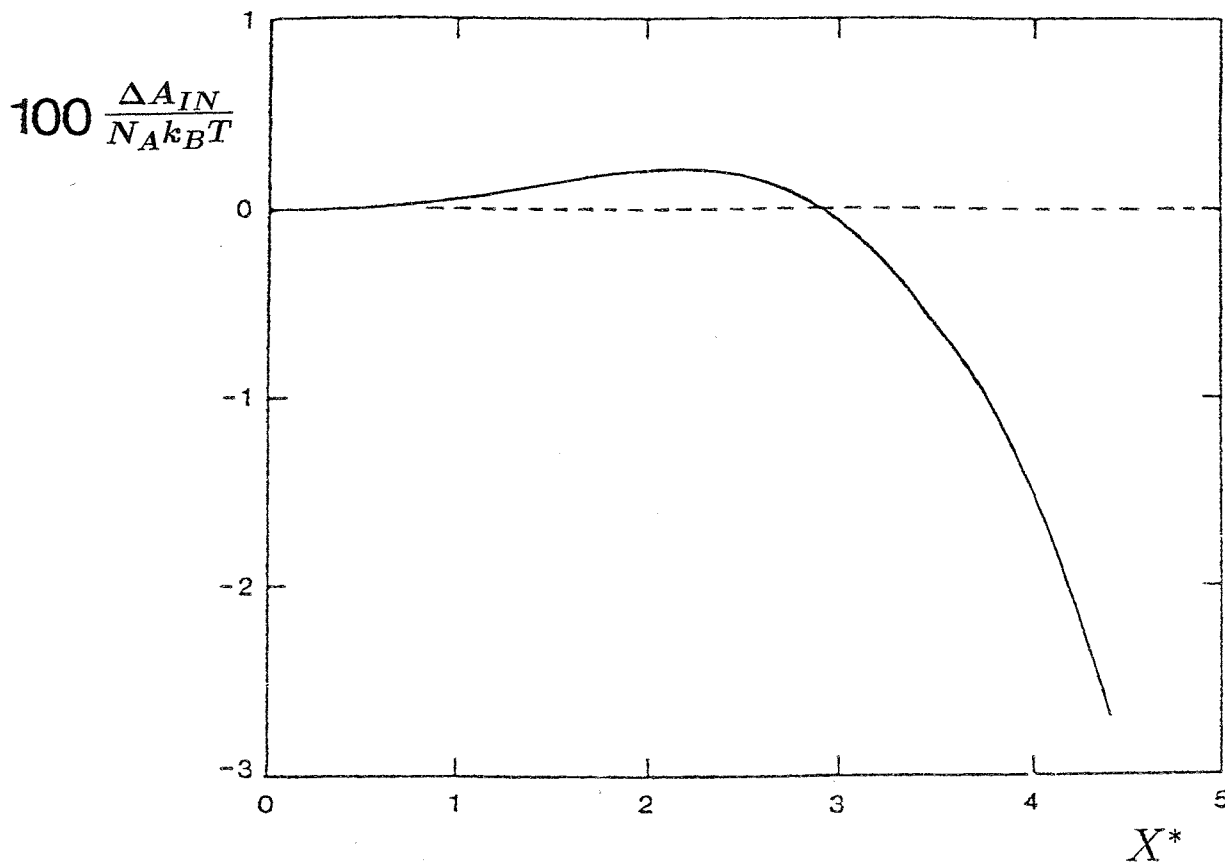
In figures 2.3a and 2.3b we show the order parameter  $\bar{P}_2$  and the scaled free energy difference  $\Delta A_{IN}/N_A k_B T$  respectively as a function of scaled temperature  $k_B T/\epsilon$ . The  $N - I$  transition is found to occur a scaled temperature of 0.22029 (providing the volume is constant) with corresponding values of  $\bar{P}_2 = 0.429$ ,  $\bar{P}_4 = 0.120$  and  $\Delta S_{NI}/R = 0.418$ .

Figure 2.1: The second rank orientational order parameter,  $\overline{P}_2$ , as a function of the scaled strength parameter,  $X^*$ , in the Maier-Saupe theory [4].



We note that there are three branches of the temperature profile of the order parameter. First of all, there are the *trivial* solutions, that is,  $\overline{P}_2 = 0$  is a solution of the self-consistency equations at all values of scaled temperature and corresponds to the isotropic phase. This will only be the thermodynamically stable phase provided its free energy is less than that of the nematic at the same temperature, that is, when  $\Delta A_{IN} > 0$ . Thus there is a stable nematic phase where  $\Delta A_{IN} < 0$  upto the transition at  $k_B T / \epsilon = 0.22029$ . At scaled temperatures in excess of this, the isotropic solution becomes thermodynamically stable. In addition to these two branches there is a third one

Figure 2.2: The molar orientational free energy as a function of the scaled strength parameter in the Maier-Saupe theory [4].



(dotted). Upon increasing the temperature above the transition the nematic ( $\overline{P}_2 \neq 0$ ) branch continues as a set of metastable solutions. The curve bends back on itself so that there is a maximum temperature on this curve beyond which the nematic phase is absolutely unstable; this is referred to as the limit of metastability. In this case it corresponds to the superheating limit.

On cooling from the isotropic phase to below the transition, the metastable regime of the isotropic solution can be realised. This terminates at the limit of supercooling metastability at a scaled temperature of 0.2. Below this, the isotropic solutions are

unstable solutions (ie, they correspond to maxima in the free energy). At the supercooling limit a second order nematic-isotropic transition would occur, if there were no first order transition. This can be shown by performing a perturbation-bifurcation analysis to locate the point at which the nematic solution branches away from the isotropic solution continuously. That is, the exponentials in the expression for the order parameter are expanded in the low order limit and truncated after the second (ie, first order) term. Using the orthogonality properties of the Legendre polynomials to simplify the expression thus obtained yields

$$\bar{P}_2 = \frac{\int (1 + (\epsilon \bar{P}_2 / k_B T) P_2(\cos \beta)) P_2(\cos \beta) \sin \beta d\beta}{\int (1 + (\epsilon \bar{P}_2 / k_B T) P_2(\cos \beta)) \sin \beta d\beta} = \frac{\epsilon \bar{P}_2}{5 k_B T}. \quad (2.87)$$

Thus,

$$\bar{P}_2 - \frac{\epsilon \bar{P}_2}{5 k_B T} = 0,$$

$$\bar{P}_2 \left( 1 - \frac{\epsilon}{5 k_B T} \right) = 0. \quad (2.88)$$

This implies two possibilities, one of them clearly being  $\bar{P}_2 = 0$ . The other possibility implies that  $\bar{P}_2$  is allowed to become non-zero in the vanishingly small order parameter limit when

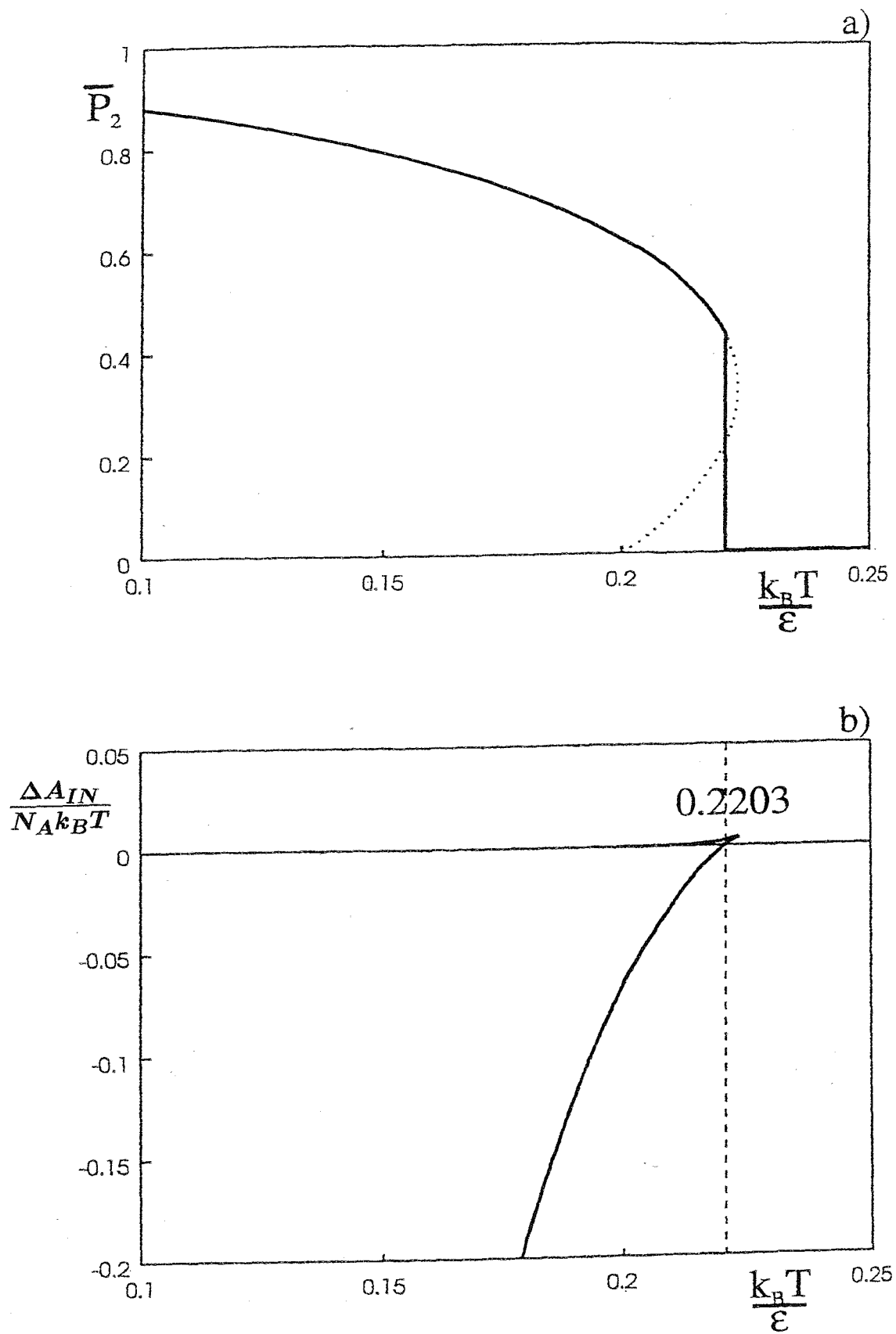
$$1 - \frac{\epsilon}{5 k_B T} = 0. \quad (2.89)$$

This implies that

$$\frac{k_B T}{\epsilon} = 1/5, \quad (2.90)$$

which represents the bifurcation point on the abscissa,  $k_B T^* / \epsilon = 0.2$ , where  $T^*$  is known as the divergence temperature.

Figure 2.3: The temperature dependence of a) the second rank orientational order parameter and b) the difference in free energy between the isotropic and nematic phase (Maier-Saupe) [14].



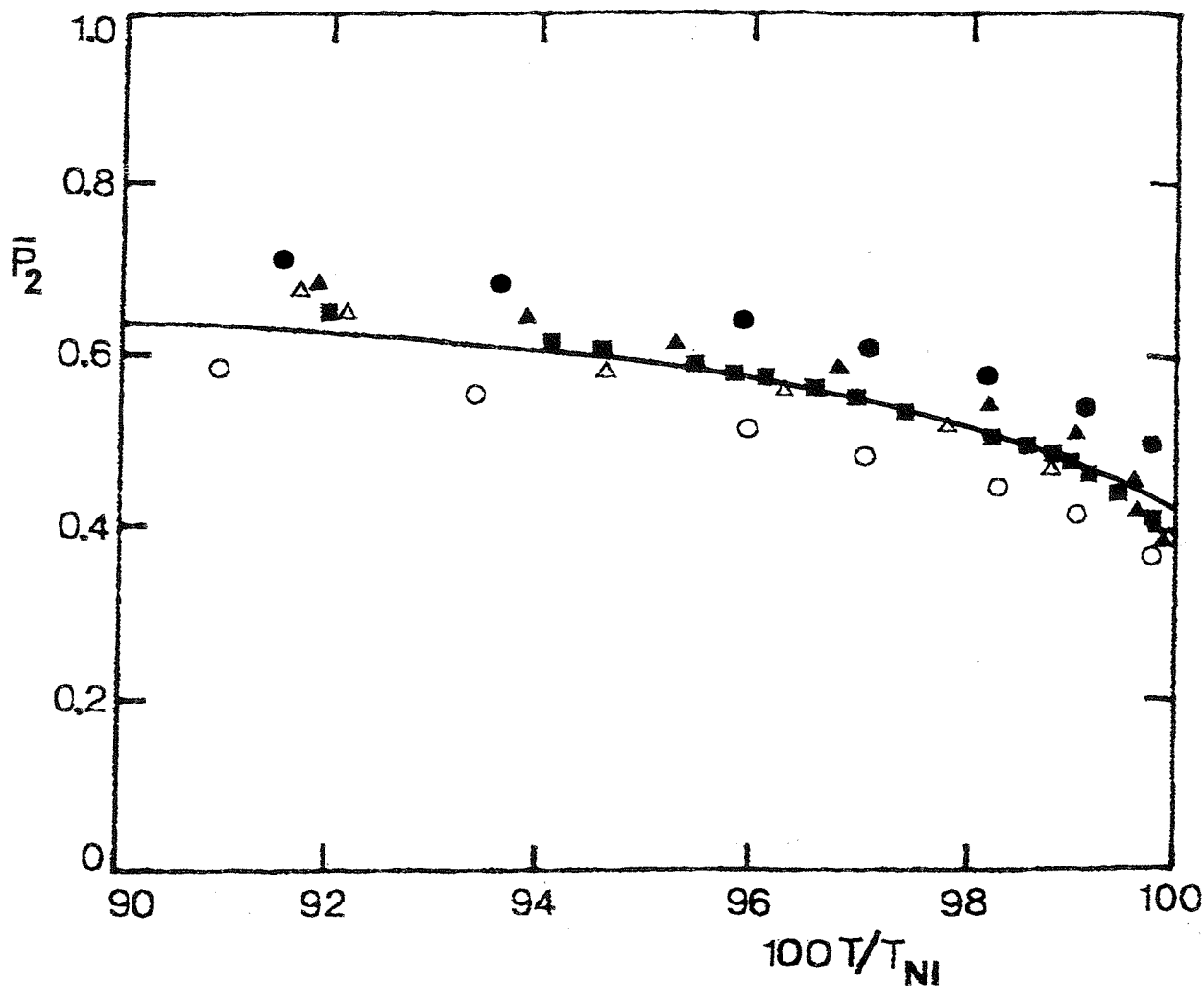


We note that the set of thermodynamic solutions over the entire temperature range is a unique curve with a unique scaled transition temperature. We have, however, scaled the temperature with the unknown intrinsic coefficient, which is taken to vary from material to material. To remove this dependence and make contact with experiment, we invoke the concept of reduced temperature,  $(k_B T / \epsilon) / (k_B T_{NI} / \epsilon) = T / T_{NI}$  and so the phase transition of any substance occurs at the same point on the abscissa. Clearly, then if the order parameter is plotted as a function of reduced temperature, we can see that the Maier-Saupe theory predicts that the order parameter of a nematic is a universal function of reduced temperature. Experimental investigations find that for a wide variety of materials, the results do indeed scatter about a common curve close to that predicted by the Maier-Saupe theory (see figure 2.4).

Another major feature of the theory is that the entropy change at the transition is independent of the form assumed for the dependence of the strength parameter on the order parameter. This is to be contrasted with the latent heat at constant volume which clearly does require specification of this relationship. The entropy change is also predicted to be independent of the molecular structure; this is in broad general agreement with experiment.

The question does arise, however, as to the source of any disagreements between the properties of real nematogens and the predictions of the Maier-Saupe theory. There are two major elements to the Maier-Saupe theory. The first is the molecular field approximation and the second is the form of the potential energy within that approximation. Any disagreements could arise from either of these assumptions. This is where the utility of computer simulations makes itself felt, for one key feature of computer simulations is that they can provide essentially exact results for a given model (ie, pair potential). Thus we are able to set up a model that conforms to that of Maier-Saupe theory, and compare the results to those of the theory. Any discrepancies between the simulation results and the predictions of the theory are then due to the molecular field approximation itself.

Figure 2.4: The temperature dependence of  $\overline{P}_2$ , at constant pressure, for a variety of mesogenic compounds. The curve is predicted by the Maier-Saupe theory. [1]



If these are significant, it means that the severity of the molecular field approximation renders theory based upon it quantitatively inadequate. Thus Lebwohl and Lasher [15] proposed a computer model with which to test the Maier-Saupe theory. In their model, cylindrically symmetric molecules are placed on the sites of a simple cubic lattice. These molecules then interact with nearest neighbours through a pair potential of the same form as that from which the Maier-Saupe theory can be considered to be derived (ie, in the pair potential approach, using the spherical harmonic addition theorem [2]).

	$k_B T_{NI}/\epsilon$	$\Delta S_{NI}/R$	$\overline{P}_2^{NI}$
Maier-Saupe	0.22	0.42	0.43
Monte Carlo	0.19	0.05	0.27

Table 2.1: A comparison of the predictions of the Maier-Saupe theory with Monte Carlo simulation results for the Lebwohl-Lasher model [15].

Table 2.1 shows a comparison of the results of the Monte Carlo simulation of Lebwohl and Lasher with the predictions of the Maier-Saupe theory.

The transition temperature is overestimated by Maier-Saupe theory by about 20% and the value of the order parameter is overestimated by about 25%. More serious is the discrepancy in the entropy of transition which is grossly overestimated, that is by a factor of about eight. It is to be concluded, therefore, that the errors are caused by the molecular field approximation itself rather than the model. Consequently any theory which assumes the molecular field approximation is likely to be quantitatively inadequate, but may be successfully employed, however, to give qualitative insight and semi-quantitative results. We can obtain further insight by looking to results from experiments based on systems that closely resemble the Maier-Saupe model. Thus PAA, which is a rigid molecule that conforms closely to the ideal of cylindrical symmetry (see chapter 1) and exhibits a nematic phase, provides a useful comparison with both theory and simulation. The value of  $\epsilon$  is not readily obtainable from experiment [16], and so it is not possible to give a comparison of the scaled transition temperatures  $k_B T_{NI}/\epsilon$ . The transitional entropy change  $\Delta S/R$  is found to be 0.17. This is not directly comparable with the Maier-Saupe value, since the latter refers to the transition at constant volume and the experimental value is at constant pressure. The experimental entropy change at constant volume can, however, be estimated from that at constant pressure [17] and is found to be about 0.05, that is, essentially the same value obtained in the simulation. This confirms the extremely poor status of the theory in predicting the entropy of transition quantitatively. The predicted constancy of the entropy of transition is, however, in broad qualitative agreement with experiment. The transitional order parameter is found to be 0.4, just slightly less than the value predicted by the Maier-Saupe theory.

## 2.8.5 Numerical Methodologies in Molecular Field Theory

There are three main ways of obtaining the temperature profiles of the order parameters that appear in the potential of mean torque in a molecular field calculation. We illustrate them here with reference to the Maier-Saupe case for simplicity. The first is to use the non-iterative, non-minimisation approach which we have illustrated in section (2.8.4) in the Maier-Saupe calculation. This method is applicable if there is only one independent parameter, as in the Maier-Saupe theory itself or some variant where all parameters appearing are ultimately controlled by one parameter. In such cases the potential(s) of mean torque can be written in terms of a single strength parameter analogue.

The second way is solving the self-consistency equations. That is, there is a defining equation for each order parameter in the potential of mean torque involving the distribution function. In the Maier-Saupe theory we have just  $\bar{P}_2$  and from (2.78, 2.79) its equation is

$$\bar{P}_2 = Z^{-1} \int P_2(\cos \beta) \exp(\epsilon \bar{P}_2 P_2(\cos \beta)/k_B T) \sin \beta d\beta. \quad (2.91)$$

Thus the order parameter occurs *self-consistently* on the right and the left; we have a self-consistency equation. One way of solving the self-consistency equations is an iterative method where a guess (or “seed”) value of each order parameter is input into the equation defining it, the result is evaluated by numerical integration, and these numbers input again. Depending on the seeds chosen, the numbers going in and coming out should converge to constant values. This is then repeated for a number of different scaled temperatures. This method is probably best suited to situations where there are few parameters, although in the case where there is just one as in the Maier-Saupe theory parameter its utility is dubious, since the non-iterative method discussed in section (2.8.4) is far better. Another way is by minimising the sum of the squared differences between the order parameters and their defining equations, treating the order parameters on both sides of these equations as fitting parameters. At the minimum of this function there will be a combination of order parameters that

solve all the self-consistency equations simultaneously. Not only should the function be minimised, but the function value at the minimum should also be zero. This technique is of general applicability and is particularly useful when there are multiple order parameters in the potential of mean torque. It is also indispensable in certain situations where other methods cannot be brought to bear as we shall see later.

The final way of obtaining the order parameters is that of minimising the orientational configurational free energy of the system with respect to the order parameter(s) [18]. This is the methodology of choice where it is applicable, since if a global minimum is found, we know by definition we have the thermodynamic solution (ie, the order parameters for the stable states only). This contrasts with solving the self-consistency equations, which will give all the solutions to the equations, but some of them will be thermodynamically metastable (or even unstable) solutions (although these could be of interest). These solutions will, in general, need sorting through (by calculation of the corresponding free energies) to determine which is the thermodynamic one at each state point. Moreover, the number of numerical evaluations of integrals in the free energy minimisation methodology is less because the free energy contains only one integral, the partition function. The self-consistency equations (or, more precisely, the error function obtained from them) contains  $n + 1$  integrals, where  $n$  is the number of order parameters. The only problems with free energy minimisation come about in two ways, one way relatively trivial, the other more fundamental. The first way is that the free energy may not be so easy to minimise as the expression for the error in the self-consistency equation approach. The more fundamental one is that there are some cases where the free energy minimisation may be inapplicable even in principle, as we shall see later. In certain instances this problem may be remediated by casting the free energy in a different form; in others this cannot be done. We shall discuss these problems in depth later in Chapters 3 and 4.

## 2.9 Uniaxial Phase of Rigid Biaxial Particles

### 2.9.1 Variational Derivation of the Distribution Function and the Potential of Mean Torque

In section (2.8.3) we derived the distribution function and potential of mean torque for a uniaxial (ie, cylindrically symmetric) particle in a uniaxial phase within the molecular field approximation. In general, however, liquid crystal molecules are not cylindrically symmetric but tend to be more lath-like in shape. We say they are biaxial, that is, all axes perpendicular to the near-symmetry axis of the molecule are not equivalent. The means for specifying the orientation of the molecule and hence the order parameters is then more complicated. This is exacerbated by the fact that, away from uniaxial symmetry, the symmetry axes of a molecule in general depend upon which molecular tensorial property is being considered. Thus we have to choose a particular second rank property as the definition. The one that is chosen is the Saupe ordering matrix which is given as

$$S_{ab} = (3\overline{l_a l_b} - \delta_{ab})/2, \quad (2.92)$$

where  $l_a$  is the direction cosine between the director and the direction of the  $a$  molecular axis increasing (with  $a \equiv x, y, z \equiv 1, 2, 3$ ) and the bar indicates a molecular average. Here we are assuming an arbitrary cartesian axis system set in the molecule. The principal axes of this real symmetric tensor are then used to define the orientation of the molecule. It is conventional to label the axis (ie, eigenvector) corresponding to the largest eigenvalue  $z$  so that the eigenvalue is  $S_{zz}$ . The next largest eigenvalue is taken to be  $S_{xx}$  and the smallest  $S_{yy}$  (so that  $S_{xx} - S_{yy}$  is positive) which then defines the  $x$  and  $y$  axes of the principal molecular frame. The quantity  $S_{zz}$  is referred to as the *major* order parameter and  $(S_{xx} - S_{yy})$  as the *biaxial* order parameter. Now we have defined the molecular symmetry axes we may proceed to the theoretical definition of molecular orientation that we require. Now, two Euler angles, which we shall refer to

as  $\beta$  and  $\gamma$ , are employed to define the orientation of the director of the phase with respect to the molecular axis system (see Chapter 1).

The orientational order of the system is then completely described by an infinite set of tensor order parameters of all even orders. By analogy with the Maier-Saupe theory, if we assume that the most important interactions are second rank in nature (ie, they dominate the single particle internal energy) then the orientational order of the system may be taken to be described by a matrix of second rank order parameters. The internal energy is assumed to be a function of the scalar product of two second rank ordering tensors to give a quadratic expression as in the Maier-Saupe theory. The second rank ordering tensors each have five components  $\overline{C}_{2m}$  ( $m = 0, \pm 1, \pm 2$ ) in irreducible form and the strength parameter now takes the form of a second rank supertensor with  $5^2$  elements. To construct the internal energy we assume that pair interactions predominate and so we take the scalar product of the second rank tensor order parameter of the first molecule of the pair with that of the second molecule. In addition, we expect that the coefficient should itself be a molecular property, and so in the case of biaxial molecules it should also be a second rank tensorial property related to the interaction between the two molecules. Thus, if we denote the first molecule by  $m$  and the second by  $n$  we form the single molecule internal energy as a scalar invariant from the tensor order parameters  $\overline{C}_{2m}$ ,  $\overline{C}_{2n}$  for the pair of molecules and the second rank supertensor  $u_{2mn}$  describing the interactions between the molecules. As in the case of uniaxial phases composed of uniaxial particles, we include a factor of  $1/2$  to retain consistency with pre-existing notation. The internal energy is then assumed to have the form

$$U = -\frac{1}{2} \sum_m \sum_n u_{2mn} \overline{C}_{2m} \overline{C}_{2n}. \quad (2.93)$$

The entropy within the molecular field approximation is again found from the singlet orientational distribution function, but this time using the analogue  $f(\omega)$  involving the two angles  $\beta, \gamma \equiv \omega$ , as

$$S = -k_B \int f(\omega) \ln f(\omega) d\omega. \quad (2.94)$$

The Hemholtz free energy per molecule is then

$$A = -\frac{1}{2} \sum_m \sum_n u_{2mn} \bar{C}_{2m} \bar{C}_{2n} + k_B T \int f(\omega) \ln f(\omega) d\omega. \quad (2.95)$$

We now proceed to minimise the free energy with respect to fluctuations in the distribution function in a manner analogous to section (2.8.3), that is, we require that

$$\delta A = 0. \quad (2.96)$$

Now

$$\delta A = -\frac{1}{2} \sum_m \sum_n u_{2mn} (\delta \bar{C}_{2m} \bar{C}_{2n} + \bar{C}_{2m} \delta \bar{C}_{2n}) + k_B T \int \delta f(\omega) [\ln f(\omega) + 1] d\omega, \quad (2.97)$$

where the  $\delta \bar{C}_{2n}$  are the variations in the ordering tensor components

$$\delta \bar{C}_{2n} = \int C_{2n}(\omega) \delta f(\omega) d\omega. \quad (2.98)$$

The variation in the free energy is then

$$\delta A = \int \left( - \sum_m \sum_n u_{2mn} \bar{C}_{2m} C_{2n}(\omega) + k_B T [\ln f(\omega) + 1] \right) \delta f(\omega) d\omega. \quad (2.99)$$

We must take account of the constraint that the distribution is normalised, that is,

$$\int \delta f(\omega) d\omega = 0. \quad (2.100)$$

To form the complete variational equation we multiply the constraint equation by the Lagrange undetermined multiplier  $\lambda$  and add the result to the variation (2.96) in  $A$  to obtain

$$\int \left( - \sum_m \sum_n u_{2mn} \bar{C}_{2m} C_{2n}(\omega) + k_B T [\ln f(\omega) + 1] + \lambda \right) \delta f(\omega) d\omega = 0. \quad (2.101)$$

This result must hold for any fluctuation  $\delta f(\omega)$  and so we require that

$$- \sum_m \sum_n u_{2mn} \bar{C}_{2m} C_{2n}(\omega) + k_B T [\ln f(\omega) + 1] + \lambda = 0. \quad (2.102)$$



The single particle orientational distribution is then

$$f(\omega) = Z^{-1} \exp \left( \sum_m \sum_n u_{2mn} \bar{C}_{2m} C_{2n}(\omega) / k_B T \right) \quad (2.103)$$

and the potential of mean torque for a biaxial particle in a uniaxial phase is

$$U(\omega) = - \sum_m \sum_n u_{2mn} \bar{C}_{2m} C_{2n}(\omega). \quad (2.104)$$

We note that this same form of potential has also been derived from the pair potential by Luckhurst, Zannoni, Nordio, and Segre [19].

In the principal axis system of the ordering tensor the  $\bar{C}_{2m}$  simplify as

$$\bar{C}_{2\pm 1} = 0 \quad \bar{C}_{22} = \bar{C}_{2-2}. \quad (2.105)$$

The  $u_{2mn}$  also simplify, although the reasons for this are not quite so clear. If we suppose for the moment that the predominant interaction contributing to the  $u_{2mn}$  is dispersion forces then we might write the interaction between the two molecules in terms of their polarisability tensors in irreducible form as

$$u_{2mn} = \alpha_{2m} \alpha_{2n}. \quad (2.106)$$

Then

$$u_{200} = \alpha_{20} \alpha_{20}. \quad (2.107)$$

Also, since

$$\alpha_{2\pm 2} = (\alpha_{xx} - \alpha_{yy})/2 \pm i2\alpha_{xy} \quad (2.108)$$

and we are by definition dealing with a principal axis system

$$\alpha_{22} = \alpha_{2-2}. \quad (2.109)$$

Then the  $u_{2mn}$  simplify as

$$u_{220} = u_{202} = u_{2-20} = u_{20-2} \quad u_{222} = u_{22-2} = u_{2-22} = u_{2-2-2}. \quad (2.110)$$

Therefore only three elements of the intrinsic interaction tensor are required, namely  $u_{200}$ ,  $u_{220}$  and  $u_{222}$ , and only two of the order parameters, namely  $\bar{C}_{20}$  and  $\bar{C}_{22}$ . The potential of mean torque can then be written

$$U(\omega) = -\{(u_{220}\bar{C}_{20} + 2u_{222}\bar{C}_{22})C_{2-2}(\omega) + (u_{200}\bar{C}_{20} + 2u_{220}\bar{C}_{22})C_{20}(\omega) \\ + (u_{220}\bar{C}_{20} + 2u_{222}\bar{C}_{22})C_{22}(\omega)\}. \quad (2.111)$$

This can be rewritten in terms of the Euler angles  $\alpha$  and  $\beta$  by substituting explicit expressions for the  $C_{20}(\beta, \gamma)$ ,  $C_{2\pm 2}(\beta, \gamma)$  (see Appendix 1B) as

$$U(\beta, \gamma) = -\{(u_{220}\bar{C}_{20} + 2u_{222}\bar{C}_{22})\sqrt{\frac{3}{8}}\sin^2\beta e^{-2i\gamma} + (u_{200}\bar{C}_{20} + 2u_{220}\bar{C}_{22})P_2(\cos\beta) \\ + (u_{220}\bar{C}_{20} + 2u_{222}\bar{C}_{22})\sqrt{\frac{3}{8}}\sin^2\beta e^{2i\gamma}\} \quad (2.112)$$

which simplifies to

$$U(\beta, \gamma) = -\{(u_{200}\bar{C}_{20} + 2u_{220}\bar{C}_{22})P_2(\cos\beta) + 2(u_{220}\bar{C}_{20} + 2u_{222}\bar{C}_{22})\sqrt{\frac{3}{8}}\sin^2\beta \cos 2\gamma\}. \quad (2.113)$$

The number of adjustable parameters  $u_{2mn}$  may be further reduced by invoking a geometric mean approximation for  $u_{220}$ , in other words  $u_{220} = (u_{200}u_{222})^{1/2}$ , and rewriting equation (2.113) in terms of a molecular biaxiality parameter  $\lambda = (u_{222}/u_{200})^{1/2}$  as

$$U(\beta, \gamma) = -\{u_{200}(\bar{C}_{20} + 2\lambda\bar{C}_{22})P_2(\cos\beta) + 2\lambda u_{200}(\bar{C}_{20} + 2\lambda\bar{C}_{22})\sin^2\beta \cos 2\gamma\}. \quad (2.114)$$

We note that the geometric mean approximation for  $u_{220}$  is only exact for dispersion forces, however. Since  $u_{200}(\bar{C}_{20} + 2\lambda\bar{C}_{22})$  is a common factor the potential of mean torque can be further simplified by defining

$$X_{20} = u_{200}(\bar{C}_{20} + 2\lambda\bar{C}_{22}) \quad (2.115)$$

giving

$$U(\beta, \gamma) = -X_{20}\{P_2(\cos\beta) + 2\lambda\sin^2\beta \cos 2\gamma\}. \quad (2.116)$$

It is also conventional to define

$$X_{22} = \lambda X_{20}. \quad (2.117)$$

Invoking the geometric mean approximation for  $u_{220}$  thus renders the ratio  $X_{22}/X_{20}$  ( $= \lambda$ ) temperature-independent. The potential of mean torque is then finally written as

$$U(\beta, \gamma) = -\{ X_{20} P_2(\cos \beta) + 2X_{22} \sin^2 \beta \cos 2\gamma \}. \quad (2.118)$$

We note that in the limit that the molecular biaxiality is zero (ie,  $\lambda = 0$ ) this reduces to

$$U(\beta) = -X_{20} P_2(\cos \beta) = -X P_2(\cos \beta), \quad (2.119)$$

which is just the Maier-Saupe potential for a uniaxial particle in a uniaxial phase, as expected.

## 2.9.2 Predictions of the Theory

From the expression for the potential of mean torque we can calculate the orientational order parameters as averages over the associated distribution function. That is,

$$\bar{C}_{20} = Z^{-1} \iint P_2(\cos \beta) \exp (X_{20}^* P_2(\cos \beta) + 2X_{22}^* \sin^2 \beta \cos 2\gamma) \sin \beta d\beta d\gamma \quad (2.120)$$

and

$$\bar{C}_{22} = Z^{-1} \iint \sin^2 \beta \cos 2\gamma \exp (X_{20}^* P_2(\cos \beta) + 2X_{22}^* \sin^2 \beta \cos 2\gamma) \sin \beta d\beta d\gamma, \quad (2.121)$$

where here the superscript \* denotes division by  $k_B T$  rather than complex conjugation and the rotational partition function is

$$Z = \iint \exp (X_{20}^* P_2(\cos \beta) + 2X_{22}^* \sin^2 \beta \cos 2\gamma) \sin \beta d\beta d\gamma. \quad (2.122)$$

The double integrals may be evaluated as one dimensional integrals involving modified Bessel functions of the first kind. That is, an  $n$ th order modified Bessel function is written (in its integral representation) as

$$I_n(x) = \pi^{-1} \int_0^\pi \cos n\gamma \exp(x \cos \gamma) d\gamma \quad (2.123)$$

and the integrals may be written

$$\bar{C}_{20} = 2\pi Z^{-1} \int_0^\pi P_2(\cos \beta) I_0(2X_{22} \sin^2 \beta/k_B T) \exp(X_{20} P_2(\cos \beta)/k_B T) \sin \beta d\beta \quad (2.124)$$

$$\bar{C}_{22} = 2\pi Z^{-1} \int_0^\pi \sin^2 \beta I_1(2X_{22} \sin^2 \beta/k_B T) \exp(X_{20} P_2(\cos \beta)/k_B T) \sin \beta d\beta \quad (2.125)$$

with

$$Z = 2\pi \int_0^\pi I_0(2X_{22} \sin^2 \beta/k_B T) \exp(X_{20} P_2(\cos \beta)/k_B T) \sin \beta d\beta. \quad (2.126)$$

The orientational partition function and order parameters are thus evaluated using one dimensional numerical integrations for given values of  $X_{20}^*$  ( $\equiv X_{20}/k_B T$ ) and  $X_{22}^*$  ( $\equiv X_{22}/k_B T$ ) but with their ratio constant.

Again, as in the case of uniaxial particles, the order parameters at the transition are obtained as those for which the difference in the free energy between isotropic and nematic phases is zero. We have from the potential of mean torque that the single particle internal energy is

$$U = -\frac{N_A}{2}(X_{20}\bar{C}_{20} + 2X_{22}\bar{C}_{22}) \quad (2.127)$$

and the orientational entropy is

$$S = -\frac{N_A}{T}(X_{20}\bar{C}_{20} + 2X_{22}\bar{C}_{22}) + N_A k_B \ln Z. \quad (2.128)$$

The molar orientational Helmholtz free energy is, therefore,

$$A = \frac{N_A}{2}(X_{20}\bar{C}_{20} + 2X_{22}\bar{C}_{22}) - N_A k_B T \ln Z. \quad (2.129)$$

Now in the isotropic phase the order parameters are zero and the rotational partition function reduces to  $4\pi$ . The free energy difference,  $\Delta A_{IN}$ , between isotropic and nematic phases is then given by

$$\Delta A_{IN} = A_N - A_I = \frac{N_A}{2}(X_{20}\bar{C}_{20} + 2X_{22}\bar{C}_{22}) - N_A k_B T \ln \frac{Z_N}{4\pi}. \quad (2.130)$$

This expression must vanish at the  $N - I$  transition which can therefore be located in an analogous way to that of uniaxial particles. Alternatively, the transitional order parameters could be obtained as those corresponding to the the values of  $X_{20}^*, X_{22}^*$  which satisfy the equation

$$\frac{X_{20}^* \bar{C}_{20} + 2X_{22}^* \bar{C}_{22}}{2} = \ln \frac{Z}{4\pi}. \quad (2.131)$$

As in the case of uniaxial particles, there is always an isotropic solution in which the order parameters are zero. In the nematic phase, however, there is no unique solution, but a set of solutions depending on the value of  $\lambda$  taken, which must therefore be specified.

The nematic-isotropic transition temperature is then obtained from

$$\frac{k_B T_{NI}}{u_{200}} = \frac{\bar{C}_{20}^{NI} + 2\lambda \bar{C}_{22}^{NI}}{X_{20}^{*NI}}, \quad (2.132)$$

with  $\lambda = X_{22}^{*NI}/X_{20}^{*NI}$ .

From the values of  $X_{20}^{*NI}$ ,  $X_{22}^{*NI}$  and the corresponding transitional order parameters, the entropy change at the transition is calculated as

$$\frac{\Delta S_{NI}}{R} = X_{20}^{*NI} \bar{C}_{20}^{NI} + 2X_{22}^{*NI} \bar{C}_{22}^{NI} + \ln \frac{4\pi}{Z_{NI}}. \quad (2.133)$$

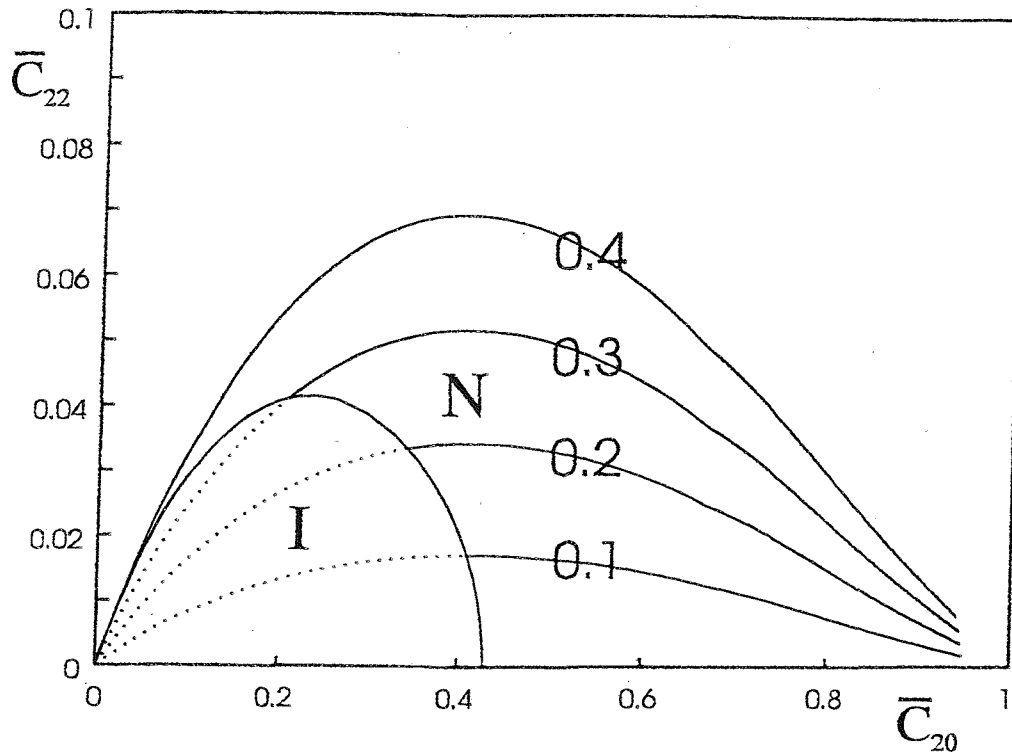
The values of the order parameters, transition temperatures and entropies of transition for a range of biaxialities as calculated by this procedure are given in table 2.2. In addition, in figure 2.5 we show the biaxial order parameter plotted against the major order parameter for four different biaxialities, namely 0.1, 0.2, 0.3 and 0.4. Figure 2.5 also shows the solutions to the self-consistency equations for the order parameters at the  $N - I$  transition.

$\lambda$	$\overline{C}_{20}^{NI}$	$\overline{C}_{22}^{NI}$	$k_B T_{NI}/u_{200}$	$\Delta S_{NI}/R$
0.000	0.429	0.000	0.220	0.418
0.050	0.424	0.009	0.221	0.410
0.100	0.409	0.017	0.222	0.384
0.150	0.382	0.026	0.224	0.338
0.200	0.341	0.034	0.228	0.276
0.250	0.284	0.040	0.233	0.198
0.300	0.208	0.041	0.240	0.113
0.350	0.115	0.032	0.250	0.038
0.400	0.016	0.006	0.264	0.008

Table 2.2: The order parameters, scaled temperature and entropy change at the nematic-isotropic transition for different values of the biaxiality parameter  $\lambda$ .

We show results only for positive values of  $\lambda$  since reversing the sign of the value of  $\lambda$  simply corresponds to an interchange of the definitions of  $x$  and  $y$  axes. We see that the scaled temperature of the  $N - I$  transition increases as a function of increasing molecular biaxiality. This seems somewhat surprising initially, but may be understood as follows. We have that for a given value of  $u_{200}$  the transition temperature is increasing with increasing  $\lambda$ . But for a constant value of  $u_{200}$ , increasing  $\lambda$  increases the overall anisotropy of the molecule by increasing  $u_{220}$  and  $u_{222}$ . The orientational internal energy therefore becomes more negative and leads to an increase in the nematic range. The transitional value of the second rank order parameter  $\overline{C}_{20}^{NI}$  is seen to decrease with increasing molecular biaxiality. Thus, for a rod-like molecule with uniaxial symmetry, the order parameter of the long axis (which in this case is the molecular symmetry axis) is high and the biaxiality is zero. If the molecular biaxiality is now increased the order parameter of this axis decreases until at  $\lambda = 1/\sqrt{6}$  the molecule becomes disc-like. At this point the molecule would tend to align orthogonal to the director with a negative order parameter, except that the axes have now changed such that the biaxiality is by

Figure 2.5: The order parameter  $\bar{C}_{20}$  plotted against the biaxial order parameter  $\bar{C}_{22}$ , calculated from the molecular field theory of uniaxial phases of biaxial particles, for biaxiality values of 0.1, 0.2, 0.3 and 0.4. The values of the order parameters at the  $N-I$  transition are also indicated on the plot. [14]



definition a maximum at  $\sqrt{6}$ . The near-symmetry axis of the molecule then still tends to align with the director (the symmetry axis of the phase) with an order parameter that is again positive. If the molecular anisotropy continues to change such that the disc-like molecule becomes increasingly uniaxial about the near-symmetry axis, then the biaxiality begins to decrease from the maximum value of  $\sqrt{6}$ . There is a concomitant increase in the order parameter of the axis, with the same values being obtained as for rod-like molecules of the equal biaxiality. This continues until, at  $\lambda = 0$ , the molecule is again perfectly uniaxial and  $\bar{C}_{20}^{NI}$  again takes on its maximum value, but

now for the uniaxial symmetry axis of the disc. The order parameter  $\overline{C}_{22}^{NI}$  is a measure of the molecular biaxiality and increases as the value of the biaxiality parameter is increased. The entropy of transition  $\Delta S_{NI}/R$  decreases markedly with increasing molecular biaxiality due to the reduction in  $\overline{C}_{20}^{NI}$ . Increasing the molecular biaxiality parameter is also found to affect the temperature dependence of the second rank order parameter, particularly the slope of the curve in the neighbourhood of the transition [16]. The degree of molecular biaxiality thus clearly makes a large difference to the transitional properties. Consequently any theory of the nematic mesophase based on the assumption of cylindrical symmetry of the nematogenic molecules is likely to be quantitatively inadequate.



## Appendix 2A: The Calculus of Variations

### 2A.1 Introduction

The solution to a great many problems in physics can be stated in terms of some quantity taking its minimum value. In ordinary calculus we find the turning (or stationary) points of a function by differentiating with respect to the independent variable and setting the result equal to zero. We then rely on the physics or further mathematical tests to characterise the stationary points if necessary. In the calculus of variations we wish to know which *function* (as opposed to which value of a variable) makes stationary (eg, a minimum) some quantity that is a function of this arbitrary function. Rather than being a function of a variable, the quantity is a function of a function and is known as a *functional*. Thus we have, effectively, to differentiate with respect to the unknown arbitrary function rather than a variable; the procedure is known as *functional differentiation*. We then similarly set the result equal to zero. This is saying that the variation in the quantity with respect to variations in the function is zero and the quantity is *functionally stationary*. In the calculus of variations problems are often stated by asserting that a certain quantity is to be minimised. Thus we often talk of *functional minimisation*. What we actually always do in practise, however, is the functional analogue of setting the derivative equal to zero. The question of whether we actually have a minimum, maximum or neither is, in general, a difficult mathematical problem [21]. Fortunately, however, making the relevant quantity stationary is usually all that is necessary. This is particularly true in the major theoretical underpinnings of mathematical physics and in view of the links between these areas provided by such stationary functionals, the concept has the status of a fundamental unifying principle. For instance, in the propagation of electromagnetic radiation we have Fermat's principle of "least" time, which becomes exact in the short wavelength limit where electrodynamics reduces to linear optics. This principle went on to be used in the historical development of quantum mechanics, appearing as the particle-wave analogue,

the principle of least phase length, which lead to the development of the Schroedinger equation. Again, in classical mechanics we have the concept that a system behaves in such a way that the integral of the Lagrangian between any two arbitrary points in time (the *action integral*) is a stationary quantity. This is Hamilton's principle (of least action) and leads directly to the Lagrangian form of the equations of motion. Under a canonical transformation with the introduction of the concept of momentum, these become the somewhat more tractable canonical or "Hamiltonian" equations of motion. However, for reasons already alluded to, the Lagrangian is to be viewed ultimately as the more fundamental quantity as a matter of principle.

## 2A.2 The Problem

The general calculus of variations problem, then, may be stated more precisely as follows. Given an integral of the form

$$I = \int_{x_1}^{x_2} F(x, y, y') dx \quad (y' \equiv dy/dx), \quad (2A.1)$$

the limits  $x_1, x_2$  and the form of  $F$ , we are required to find the curve (function)  $y(x)$  that makes the integral have the smallest possible value (or stationary value). In a more general case  $F$  might be a function  $F(x, \{y\}, \{y'\})$  of a set of dependent variables  $\{y\}$ . For example, the Lagrangian is  $L(t, q_i, \dot{q}_i)$  (where the  $q_i$  are the cartesian components of the position vectors of the particles  $i$  of the system) and so the action integral to be made stationary is

$$I = \int_{t_1}^{t_2} L(t, q_i, \dot{q}_i) dt. \quad (2A.2)$$

In other cases, there may be a single dependent variable, but with a set of independent variables  $\{x\}$  (see later) and so then we have

$$I = \int_{\{x\}_1}^{\{x\}_2} F(\{x\}, y, \{y'\}) d\{x\}. \quad (2A.3)$$

In the most general possible case we might in principle have a set of independent and dependent variables and so the integral would then be

$$I = \int_{\{x\}_1}^{\{x\}_2} F(\{x\}, \{y\}, \{y'\}) d\{x\}. \quad (2A.4)$$

Let us now see more precisely and in greater detail what we really mean by making an integral stationary with respect to a function and how we go about doing this. For the moment it will be sufficient for our purposes, given our concern with molecular field theory, to illustrate it by reference to a system with one independent and one dependent variable. The integral in (2A.1) is to be made stationary with respect to fluctuations in the “path” between  $x_1$  and  $x_2$ , that is, in the functional form of  $y(x)$ . Until now we have been using  $y(x)$  to denote all the *varied paths* from  $x_1$  to  $x_2$  with respect to which the integral is to be made stationary, with just the one particular  $y(x)$  being the solution we require. This path corresponds to the extremum and is referred to as the *extremal*. For the moment we shall change our notation slightly for sake of convenience and precision. If we now denote the arbitrary function by  $Y$  then we can construct the varied paths  $Y(x)$  as

$$Y(x, \epsilon) = y(x) + \epsilon\eta(x), \quad (2A.5)$$

where  $y(x)$  is now strictly the desired extremal and  $\epsilon$  is a parameter that controls the relative contribution of the function  $\eta(x)$  to the varied paths. Here  $\eta(x)$  is any arbitrary function that has a continuous second derivative and that obeys the constraints

$$\eta(x_1) = \eta(x_2) = 0 \quad (2A.6)$$

so that at the endpoints  $x_1, x_2$  of the path we necessarily have

$$Y(x_1, \epsilon) = y(x_1)$$

$$Y(x_2, \epsilon) = y(x_2) \quad (2A.7)$$

as required. Then we have

$$I(\epsilon) = \int_{x_1}^{x_2} F(x, Y, Y') dx. \quad (2A.8)$$

The most important thing to note now is that when  $\epsilon = 0$ ,  $Y(x, 0) = y(x)$ . We are now in a position to state precisely what we mean by making the quantity  $I$  stationary with respect to fluctuations in the dependent variable function in the integrand. What we require is that the derivative of  $I(\epsilon)$  with respect to the fluctuation parameter  $\epsilon$  of the varied paths is zero when this parameter is itself zero, for *any arbitrary fluctuation* function  $\eta(x)$ . That is,

$$\left(\frac{dI}{d\epsilon}\right)_{\epsilon=0} = 0 \quad (2A.9)$$

for any arbitrary fluctuation  $\eta(x)$ . Since  $\epsilon$  is not a function of the variable of integration,

$$\left(\frac{dI}{d\epsilon}\right)_{\epsilon=0} = \int \left(dF(x, Y, Y')/d\epsilon\right)_{\epsilon=0} dx \quad (2A.10)$$

$$= \int \left[ \left(\frac{\partial F}{\partial x} \frac{dx}{d\epsilon}\right)_{\epsilon=0} + \left(\frac{\partial F}{\partial Y} \frac{dY}{d\epsilon}\right)_{\epsilon=0} + \left(\frac{\partial F}{\partial Y'} \frac{dY'}{d\epsilon}\right)_{\epsilon=0} \right] dx. \quad (2A.11)$$

Now  $x$  is not a function of  $\epsilon$  so that  $dx/d\epsilon = 0$  giving

$$\left(\frac{dI}{d\epsilon}\right)_{\epsilon=0} = \int \left[ \left(\frac{\partial F}{\partial Y} \frac{dY}{d\epsilon}\right)_{\epsilon=0} + \left(\frac{\partial F}{\partial Y'} \frac{dY'}{d\epsilon}\right)_{\epsilon=0} \right] dx. \quad (2A.12)$$

Also, from (2A.5),

$$\frac{dY}{d\epsilon} = \eta(x) \quad (2A.13)$$

and

$$\frac{dY'}{d\epsilon} = \eta'(x) \quad (2A.14)$$

so that

$$\left(\frac{dI}{d\epsilon}\right)_{\epsilon=0} = \int \left[ \left(\frac{\partial F}{\partial Y} \eta(x)\right)_{\epsilon=0} + \left(\frac{\partial F}{\partial Y'} \eta'(x)\right)_{\epsilon=0} \right] dx. \quad (2A.15)$$

But, at  $\epsilon = 0$ , as we have already noted,  $Y = y$  and so

$$\left(\frac{dI}{d\epsilon}\right)_{\epsilon=0} = \int \left[ \frac{\partial F}{\partial y} \eta(x) + \frac{\partial F}{\partial y'} \eta'(x) \right] dx. \quad (2A.16)$$

The required solutions are then obtained by setting

$$\int \left[ \frac{\partial F}{\partial y} \eta(x) + \frac{\partial F}{\partial y'} \eta'(x) \right] dx = 0. \quad (2A.17)$$

If  $y''$  is continuous, we can integrate the second term by parts as

$$\int_{x_1}^{x_2} \frac{\partial F}{\partial y'} \eta'(x) dx = \left[ \frac{\partial F}{\partial y'} \eta(x) \right]_{x_1}^{x_2} - \int_{x_1}^{x_2} \frac{d}{dx} \left( \frac{\partial F}{\partial y'} \right) \eta(x) dx. \quad (2A.18)$$

The integrated term is zero because  $\eta(x)$  is by definition zero at  $x_1$  and  $x_2$  and so we obtain

$$\int \left[ \frac{\partial F}{\partial y} - \frac{d}{dx} \frac{\partial F}{\partial y'} \right] \eta(x) dx = 0. \quad (2A.19)$$

The integral must vanish for any arbitrary fluctuation  $\eta(x)$  and so the remaining factor in the integrand must vanish, giving the well-known Euler-Lagrange equation

$$\frac{d}{dx} \frac{\partial F}{\partial y'} - \frac{\partial F}{\partial y} = 0. \quad (2A.20)$$

This is the standard equation we have in principle to solve in any calculus of variations problem. In many cases, however, there may be constraints or relationships in the physics of the situation that need to be somehow included (eg boundary conditions) without which satisfactory solution of the equation may not be possible. For instance it may simply be insoluble (most likely when boundary conditions need to be imposed) or it may be that any arbitrary  $y(x)$  will satisfy (due to physical relationships between certain quantities that have not been built in). In such cases we apply the method of undetermined multipliers due to Lagrange. This method is generally applicable to variational-type problems whether involving ordinary minimisation or functional minimisation and proceeds as follows. We identify the constraints and write equations expressing those constraints. We then manipulate each of these constraint equations into the form that some expression is equal to zero. Clearly, if we now add this expression to the main variational expression the sum is still equal to zero. However, this would also be true if we added the constraint expression multiplied by any arbitrary constant. So in general the solution requires the inclusion of this unknown

multiplier (commonly referred to as the Lagrange undetermined multiplier), one for each constraint. The resulting equation can then be solved as a purely mathematical exercise confident that any constraints and interrelationships are fully accounted for. The Lagrange multiplier(s) may then be determined at the end if desired, although in many cases it turns out not to be necessary.

Strictly, in the case of the calculus of variations, we should say that we include the constraint with its Lagrange multiplier in the integral to be made stationary. That is, we write each constraint  $i$  as an integral over the same range(s) of the same variable(s) in the form

$$\int_{x_1}^{x_2} c_i dx = k_i, \quad (2A.21)$$

where  $k_i$  is a constant. The differential with respect to  $\epsilon$  of this integral is then zero and so we can add the integral to the main variational equation (after multiplying by the Lagrange undetermined multiplier  $\lambda_i$ ). The total integral to be made stationary would be then

$$I = \int_{x_1}^{x_2} \left( F(x, y, y') + \sum_i \lambda_i c_i \right) dx. \quad (2A.22)$$

The total variational equation with constraints included is then just (2A.9) with  $I$  as in (2A.22). The formal analysis proceeds just as before but with  $F$  replaced by  $F + \lambda_i c_i$ , ultimately giving for the Euler-Lagrange equation in the presence of constraints

$$\frac{d}{dx} \frac{\partial}{\partial y'} \left( F + \sum_i \lambda_i c_i \right) - \frac{\partial}{\partial y} \left( F + \sum_i \lambda_i c_i \right) = 0. \quad (2A.23)$$

We note, however, that in certain cases we can write this in another, simpler way, as we shall see later.

### 2A.3 Variational Notation

There is an older more traditional notation for the calculus of variations involving the symbol  $\delta$ . It is the one most commonly employed in practise in applications,

particularly in the theory of liquid crystals (at various length scales), and it is therefore the one we shall adopt. We shall now therefore define it in terms of the foregoing notation. The symbol  $\delta$  is used to denote essentially what we have hitherto referred to as differentiation with respect to the fluctuation parameter  $\epsilon$ . Instead of saying that the required condition is that  $I$  is stationary, we say that the *variation of  $I$*  is zero. That is,

$$\delta I = 0, \quad (2A.24)$$

where

$$\delta I = \left( \frac{dI}{d\epsilon} \right)_{\epsilon=0} d\epsilon \quad (2A.25)$$

is the variation of  $I$ . So the symbol  $\delta$  when applied to the integral denotes differentiation with respect to the parameter  $\epsilon$  of the fluctuation term, evaluated at  $\epsilon = 0$ . Just as before,  $\epsilon$  is not a function of the variable of integration and so

$$\delta \int F(x, Y, Y') dx = \int \delta F(x, Y, Y') dx, \quad (2A.26)$$

where

$$\delta F(x, Y, Y') = \left( \frac{\partial F}{\partial x} \frac{dx}{d\epsilon} \right)_{\epsilon=0} d\epsilon + \left( \frac{\partial F}{\partial Y} \frac{dY}{d\epsilon} \right)_{\epsilon=0} d\epsilon + \left( \frac{\partial F}{\partial Y'} \frac{dY'}{d\epsilon} \right)_{\epsilon=0} d\epsilon. \quad (2A.27)$$

Again,  $x$  is not a function of  $\epsilon$  and so the meaning of  $\delta F$  is then

$$\begin{aligned} \delta F(x, Y, Y') &= \left( \frac{\partial F}{\partial Y} \frac{dY}{d\epsilon} \right)_{\epsilon=0} d\epsilon + \left( \frac{\partial F}{\partial Y'} \frac{dY'}{d\epsilon} \right)_{\epsilon=0} d\epsilon, \\ &= \left( \frac{\partial F}{\partial Y} \right)_{\epsilon=0} \left( \frac{dY}{d\epsilon} \right)_{\epsilon=0} d\epsilon + \left( \frac{\partial F}{\partial Y'} \right)_{\epsilon=0} \left( \frac{dY'}{d\epsilon} \right)_{\epsilon=0} d\epsilon. \end{aligned} \quad (2A.28)$$

We note that the total derivative  $dY$  is

$$dY(x, \epsilon) = \frac{\partial Y}{\partial x} dx + \frac{\partial Y}{\partial \epsilon} d\epsilon. \quad (2A.29)$$

Now  $x$  and  $\epsilon$  are independent variables, so

$$\frac{dY}{d\epsilon} = \frac{\partial Y}{\partial x} \frac{dx}{d\epsilon} + \frac{\partial Y}{\partial \epsilon} \frac{d\epsilon}{d\epsilon},$$

$$\frac{dY}{d\epsilon} = \frac{\partial Y}{\partial \epsilon}. \quad (2A.30)$$

So we see that (2A.28) is just the total differential  $dF = (\partial F/\partial \epsilon)_{\epsilon=0} d\epsilon$  of the function  $F(x, Y(x, \epsilon), Y'(x, \epsilon))$  at  $\epsilon = 0$  with  $\epsilon$  considered as the only variable. That is,

$$\begin{aligned} dF &= \frac{\partial F}{\partial Y} dY + \frac{\partial F}{\partial Y'} dY', \\ &= \frac{\partial F}{\partial Y} \frac{\partial Y}{\partial \epsilon} d\epsilon + \frac{\partial F}{\partial Y'} \frac{\partial Y'}{\partial \epsilon} d\epsilon, \\ &= \frac{\partial F}{\partial Y} \frac{dY}{d\epsilon} d\epsilon + \frac{\partial F}{\partial Y'} \frac{dY'}{d\epsilon} d\epsilon. \end{aligned} \quad (2A.31)$$

We note that in (2A.28) and (2A.31) terms appear in  $Y$  and  $Y'$  of the same form as in the definition (2A.25) of  $\delta I$ . So, using the  $\delta$  notation consistently to mean the variation in some quantity, we can rewrite this as

$$\delta F(x, Y, Y') = \left( \frac{\partial F}{\partial Y} \right)_{\epsilon=0} \delta Y + \left( \frac{\partial F}{\partial Y'} \right)_{\epsilon=0} \delta Y'. \quad (2A.32)$$

Now  $\epsilon = 0$  is completely synonymous with saying  $Y = y$  so this simplifies to

$$\delta F = \frac{\partial F}{\partial y} \delta Y + \frac{\partial F}{\partial y'} \delta Y'. \quad (2A.33)$$

But

$$\delta Y = \left( \frac{dY}{d\epsilon} \right)_{\epsilon=0} d\epsilon = \delta y \quad (2A.34)$$

so

$$\delta F = \frac{\partial F}{\partial y} \delta y + \frac{\partial F}{\partial y'} \delta y'. \quad (2A.35)$$

The variation in the dependent variable can then be defined severally as

$$\delta y = \left( \frac{dY}{d\epsilon} \right)_{\epsilon=0} d\epsilon = \frac{\partial Y}{\partial \epsilon} d\epsilon = \eta(x) d\epsilon. \quad (2A.36)$$

So we see that the *variation* in the dependent variable is essentially just the *fluctuation* in it. As with the integrand  $F$  its variation can be considered to be just the total



differential (in this case  $dY(\epsilon)$ ) with  $\epsilon$  considered as the only variable. The meaning of  $\delta y'$  is similarly defined as

$$\delta y' = \left( \frac{dY'}{d\epsilon} \right)_{\epsilon=0} d\epsilon = \frac{\partial Y'}{\partial \epsilon} d\epsilon = \eta'(x) d\epsilon. \quad (2A.37)$$

We also note, in passing, that this is identical to

$$\frac{d}{dx}(\delta y) = \frac{d}{dx}(\eta(x) d\epsilon) = \eta'(x) d\epsilon, \quad (2A.38)$$

so that  $d$  and  $\delta$  commute. The application of  $\delta$  to a quantity may be compared with

$$df(a, b, c, \dots) = \frac{\partial f}{\partial a} da + \frac{\partial f}{\partial b} db + \frac{\partial f}{\partial c} dc + \dots \quad (2A.39)$$

and

$$\delta f(a, b, c, \dots) \approx \frac{\partial f}{\partial a} \delta a + \frac{\partial f}{\partial b} \delta b + \frac{\partial f}{\partial c} \delta c + \dots, \quad (2A.40)$$

where here  $\delta$  takes its usual mathematical meaning as a small but non-infinitesimal change.

The  $\delta$  notation can be thought of intuitively as the total derivative (but using the same symbol as its counterpart for small non-infinitesimal changes), except that it should be remembered that we are really differentiating with respect to the fluctuation parameter  $\epsilon$  only (ie, considering  $\epsilon$  to be the sole variable) and evaluating at  $\epsilon = 0$ . Normally, however, it can be used fairly simply and intuitively as a pseudo-differential operator with the usual properties of  $\delta$  in mathematics (but noting that it is exact). We just need to know in any given problem at hand what quantities involved are affected by a non-zero variation in the dependent variable  $y$  and thence suffer a non-vanishing variation themselves. This will be made clearer in the next section where we discuss some general classes of problems including that within which falls the elaboration employed in molecular field theory.

## 2A.4 Application to Multivariate Problems

In this section we consider problems with multiple variables. To begin with we analyse the case where there is one independent variable and multiple dependent ones. Such a case is well-illustrated by application of Hamilton's principle to obtain the Lagrangian equations of motion. The single independent variable (ie, the variable of integration) is  $t$ , the time, and the dependent variables are the  $q_i$ , the cartesian components of the particle positions. The stationary variational condition is

$$\left(\frac{dI}{d\epsilon}\right)_{\epsilon=0} = \left(\frac{dI}{d\epsilon}\right)_{\epsilon=0} d\epsilon = \delta I = 0 \quad (2A.41)$$

and the integral to be made stationary is that given in (2A.2), where the Lagrangian is

$$L(t, q_i, \dot{q}_i) = T(t, \dot{q}_i) - V(t, q_i) \quad (2A.42)$$

and  $T$  here is the kinetic energy. Now  $\delta I$  is

$$\delta \int L(t, q_i, \dot{q}_i) dt = \int \delta L(t, q_i, \dot{q}_i) dt \quad (2A.43)$$

and  $\delta L$  is

$$\delta L(t, q_i, \dot{q}_i) = \sum_i \frac{\partial L}{\partial q_i} \delta q_i + \frac{\partial L}{\partial \dot{q}_i} \delta \dot{q}_i. \quad (2A.44)$$

This we may simplify by considering for the moment just the terms in  $\delta \dot{q}_i$ . From section 2A.3 (equation (2A.38)) we have that  $d$  and  $\delta$  commute. Alternatively we can see this by writing

$$\dot{q}_i + \delta \dot{q}_i = \frac{d}{dt}(q_i + \delta q_i) \quad (2A.45)$$

from which we obtain

$$\begin{aligned} \delta \dot{q}_i &= \frac{d}{dt}(q_i + \delta q_i - q_i), \\ \delta \dot{q}_i &= \frac{d}{dt} \delta q_i. \end{aligned} \quad (2A.46)$$

In any case each of the  $\delta\dot{q}_i$  terms may be written

$$\int \frac{\partial L}{\partial \dot{q}_i} \delta\dot{q}_i dt = \int \frac{\partial L}{\partial \dot{q}_i} \frac{d}{dt} \delta q_i dt, \quad (2A.47)$$

which we can integrate by parts

$$\int \frac{\partial L}{\partial \dot{q}_i} \frac{d}{dt} \delta q_i dt = \left[ \frac{\partial L}{\partial \dot{q}_i} \delta q_i \right]_{t_1}^{t_2} - \int_{t_1}^{t_2} \frac{d}{dt} \left[ \frac{\partial L}{\partial \dot{q}_i} \right] \delta q_i dt. \quad (2A.48)$$

Now since  $t_1$  and  $t_2$  are the end-points of integration at which, by definition, any variations are zero, the first term on the right hand side of (2A.48) must vanish. Then all the terms (integrals) involving  $\delta\dot{q}_i$  take the form of the second term, that is,

$$\int \frac{\partial L}{\partial \dot{q}_i} \delta\dot{q}_i dt = - \int_{t_1}^{t_2} \frac{d}{dt} \left[ \frac{\partial L}{\partial \dot{q}_i} \right] \delta q_i dt. \quad (2A.49)$$

The variational equation

$$\int_{t_1}^{t_2} \sum_i \left[ \frac{\partial L}{\partial q_i} \delta q_i + \frac{\partial L}{\partial \dot{q}_i} \delta\dot{q}_i \right] dt = 0 \quad (2A.50)$$

is rewritten by taking the negative as

$$\int_{t_1}^{t_2} \sum_i \left[ - \frac{\partial L}{\partial q_i} \delta q_i - \frac{\partial L}{\partial \dot{q}_i} \delta\dot{q}_i \right] dt = 0. \quad (2A.51)$$

We then substitute for the  $-(\partial L/\partial \dot{q}_i) \delta\dot{q}_i$  integrals from (2A.49) giving

$$\int_{t_1}^{t_2} \sum_i \left[ \frac{d}{dt} \left( \frac{\partial L}{\partial \dot{q}_i} \right) \delta q_i - \frac{\partial L}{\partial q_i} \delta q_i \right] dt = 0, \quad (2A.52)$$

which simplifies to

$$\int_{t_1}^{t_2} \sum_i \left[ \frac{d}{dt} \left( \frac{\partial L}{\partial \dot{q}_i} \right) - \frac{\partial L}{\partial q_i} \right] \delta q_i dt = 0. \quad (2A.53)$$

This equation must hold for any arbitrary variation  $\delta q_i$  in any of the  $q_i$ . It turns out that this requires each individual term in the summation over  $i$  to vanish. In other words we must have

$$\frac{d}{dt} \left( \frac{\partial L}{\partial \dot{q}_i} \right) - \frac{\partial L}{\partial q_i} = 0 \quad \forall i, \quad (2A.54)$$

thus giving rise to a set of coupled second order differential equations—a set of Euler-Lagrange equations. In this specific and very important case these equations are referred to as the Lagrangian equations of motion.

Next, we consider the general case where there are multiple variables of integration and one dependent variable. The stationary variational condition is (2A.41) as before, but  $\delta I$  is now

$$\delta \int F(\{x\}, y, \{y'\}) d\{x\} = \int \delta F(\{x\}, y, \{y'\}) d\{x\} \quad (2A.55)$$

and  $\delta F$  is

$$\delta F(\{x\}, y, \{y'\}) = \frac{\partial F}{\partial y} \delta y + \sum_i \frac{\partial F}{\partial y'_i} \delta y'_i, \quad (2A.56)$$

where  $y'_i = dy/dx_i$  and  $i$  labels the independent variables. This we may simplify by considering for the moment just the terms in  $\delta y'_i$ . Again we recall that  $d$  and  $\delta$  commute:

$$y'_i + \delta y'_i = \frac{d}{dx_i}(y\{x\} + \delta y\{x\}),$$

$$\delta y'_i = \frac{d}{dx_i}(y\{x\} + \delta y\{x\} - y\{x\}),$$

$$\delta y'_i = \frac{d}{dx_i} \delta y\{x\}. \quad (2A.57)$$

Each of the  $\delta y'_i$  terms is then written

$$\int \frac{\partial F}{\partial y'_i} \delta y'_i d\{x\} = \int \frac{\partial F}{\partial y'_i} \frac{d}{dx_i} \delta y d\{x\}, \quad (2A.58)$$

which we integrate by parts

$$\int \frac{\partial F}{\partial y'_i} \frac{d}{dx_i} \delta y d\{x\} = \left[ \frac{\partial F}{\partial y'_i} \delta y \right]_{\{x\}_1}^{\{x\}_2} - \int_{\{x\}_1}^{\{x\}_2} \frac{d}{dx_i} \left[ \frac{\partial F}{\partial y'_i} \right] \delta y d\{x\}. \quad (2A.59)$$

Again, since  $\{x\}_1$  and  $\{x\}_2$  are the end-points of integration the first term on the right hand side of (2A.59) vanishes and so all the integrals involving the  $\delta y'_i$  take the form

$$\int \frac{\partial F}{\partial y'_i} \delta y'_i d\{x\} = - \int_{\{x\}_1}^{\{x\}_2} \frac{d}{dx_i} \left[ \frac{\partial F}{\partial y'_i} \right] \delta y d\{x\}. \quad (2A.60)$$

We then substitute (2A.60) into the variational equation

$$\int_{\{x\}_1}^{\{x\}_2} \left[ \frac{\partial F}{\partial y} \delta y + \sum_i \frac{\partial F}{\partial y'_i} \delta y'_i \right] d\{x\} = 0 \quad (2A.61)$$

giving

$$\int_{\{x\}_1}^{\{x\}_2} \left[ \frac{\partial F}{\partial y} \delta y - \sum_i \frac{d}{dx_i} \left( \frac{\partial F}{\partial y} \right) \delta y \right] d\{x\} = 0 \quad (2A.62)$$

which simplifies to

$$\int_{\{x\}_1}^{\{x\}_2} \left[ \sum_i \frac{d}{dx_i} \left( \frac{\partial F}{\partial y} \right) - \frac{\partial F}{\partial y} \right] \delta y d\{x\} = 0. \quad (2A.63)$$

This equation must hold for any arbitrary fluctuation  $\delta y$  and so in the absence of any constraints the Euler-Lagrange equation would be the condition that the remaining factor in the integrand vanish. That is,

$$\sum_i \frac{d}{dx_i} \left( \frac{\partial F}{\partial y} \right) - \frac{\partial F}{\partial y} = 0. \quad (2A.64)$$

In the presence of constraints, each constraint  $j$  is written in the form (2A.21) and the integral to be made stationary is of the form (2A.22), namely in this case

$$I = \int_{\{x\}_1}^{\{x\}_2} \left( F(\{x\}, y, \{y'\}) + \sum_j \lambda_j c_j \right) d\{x\}. \quad (2A.65)$$

At this point we could simply write the Euler-Lagrange equation in the earlier form (2A.23), substituting  $F + \sum_j \lambda_j c_j$  for  $F$ . However, if the constraints

$$\delta \int c_j d\{x\} = \int \delta c_j d\{x\} = 0 \quad (2A.66)$$

can be written in the form

$$\int s_j \delta y d\{x\} = 0 \quad (2A.67)$$

(where  $\delta c_j = s_j \delta y$ ) then equation (2A.61) becomes

$$\int_{\{x\}_1}^{\{x\}_2} \left[ \frac{\partial F}{\partial y} \delta y + \sum_i \frac{\partial F}{\partial y'_i} \delta y'_i + \sum_j \lambda_j s_j \delta y \right] d\{x\} = 0 \quad (2A.68)$$

giving

$$\int_{\{x\}_1}^{\{x\}_2} \left[ \frac{\partial F}{\partial y} \delta y - \sum_i \frac{d}{dx_i} \left( \frac{\partial F}{\partial y} \right) \delta y + \sum_j \lambda_j s_j \delta y \right] d\{x\} = 0, \quad (2A.69)$$

which simplifies to

$$\int_{\{x\}_1}^{\{x\}_2} \left[ \sum_i \frac{d}{dx_i} \left( \frac{\partial F}{\partial y} \right) - \frac{\partial F}{\partial y} - \sum_j \lambda_j s_j \right] \delta y d\{x\} = 0. \quad (2A.70)$$

The Euler-Lagrange equation is then

$$\sum_i \frac{d}{dx_i} \left( \frac{\partial F}{\partial y} \right) - \frac{\partial F}{\partial y} - \sum_j \lambda_j s_j = 0. \quad (2A.71)$$

It turns out that this method of including constraints is the one that is more useful for our purposes and the one employed in molecular field theory.

Finally we note that in the most general multivariate case we could possibly have (multiple independent and dependent variables), we obtain a set of Euler-Lagrange equations of the form (2A.64) or (2A.71), one for each dependent variable.

## 2A.5 Application to Distribution Functions in Statistical Mechanics

Apart from the formal underlying basis of theoretical mechanics/electromagnetics we can also apply the same mathematical technique in classical statistical mechanics to obtain the equilibrium distribution functions of systems. In fact, this application turns out to be just a limiting case of the many independent variable, single dependent variable case already discussed. That is, the equilibrium distribution of a system over the degrees of freedom available to it is by definition that which minimises the thermodynamic potential function. In the familiar canonical ensemble this is the Helmholtz free energy. This suggests that we should make the free energy stationary with respect to fluctuations in the distribution function. To do this, we must be able to write the free energy in such a way as to conform to the structure of the problem already given. In a system with one degree of freedom we would have to be able to write the free energy

in the form (2A.1) with  $y = y(x)$  being the distribution function over the single degree of freedom  $x$ . More generally, in a system with multiple degrees of freedom  $\{x\}$  we would have to be able to write the free energy in the form (2A.3) with the distribution function now being  $y = y\{x\}$ , a many-body distribution. That this is always possible can be seen as follows. The bulk internal energy,  $U$ , is

$$U = \langle U\{x\} \rangle_{P\{x\}}, \quad (2A.72)$$

where  $P\{x\}$  is the many-body distribution function, and the entropy is

$$S = -N_A k_B \int P\{x\} \ln P\{x\} d\{x\}. \quad (2A.73)$$

Thus the Helmholtz free energy is

$$A = U + N_A k_B T \int P\{x\} \ln P\{x\} d\{x\}. \quad (2A.74)$$

However, since  $U$  is averaged over  $P\{x\}$ , it is not a function of the variables of integration. In addition,  $k_B$  and  $T$  are not functions of the degrees of freedom either. Therefore the free energy can be written as a single integral

$$I = A = \int_{\{x\}_1}^{\{x\}_2} \left( U/X + k_B T P\{x\} \ln P\{x\} \right) d\{x\}, \quad (2A.75)$$

where

$$X = \int_{\{x\}_1}^{\{x\}_2} d\{x\}. \quad (2A.76)$$

Alternatively we can use the fact that the definition of  $\langle U\{x\} \rangle_{P\{x\}}$ ,

$$\langle U\{x\} \rangle_{P\{x\}} = \int_{\{x\}_1}^{\{x\}_2} U\{x\} P\{x\} d\{x\}, \quad (2A.77)$$

involves integration over the same ranges of the same variables, and write the free energy as

$$A = \int_{\{x\}_1}^{\{x\}_2} \left( U\{x\} P\{x\} + k_B T P\{x\} \ln P\{x\} \right) d\{x\}. \quad (2A.78)$$

While the latter would appear to be the most straightforward, both manipulations will turn out to be useful.

We can obtain the Euler-Lagrange equation in this instance as follows (although as we shall see later this is not actually necessary in this class of problems). The stationary variational condition is, of course, (2A.41) as before. The integrand in (2A.75) is thus identified with that in the general definition of the problem given in (2A.3), and so in this case we would have in principle

$$F = F(\{x\}, P\{x\}, \{P'\}). \quad (2A.79)$$

Then  $\delta I$  would be

$$\delta \int F(\{x\}, P\{x\}, \{P'\}) d\{x\} = \int \delta F(\{x\}, P\{x\}, \{P'\}) d\{x\} \quad (2A.80)$$

with  $\delta F$  as

$$\delta F(\{x\}, P\{x\}, \{P'\}) = \frac{\partial F}{\partial P\{x\}} \delta P\{x\} + \sum_i \frac{\partial F}{\partial P'_i} \delta P'_i, \quad (2A.81)$$

where  $P'_i = dP/dx_i$  and  $i$  labels the degrees of freedom. The analysis would then proceed as for the many independent variable case with  $P\{x\}$  replacing  $y$ ,  $\{P'_i\{x\}\}$  replacing  $\{y'_i\}$  and a single constraint, namely that the distribution be normalised. The latter is expressed in the form (2A.21) simply as

$$\int P\{x\} d\{x\} = k, \quad (2A.82)$$

where  $k = 1$ . In other words the variation (2A.66,2A.67) in the integral must be zero

$$\delta \int P\{x\} d\{x\} = \int \delta P\{x\} d\{x\} = 0, \quad (2A.83)$$

where  $c_j = c = P\{x\}$  and  $s_j = s = 1$ . This would then be added to the main variational equation, inserting the Lagrange multiplier  $\lambda$ ,

$$\delta \int F d\{x\} + \lambda \delta \int P d\{x\} = 0. \quad (2A.84)$$

The integral (2A.75) to be made stationary is then

$$I = \int (F + \lambda P) d\{x\}, \quad (2A.85)$$



where  $F + \lambda P$  now replaces  $F$ . The variational condition (2A.41) is then

$$\int \delta(F + \lambda P) d\{x\} = \int (\delta F + \lambda \delta P) d\{x\} = 0, \quad (2A.86)$$

which ultimately becomes the same as the analogue of (2A.62) but modified with the constraint as

$$\int_{\{x\}_1}^{\{x\}_2} \left[ \sum_i \frac{d}{dx_i} \left( \frac{\partial F}{\partial P\{x\}} \right) \delta P\{x\} - \frac{\partial F}{\partial P\{x\}} \delta P\{x\} - \lambda \delta P\{x\} \right] d\{x\} = 0, \quad (2A.87)$$

giving

$$\int_{\{x\}_1}^{\{x\}_2} \left[ \sum_i \frac{d}{dx_i} \left( \frac{\partial F}{\partial P\{x\}} \right) - \frac{\partial F}{\partial P\{x\}} - \lambda \right] \delta P\{x\} d\{x\} = 0. \quad (2A.88)$$

The Euler-Lagrange equation with the constraint would then be obtained as

$$\sum_i \frac{d}{dx_i} \left( \frac{\partial F}{\partial P\{x\}} \right) - \frac{\partial F}{\partial P\{x\}} - \lambda = 0. \quad (2A.89)$$

However, the analysis in the case where the integral to be made stationary is the free energy simplifies from the completely general formal case, since the integrand  $F$  is not explicitly a function of the gradients  $\{P'\}$  of the distribution, and so the partial derivatives with respect to them vanish. Therefore the Euler-Lagrange equation simplifies to

$$\frac{\partial F}{\partial P\{x\}} + \lambda = 0. \quad (2A.90)$$

Indeed, the situation simplifies even further in this class of problems since, as we mentioned earlier, proceeding with this analysis all the way to the Euler-Lagrange equation is not actually necessary. Fortunately, we are able to obtain the distribution function in terms of relationships between physically meaningful quantities without having to cast the problem in its most general form and then solve the resulting differential equation explicitly.

The crucial feature in the statistical physics that enables us to obtain the distribution with such ease is the known relationship between the internal energy contribution to

the free energy and the distribution function we are trying to find. This may either be a direct relationship, or, in certain approximations of the statistical mechanics, through some parameter relating to the system which is itself an average over the distribution, thereby again providing the required relationship, albeit indirectly. It is the latter situation which obtains in the the molecular field theory of nematics, and the distribution function-related parameter from which the internal energy is constructed is the order parameter. We note that in such approximate treatments there may be more than one parameter, depending on the level of the theory.

In the general case of the many body distribution the analysis proceeds as follows. The free energy is  $U - TS$  where  $U$  is given by (2A.72) and  $S$  is given by (2A.73). If we write the free energy first of all as in (2A.78) then

$$\begin{aligned}
\delta I = \delta A &= \int \left( U\{x\} \delta P\{x\} + k_B T \delta [P\{x\} \ln P\{x\}] \right) d\{x\} \\
&= \int \left( U\{x\} \delta P\{x\} + k_B T [ \delta P\{x\} \ln P\{x\} + P\{x\} \delta (\ln P\{x\}) ] \right) d\{x\} \\
&= \int \left( U\{x\} \delta P\{x\} + k_B T [ \delta P\{x\} \ln P\{x\} + \delta P\{x\} ] \right) d\{x\}. \tag{2A.91}
\end{aligned}$$

We now take account of the constraint

$$\int P\{x\} d\{x\} = 1, \tag{2A.92}$$

which we write as,

$$\delta \int P\{x\} d\{x\} = 0 \tag{2A.93}$$

to give

$$\int \left( U\{x\} \delta P\{x\} + k_B T [ \delta P\{x\} \ln P\{x\} + \delta P\{x\} ] \right) d\{x\} + \lambda \delta \int P\{x\} d\{x\} = 0, \tag{2A.94}$$

which reduces to

$$\int \left( U\{x\} + k_B T [ \ln P\{x\} + 1 ] + \lambda \right) \delta P\{x\} d\{x\} = 0. \tag{2A.95}$$

This has to be true for any arbitrary  $\delta P\{x\}$  so we must have

$$U\{x\} + k_B T [\ln P\{x\} + 1] + \lambda = 0, \quad (2A.96)$$

which we solve to obtain the distribution as

$$P\{x\} = \exp [-(U\{x\} + \lambda)/k_B T - 1]. \quad (2A.97)$$

But this is just the Boltzmann distribution

$$P\{x\} = \exp (-U\{x\}/k_B T) \exp (-\lambda/k_B T - 1) \propto \exp (-U\{x\}/k_B T) \quad (2A.98)$$

if we identify the constant of proportionality as the normalising inverse partition function. That is,

$$P\{x\} = Z^{-1} \exp (-U\{x\}/k_B T), \quad (2A.99)$$

where

$$Z^{-1} = \exp (-\lambda/k_B T - 1). \quad (2A.100)$$

In this case the variational analysis has not afforded us anything other than what we already know—that the distribution  $P\{x\}$  over the states  $\{x\}$  is just the Boltzmann distribution for the corresponding energies  $U\{x\}$ . This situation changes, however, in approximations of the statistical mechanics in which we are able to construct  $U$  in terms of some parameter(s) which are themselves averages over the distribution function, rather than in terms of the distribution directly. In these cases we obtain an explicit form for the function  $U\{x\}$  (where  $\{x\}$  may now represent one or more degrees of freedom) in terms of the parameters and their non-ensemble averaged counterparts. We shall now demonstrate how this comes about. We imagine that there is some function  $p\{x\}$ , the ensemble average of which is  $\bar{p}$  (or in general  $p_i\{x\}$  and  $\bar{p}_i$  where  $i$  labels the functions and corresponding parameters). We assume that the energy  $U$  can be written as some power of  $\bar{p}$  for which the most general expression would be  $a\bar{p}^n$  (where  $a$  is an arbitrary coefficient) or, for more than one parameter,  $\sum_i a_i \bar{p}_i^{n_i}$ . Of course, the contribution from each parameter might be better represented by a power

series, rather than a single term of given order, but that does not affect the essentials of the analysis presented here.

Staying with a single parameter  $\bar{p}$  for the moment, we see that if the energy is other than linear in the parameter then we are unable to combine energy and entropy integrals in the straightforward manner of (2A.78). Instead, the integral to be made stationary can be made to conform to the formal definition by integrating  $U$  itself and renormalising as in (2A.75). However, once we have established that the free energy can be written in this way, the fact that this integral is equal to the free energy which is equal to the sum of two separate terms, and that  $\delta$  is distributive over addition means that we may write

$$\delta A = \delta U(\bar{p}) - T\delta S$$

$$= a' \delta [(\bar{p})^n] + k_B T \int \delta [P\{x\} \ln P\{x\}] d\{x\} \quad (2A.101)$$

$$= a' n (\bar{p})^{n-1} \delta \bar{p} + k_B T \int [1 + \ln P\{x\}] \delta P\{x\} d\{x\}. \quad (2A.102)$$

The fact that we do not yet have this expression in the form of a single integral is not, in itself, critical. The feature that is critical in these analyses, however, is having the final equation for the variation in the quantity (here the free energy) as a single integral. Only then can we factor out the fluctuation in the distribution from the integrand and assert that the remainder vanishes to obtain the distribution, and thence the energy function. To achieve this, we invoke the definition of  $\bar{p}$  in terms of the distribution function

$$\bar{p} = \int p\{x\} P\{x\} d\{x\} \quad (2A.103)$$

which implies that

$$\delta \bar{p} = \int p\{x\} \delta P\{x\} d\{x\}. \quad (2A.104)$$

Thus we may write

$$\begin{aligned}\delta A &= \int a' n \bar{p}^{n-1} p\{x\} \delta P\{x\} d\{x\} + k_B T \int [1 + \ln P\{x\}] \delta P\{x\} d\{x\}. \\ &= \int \left( a \bar{p}^{n-1} p\{x\} \delta P\{x\} + k_B T [1 + \ln P\{x\}] \delta P\{x\} \right) d\{x\} = 0,\end{aligned}\quad (2A.105)$$

where  $a = a'/n$ . We now take into account the constraint that the distribution is normalised,

$$\int \delta P\{x\} d\{x\} = 0,\quad (2A.106)$$

which we add to the equation inserting the Lagrange multiplier  $\lambda$  to give

$$\int \left( a \bar{p}^{n-1} p\{x\} \delta P\{x\} + k_B T [1 + \ln P\{x\}] \delta P\{x\} + \lambda \delta P\{x\} \right) d\{x\} = 0.\quad (2A.107)$$

The stationary variational condition is then

$$\int \left( a \bar{p}^{n-1} p\{x\} + k_B T [1 + \ln P\{x\}] + \lambda \right) \delta P\{x\} d\{x\} = 0,\quad (2A.108)$$

which implies

$$a \bar{p}^{n-1} p\{x\} + k_B T [1 + \ln P\{x\}] + \lambda = 0,\quad (2A.109)$$

solution of which yields

$$P\{x\} = \exp(-a \bar{p}^{n-1} p\{x\}/k_B T) \exp(-1 - \lambda/k_B T).\quad (2A.110)$$

If we identify the constant of proportionality in the Boltzmann distribution,  $Z^{-1}$ , as

$$Z^{-1} = \exp(-1 - \lambda/k_B T)\quad (2A.111)$$

then the energy function in the Boltzmann factor is

$$U\{x\} = a \bar{p}^{n-1} p\{x\}.\quad (2A.112)$$

Thus the variational analysis has given us the energy of a state as a function of the degree(s) of freedom of the system.

In the case where multiple parameters are taken to be important in determining the bulk thermodynamic energy, the analysis is the same except that we now have

$$\begin{aligned}\delta U\{\bar{p}_i\} &= \sum_i a'_i \delta[\bar{p}_i^{n_i}] \\ &= \sum_i a_i \bar{p}_i^{n_i-1} \delta\bar{p}_i,\end{aligned}\tag{2A.113}$$

where  $a_i = a'_i n_i$ . Then for each  $\delta\bar{p}_i$  we have

$$\delta\bar{p}_i = \int p_i\{x\} \delta P\{x\} d\{x\}\tag{2A.114}$$

so that

$$\delta U\{\bar{p}_i\} = \int \left( \sum_i a_i \bar{p}_i^{n_i-1} p_i\{x\} \right) \delta P\{x\} d\{x\}.\tag{2A.115}$$

This equation for  $\delta U$  and the constraint equation are then combined with the entropy term integral to give

$$\int \left( \sum_i a_i \bar{p}_i^{n_i-1} p_i\{x\} + k_B T [1 + \ln P\{x\}] + \lambda \right) \delta P\{x\} d\{x\} = 0.\tag{2A.116}$$

This implies

$$\sum_i a_i \bar{p}_i^{n_i-1} p_i\{x\} + k_B T [1 + \ln P\{x\}] + \lambda = 0,\tag{2A.117}$$

from which we obtain the distribution as

$$P\{x\} = \exp\left(-\sum_i a_i \bar{p}_i^{n_i-1} p_i\{x\}/k_B T\right) \exp(-1 - \lambda/k_B T)\tag{2A.118}$$

and the energy function as

$$U\{x\} = \sum_i a_i \bar{p}_i^{n_i-1} p_i\{x\}.\tag{2A.119}$$

A similar kind of analysis obtains whether we consider many parameters to be important taken to the same or differing order, or one parameter in a power series or some combination of all of these.

In the molecular field theory of nematics the parameters are the order parameters, functions of the angular variables of interest averaged over the corresponding distribution function. In the case of uniaxial phases of uniaxial particles, we have only one degree of freedom,  $\beta$ , the polar angle. The angular functions are then the  $P_L(\cos \beta)$  and the parameters are the averages of these, the  $\bar{P}_L$ . According to de Gennes [5] the orientational configurational internal energy of a liquid crystal is quadratic in the order parameter(s), and so we take  $n_i = n = 2 \forall i$ .

In the variational derivation of the Maier-Saupe theory, the second rank order parameter,  $\bar{P}_2$ , is taken to predominate the internal energy. The coefficient we have been calling  $a'$  is written as  $-\epsilon/2$  so that with  $n = 2$  we have  $a = a'n = -\epsilon$ . The distribution, which we now write as  $f(\beta)$ , is then

$$f(\beta) = \exp(\epsilon \bar{P}_2 P_2(\cos \beta)/k_B T) \exp(-1 - \lambda/k_B T), \quad (2A.120)$$

that is,

$$f(\beta) = Z^{-1} \exp(\epsilon \bar{P}_2 P_2(\cos \beta)/k_B T) \quad (2A.121)$$

with

$$Z^{-1} = \exp(-1 - \lambda/k_B T). \quad (2A.122)$$

The energy function here is the rotational analogue of the potential of mean force, that is, the *potential of mean torque*

$$U(\beta) = -\epsilon \bar{P}_2 P_2(\cos \beta), \quad (2A.123)$$

which is the Maier-Saupe result.

A more general variational derivation is obtained by considering all the  $\bar{P}_L$  to be important in principle in determining the internal energy. In this case we have  $a'_i = -\epsilon_L/2$  and  $a_i = a'_i n = -\epsilon_L$ , thus giving the distribution as

$$f(\beta) = \exp\left(\sum_L \epsilon_L \bar{P}_L P_L(\cos \beta)/k_B T\right) \exp(-1 - \lambda/k_B T)$$

$$= Z^{-1} \exp \left( \sum_L \epsilon_L \bar{P}_L P_L(\cos \beta) / k_B T \right). \quad (2A.124)$$

The potential of mean torque is then

$$U(\beta) = - \sum_L \epsilon_L \bar{P}_L P_L(\cos \beta). \quad (2A.125)$$

So we see that the Maier-Saupe result is really a limiting case in which we take only the first term in the generalised molecular field theory potential.





## References

- [1] G. R. Luckhurst in *The Molecular Physics of Liquid Crystals*, edited by G. R. Luckhurst and G. W. Gray, Academic Press, London, Chapter 3 (1979).
- [2] R. L. Humphries, P. G. James and G. R. Luckhurst, *J. Chem. Soc. Faraday Trans. II*, **68**, 1031 (1972).
- [3] T. D. Schultz in *Liquid Crystals3*, edited by G. H. Brown and M. M. Labes, Gordon and Breach, p. 263 (1972).
- [4] C. Zannoni, PhD thesis, University of Southampton (1975).
- [5] P. G. de Gennes and J. Prost, *The Physics of Liquid Crystals*, second edition, Clarendon Press, Oxford (1993).
- [6] A. Wulf, *J. Chem. Phys.*, **55**, 4512 (1971).
- [7] L. Shen, H. K. Sim, Y. M. Shih and C.-W. Woo, *Mol. Cryst. Liq. Cryst.*, **39**, 229 (1977); M. A. Lee and C.-W. Woo, *Phys. Rev. A*, **16**, 750 (1977); V. T. Rajan and C.-W. Woo, *ibid.* **17**, 382 (1978).
- [8] J. P. Hansen and I. R. McDonald, *Theory of Simple Fluids*, Academic Press (1976).
- [9] W. Maier and A. Saupe, *Z. Naturforsch.*, **13a**, 564 (1958).
- [10] W. Maier and A. Saupe, *Z. Naturforsch.*, **14a**, 882 (1959).
- [11] W. Maier and A. Saupe, *Z. Naturforsch.*, **15a**, 287 (1960).
- [12] L. Neel, *Comptes Rendues*, **203**, 304 (1936).
- [13] J. S. Smart, *Am. J. Phys.*, **23**, 356 (1955).
- [14] S. J. Roskilly, PhD Thesis, University of Southampton (1994).
- [15] P. A. Lebwohl and G. Lasher, *Phys. Rev. A.*, **6**, 426 (1972).

- [16] See, for example, G. R. Luckhurst in *The Molecular Physics of Liquid Crystals*, edited by G. R. Luckhurst and G. W. Gray, Academic Press, London, Chapter 3 (1979).
- [17] G. R. Luckhurst and P. Simpson, *Mol. Phys.*, **47**, 251 (1982).
- [18] F. Biscarini, C. Zannoni, C. Chiccoli and P. Pasini, *Mol. Phys.*, **73**, 439 (1991).
- [19] G. R. Luckhurst, C. Zannoni, P. L. Nordio and U. Segre, *Mol. Phys.*, **30**, 1345 (1975).
- [20] M. Boas, *Mathematical Methods in the Physical Sciences*, Wiley, New York (1983).
- [21] R. Weinstock, *Calculus of Variations with Applications to Physics and Engineering*, McGraw-Hill, New York (1952).

# Chapter 3: Electric Field Polarisation of Nematic Liquid Crystals: A Molecular Field Theory

## 3.1 Aims and Rationale

In the absence of external fields, a nematic liquid crystal is a non-polar, non-ferroelectric phase; however, there is interest in making polarised systems because of their potential non-linear optical properties. One way that has been conceived for achieving this is to polarise (or pole) a nematic and then lower the temperature into a glassy nematic phase, hoping that the induced polarisation is preserved. It turns out that a nematic is more readily polarised by an electric field than a normal isotropic liquid [1], which would seem to confer a definite advantage on the technique. A polarised nematic glass is obtained via application of a static external field to a nematic liquid crystal polymer; with the field still being applied, the temperature is then lowered below that of its glass transition,  $T_{NgN}$ .

The aim of this study is to quantify the benefit of poling a nematic in terms of the long range polar order induced in the liquid crystal phase as a function of the electric field strength at a specified temperature. We would like to estimate the poling fields required and to investigate what factors influence the poling of nematics at a molecular level. The relevant choice of temperature is  $T_{NgN}$ , the temperature at which the induced polarisation (and nematic order) becomes frozen into the glass. There have been a number of previous attempts to develop a theory for this; the most complete of these appears to be that of Picken and van der Vorst [2], the Maier-Saupe-van der Vorst-Picken (MSVP) theory. Their theory, however, has certain deficiencies, as we shall see and we seek to rectify these here.

## 3.2 Formal Development of the Theory

In Chapter 2 we obtained the potential of mean torque for a uniaxial nematic in the absence of external fields. We must now make this complete in the context of the problem at hand and introduce the terms in the energy which arise from the direct interaction of the field with the test molecule.

The energy of interaction of the molecule with the electric field has two contributions. First, we have an energy resulting from the fact that the molecule has an anisotropic polarisability, hyperpolarisability, second hyperpolarisability and so on. The electric field interacts with these to induce electrical multipole moments which then interact with the field, giving rise to an energy. Secondly, there is also an energy coming from the interaction of the electric field with the permanent multipole moments of the molecule that result from the unevenness (anisotropy) in the molecular charge distribution. Assuming that the electric field-induced dipole interaction is dominant then the induction energy is

$$U_{\text{ind}} = -\Delta\alpha E^2 P_2(\cos \beta) - \Delta\beta E^3 P_3(\cos \beta) - \Delta\gamma E^4 P_4(\cos \beta) - \dots, \quad (3.1)$$

where  $E$  is the magnitude of the electric field, the angular dependence of the anisotropic potential energy terms being represented by the corresponding Legendre polynomials. Here  $\Delta\alpha$  is the anisotropy in the polarisability,  $\Delta\beta$  is that in the first hyperpolarisability,  $\Delta\gamma$  is that in the second hyperpolarisability and so on.

The energy due to the interaction of the permanent electrical moments of the molecule with the field is given by the sum of contributions from each of the electrical multipoles. That is,

$$U_{\text{perm}} = -\mu E P_1(\cos \beta) - Q E^2 P_2(\cos \beta) - O E^3 P_3(\cos \beta) \dots, \quad (3.2)$$

where the electric charge dipole is

$$\mu = \sum_i q_i r_i \quad (3.3)$$

( $q_i$  here being the charge at a distance  $r_i$  from some point of origin  $i$ ), the quadrupole is

$$Q = \sum_i q_i r_i^2, \quad (3.4)$$

the octopole is

$$O = \sum_i q_i r_i^3 \quad (3.5)$$

and so on. The total energy of interaction of the molecule with the electric field is then

$$U_{\text{elec}} = U_{\text{ind}} + U_{\text{perm}}, \quad (3.6)$$

which we can rewrite in a simple general form as

$$U_{\text{elec}} = - \sum_L x_L E^L P_L(\cos \beta). \quad (3.7)$$

Thus it can be seen that the permanent electric dipole alone contributes to  $x_1$ , the electric quadrupole and the polarisability anisotropy are both included in the coefficient  $x_2$  multiplying the quadratic term, the octopole and the first hyperpolarisability anisotropy contribute to  $x_3$  multiplying the cubic term, and so on.

Combining this with the general result derived in Chapter 2 (with allowance for non-zero odd rank order parameters) the complete, formally exact expression for the potential of mean torque for a nematic monodomain in the presence of a uniform static electric field is then

$$U(\beta) = - \sum_{L \text{ even}} u_L \bar{P}_L P_L(\cos \beta) - \sum_{L \text{ odd}} u_L \bar{P}_L P_L(\cos \beta) - \sum_L x_L E^L P_L(\cos \beta). \quad (3.8)$$

The expansion (3.8) is believed to converge quite rapidly except for the molecular field summations in the high order limit, since, except in the limit of high order, the order parameters normally diminish rapidly with increasing rank. If we assume, in a manner similar to the Maier-Saupe theory, that to a good approximation the summations may be truncated at the first term then equation (3.8) becomes

$$U(\beta) = -\{\epsilon_2 \bar{P}_2 P_2(\cos \beta) + \epsilon_1 \bar{P}_1 P_1(\cos \beta) + \mu E P_1(\cos \beta)\}, \quad (3.9)$$

which is the potential of mean torque we have used and where the  $u_L$  are now the  $\epsilon_L$  by convention. We note that if the potential of mean torque (in the absence of a field but acknowledging the existence of odd rank order parameters) is obtained from a variational analysis then  $\epsilon_2$  and  $\epsilon_1$  are just arbitrary coefficients bearing no definite relationship to the molecular structure. However, clearly there physically must be a relationship and we need to understand the molecular factors determining their values. In the case of the coefficient  $\epsilon_2$  of the second rank term that appears in the Maier-Saupe theory, it is understood to reflect the anisotropy of the molecule or, more strictly, the anisotropy in the intermolecular potential. In other words  $\epsilon_2$  should contain contributions from all anisotropic intermolecular interactions that are quadrupolar (second rank) in form. Similarly,  $\epsilon_1$  will contain contributions from all anisotropic interactions of first rank polar (ie, dipolar) character, whether this be the first moment of the charge distribution (electric dipole) or of the mass distribution (shape dipole) or some combination of the these.

### 3.3 Methodological Application

In this section we apply the theoretical development given in section 3.2 and discuss the methodology we have employed, comparing it to the previous theoretical studies undertaken by Picken and van der Vorst [2]. To do this, let us recapitulate briefly that which we require from the Maier-Saupe theory and extend it to the problem at hand. As we have already seen (see Chapter 2) the potential of mean torque of the Maier-Saupe theory for a molecule of  $D_{\infty h}$  symmetry in a necessarily non-polar phase is

$$U(\beta) = -\epsilon_2 \bar{P}_2 P_2(\cos \beta). \quad (3.10)$$

According to the Maier-Saupe theory the system undergoes a first order transition between the nematic and isotropic phases. The transition temperature is related to

the intrinsic strength parameter  $\epsilon_2$  by

$$T_{\text{NI}} = 0.2203 \epsilon_2 / k_B. \quad (3.11)$$

In the poling experiment, the molecule is now of  $C_{\infty v}$  (rather than  $D_{\infty h}$ ) symmetry; to maximise the polarisation achieved it has a substantial electrical dipole moment. To allow for the influence of the poling field van der Vorst and Picken [2] added two terms to this potential; these were

$$U_{\text{elec}} = -\{\mu E P_1(\cos \beta) + \frac{1}{3} \Delta \alpha E^2 P_2(\cos \beta)\}, \quad (3.12)$$

where  $\Delta \alpha$  is the anisotropy in the molecular polarisability ( $\alpha_{\parallel} - \alpha_{\perp}$ ),  $\parallel$  and  $\perp$  here referring to parallel and perpendicular to the molecular symmetry axes (not the director). The effect of the electric field in inducing polar order is reflected predominantly by the first rank order parameter,  $\bar{P}_1$ . The existence of this non-vanishing order parameter generates a polar molecular field to which the molecule can couple; to leading order within the molecular field approximation this demands the addition of the term

$$-\epsilon_1 \bar{P}_1 P_1(\cos \beta), \quad (3.13)$$

to the total potential of mean torque.

In fact, even in zero field this term should be included for a system of particles with  $C_{\infty v}$  symmetry [3]. The potential of mean torque then takes the form

$$U(\beta) = -\{\epsilon_2 \bar{P}_2 P_2(\cos \beta) + \epsilon_1 \bar{P}_1 P_1(\cos \beta)\}. \quad (3.14)$$

The molecular field coefficients ( $\epsilon_1$  and  $\epsilon_2$ ) are defined to be positive. The positive sense of the  $z$  axis (director) is then defined as that of the polarisation so that the polar order parameter  $\bar{P}_1$  is necessarily positive. Molecular field calculations [3] based on this potential show that the system may exhibit a polar nematic ( $N_p$ ) phase ( $\bar{P}_1 \neq 0, \bar{P}_2 \neq 0$ ), a non-polar nematic ( $N$ ) phase ( $\bar{P}_1 = 0, \bar{P}_2 \neq 0$ ) and an isotropic phase ( $\bar{P}_1 = 0, \bar{P}_2 = 0$ ). Whether it exhibits all these phases, and at what temperatures the transitions between them occur, is determined by the ratio  $\epsilon_1/\epsilon_2$ , that is, on the

relative importance of the first rank to the second rank term in the potential for the material. Depending on this ratio the system will undergo a second order transition from the polar to the non-polar nematic phase followed by a first order transition to the isotropic phase at a higher temperature. As the relative importance of the first rank term is increased the temperature of the  $N_p - N$  transition increases towards that of the  $N - I$  transition, so that the non-polar nematic range is progressively reduced. For sufficiently large values of  $\epsilon_1/\epsilon_2$  the transition from the polar nematic overtakes the  $N - I$  transition and there is a first order transition directly from the polar nematic to the isotropic phase [3]. In modelling the behaviour of real nematics, however, the polar molecular field term is usually ignored, even if (as is the case with most real nematics) the molecules possess a significant dipole moment. This neglect can be justified for two main reasons, to which we have already alluded in Chapter 2. One is that in a molecular field analysis starting from a pair potential the intermolecular vector is usually assumed to have a spherically symmetric probability density distribution function. As a direct result of the symmetry assumed for the distribution of the intermolecular vector all electrostatic contributions to the single particle potential necessarily vanish [4]. In real nematics, to be sure, the intermolecular vector has an anisotropic distribution and so electrostatic contributions will make a contribution [5]. One way in which they can be accounted for is to employ a variational derivation of the potential of mean torque [6]. Then provided that the order parameters  $\bar{P}_1$  and  $\bar{P}_2$  provide the dominant contributions to the anisotropic internal potential energy, the potential of mean torque is that given in (3.14) but the molecular significance of  $\epsilon_1$  and  $\epsilon_2$  is lost. The other main reason why the polar molecular field is often ignored is that no polar nematic phase has been observed for real nematics; the theoretical effect of the dipolar contribution only occurs at temperatures outside their nematic range. This observation enables us to place an upper limit on the ratio  $\epsilon_1/\epsilon_2$ , as we shall see.

While the foregoing observation implies that, within molecular field theory, the dipolar contribution may be safely ignored in the absence of a poling field the situation changes dramatically when an electric field is applied. This is due to the lowering of



the symmetry of the phase which inevitably results from the field-induced generation of polar order (see previous discussion in section 2.8.2). The polar molecular field contribution is necessarily non-vanishing due to the non-zero value of  $\bar{P}_1$  induced by the applied field. Formally, therefore, it is incorrect to exclude the term in  $\bar{P}_1$  from the single molecule potential as van der Vorst and Picken have done [2]. At a pragmatic level, however, their neglect of its effects may be justifiable. To see if this is so, we have investigated the electric field dependence of the order parameters  $\bar{P}_1$ ,  $\bar{P}_2$  and  $\bar{P}_3$ . We have included the evaluation of the third rank order parameter in the calculations because it is related to the non-linear optical coefficient and is therefore important for one of the main potential applications of these polarised systems. The total potential of mean torque which we have employed (and which we have already derived in a more formal way in section 3.2) is

$$U(\beta) = -\{\epsilon_2 \bar{P}_2 P_2(\cos \beta) + \epsilon_1 \bar{P}_1 P_1(\cos \beta) + \mu E P_1(\cos \beta)\}. \quad (3.15)$$

The quadratic term in the electric field (see equation (3.8)), which van der Vorst and Picken chose to represent via the polarisability only, excluding the quadrupolar contribution [2], has been suppressed. This simplification is justified because the term does not contribute significantly to the polarisation of the nematic. It is only important when calculating the coefficient of  $P_2(\cos \beta)$ , and hence  $\bar{P}_2$  which does not directly influence on  $\bar{P}_1$ .

### 3.4 The Free Energy

The orientational part of the configurational Helmholtz free energy of the system may be obtained by the means described in Chapter 2. In this case, we have that the internal energy is

$$\begin{aligned} U &= N_A \bar{U} = -\frac{N_A}{2} \left\langle \epsilon_1 \bar{P}_1 P_1(\cos \beta) + \epsilon_2 \bar{P}_2 P_2(\cos \beta) \right\rangle_{f(\beta)} \\ &= -\frac{N_A}{2} \left( \left\langle \epsilon_1 \bar{P}_1 P_1(\cos \beta) \right\rangle_{f(\beta)} + \left\langle \epsilon_2 \bar{P}_2 P_2(\cos \beta) \right\rangle_{f(\beta)} \right) \end{aligned}$$

$$= -\frac{N_A}{2}(\epsilon_1 \bar{P}_1^2 + \epsilon_2 \bar{P}_2^2). \quad (3.16)$$

Thus the free energy is given by

$$\begin{aligned} A &= -N_A \bar{U} - N_A k_B T \ln Z \\ &= \frac{N_A}{2}(\epsilon_1 \bar{P}_1^2 + \epsilon_2 \bar{P}_2^2) - N_A k_B T \ln Z, \end{aligned} \quad (3.17)$$

with  $Z$  as

$$Z = \int \exp\left(\{\epsilon_2 \bar{P}_2 P_2(\cos \beta) + (\epsilon_1 \bar{P}_1 + \mu E) P_1(\cos \beta)\} / k_B T\right) \sin \beta d\beta. \quad (3.18)$$

### 3.5 Evaluating the Orientational Order Parameters

The order parameters for any given temperature and field strength were obtained by minimising the molar orientational Helmholtz free energy

$$A = N_A(\epsilon_1 \bar{P}_1^2 + \epsilon_2 \bar{P}_2^2)/2 - RT \ln Z \quad (3.19)$$

with respect to the two degrees of freedom of the system, namely the two order parameters  $\bar{P}_1$  and  $\bar{P}_2$ . Having obtained the order parameters that occur in the potential of mean torque (and hence the free energy), the third rank order parameter was obtained from the distribution function as

$$\bar{P}_3 = Z^{-1} \int_0^\pi P_3(\cos \beta) \exp(-U(\beta)/k_B T) \sin \beta d\beta, \quad (3.20)$$

with  $U(\beta)$  is as given in equation (3.15).

### 3.6 Results and Discussion

In order to investigate the significance of the polar molecular field we have calculated the electric field dependence of the order parameters employing the same choice of

parameters used in the original calculation by Picken and van der Vorst [2]. Thus the temperature of the system was set to 380  $K$ , which is taken to be the glass transition temperature, while the  $N - I$  transition temperature,  $T_{NI}$  was set to either 420  $K$  or 340  $K$  so that the calculations would correspond to an initially nematic or initially isotropic phase, respectively. The coefficient,  $\epsilon_2$  was calculated from the transition temperatures using the Maier-Saupe result given in Section 2.8.4. Realistic values of  $\epsilon_1$  were obtained as follows. Since the molecular field theory based on the potential of mean torque given in (3.14) reveals that  $T_{N-N_p}$  is determined by the ratio  $\epsilon_1/\epsilon_2$  [7, 3], the value of  $\epsilon_1$  could be found if this temperature were known. No polar nematics have ever been observed, however, and so we are only able to place an upper limit on the reduced temperature for this transition and hence on the ratio  $\epsilon_1/\epsilon_2$ . Assuming the nematic range to be less than 100  $K$  the reduced transition temperature will be ca. 0.76 or higher based on  $T_{NI} = 420$   $K$ ; consequently we estimate that  $\epsilon_1/\epsilon_2 \leq$  ca. 0.2. We have performed the calculations for  $\epsilon_1/\epsilon_2$  equal to the upper limit, 0.2, and also half this value, namely 0.1. The range of electric fields employed was that used when poling liquid crystal side chain polymers, namely 0 – 10<sup>9</sup>  $\text{Vm}^{-1}$  [2], and the dipole moment was set to 7  $D$ , an appropriate value for such materials [2].

We begin the discussion of our results with the effect of the field on the non-polar order parameter,  $\bar{P}_2$ . Figure 3.1 shows the electric field dependence of  $\bar{P}_2$  for an initially nematic sample, for three values of  $\epsilon_1/\epsilon_2$ , namely, 0.2, 0.1 and 0. In all cases,  $\bar{P}_2$  increases with the field strength although its response is rather weak. With  $\epsilon_1/\epsilon_2$  set to zero the calculations essentially reproduce the results of the MSVP theory [2] which implies that the polarisability contribution to the quadratic term plays only a minor role. For  $\epsilon_1/\epsilon_2 \neq 0$ ,  $\bar{P}_2$  grows more rapidly with increasingly field, the rate of increase being higher the greater this ratio. The effect, however, is relatively small and the interpretation of its origin subtle. Even though the field induced growth of polar order stabilises molecular orientations less than  $\pi/2$  it destabilises those greater than this by the same amount (see equation (3.15)) so the overall effect on the potential of mean torque is zero. However, the net effect on the distribution function favours those

Figure 3.1: The dependence of the non-polar order parameter,  $\overline{P}_2$ , on the electric field,  $E$ , for three values of the ratio  $\epsilon_1/\epsilon_2$  of 0 ( $\cdots$ ), 0.1 ( $- - -$ ) and 0.2 ( $—$ ) for a nematogen with its  $N - I$  transition above the glass transition.

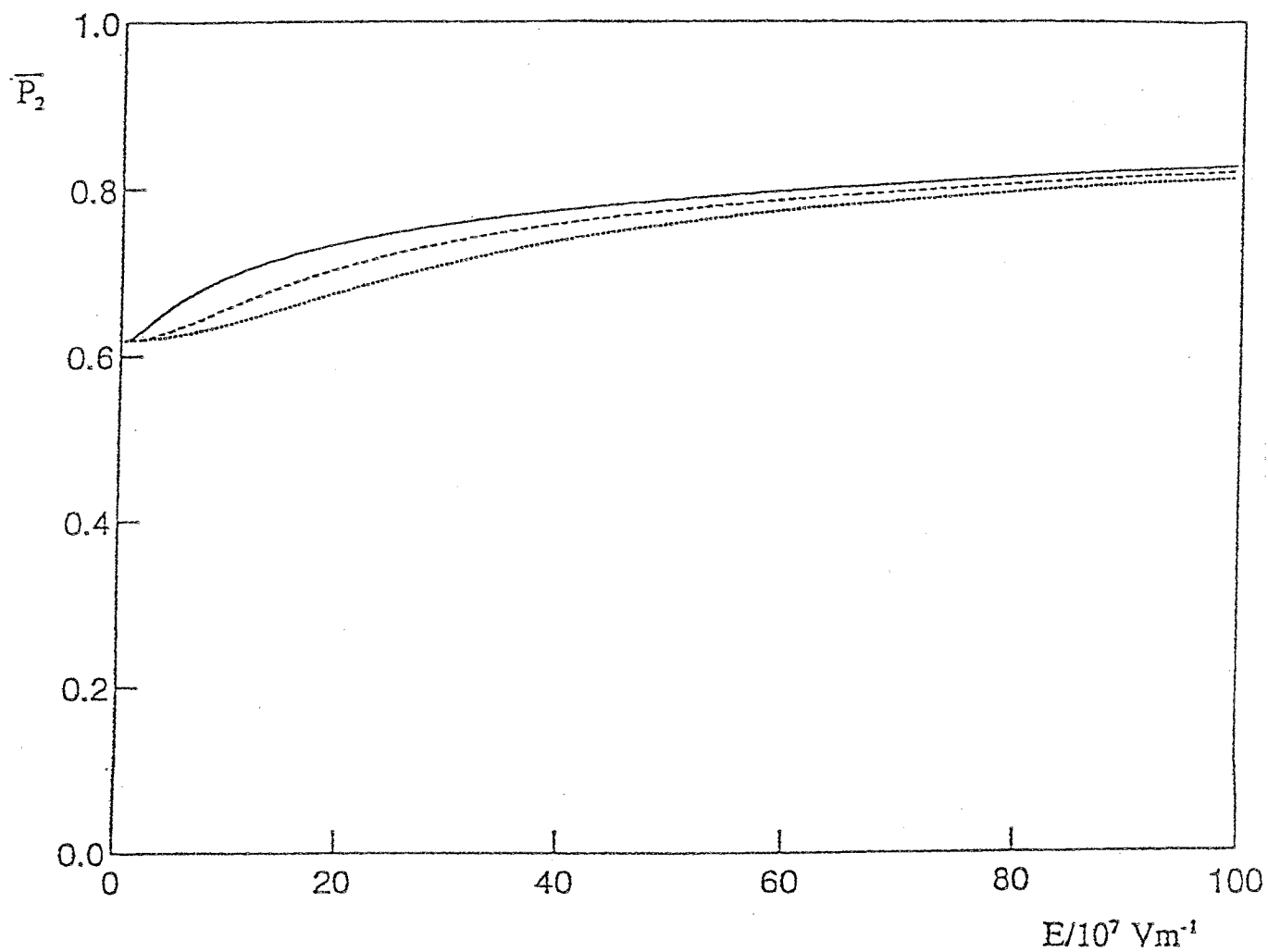
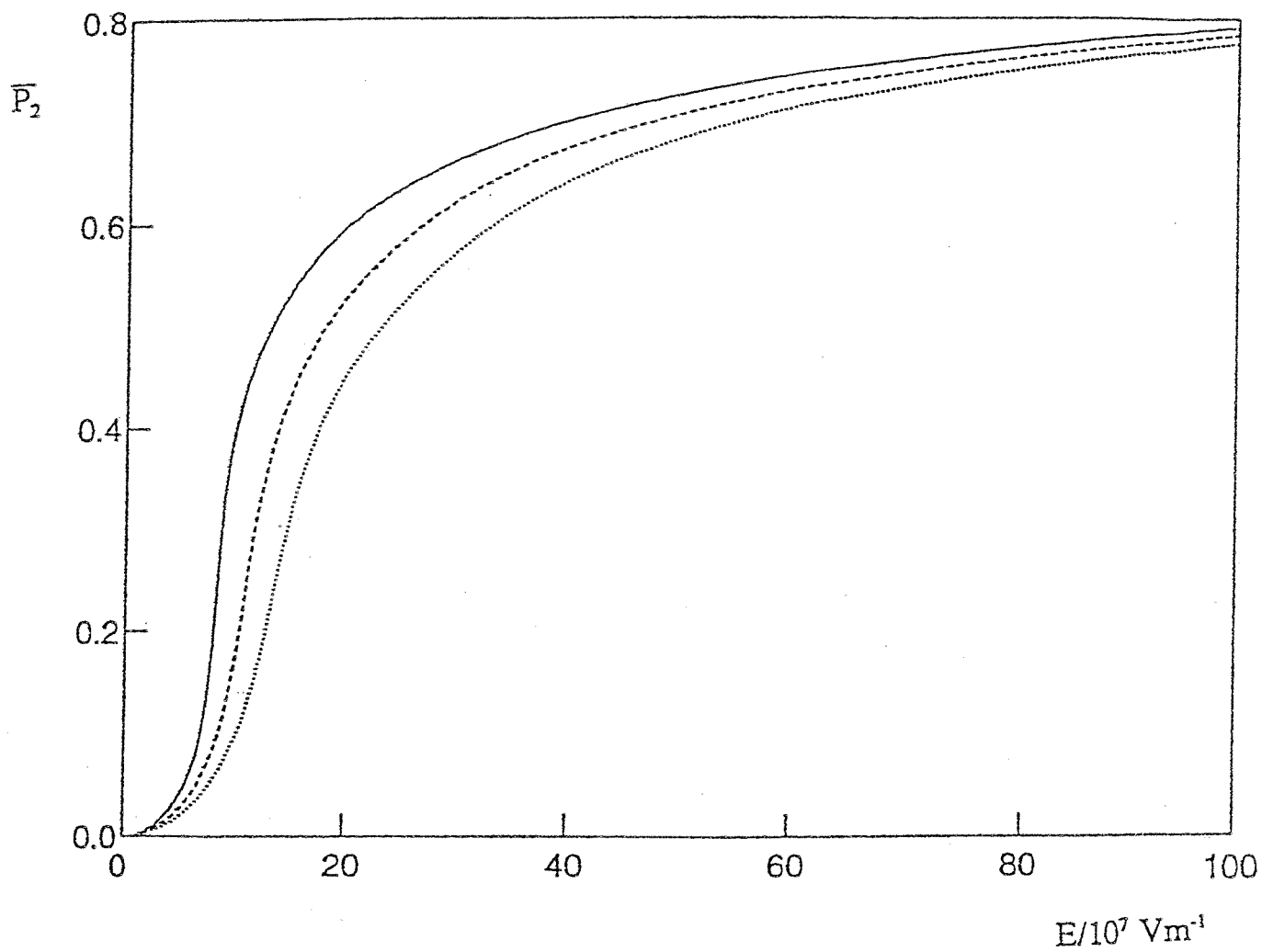


Figure 3.2: The dependence of the non-polar order parameter,  $\bar{P}_2$ , on the electric field,  $E$ , for three values of the ratio  $\epsilon_1/\epsilon_2$  of 0 ( $\cdots$ ), 0.1 ( $- - -$ ) and 0.2 ( $—$ ) for a nematogen with its  $N - I$  transition below the glass transition.



orientations parallel to the axis of polarisation more than those which are antiparallel, so that there is a small increase in  $\overline{P}_2$ , the rate of which depends on  $\epsilon_1/\epsilon_2$ . For the realistic values of this ratio which we have employed the polar molecular field in the potential of mean torque has a clear but only minor effect on the response of the second rank order parameter to the electric field when the system is already ordered. From a more formal point of view the initial response of  $\overline{P}_2$  is seen to be a second order effect, which can be seen by expanding the expression for  $\overline{P}_2$  [7](see also Appendix 3A).

This is not the case, however, when the system is initially isotropic as can be seen in figure 3.2. For small fields the induced polar order is very small, a result that can be shown, via a perturbation analysis, to have its origins in the orthogonality of  $P_1(\cos \beta)$  and  $P_2(\cos \beta)$  (see Appendix 3A) [7]. Around a certain threshold field, however, there is a dramatic acceleration in the rate of increase of  $\overline{P}_2$ . This behaviour is attributed to a field induced increase in  $T_{NI}$  so that as  $T_{NI}$  exceeds  $T_g$  the system becomes progressively more nematic. This effect leads to a much larger influence of the field and of the value of  $\epsilon_1/\epsilon_2$  on the second rank order parameter.

We now consider the ability of the polar molecular field to aid in the induction of the odd rank order parameters  $\overline{P}_1$  and  $\overline{P}_3$  by an electric field, beginning with  $\overline{P}_1$ . Figure 3.3 shows the numerically estimated field dependence for a system initially in its nematic phase for the same values of  $\epsilon_1/\epsilon_2$  as before. In all cases,  $\overline{P}_1$  increases, initially linearly, with the field. The initial response is expected from a perturbation analysis (see Appendix 3A) [7]. With further increase in the field  $\overline{P}_1$  tends to an upper limiting value of ca. 0.9 which is independent of  $\epsilon_1/\epsilon_2$ . This ratio does have a large influence on the initial rate of growth of  $\overline{P}_1$  with the field, however. Thus, the field at which  $\overline{P}_1$  reaches half its limiting value decreases from  $15.0 \times 10^7 \text{ Vm}^{-1}$  to  $5.0 \times 10^7 \text{ Vm}^{-1}$  as  $\epsilon_1/\epsilon_2$  increases from 0 through 0.1 to 0.2. This reduction in the field required to generate a given polar order, caused by the polar molecular field, has beneficial implications for the use of nematics in non-linear optics which have thus so far been overlooked, at least in their production. The practical benefit here is the lowering of the intensity of the electric field required to generate essentially limiting polar order.

Figure 3.3: The electric field dependence of the first rank polar order parameter,  $\overline{P}_1$ , calculated for three values of the ratio  $\epsilon_1/\epsilon_2$  of 0 ( $\cdots$ ), 0.1 ( $- - -$ ) and 0.2 ( $—$ ) for a nematogen with its  $N - I$  transition above the glass transition.

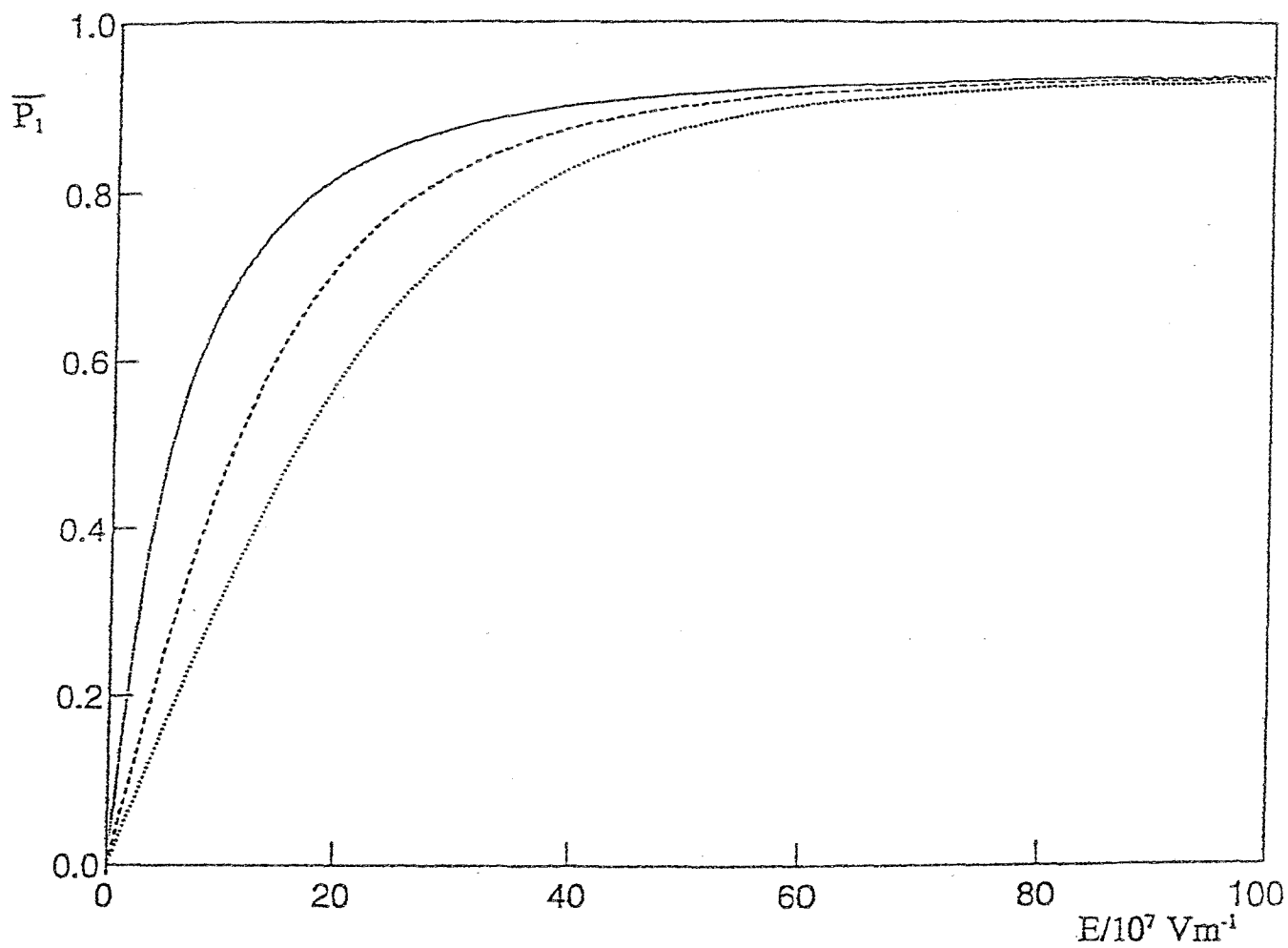
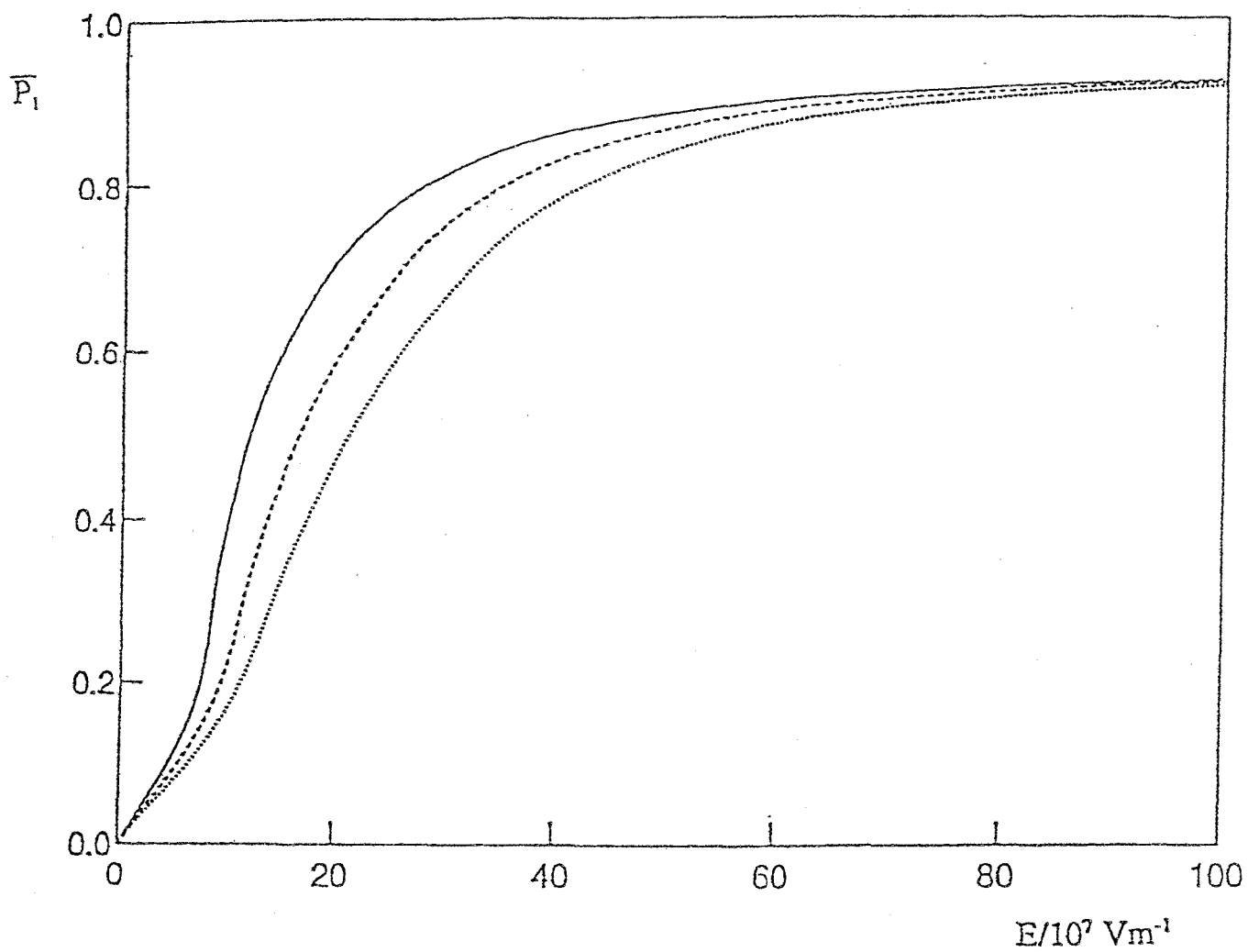


Figure 3.4: The electric field dependence of the first rank polar order parameter,  $\bar{P}_1$ , calculated for three values of the ratio  $\epsilon_1/\epsilon_2$  of 0 ( $\cdots$ ), 0.1 ( $- - -$ ) and 0.2 ( $—$ ) for a nematogen with its  $N - I$  transition below the glass transition.





A similar influence of  $\epsilon_1/\epsilon_2$  is predicted for an initially isotropic system, as we see in figure 3.4. At relatively low electric fields, since we are considering only a small perturbation to the isotropic phase, the ability of the electric field to induce polar order is weak. Even though the small applied field is assisted by a polar molecular field, the latter is also weak because it is a feedback mechanism generated by the external field itself, and so the effect of the electric field is relatively insensitive to  $\epsilon_1/\epsilon_2$ . As we go to higher fields, however, a threshold field is reached where  $T_{N_pI}$  exceeds  $T_{N_gN}$ ;  $\bar{P}_1$  then grows rapidly with increasing field. The threshold field is found to decrease with increasing  $\epsilon_1/\epsilon_2$ ; the threshold decreases from  $12 \times 10^7 \text{ Vm}^{-1}$  through  $10 \times 10^7 \text{ Vm}^{-1}$  to  $7 \times 10^7 \text{ Vm}^{-1}$  as we increase the ratio from 0 through 0.1 to 0.2. As for the initially nematic system,  $\bar{P}_1$  reaches a plateau at a limiting value of ca. 0.9 which is independent of  $\epsilon_1/\epsilon_2$ . Clearly, even above  $T_{NI}$ , quite reasonable values of this ratio significantly augment the predicted polarising power of the applied field.

Finally, we turn to the influence of the electric field on the third rank order parameter  $\bar{P}_3$ . The results for a system originally in its nematic phase, employing the same values of the ratio  $\epsilon_1/\epsilon_2$ , are shown in figure 3.5. Again we find an initial linear response, as expected from the perturbation analysis (see Appendix 3A) [7], the gradient of which increases significantly with increasing  $\epsilon_1/\epsilon_2$ . Beyond the linear regime the field-induced  $\bar{P}_3$  continues to be enhanced by a greater value of this ratio, although to a progressively lesser extent with further increase in the field, until eventually  $\bar{P}_3$  tends to a limiting value of ca. 0.7 which is insensitive to the ratio  $\epsilon_1/\epsilon_2$ . The value of the field at which  $\bar{P}_3$  attains half its limiting value is strongly dependent on this ratio and decreases from  $19.5 \times 10^7 \text{ Vm}^{-1}$  through  $13.5 \times 10^7 \text{ Vm}^{-1}$  to  $6.5 \times 10^7 \text{ Vm}^{-1}$  as  $\epsilon_1/\epsilon_2$  is increased from 0 through 0.1 to 0.2. Again, we find that for an orientationally ordered system, the inclusion of a polar molecular field of realistic strength brings about a significant reduction in the predicted field required to pole a sample. A similar advantage is predicted even for systems not originally in an orientationally ordered state, however, as can be clearly seen from figure 3.6. Relatively weak fields are unable to generate any  $\bar{P}_3$  order, a result that has its origins in the orthogonality of  $P_1(\cos \beta)$  and  $P_3(\cos \beta)$  (see Appendix 3A) [7].

Figure 3.5: The variation of the third rank polar order parameter,  $\overline{P}_3$ , with the electric field strength, calculated for three values of the ratio  $\epsilon_1/\epsilon_2$  of 0 ( $\cdots$ ), 0.1 ( $- - -$ ) and 0.2 ( $—$ ) for a nematogen with its  $N - I$  transition above the glass transition.

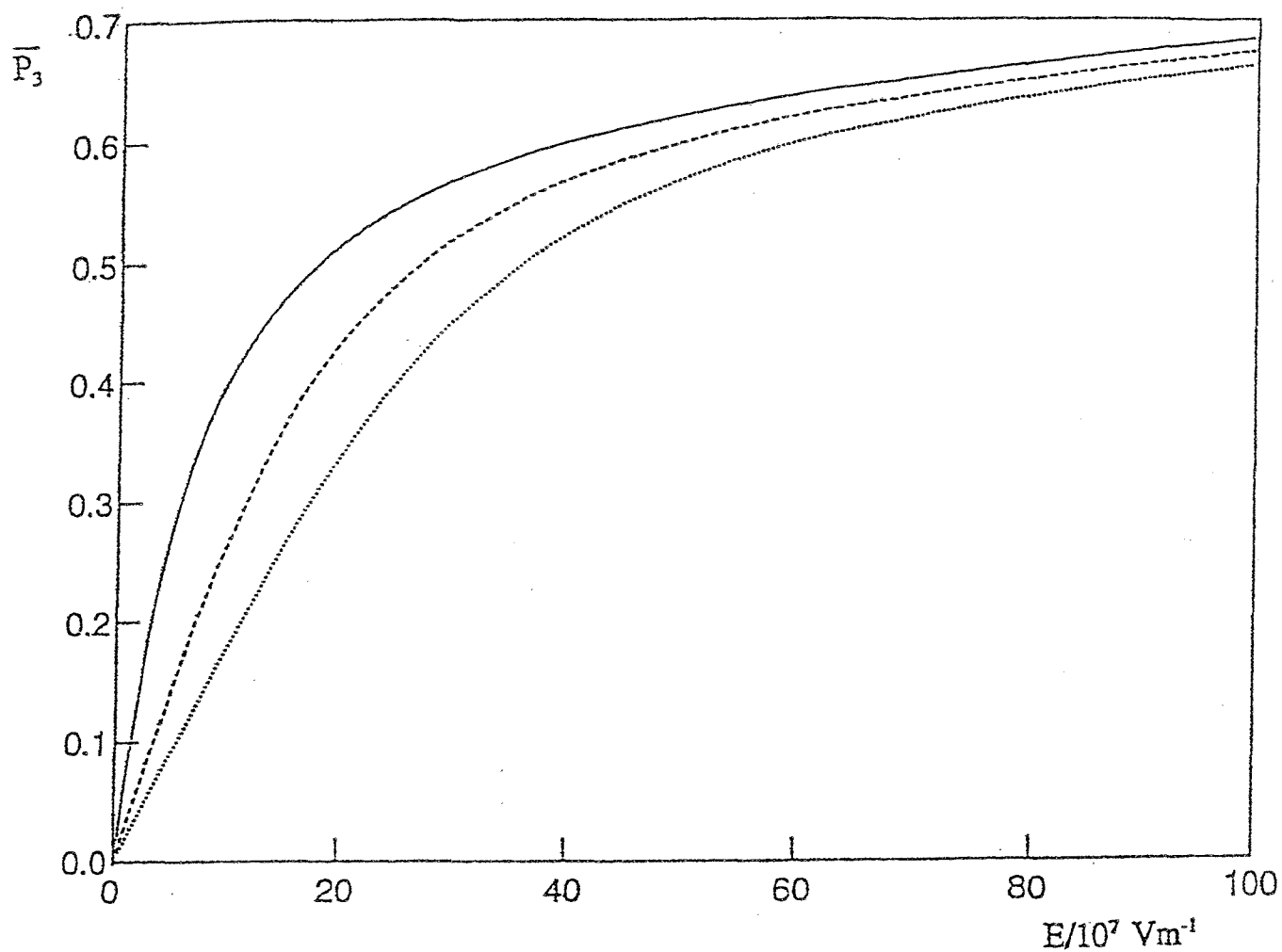
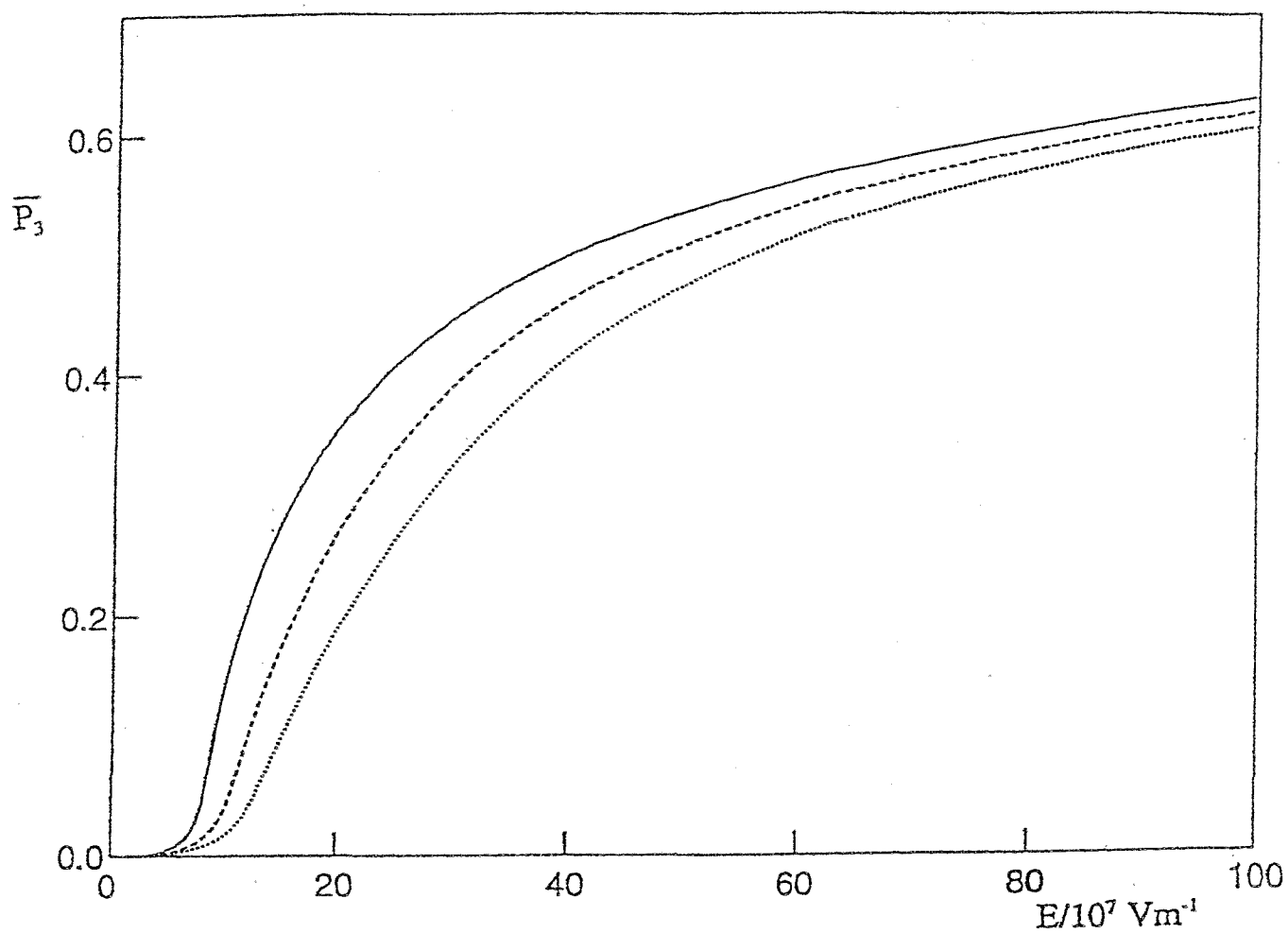


Figure 3.6: The variation of the third rank polar order parameter,  $\bar{P}_3$ , with the electric field strength, calculated for three values of the ratio  $\epsilon_1/\epsilon_2$  of 0 ( $\cdots$ ), 0.1 ( $-\cdot-\cdot$ ) and 0.2 ( $—$ ) for a nematogen with its  $N - I$  transition below the glass transition.



Above the threshold field, at which  $T_{NI}$  becomes equal to  $T_G$ ,  $\bar{P}_3$  grows rapidly, however, and the value of the third rank order parameter is again higher for a given applied field the greater the value of  $\epsilon_1/\epsilon_2$ . At high fields  $\bar{P}_3$  tends to a limiting value of ca. 0.6 which is insensitive to  $\epsilon_1/\epsilon_2$ . Again, it is clear that, for quite realistic values of  $\epsilon_1/\epsilon_2$ , the introduction of the polar molecular field term into the potential of mean torque results in a significant reduction in the strength of the electric field required to generate a specified degree of long range polar order (e.g. that required in a non-linear optical material).

### 3.7 The Problem of an Inhomogeneous Ground State

In the foregoing treatment the ground state of the system (achieved in the low temperature limit) is necessarily homogeneous, that is, ferroelectric. However, in reality this is not the most likely preferred ground state arrangement of the molecular electric dipoles, depending on the spatial arrangement of the molecules. Given the shape of nematogenic molecules and steric considerations an inhomogeneous ground state (ie, one in which there is not just one dipolar orientation throughout the system) is more likely because on average a molecule is likely to be surrounded by a higher number of others in a side to side configuration than end-to-end, and the former to have their dipoles oriented oppositely. In this case the ground state will be antiferroelectric. As we have already mentioned, however, the nature of the ground state does depend on the spatial arrangement of the molecules. If the molecules were at the sites of a face-centred cubic lattice, for instance, even though any given molecule has more neighbours side-to-side, in an infinite lattice the ground state of an array of dipoles will be antiferroelectric.

It is not possible to use the equations for a single molecule interacting with a molecular field (single site cluster molecular field theory) in a single component system to adequately describe electric field poling of a nematic that exhibits an inhomogeneous ground state.

This obtains because a single site cluster treatment, by definition, assumes that there is a single representative orientational potential function for the entire system and hence all molecules will adopt the same preferred orientation in the low temperature limit. Thus the ground state is necessarily homogeneous.

It might be thought that we could simply reverse the sign of the first rank molecular field coefficient in (3.15) to attempt to model the effect of antiferroelectric coupling between the molecules. As we have already stated, the single potential of mean torque means that there is just one molecule within the molecular field approximation that is somehow representative of all molecules. This then also applies to its preferred orientation and so the ground state cannot be correctly modelled. However, persisting with this concept, let us see what it would mean. In the absence of a field, first of all, the effect would be to cause the polar order parameter to be the same in magnitude, but opposite in sign. But this is physically indistinguishable from the case  $\epsilon_1 > 0$  and given that we might as well use the sense of the polarisation to define the first rank order parameter positively, we are then free to define  $\epsilon_1$  to be positive. In the case of an applied field an analogous situation would obtain if we were to reverse the overall sign of the total coefficient of  $P_1(\cos\beta)$  in the potentials of mean torque. However, if we were to simply reverse the sign of  $\epsilon_1$  alone, this would introduce into the first rank molecular field term a preference for the dipole to be oriented against the sense not of the surrounding molecules but of the director (or equivalently the field). This would oppose the effect of the electric field term itself and detract from it. To this extent, then, it would model antiferroelectric coupling, but in a fashion that physically is highly dubious. The potential models the energy of a single molecule, on average, as a function of orientation with respect to the director—it is an effective single body property—not between pairs or higher body interactions. Given that we have a system with a homogeneous ground state, we have to regard the polar molecular field term as a necessarily positive feedback mechanism for polar order. A negative odd rank coefficient  $\epsilon_1$  would imply that, as polar order were induced, there were some negatively cooperative mechanism by which this induced order inhibited the process generating

it. This mechanism would be somehow operating *at the single molecule level*, leading to a lower degree of induced polar order than if there were no polar molecular fields present. Thus the case  $\epsilon_1 < 0$  represents a physically impossible situation. This can also be seen from a consideration of the internal energy as one approaches the ground state (in zero field) at low temperatures. That is, the contribution to the orientational internal energy per molecule from the first rank interaction

$$\bar{U}_1 = -\epsilon_1 \bar{P}_1^2 / 2, \quad (3.21)$$

which is overall negative if  $\epsilon_1$  is positive. If  $\epsilon_1 < 0$  then the energy from the first rank interaction in the dipolar phase is overall positive and higher than in the isotropic phase (where it is zero); moreover, the contribution increases towards its maximum value as we lower the temperature into the ground state at absolute zero. This is not considered to be physically reasonable because as we approach 0 K the thermodynamic potential function becomes increasingly accurately represented by the internal energy; one would expect the polar contribution to be lower than that in the isotropic fluid since the dipolar phase would certainly be expected to be thermodynamically more stable. These pathological features are all artefacts that result from attempting to model couplings between molecules with a single effective potential energy function with respect to a single direction, the electric field-director. In addition, the free energy in this case does not possess a minimum with respect to the order parameters in the potential of mean torque. This could also be regarded as symptomatic of underlying pathology in this parameterisation of the theory. On the other hand, it may be that there are cases where the theory is correct, but the free energy still exhibits this feature. We shall postpone discussion of this possibility for the moment.

This situation, then, clearly represents a much more challenging theoretical problem, one which is beyond previous theories of poling to deal with. The effect of having antiferroelectric coupling between the molecular dipoles (or at least between the majority of them) should be such that field-induced polar order feeds back negatively and detracts from the overall polarisation and so the benefit of poling a nematic will be

somewhat less than on the basis of the MSVP theory, which is completely devoid of polar couplings. Here we present a molecular field model for poling of nematics with a predominantly antiferroelectric-type coupling, together with results of calculations based upon it.

### 3.8 The Theory

As we have already seen, the ground state arrangement of the molecular dipoles depends on the geometrical disposition of the dipoles. Therefore we have to invoke some kind of model that is reasonably plausible and accessible to physical intuition. In this spirit, we take the simple cubic lattice to provide such a model. The question now is how to treat this (or any other) model of the ground state theoretically within a molecular field theory.

An appropriate theoretical treatment of the antiferroelectric problem may be achieved by describing the phase as a mixture. That is, molecules comprising the different components of the mixture are identified by their dipolar orientations in the hypothetical ground state—dipole “up” particles being considered as one component and dipole “down” particles the other. Alternatively, we can conceptualise the different components to be identified by their lattice sites since the dipoles can switch. In the ground state there will be equal numbers of each and hence the components could each be considered to occupy one of two equivalent degenerate sub-lattices. We note that, with this identification, the nature of the interactions between neighbours on the same or different sub-lattices is different. That is, between neighbours on the same sub-lattice the coupling is ferroelectric, that between neighbours on different sub-lattices is antiferroelectric.

We now have to devise a way of describing this within the framework of a molecular field theory. We have chosen to treat the system with the Humphries-James-Luckhurst (HJL) theory of binary nematic mixtures [9], which we shall introduce in section 3.9

below (see also Chapter 4 for a formal derivation). In the absence of external fields the phase will have no overall dipolar order, as measured by the odd rank order parameters, at any temperature. There will be a transition temperature above which there will be complete randomisation of the dipole sense of both sub-lattices and below which there is no overall polar order but the odd rank order parameters of the individual sub-lattices (with respect to a common laboratory frame of reference) will be equal and opposite. At all temperatures the even rank order parameters will be identical for both sub-lattices and so at some higher transition temperature, both sets of even rank order parameters will vanish giving an overall isotropic phase. The application of an electric field along the nematic director of the phase then acts as a perturbation to this situation so that if, at the temperature of interest, the two sub-lattices have non-zero equal and opposite odd rank order parameters, the field will destabilise the dipolar arrangement of one sub-lattice and stabilise that of the other. We shall now sketch the required HJL theory of binary nematic mixtures by way of introduction before showing how to apply it to describe a nematic with a predominantly antiferroelectric dipolar coupling.

### 3.9 Introduction to the Humphries-James-Luckhurst Theory of Binary Nematic Mixtures

The HJL theory of mixtures [9] is an extension of the Maier-Saupe theory of nematics to systems of two components of differing anisometry. Here we give an intuitive extension of the Maier-Saupe theory; the equations we shall derive can also be obtained from a variational analysis (see Chapter 4).

We begin by writing down the potentials of mean torque,  $U_A(\beta)$  and  $U_B(\beta)$ , for each of the chemical species  $A$  and  $B$ . Each potential of mean torque will have contributions arising from both the molecular field generated by like particles and that from unlike



particles. We write

$$U_A(\beta) = U_{AA}(\beta) + U_{AB}(\beta), \quad (3.22)$$

with an analogous expression for  $U_B(\beta)$ . For a system of pure  $A$  we would write down the standard Maier-Saupe potential

$$U(\beta) = -\epsilon \bar{P}_2 P_2(\cos \beta), \quad (3.23)$$

which in this case we can rewrite more suggestively as

$$\begin{aligned} U_A(\beta) &= -\epsilon_{AA} \bar{P}_{2A} P_2(\cos \beta), \\ &= U_{AA}(\beta), \end{aligned} \quad (3.24)$$

where the subscripts on the coefficient  $\epsilon$  indicate that the intrinsic strength parameter is that associated with the interaction between particles of type  $A$  and there is an analogous expression for  $U_B(\beta) = U_{BB}(\beta)$  in a system of pure  $B$ . In a mixture of  $A$  and  $B$ ,  $U_A(\beta)$  now has a contribution  $U_{AB}(\beta)$ . For a test particle  $A$  immersed in pure  $B$

$$U_{AB}(\beta) = -\epsilon_{AB} \bar{P}_{2B} P_2(\cos \beta), \quad (3.25)$$

where  $\epsilon_{AB}$  is the intrinsic strength parameter for the interaction between unlike particles. We must now take into account the influence of the composition on the molecular field contributions from  $A$  and  $B$  to the total potential of mean torque of a test particle  $A$ . We expect that the molecular field experienced by a test particle due to a particular molecular type to be related to the number of such molecules in its vicinity, which will be proportional to the number of these molecules around it. If we assume a simple proportional relationship (ie, random mixing) then the molecular field will be proportional to the number density and hence to the total number of particles,  $N_A$  or  $N_B$ , of the given type. It seems reasonable to suppose then that we can take account of the composition by introducing composition proportionate weighting factors into equations (3.24) and (3.25) (which give the contribution of particles  $A$  or  $B$  in pure  $A$

or pure  $B$  respectively) such that in the limits (3.24) or (3.25) obtains. Given that we must regain (3.24) and (3.25) in the composition limits we require that the weightings be normalised. It would thus seem sensible to divide  $N_A$  or  $N_B$  by the total number of particles,  $(N_A + N_B)$ , so that the weightings become mole fractions. Therefore,

$$\begin{aligned}
 U_A(\beta) &= U_{AA}(\beta) + U_{AB}(\beta) \\
 &= -\{N_A/(N_A + N_B)\} \epsilon_{AA} \bar{P}_{2A} P_2(\cos \beta) - \{N_B/(N_A + N_B)\} \epsilon_{AB} \bar{P}_{2B} P_2(\cos \beta) \\
 &= -\{(1-x) \epsilon_{AA} \bar{P}_{2A} + x \epsilon_{AB} \bar{P}_{2B}\} P_2(\cos \beta), \tag{3.26}
 \end{aligned}$$

where  $x$  is the mole fraction of component  $B$ . The analogous expression for  $U_B(\beta)$  is then

$$U_B(\beta) = -\{x \epsilon_{BB} \bar{P}_{2B} + (1-x) \epsilon_{AB} \bar{P}_{2A}\} P_2(\cos \beta). \tag{3.27}$$

The weightings thus represent normalised probabilities that a given intermolecular interaction with the test particle will be with a particle of a given type assuming random mixing. Equations (3.26) and (3.27), then, form the starting point of the theory. The free energy within the molecular field approximation may be obtained either from the partition function or distribution function (see sections 2.6, 2.7) and is written as

$$A = \{(1-x)^2 \epsilon_{AA} \bar{P}_{2A}^2 + 2x(1-x) \epsilon_{AB} \bar{P}_{2A} \bar{P}_{2B} + x^2 \epsilon_{BB} \bar{P}_{2B}^2\} / 2$$

$$-(1-x)k_B T \ln Z_A - xk_B T \ln Z_B,$$

$$Z_A = \int_0^\pi \exp(-U_A(\beta)/k_B T) \sin \beta d\beta, \quad Z_B = \int_0^\pi \exp(-U_B(\beta)/k_B T) \sin \beta d\beta. \tag{3.28}$$

It is to be noted, however, that the free energy expression we have developed ignores phase separation. We shall now adapt this mixture theory to the problem at hand.

### 3.10 Adaptation of the HJL Theory to Model Nematics with Predominantly Antiferroelectric Coupling

We now extend the HJL theory to include both first and second rank interactions in addition to the direct interaction of the electric field, consistent with the formal demands of the molecular field theory. The potentials of mean torque for the molecules on the two sub-lattices are given by

$$U_A(\beta) = -\{(\epsilon_{2AA}\bar{P}_{2A} + \epsilon_{2AB}\bar{P}_{2B})P_2(\cos\beta) + (\epsilon_{1AA}\bar{P}_{1A} + \epsilon_{1AB}\bar{P}_{1B} + \mu E)P_1(\cos\beta)\}/2$$

$$U_B(\beta) = -\{(\epsilon_{2BB}\bar{P}_{2B} + \epsilon_{2AB}\bar{P}_{2B})P_2(\cos\beta) + (\epsilon_{1BB}\bar{P}_{1B} + \epsilon_{1AB}\bar{P}_{1A} + \mu E)P_1(\cos\beta)\}/2,$$
(3.29)

where  $\epsilon_{2BB} = \epsilon_{2AA}$  and  $\epsilon_{1BB} = \epsilon_{1AA}$  since the molecule types  $A$  and  $B$  are chemically identical. The free energy per molecule of sub-lattice  $A$  is then

$$A_A = \{\epsilon_{2AA}\bar{P}_{2A}^2 + \epsilon_{2AB}\bar{P}_{2A}\bar{P}_{2B} + \epsilon_{1AA}\bar{P}_{1A}^2 + \epsilon_{1AB}\bar{P}_{1A}\bar{P}_{1B}\}/2 - k_B T \ln Z_A,$$

$$Z_A = \int_0^\pi \exp(-U_A(\beta)/k_B T) \sin\beta \, d\beta.$$
(3.30)

The corresponding equation for sub-lattice  $B$  is

$$A_B = \{\epsilon_{2AA}\bar{P}_{2B}^2 + \epsilon_{2AB}\bar{P}_{2A}\bar{P}_{2B} + \epsilon_{1AA}\bar{P}_{1B}^2 + \epsilon_{1AB}\bar{P}_{1A}\bar{P}_{1B}\}/2 - k_B T \ln Z_B,$$

$$Z_B = \int_0^\pi \exp(-U_B(\beta)/k_B T) \sin\beta \, d\beta.$$
(3.31)

The total orientational free energy per particle of the whole phase is then

$$A = (1-x)A_A + xA_B = (A_A + A_B)/2,$$

$$A = [ \{\epsilon_{2AA}(\bar{P}_{2A}^2 + \bar{P}_{2B}^2) + 2\epsilon_{2AB}\bar{P}_{2A}\bar{P}_{2B} + \epsilon_{1AA}(\bar{P}_{1A}^2 + \bar{P}_{1B}^2) + 2\epsilon_{1AB}\bar{P}_{1A}\bar{P}_{1B}\}/2$$

$$- k_B T \ln Z_A - k_B T \ln Z_B ] / 2.$$
(3.32)

In order to obtain reasonable values of the molecular field coefficients appearing in the free energy we need to invoke some model for the mutual spatial disposition of the dipoles in the ground state. Here, as stated earlier, we envisage that the molecules occupy the sites of a simple cubic lattice. In the ground state any given molecule will have four nearest neighbours with opposite dipole sense to its own and two with the same sense. If we imagine that only the nearest neighbours interact then  $\epsilon_{2AA} = \epsilon_{2AB}/2$  and  $\epsilon_{1AA} = -\epsilon_{1AB}/2$ . That is, there are twice as many  $A-B$  interactions as  $A-A$  interactions and, in the case of the first rank coefficients, not only this, but the  $A-A$  coupling is ferroelectric as in the homogeneous system (ie,  $\epsilon_{1AA}$  is positive) and the  $A-B$  coupling is antiferroelectric (ie,  $\epsilon_{1AB}$  is negative). We scale the temperature using the dominant interaction,  $\epsilon_{2AB}$  (ie, the scaled temperature is  $T^* = k_B T / \epsilon_{2AB}$ ) and then express the other coefficients scaled with  $\epsilon_{2AB}$ . Thus  $\epsilon_{2AA}/\epsilon_{2AB} = 0.5$ ,  $\epsilon_{1AB}/\epsilon_{2AB} = -0.2$  or  $-0.1$ , say, and then  $\epsilon_{1AA}/\epsilon_{2AB} = (\epsilon_{1AA}/\epsilon_{1AB})(\epsilon_{1AB}/\epsilon_{2AB}) = -0.1$  or  $-0.05$ . The electric field is then also scaled as  $\mu E / \epsilon_{2AB}$ . This choice of scaling retains the connection, through the bona-fide mixtures theory, to the Maier-Saupe-like theory for homogeneous systems developed previously (section 3.2). The actual choice of values then preserves the correspondance with the values of the parameters employed there and in the MSVP theory. We note, however, that we have invoked a model to obtain particular numerical relationships between the molecular field coefficients. These relationships are model-dependent and are then really parameters themselves. That is, the most general system of equations within this theoretical framework would have the numerical factors included implicitly in the molecular field coefficients and then any model could be accounted for by varying the parameters. We are thus able to set up a theory to describe the antiferroelectric ground state nematic, but at the expense of model dependency (or, equivalently, further parameterisation). If we wish we may include next nearest neighbour interactions (or even further coordination shells) from the numbers of such neighbours  $A$  and  $B$ , the proportionate extra distance from the test particle and the likely distance dependence of the interaction (inverse sixth power for second rank and inverse third power for first rank). Likewise, we may decide to change to a different lattice. The need to pursue such possibilities is not so clear, however.

## 3.11 Methodology

As we have already seen in Chapter 2, there are a variety of methodologies for obtaining the order parameters in molecular field calculations. The two main ones are minimisation of the equilibrium free energy over the order parameters and solution of the self-consistency equations.

### 3.11.1 Minimisation of the Free Energy

It was our intention to minimise the free energy (3.32) with respect to the order parameters  $\bar{P}_{1A}$ ,  $\bar{P}_{1B}$ ,  $\bar{P}_{2A}$  and  $\bar{P}_{2B}$ . This would be done at the same temperatures and over the same range of electric fields as before, employing the scaled parameters consistent with the model outlined above in which there are only nearest neighbour interactions.

We were, however, unable to find a minimum numerically in the free energy hypersurface  $A(\bar{P}_{1A}, \bar{P}_{1B}, \bar{P}_{2A}, \bar{P}_{2B})$  for any values of the applied field and at any temperature.

We hypothesised that there may be, in fact, no minimum to be found. To investigate this possibility, we removed the second rank terms from the equations to leave the free energy as a function of the two order parameters which are most essential for our purposes in studying the polar order, namely the polar order parameters  $\bar{P}_{1A}$  and  $\bar{P}_{1B}$ . Even though the removal of the second rank terms is quantitatively incorrect, it should, it was hoped, preserve the essential qualitative features of the free energy surface that are of interest in investigating the odd rank order parameters. Exhaustive calculations of the surface of such a simplified system for an extensive range of scaled temperatures and fields revealed that there is invariably no true minimum in the surface, in fact, but rather a saddle point.

We then proceeded to explore a variety of other models (with both first and second rank interactions) within the same general theoretical structure we have just given, attempting to minimise the free energy over the order parameters appearing in the

potentials. This corresponds to changing the parameterisation of the intrinsic molecular field coefficients to correspond to whatever model is desired. Even after an exhaustive search we were unable to obtain the order parameters by this means for any arbitrary model for the interparticle couplings, for any field or temperature.

It would appear then, that whilst the free energy minimisation methodology works successfully in the case of the molecular field theory for single component systems (and hence homogeneous ground states), there are clearly cases, such as these, where it is inapplicable in its usual formulation. We now turn our attention to the origins of this feature of the adaptation of binary mixture theory to antiferroelectric coupling in nematics.

In some cases it is possible to see analytically that the surface cannot possess a minimum. Specifically, if we consider a system in which there are no “like” interactions it is possible to show from the structure of the free energy that the surface cannot contain a minimum with respect to the order parameters in the potentials. However, this result is not capable of being generalised to models with an arbitrary mixture of “like” and “unlike” interactions [7].

A more general possibility is that in cases where the approach fails the order parameters being treated as separate variational parameters are not truly independent. That, is unless the free energy function is written in terms of a minimum number of degrees of freedom (ie, order parameters) the corresponding surface will not possess a minimum [8]. If so, then the problem would appear to revolve around the correct definition of a minimum number of independent order parameters of the system. In the case of the system of interest here we may glean some clue regarding the minimum number of independent order parameters and how they relate to those appearing in the potential of mean torque by considering limiting cases. Specifically, in the simplified model (first rank interactions only) under conditions of zero field,  $\overline{P}_{1B} = -\overline{P}_{1A}$ , so that there is only one independent order parameter rather than two. In the full model we have in addition  $\overline{P}_{2B} = \overline{P}_{2A}$ , so that again there are only half the number of independent order

parameters as appear in the potentials of mean torque, that is, only one independent order parameter for each of first and second rank. If we make the explicit substitutions  $\overline{P}_{2B} = \overline{P}_{2A}$  and  $\overline{P}_{1B} = -\overline{P}_{1A}$  into the the free energy expression to obtain  $A(\overline{P}_{1A}, \overline{P}_{2A})$  we find that indeed the surface possesses a global minimum. Minimisation then yields the equilibrium order parameters  $\overline{P}_{1A}$  and  $\overline{P}_{2A}$  from which any other required order parameters may thence be obtained. Indeed this is the technique we employed to obtain the zero field phase diagram for the system (see section 3.12 for results and discussion).

It might have initially been assumed that for non-zero values of the electric field the effect of the field would be to destroy any such relationship between the order parameters rendering all the order parameters in the potentials independent. Clearly this is not the case, however. While the simple relationships between the order parameters of the same rank in the two sub-lattices will obviously no longer hold, there may still be only the same number of independent order parameters, with these relationships being obtained in the low field limit. It seems likely that an analogous situation still obtains in which both sub-lattice order parameters of the same rank are still related, but now in a more complicated way through the field. If this were the case, we might presume to substitute this relationship into the the free energy expression in an analogous way to the case in zero field and obtain the order parameters similarly. Unfortunately, however, it is not possible to obtain an analytic relationship, since the integrals defining the order parameters are non-analytic. So if a relationship does exist, we could only obtain approximations to it, even assuming such manipulations to be applicable in this case. A perturbation analysis shows that the order parameters of given rank in the two sub-lattices are related to their zero field values. Given that their zero field values are clearly related to each other, as we have seen, it follows that the values for non-zero fields must be related to each other also [7]. It would also appear that this result obtains to whatever order the perturbation expansions are taken in the field, increasing order giving approximations valid to higher and higher fields. Not only are the order parameters related to each other through the field, and that in a non-analytic way, but the required range of fields extends into the very high field regime, where any

manageable number of terms in the expansion would be utterly inadequate. Thus we cannot express the relationship between the sub-lattice order parameters of the same rank analytically in a way that is satisfactory for our purposes. Therefore we cannot even in principle rewrite  $A(\bar{P}_{1A}, \bar{P}_{1B}, \bar{P}_{2A}, \bar{P}_{2B})$  as  $A(\bar{P}_{1A}, \bar{P}_{2A})$ . This constitutes a fundamental flaw in the free energy minimisation methodology in this type of molecular field theory, one that is not susceptible to any straightforward simple reformulation of the free energy expression. We are forced then, to look to another methodology, that of next choice being solution of the self-consistency equations, or something equivalent (see section 3.11.2 below).

### 3.11.2 Solution of the Self-Consistency Equations

The self-consistency equations here are

$$\begin{aligned}\bar{P}_{1A} &= Z_A^{-1} \int_0^\pi P_1(\cos \beta) \exp(-U_A(\beta)/k_B T) \sin \beta d\beta, \\ \bar{P}_{1B} &= Z_B^{-1} \int_0^\pi P_1(\cos \beta) \exp(-U_B(\beta)/k_B T) \sin \beta d\beta, \\ \bar{P}_{2A} &= Z_A^{-1} \int_0^\pi P_2(\cos \beta) \exp(-U_A(\beta)/k_B T) \sin \beta d\beta, \\ \bar{P}_{2B} &= Z_B^{-1} \int_0^\pi P_2(\cos \beta) \exp(-U_B(\beta)/k_B T) \sin \beta d\beta.\end{aligned}\tag{3.33}$$

These are to be solved simultaneously. The integrals are non-analytic so numerical solutions must be sought. In practise, this was achieved by minimising the sum of the squares of the differences between the left and right sides of the equations. At the minimum with respect to  $\bar{P}_{1A}, \bar{P}_{1B}, \bar{P}_{2A}, \bar{P}_{2B}$  the function is zero.

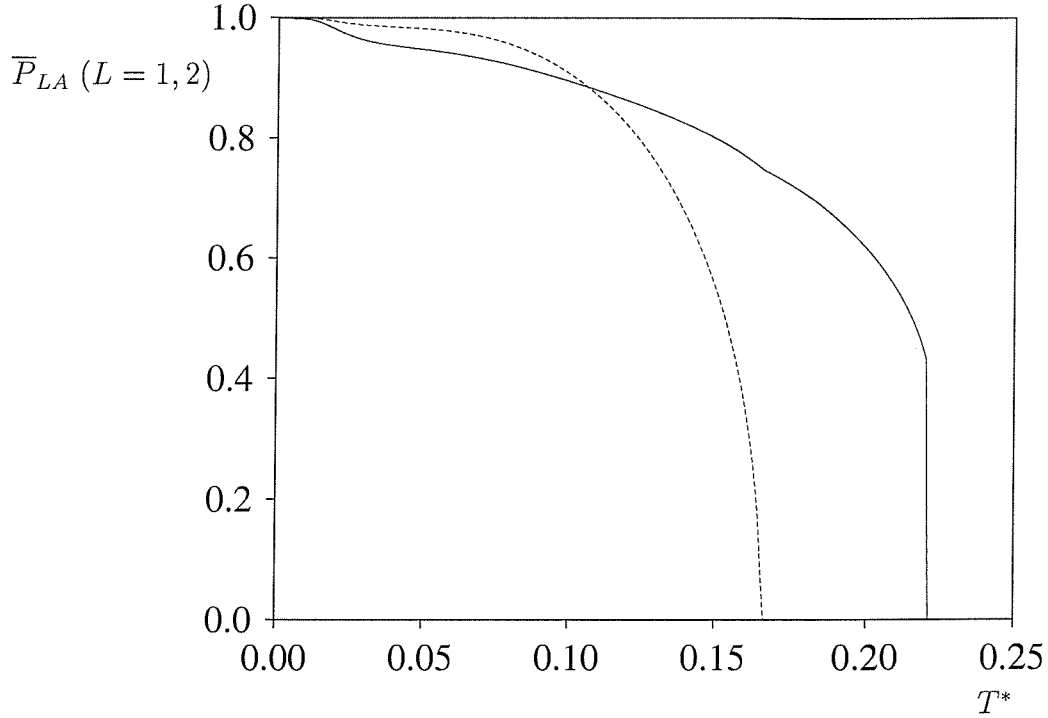
## 3.12 Results and Discussion

We begin discussion of the results by presenting the zero field phase diagram (see figure 3.7). We find a second order transition between a non-polar antiferroelectric ne-



matic and a non-polar non-antiferroelectric nematic (which one would expect is probably the type of nematic normally observed experimentally). The transition occurs at a scaled temperature  $T^* = k_B T / \epsilon_{2AB}$  of 0.1667 and is second order due to the vector nature of the order parameter involved [10]. The scaled transition temperature is consistent with a perturbation-bifurcation analysis. We also see a first order transition at  $T^* = 0.2203$ , as expected from the Maier-Saupe theory.

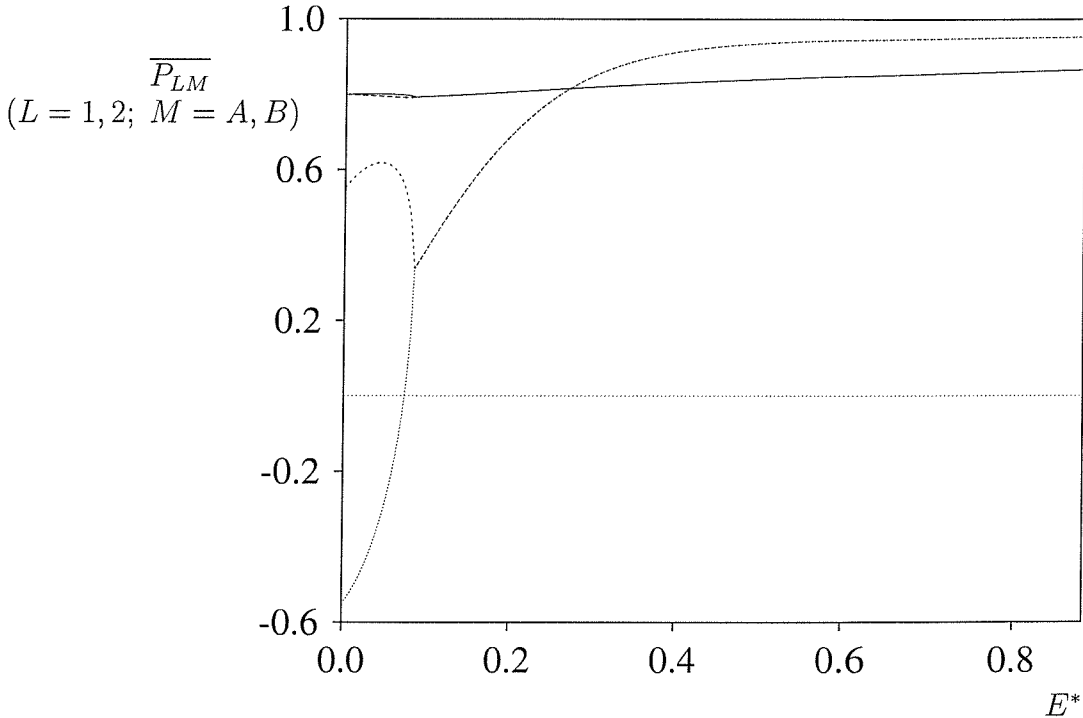
Figure 3.7: The order parameters  $\bar{P}_{2A}$  (—) and  $\bar{P}_{1A}$  (- -) as a function of scaled temperature,  $T^*$ , in zero field.



We now turn our attention to the system at a temperature below the second order transition in the presence of the field (see figure 3.8). It is to be noted that the extreme high field limit of the abscissa in scaled units in figures 3.8–3.12 is the same as that in the ferroelectric poling case, which corresponds to  $100 \times 10^7 \text{ Vm}^{-1}$  in the MSVP theory [2]. As we go to high fields we find that the symmetry of the sub-lattice order parameters of the same rank is gradually lost, albeit a negligible effect for those of second rank.  $\bar{P}_1^A$  grows, whilst  $\bar{P}_1^B$  diminishes in magnitude until it passes through

zero to become positive and from then on continues to increase. As the field continues to increase the order parameters begin to approach one another again,  $\overline{P}_1^A$  beginning to decrease and  $\overline{P}_1^B$  increasing, these effects occurring at an accelerating rate, until they reach a common value. From then on they remain together and increase, initially linearly, before reaching a plateau of ca. 0.9 in the limit of high field. We note that the behaviour of the first rank order parameters around the transition is consistent with the Landau theory of second order phase transitions [10]. That is, whilst the order parameter itself changes continuously,  $\overline{P}_1(E^*)$  is not everywhere smooth. Rather than the gradient changing continuously through the transition as one might have expected, its magnitude increases without limit as we approach the transition from below until, at the transition itself, it suffers an infinite jump discontinuity down to some finite value.

Figure 3.8: The order parameters  $\overline{P}_{2A}$  (—),  $\overline{P}_{2B}$  (---),  $\overline{P}_{1A}$  (- - -) and  $\overline{P}_{1B}$  (···) as a function of scaled electric field,  $E^* = \mu E/\epsilon_2$ , at a scaled temperature  $T^*$  of 0.15.



The effect on the second rank order parameter is rather diminutive; the second rank order of the A sub-lattice increases whilst that for the B sub-lattice decreases. At the point where the  $\overline{P}_1$  order parameters begin to come together the  $\overline{P}_2$  order parameters also begin to come back together and reach a common value coincident with the transition in the  $\overline{P}_1$  order parameters. After this the second rank order parameters remain together increasing only very slightly with the field.

We seem to have found a second order transition between a system wherein the odd rank order parameters on the sub-lattices are different and one in which they are the same. What are we to call these phases ? The terms ferroelectric and antiferroelectric are usually used to refer to interactions, that is, the orientation preference of a pair of dipoles in their ground state. Ferroelectric coupling denotes a preference for parallel alignment with respect to each other and the intermolecular vector, whilst antiferroelectric coupling refers to an antiparallel mutual disposition and an orthogonal alignment with respect to the intermolecular axis. In this document we have already been extending this terminology somewhat intuitively to refer to bulk configurations of dipoles, but we shall now, to remove ambiguity, make this more precise in the particular case of our model where we treat the system as if there were two sub-lattices identified by the hypothetical ground state dipolar orientations. We define (for our system) *ferroelectric* to mean a phase in which the polar order in the two sub-lattices is the same and *antiferroelectric* to mean a phase in which it is different. Thus we have a *field-induced antiferroelectric-ferroelectric transition*.

Now we note that it is generally assumed that we do not have *long-range* antiferroelectric ordering in nematics, even though both an intrinsically antiferroelectric nematic phase and a non-dipolar nematic will have no overall polarisation in zero field. Thus we ought to perform the calculations at a higher temperature, above the second order transition on the phase diagram. Indeed, the values of scaled temperature comparable to those employed in the previous study [2] and in the initial homogeneous ground state theory in this Thesis are well above the temperature of this transition. So we

now consider this temperature regime to facilitate comparison with previous work and experimental regimes. Figures 3.9 and 3.10 show the two lowest order odd rank order parameters as a function of poling field strength at the glass transition temperature of 380 K for three values of the relative strength of the polar couplings, namely those analogous to  $\epsilon_1/\epsilon_2 = 0, 0.1$  and  $0.2$  in the initial study (ie, on systems with a ferroelectric ground state). The connection between the parameterisations of the two theories is as follows. Given that we have scaled the temperature with  $\epsilon_{2AB}$  by default, since it is the largest second rank coefficient, the other coefficients are all scaled by it. Then, to compare like with like, the analogue of  $\epsilon_1/\epsilon_2$  has to be  $\epsilon_{1AB}/\epsilon_{2AB}$ , which should then be set to magnitudes of  $0, 0.1$  and  $0.2$ . Since  $\epsilon_{1AB}$  is negative and of opposite sign to  $\epsilon_1 > 0$ , strictly we might say that we are really performing the calculation for  $\epsilon_1/\epsilon_2 = 0, -0.1$  and  $-0.2$ . The figures 3.9 and 3.11 show the results of the calculation assuming a  $T_{NI}$  of 420 K (ie, the system is initially in the nematic phase before poling) whilst 3.10 and 3.12 show those assuming a  $T_{NI}$  of 340 K (ie, initially isotropic). It is to be noted that, above the transition to the non-dipolar phase, order parameters of the same rank are identical between the two sub-lattices over the whole field range and for all ranks. The forms of all the graphs are the same as for the previous study of the homogeneous ground state system with ferroelectric coupling, but the response of the order parameters is muted. In addition, the effect of the polar coupling is seen to be much smaller than in the previous study, where it was enhancing, rather than detracting from the field. We also note the faster response of the initially nematic phase by comparison with the initially isotropic phase.

Thus for  $\overline{P}_1$  in the initially nematic phase we have an initial linear response before tailing off to a plateau in the limit of high field. The influence of steadily increasing the strength of the polar coupling is to steadily decrease the polar order for a given field until we reach the high field limit, which is insensitive to the polar coupling. We note that the largest response is when  $\epsilon_1/\epsilon_2 = 0$ , as in the MSVP theory [2].  $\overline{P}_1$  in the initially isotropic phase, as before, shows an initial, but shallower, linear response followed by a fairly sudden rise as  $T_{NI}$ , which has been raised by the field, overtakes

Figure 3.9: The first rank order parameter as a function of the scaled electric field,  $E^*$ , for an initially nematic sample for three values of the relative strength of the polar couplings, namely  $\epsilon_1/\epsilon_2 = 0$  ( $\cdots$ ), 0.1 ( $- - -$ ) and 0.2 ( $—$ ).

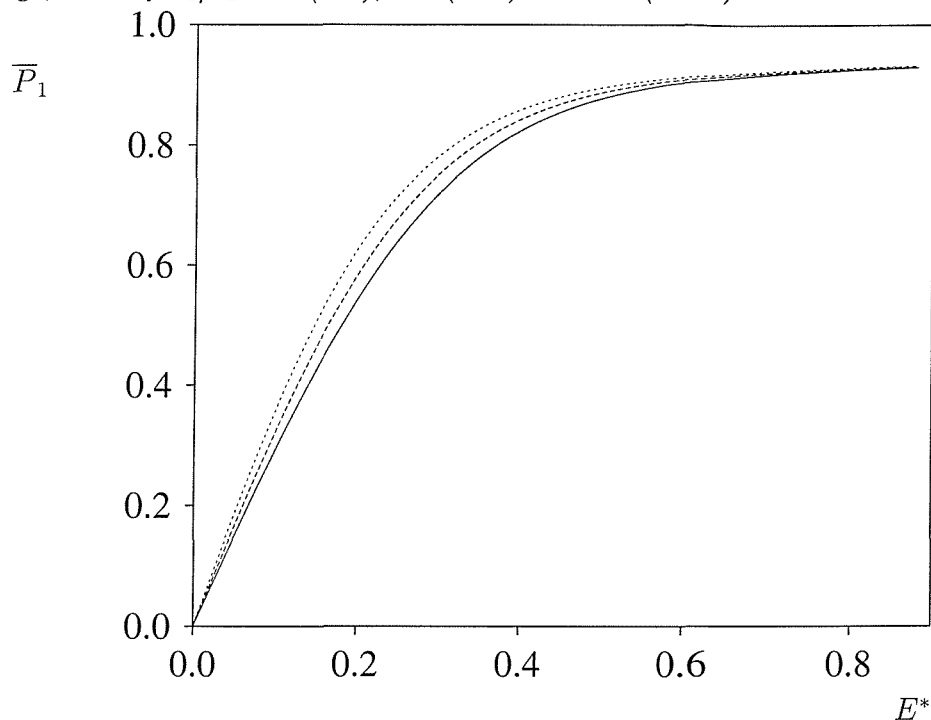
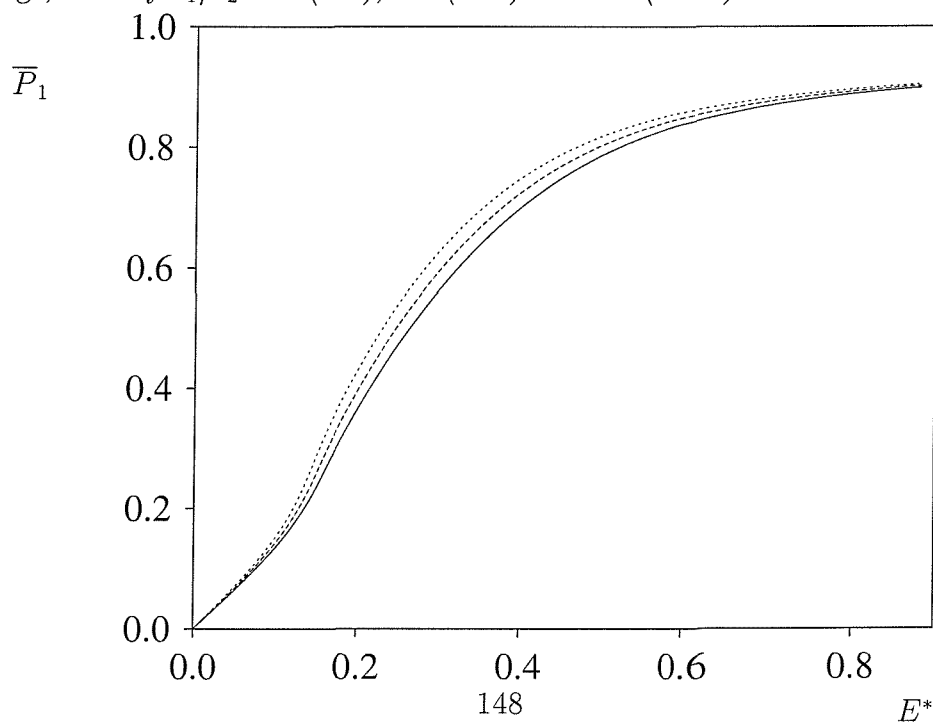


Figure 3.10: The first rank order parameter as a function of the scaled electric field,  $E^*$ , for an initially isotropic sample for three values of the relative strength of the polar couplings, namely  $\epsilon_1/\epsilon_2 = 0$  ( $\cdots$ ), 0.1 ( $- - -$ ) and 0.2 ( $—$ ).



the glass transition temperature. It then attains a limiting value, independent of the polar coupling strength. Again the response is less sensitive to the inclusion of  $\epsilon_1/\epsilon_2$  but is still somewhat diminished by it.

The response of  $\bar{P}_3$  (figures 3.11 and 3.11) also shows this decreased sensitivity to the polar coupling by comparison, while still retaining the same form as before. In the initially isotropic phase it shows a zeroth response initially (this has its origins in the orthogonality of Legendre polynomials of differing ranks) and then a sharp rise as the field-induced elevation of  $T_{NI}$  begins to take effect, eventually reaching a high field limiting value independent of  $\epsilon_1/\epsilon_2$ . In the initially nematic case we have qualitatively the same behaviour as before; the high field limit of the order is simply lower.

Figure 3.11: The third rank order parameter as a function of the scaled electric field,  $E^*$ , for an initially nematic sample for three values of the relative strength of the polar couplings, namely  $\epsilon_1/\epsilon_2 = 0$  ( $\cdots$ ), 0.1 ( $- - -$ ) and 0.2 ( $—$ ).

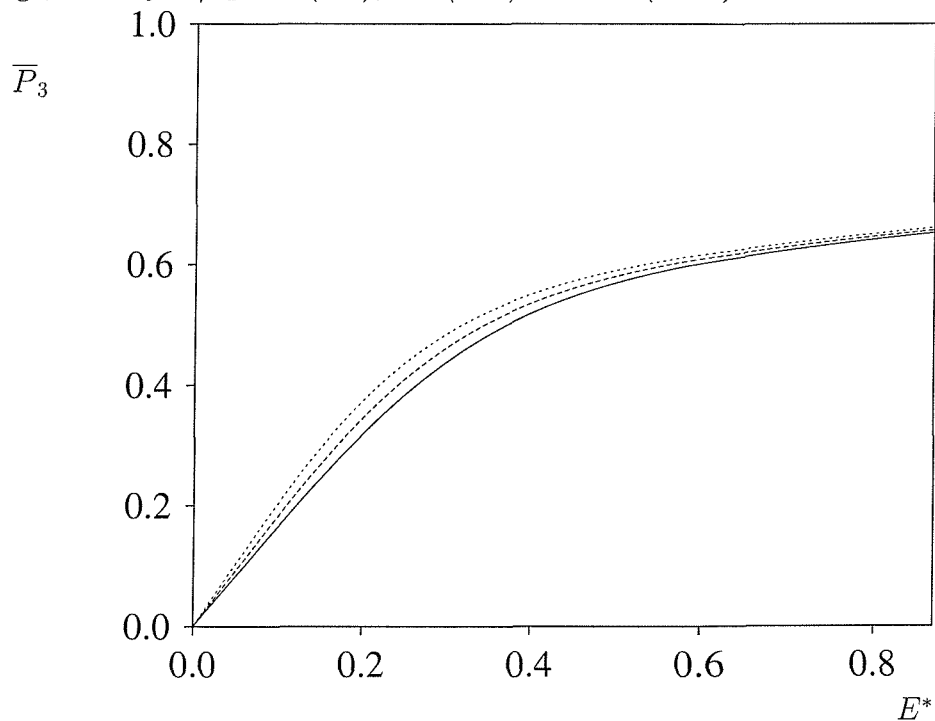
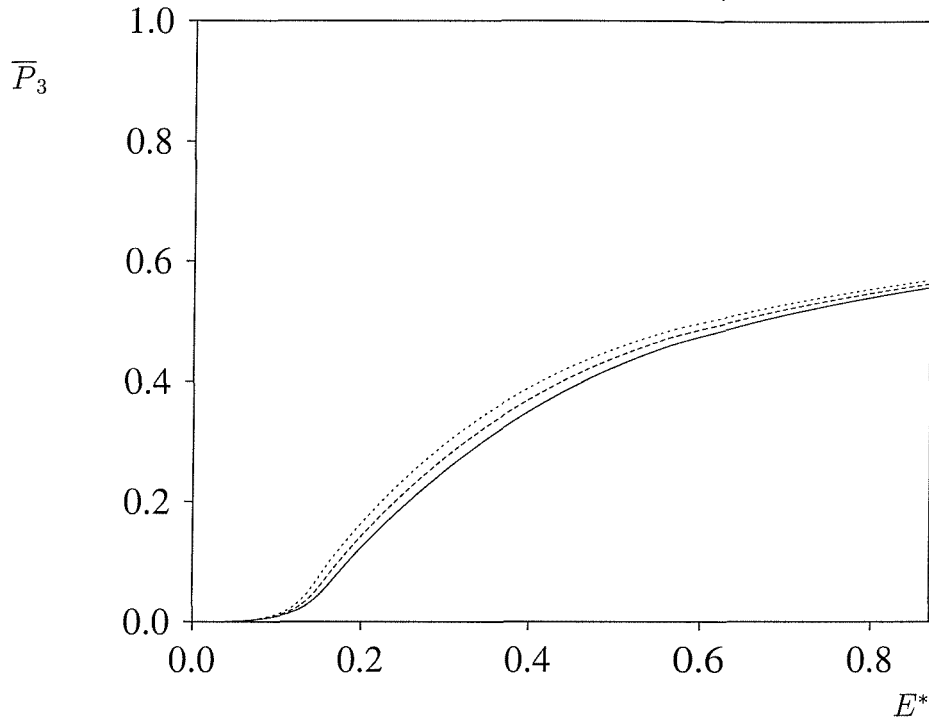


Figure 3.12: The third rank order parameter as a function of the scaled electric field,  $E^*$ , for an initially isotropic sample for three values of the relative strength of the polar couplings, namely  $\epsilon_1/\epsilon_2 = 0$  ( $\cdots$ ), 0.1 ( $- - -$ ) and 0.2 ( $—$ ).



### 3.13 Conclusions

For a nematic where the polar couplings are ferroelectric in nature, the initial study we have undertaken shows that they have a significant beneficial effect on the polar order induced by a given field by comparison with the MSVP theory [2]. If, however, the polar coupling is predominantly antiferroelectric in nature then the polar order generated is diminished by comparison. Just how predominant the antiferroelectric coupling is will determine the size of this effect and in our model there is not total dominance of the antiferroelectric coupling and so the effect of the inclusion of odd rank molecular field terms in the single particle potential is apparent, but not as significant as for the ferroelectric coupling case. Our model for the anti-coupling is, however,

physically reasonable. Thus we would predict that the polarisation obtained from a real nematic will be very significantly less than on the basis of the ferroelectric coupling model, and still somewhat less than on the basis of a model completely devoid of polar couplings [2]. Of the two possibilities, it would seem that antiferroelectric coupling is much more likely to be the norm for nematics than ferroelectric coupling and so we are forced to conclude that, by comparison with our initial single component theory for homogeneous ground states and the work of others [2], the potential advantage of poling nematics, even in principle, has now to be regarded as less than has been previously suggested.



## Appendix 3A: Proofs and Derivations

1. Perturbation analysis for the order parameters  $\bar{P}_L$  of a polarised ferroelectric ground state system initially in the nematic phase.

The essence of a perturbation analysis is to identify a dominant contribution to some quantity of interest (if there is one) and factor it out to leave the smaller remaining factor. The dominant quantity is normally identified with some known quantity or standard theoretical point of reference about which the actual situation is a perturbation. The small remaining factor is expanded and there will be some regime in which this expansion may be truncated to a good approximation. In this case we require the order parameter which is by definition

$$\bar{P}_L = Z^{-1} \int_{-1}^1 P_L(\cos \beta) \exp \left( \{ \epsilon_2 \bar{P}_2 P_2(\cos \beta) + (\mu E + \epsilon_1 \bar{P}_1) P_1(\cos \beta) \} / k_B T \right),$$

$$Z = \int_{-1}^1 \exp \left( \{ \epsilon_2 \bar{P}_2 P_2(\cos \beta) + (\mu E + \epsilon_1 \bar{P}_1) P_1(\cos \beta) \} / k_B T \right). \quad (3A.1)$$

Now in a non-polar nematic in the absence of external fields the dominant order parameter is  $\bar{P}_2$  and the dominant term in the potential of mean torque is the Maier-Saupe contribution. Thus, if the electric field is weak then we may write the partition function as

$$Z = \int \exp \left( \epsilon_2 \bar{P}_2 P_2(\cos \beta) / k_B T \right) \exp \left( \{ \mu E + \epsilon_1 \bar{P}_1 \} P_1(\cos \beta) / k_B T \right) d \cos \beta \quad (3A.2)$$

and expand the second exponential as

$$Z = \int \exp \left( \epsilon_2 \bar{P}_2 P_2(\cos \beta) / k_B T \right) \left[ 1 + (\mu E + \epsilon_1 \bar{P}_1) P_1(\cos \beta) / k_B T + \dots \right] d \cos \beta. \quad (3A.3)$$

If the electric field is small enough then to a good approximation we may truncate the expansion at first order to obtain

$$\begin{aligned}
Z &\sim \int \exp\left(\epsilon_2 \bar{P}_2 P_2(\cos \beta)/k_B T\right) d \cos \beta \\
&+ \left(\frac{\mu E + \epsilon_1 \bar{P}_1}{k_B T}\right) P_1(\cos \beta) \int_{-1}^1 P_1(\cos \beta) \exp\left(\epsilon_2 \bar{P}_2 P_2(\cos \beta)/k_B T\right) d \cos \beta.
\end{aligned} \tag{3A.4}$$

The integral in the second term is of the form

$$\int_{-a}^a x \exp\left\{b(3x^2 - 1)/2\right\} dx,$$

that is, the integrand is an odd function and the range of integration is symmetrical about zero so the integral must vanish. Therefore the first order perturbation approximation for the partition function is

$$Z \sim \int \exp\left(\epsilon_2 \bar{P}_2 P_2(\cos \beta)/k_B T\right) d \cos \beta.$$

If we then approximate  $\bar{P}_2$  to that where the ordering is dictated by the Maier-Saupe potential then

$$Z \sim Z_0, \tag{3A.5}$$

the partition function for the unperturbed nematic. Equation (3A.1) can then be written approximately as

$$\begin{aligned}
\bar{P}_L &\sim Z_0^{-1} \int P_L(\cos \beta) \exp\left(\epsilon_2 \bar{P}_2 P_2(\cos \beta)/k_B T\right) \\
&\times \exp\left(\{\mu E + \epsilon_1 \bar{P}_1\} P_1(\cos \beta)/k_B T\right) d \cos \beta.
\end{aligned} \tag{3A.6}$$

If we now expand the second exponential in a manner consistent with the treatment of the partition function then this becomes

$$\begin{aligned}
\bar{P}_L &\sim Z_0^{-1} \int P_L(\cos \beta) \exp\left(\epsilon_2 \bar{P}_2 P_2(\cos \beta)/k_B T\right) \\
&\times \left[1 + \left(\frac{\mu E + \epsilon_1 \bar{P}_1}{k_B T}\right) P_1(\cos \beta)\right] d \cos \beta
\end{aligned}$$

$$\begin{aligned}
&= Z_0^{-1} \left\{ \int P_L(\cos \beta) \exp \left( \epsilon_2 \bar{P}_2 P_2(\cos \beta) / k_B T \right) d \cos \beta \right. \\
&+ \left. \left( \frac{\mu E + \epsilon_1 \bar{P}_1}{k_B T} \right) \int P_1(\cos \beta) P_L(\cos \beta) \exp \left( \frac{\epsilon_2 \bar{P}_2 P_2(\cos \beta)}{k_B T} \right) d \cos \beta \right\}. \quad (3A.7)
\end{aligned}$$

Now for all  $L$  of odd parity the first term here vanishes by symmetry. As an example we consider the case where  $L = 1$ . Here,

$$\bar{P}_1 \sim Z_0^{-1} \left( \frac{\mu E + \epsilon_1 \bar{P}_1}{k_B T} \right) \int P_1(\cos \beta)^2 \exp \left( \frac{\epsilon_2 \bar{P}_2 P_2(\cos \beta)}{k_B T} \right) d \cos \beta. \quad (3A.8)$$

From the properties of the Legendre polynomials and Clebsch-Gordan coupling (or otherwise) we can write

$$P_1(\cos \beta)^2 = \frac{2}{3} P_2(\cos \beta) + \frac{1}{3} \quad (3A.9)$$

so that

$$\begin{aligned}
\bar{P}_1 \sim Z_0^{-1} \left( \frac{\mu E + \epsilon_1 \bar{P}_1}{k_B T} \right) &\left\{ \frac{2}{3} \int P_2(\cos \beta) \exp \left( \frac{\epsilon_2 \bar{P}_2 P_2(\cos \beta)}{k_B T} \right) d \cos \beta \right. \\
&+ \left. \frac{1}{3} \int \exp \left( \frac{\epsilon_2 \bar{P}_2 P_2(\cos \beta)}{k_B T} \right) d \cos \beta \right\} \quad (3A.10)
\end{aligned}$$

Again, approximating  $\bar{P}_2$  as that for the unperturbed nematic,  $\bar{P}_2^0$ , (and assuming that the potential of mean torque is also approximately that for the unperturbed nematic)

$$\begin{aligned}
\bar{P}_1 \sim \left( \frac{\mu E + \epsilon_1 \bar{P}_1}{k_B T} \right) &\left\{ \frac{2}{3} \bar{P}_2^0 + \frac{1}{3} Z_0^{-1} Z_0 \right\} \\
&= \left( \frac{\mu E + \epsilon_1 \bar{P}_1}{3 k_B T} \right) (2 \bar{P}_2^0 + 1), \quad (3A.11)
\end{aligned}$$

which rearranges to

$$\bar{P}_1 \sim \mu E / \left\{ \frac{3 k_B T}{2 \bar{P}_2^0 + 1} - \epsilon_1 \right\}. \quad (3A.12)$$

Thus an initial linear response of  $\bar{P}_1$  to the field is predicted to first order in the perturbation analysis.

A similar analysis for the other rank order parameters can give rise to some kind of field dependence to first order, although it is to be noted that, as we consider higher fields, the perturbation analysis would have to be taken to higher order for it to be a good approximation, and thus in higher field regimes the predicted dependence changes.

As another example of relevance we could consider  $\overline{P}_3$ . The order parameter is of odd rank so the first term in (3A.7) vanishes. The dependence on the field that we obtain from the second term then depends on the nature of  $P_1(\cos \beta)P_3(\cos \beta)$ . The product of two Legendre polynomials may be written as a Clebsch-Gordan series as

$$P_L(\cos \beta)P_{L'}(\cos \beta) = \sum_J C(LL', J00)^2 P_J(\cos \beta), \quad (3A.13)$$

where  $J = |L - L'|, |L - L'| + 1, \dots, |L + L'|$  and  $C(LL', J00)$  is a Clebsch-Gordan coefficient. Here the Clebsch-Gordan coupling yields a linear dependence of  $\overline{P}_3$  on the field. The same is not true of the second rank order parameter,  $\overline{P}_2$ , however. In this case both terms of (3A.7) survive, but the first is identified as just the Maier-Saupe  $\overline{P}_2$  and the second involves Clebsch-Gordan coupling between  $P_1(\cos \beta)$  and  $P_2(\cos \beta)$ , which gives only odd rank polynomials (so the Clebsch-Gordan coefficient of the  $P_2(\cos \beta)$  term in the series vanishes). These give rise to quantities that are identified as the Maier-Saupe values of  $\overline{P}_1$  and  $\overline{P}_3$ , which are zero and thus we obtain simply

$$\overline{P}_2 = \overline{P}_2^0, \quad (3A.14)$$

and a zeroth dependence on the field.

2. Perturbation analysis for the order parameters  $\overline{P}_L$  of a polarised ferroelectric ground state system initially in the isotropic phase.

A perturbation analysis is also available for the case of poling an initially isotropic material. Here there is no dominant interaction to factor out, but we know from experiment that the order parameters induced in an isotropic fluid by a weak (or

even a fairly strong) field are very small. Hence we can expand the total Boltzmann factor (ie, the Boltzmann factor for the total anisotropic potential energy) and truncate the expansion at the linear term to obtain a good approximation of the field dependence in the low field regime. Here then

$$\begin{aligned}
Z &\sim \int \left[ 1 + \left( \epsilon_2 \bar{P}_2 P_2(\cos \beta) + (\mu E + \epsilon_1 \bar{P}_1) P_1(\cos \beta) \right) / k_B T \right] d \cos \beta \\
&= \int d \cos \beta + \left( \frac{\mu E + \epsilon_1 \bar{P}_1}{k_B T} \right) \int P_1(\cos \beta) d \cos \beta + \frac{\epsilon_2 \bar{P}_2}{k_B T} \int P_2(\cos \beta) d \cos \beta
\end{aligned} \tag{3A.15}$$

Therefore,

$$Z \sim 2, \tag{3A.16}$$

that is, the value obtained by setting all the  $\bar{P}_L$  and the field to zero, the isotropic partition function. Therefore,

$$\begin{aligned}
\bar{P}_L &\sim \frac{1}{2} \left\{ \int P_L(\cos \beta) d \cos \beta + \frac{\epsilon_2 \bar{P}_2}{k_B T} \int P_2(\cos \beta) P_L(\cos \beta) d \cos \beta \right. \\
&\quad \left. + \left( \frac{\mu E + \epsilon_1 \bar{P}_1}{k_B T} \right) \int P_1(\cos \beta) P_L(\cos \beta) d \cos \beta \right\} \\
&= \frac{1}{2} \left\{ 0 + \frac{\epsilon_2 \bar{P}_2}{k_B T} \left( \frac{2}{2L+1} \right) \delta_{2L} + \left( \frac{\mu E + \epsilon_1 \bar{P}_1}{k_B T} \right) \left( \frac{2}{2L+1} \right) \delta_{1L} \right\},
\end{aligned} \tag{3A.17}$$

where  $\delta_{LL'}$  is a Kronecker delta. Thus, for all  $L > 2$  then all terms vanish and so all corresponding  $\bar{P}_L$  are predicted to show no response to the field.

For  $L = 1$  we have

$$\bar{P}_1 \sim \frac{1}{2} \left( \frac{\mu E + \epsilon_1 \bar{P}_1}{k_B T} \right) \frac{2}{3}, \tag{3A.18}$$

which rearranges to

$$\bar{P}_1 \sim \mu E / (3k_B T - \epsilon_1). \tag{3A.19}$$

We note that this is the result obtained by setting  $\overline{P}_2 = 0$  in the analogous expression for  $\overline{P}_1$  in the case of a material in a nematic phase prior to poling. Thus, for the initially isotropic phase too, a linear initial dependence of the first rank order parameter on the field is predicted.

For the case  $L = 2$  we obtain

$$\overline{P}_2 \sim \frac{1}{2} \frac{\epsilon_2 \overline{P}_2}{k_B T} \frac{2}{5} = \frac{\epsilon_2 \overline{P}_2}{5k_B T}, \quad (3A.20)$$

which implies

$$\overline{P}_2 \{1 - \epsilon_2/5k_B T\} \sim 0. \quad (3A.21)$$

Provided that  $\epsilon_2 \neq 5k_B T$  then

$$\overline{P}_2 \sim 0, \quad (3A.22)$$

and so, as with the  $\overline{P}_L$  ( $L > 2$ ), there is a zeroth initial response to the electric field.

To summarise, then, it would seem that to first order in the perturbation and with only first and second rank terms in the potential of mean torque, only  $\overline{P}_1$  order can be induced in an isotropic fluid at low electric fields. Some induction of higher rank order parameters may be obtained, however, if the perturbation expansion is taken to higher order. In addition, dependence of higher rank order parameters may also be obtained, even at first order in the perturbation, if the expansion for the potential of mean torque is taken to higher order.

## References

- [1] G. R. Meredith, J. G. van Dusen and D. J. Williams, *Macromol.*, **15**, 1385 (1982).
- [2] C. P. J. M. van der Vorst and S. J. Picken, *J. Opt. Soc. Am. B*, **7**, 320 (1990).
- [3] T. J. Krieger and H. M. James, *J. Chem. Phys.*, **22**, 796 (1954).
- [4] See, for example, G. R. Luckhurst in *The Molecular Physics of Liquid Crystals*, Chapter 4, Edited by G. R. Luckhurst and G. W. Gray, Academic Press, London (1979).
- [5] A. P. J. Emerson, R. Hashim and G. R. Luckhurst, *Mol. Phys.*, **76**, 241 (1992).
- [6] P. G. de Gennes and J. Prost, *The Physics of Liquid Crystals*, second edition, Clarendon Press, Oxford (1993).
- [7] T. H. Payne, unpublished notes.
- [8] G. R. Luckhurst, C. Zannoni, personal communications.
- [9] R. L. Humphries, P. G. James and G. R. Luckhurst, *Symp. Farad. Soc.*, **5**, 107 (1971).
- [10] L. D. Landau, *Collected Papers of L. D. Landau*, edited by D. ter Haar, Gordon and Breach, New York (1965).

# Chapter 4: A Molecular Field Theoretic Study of Order Parameters in Binary Nematic Mixtures

## 4.1 Introduction

In a liquid crystal display device it is necessary to optimise a range of properties. Pertinent considerations would include a large nematic range around room temperature, low viscosities, appropriate values of the elastic constants and large dielectric anisotropy and birefringence. It turns out that it is very difficult to achieve this using a single nematogenic compound as the liquid crystalline material. However, it has been found that the use of a mixture of compounds which exhibits a nematic state is a very powerful technique in achieving functional display devices.

In a typical liquid crystal display device a range of dopants are added to a nematic liquid crystal to form a multicomponent mixture. In order for a liquid crystal display to work, a low threshold voltage is required for switching, which in turn necessitates a large dielectric anisotropy  $\Delta\epsilon^{\text{mixt}}$ . Now

$$\Delta\epsilon^{\text{mixt}} = \sum_i x_i \Delta\epsilon_i \bar{P}_2^i, \quad (4.1)$$

where  $i$  labels the components and  $x_i$ ,  $\Delta\epsilon_i$  and  $\bar{P}_2^i$  are the mole fractions, dielectric anisotropies and order parameters of the components  $i$ , respectively. If we assume that the dielectric anisotropies of the components  $i$  are all equal ( $\Delta\epsilon$ , say) then

$$\Delta\epsilon^{\text{mixt}} = \Delta\epsilon \sum_i x_i \bar{P}_2^i \quad (4.2)$$



and since

$$\sum_i x_i \bar{P}_2^i = \bar{P}_2^{\text{mixt}} \quad (4.3)$$

the dielectric anisotropy of the mixture is seen to vary as the order parameter of the mixture

$$\Delta\epsilon^{\text{mixt}} \sim \bar{P}_2^{\text{mixt}}.$$

Moreover, in order to achieve a good contrast a large birefringence is required, but the birefringence  $\Delta n$  is also related to the dielectric anisotropy of the medium as

$$(\Delta n^{\text{mixt}})^2 \propto \Delta\epsilon^{\text{mixt}},$$

and as we have seen,  $\Delta\epsilon^{\text{mixt}}$  is expected to be proportional to  $\bar{P}_2^{\text{mixt}}$ . For this reason also then, we require a high value of  $\bar{P}_2^{\text{mixt}}$ .

It is clearly desirable to investigate the suitability of a variety of compounds for application in devices. Whilst the nematic mixture in a display device may contain many individual components, to test each component separately they are studied individually in a given nematic solvent. This is then more convenient for devising ways of obtaining standardised measures for a variety of properties of the potential additives. The way that this is most commonly employed at present is to measure the property of interest for mixtures of the test compound in a standard nematic solvent as a function of composition of the mixture, at a given absolute temperature. For a wide variety of properties it is generally found that the graph obtained from this procedure is linear; this probably results because the accessible range of compositions is very narrow due to the limits of miscibility of the test compounds. Nevertheless, this linear graph is then extrapolated to the limit of pure solute and the value there is taken to yield a hypothetical value for the property intrinsic to the pure solute [1]. This is assumed to give a measure that is somehow intrinsic to the additive itself and independent of the solvent. This manipulation clearly assumes continued linearity across the whole of the composition range. Here, the experimental interest focusses on the problem of

achieving good contrast (and low threshold voltages) and hence on measures of the power of the potential dopants to induce birefringence, or nematic ordering, in the mixture. Thus, the birefringence of mixtures is measured, at a given temperature, across the accessible part of the composition range. The extrapolation is taken to yield a measure of the hypothetical birefringence of the pure solute in the nematic state.

The aim of this research, then, is to investigate from a theoretical standpoint to what extent this extrapolation is valid and to what the limiting value really corresponds. For our purposes in performing molecular field calculations the nematic order parameter of the mixture serves as a convenient surrogate to the birefringence and is the quantity we shall focus on calculating. Such investigations have the advantage that the theory only concerns itself with the essential features that give rise to liquid crystalline behaviour. Thus we are able to probe composition regimes that are inaccessible practically due to the limits of solubility of the components. The variant of molecular field theory that we have employed for this purpose is the Humphries-James-Luckhurst (HJL) theory of binary nematic mixtures [2] that we have developed in an intuitive way and used in the studies of poling of nematics in Chapter 3. We now give a more formal derivation and apply it to the problem at hand.

## 4.2 Variational Derivation of the HJL Theory of Binary Nematic Mixtures

First we identify the dominant order parameters, which for cylindrically symmetric particles we take as  $\overline{P}_{2A}$  and  $\overline{P}_{2B}$ . We then construct the internal energy on the basis that pair interactions are predominant as

$$\overline{U} = -\frac{1}{2} (n_A^2 \epsilon_{AA} \overline{P}_{2A}^2 + 2 n_A n_B \epsilon_{AB} \overline{P}_{2A} \overline{P}_{2B} + n_B^2 \epsilon_{BB} \overline{P}_{2B}^2), \quad (4.4)$$

where  $n_A$  is the number of particles of component  $A$ ,  $\epsilon_{AB}$  is the intrinsic interaction parameter for interaction of particle type  $A$  with  $B$  and  $\overline{P}_{2A}$  is the second rank orien-

tational order parameter for component  $A$ . The internal energy per mole is then

$$\frac{\bar{U}}{n_A + n_B} = -\frac{1}{2}(x^2\epsilon_{AA}\bar{P}_{2A}^2 + 2x(1-x)\epsilon_{AB}\bar{P}_{2A}\bar{P}_{2B} + (1-x)^2\epsilon_{BB}\bar{P}_{2B}^2), \quad (4.5)$$

where  $x$  is the mole fraction of  $A$ . This form for  $\bar{U}$  assumes random mixing of the two components  $A$  and  $B$  and the equality of their molar volumes. (If the molar volumes are not approximately equal then the mole fractions should be replaced by volume fractions.) Within the molecular field approximation the entropy is additive, that is

$$S = xS_A + (1-x)S_B. \quad (4.6)$$

This obviously ignores the entropy of mixing which is valid as long as phase separation is not allowed. Within the molecular field approximation the entropy of each component is related to the singlet orientational distribution function for that component in the usual way,

$$S_A = -k_B \int f_A(\beta) \ln f_A(\beta) \sin \beta d\beta,$$

$$S_B = -k_B \int f_B(\beta) \ln f_B(\beta) \sin \beta d\beta. \quad (4.7)$$

The total molar Helmholtz free energy is then

$$A = -\{(1-x)^2\epsilon_{AA}\bar{P}_{2A}^2 + 2x(1-x)\epsilon_{AB}\bar{P}_{2A}\bar{P}_{2B} + x^2\epsilon_{BB}\bar{P}_{2B}^2\}/2$$

$$+k_B T \left\{ (1-x) \int f_A(\beta) \ln f_A(\beta) \sin \beta d\beta + x \int f_B(\beta) \ln f_B(\beta) \sin \beta d\beta \right\}. \quad (4.8)$$

The variation in  $A$  (which we set to zero) is then

$$\delta A = -\{ (1-x)^2\epsilon_{AA} 2\bar{P}_{2A} \delta\bar{P}_{2A} + 2x(1-x)\epsilon_{AB} (\bar{P}_{2A} \delta\bar{P}_{2B} + \bar{P}_{2B} \delta\bar{P}_{2A})$$

$$+ x^2\epsilon_{BB} 2\bar{P}_{2B} \delta\bar{P}_{2B} \} / 2$$

$$+k_B T \left\{ (1-x) \int \delta f_A(\beta) [\ln f_A(\beta) + 1] \sin \beta d\beta + x \int \delta f_B(\beta) [\ln f_B(\beta) + 1] \sin \beta d\beta \right\}. \quad (4.9)$$

Now the variations  $\delta \bar{P}_{2A}, \delta \bar{P}_{2B}$  in the two order parameters  $\bar{P}_{2A}, \bar{P}_{2B}$  are related to the fluctuations in the distribution functions

$$\begin{aligned}\delta \bar{P}_{2A} &= \int P_2(\cos \beta) \delta f_A(\beta) \sin \beta d\beta, \\ \delta \bar{P}_{2B} &= \int P_2(\cos \beta) \delta f_B(\beta) \sin \beta d\beta,\end{aligned}\tag{4.10}$$

and so

$$\begin{aligned}\delta A &= -\left\{ (1-x)^2 \epsilon_{AA} \bar{P}_{2A} \int P_2(\cos \beta) \delta f_A(\beta) \sin \beta d\beta \right. \\ &+ x(1-x) \epsilon_{AB} \left( \bar{P}_{2A} \int P_2(\cos \beta) \delta f_B(\beta) \sin \beta d\beta + \bar{P}_{2B} \int P_2(\cos \beta) \delta f_A(\beta) \sin \beta d\beta \right) \\ &\left. + x^2 \epsilon_{BB} \bar{P}_{2B} \int P_2(\cos \beta) \delta f_B(\beta) \sin \beta d\beta \right\} \\ &+ k_B T \left\{ (1-x) \int \delta f_A(\beta) [\ln f_A(\beta) + 1] \sin \beta d\beta + x \int \delta f_B(\beta) [\ln f_B(\beta) + 1] \sin \beta d\beta \right\}.\end{aligned}\tag{4.11}$$

This may be written as a single integral

$$\begin{aligned}\delta A &= \int \left\{ \delta f_A(\beta) \left[ - (1-x)^2 \epsilon_{AA} \bar{P}_{2A} P_2(\cos \beta) - x(1-x) \epsilon_{AB} \bar{P}_{2B} P_2(\cos \beta) \right. \right. \\ &\left. \left. + (1-x) k_B T [\ln f_A(\beta) + 1] \right] \right. \\ &\left. + \delta f_B(\beta) \left[ - x(1-x) \epsilon_{AB} \bar{P}_{2A} P_2(\cos \beta) - x^2 \epsilon_{BB} \bar{P}_{2B} P_2(\cos \beta) + x k_B T [\ln f_B(\beta) + 1] \right] \right\} \sin \beta d\beta\end{aligned}\tag{4.12}$$

We must now take account of the constraints, namely that the two distribution functions  $f_A(\beta), f_B(\beta)$  are normalised. Thus

$$\int \delta f_A(\beta) \sin \beta d\beta = 0,\tag{4.13}$$

$$\int \delta f_B(\beta) \sin \beta d\beta = 0. \quad (4.14)$$

We multiply (4.13) by the Lagrange multiplier  $\lambda_1$  and (4.14) by  $\lambda_2$  and add them to the main equation (4.12) to give

$$\begin{aligned} \int \left\{ \delta f_A(\beta) \left[ - (1-x)^2 \epsilon_{AA} \bar{P}_{2A} P_2(\cos \beta) - x(1-x) \epsilon_{AB} \bar{P}_{2B} P_2(\cos \beta) \right. \right. \\ \left. \left. + (1-x) k_B T [\ln f_A(\beta) + 1] + \lambda_1 \right] \right. \\ \left. + \delta f_B(\beta) \left[ - x(1-x) \epsilon_{AB} \bar{P}_{2A} P_2(\cos \beta) - x^2 \epsilon_{BB} \bar{P}_{2B} P_2(\cos \beta) \right. \right. \\ \left. \left. + x k_B T [\ln f_B(\beta) + 1] + \lambda_2 \right] \right\} \sin \beta d\beta = 0. \end{aligned} \quad (4.15)$$

This equation must hold for any arbitrary  $\delta f_A(\beta)$  and  $\delta f_B(\beta)$ . Here we have an integrand composed of a sum of two terms, one in which the variation in one distribution is a factor and the other in which that in the other distribution is a factor. Under such circumstances (see Appendix 2A) it turns out that the remaining factor in each term must vanish, giving a vanishing expression for each distribution, which we may then solve for that distribution. Thus we have

$$\begin{aligned} - (1-x)^2 \epsilon_{AA} \bar{P}_{2A} P_2(\cos \beta) - x(1-x) \epsilon_{AB} \bar{P}_{2B} P_2(\cos \beta) \\ + (1-x) k_B T [\ln f_A(\beta) + 1] + \lambda_1 = 0, \\ - x(1-x) \epsilon_{AB} \bar{P}_{2A} P_2(\cos \beta) - x^2 \epsilon_{BB} \bar{P}_{2B} P_2(\cos \beta) \\ + x k_B T [\ln f_B(\beta) + 1] + \lambda_2 = 0, \end{aligned} \quad (4.16)$$

which yield as the singlet orientational distribution functions

$$f_A(\beta) = \exp \left[ \frac{(1-x)^2 \epsilon_{AA} \bar{P}_{2A} P_2(\cos \beta) + x(1-x) \epsilon_{AB} \bar{P}_{2B} P_2(\cos \beta) - \lambda_1}{(1-x) k_B T} - 1 \right],$$

$$= \exp \left[ \frac{(1-x)\epsilon_{AA}\bar{P}_{2A}P_2(\cos\beta) + x\epsilon_{AB}\bar{P}_{2B}P_2(\cos\beta)}{k_B T} \right] \exp \left[ -\frac{\lambda_1}{(1-x)k_B T} - 1 \right] \quad (4.17)$$

and

$$\begin{aligned} f_B(\beta) &= \exp \left[ \frac{x^2\epsilon_{BB}\bar{P}_{2B}P_2(\cos\beta) + x(1-x)\epsilon_{AB}\bar{P}_{2A}P_2(\cos\beta) - \lambda_2}{xk_B T} - 1 \right] \\ &= \exp \left[ \frac{x\epsilon_{BB}\bar{P}_{2B}P_2(\cos\beta) + (1-x)\epsilon_{AB}\bar{P}_{2A}P_2(\cos\beta)}{k_B T} \right] \exp \left[ -\frac{\lambda_2}{xk_B T} - 1 \right]. \end{aligned} \quad (4.18)$$

The distributions are then

$$\begin{aligned} f_A(\beta) &= Z_A^{-1} \exp \left( \{ (1-x)\epsilon_{AA}\bar{P}_{2A} + x\epsilon_{AB}\bar{P}_{2B} \} P_2(\cos\beta) / k_B T \right), \\ f_B(\beta) &= Z_B^{-1} \exp \left( \{ x\epsilon_{BB}\bar{P}_{2B} + (1-x)\epsilon_{AB}\bar{P}_{2A} \} P_2(\cos\beta) / k_B T \right), \end{aligned} \quad (4.19)$$

if we identify the inverse partition functions as

$$\begin{aligned} Z_A^{-1} &= \exp \left[ -\frac{\lambda_1}{(1-x)k_B T} - 1 \right], \\ Z_B^{-1} &= \exp \left[ -\frac{\lambda_2}{xk_B T} - 1 \right]. \end{aligned} \quad (4.20)$$

Accordingly, the potentials of mean torque for the particle types *A* and *B* of the mixture are then

$$\begin{aligned} U_A(\beta) &= -\{ (1-x)\epsilon_{AA}\bar{P}_{2A} + x\epsilon_{AB}\bar{P}_{2B} \} P_2(\cos\beta), \\ U_B(\beta) &= -\{ x\epsilon_{BB}\bar{P}_{2B} + (1-x)\epsilon_{AB}\bar{P}_{2A} \} P_2(\cos\beta), \end{aligned} \quad (4.21)$$

respectively.

### 4.3 Application

Here we take *B* to be the additive so that its mole fraction is *x*; that of the liquid crystal solvent is then  $1-x$ . The coefficients  $\epsilon_{MN}$  in the potentials of mean torque

represent the intrinsic molecular field interaction coefficients for a particle of type  $M$  in the molecular field generated by a particle of type  $N$ . We note that  $\epsilon_{MN} = \epsilon_{NM}$  so that  $\epsilon_{BA} = \epsilon_{AB}$ . We construct the Helmholtz free energy as follows. The free energy of component  $A$  is

$$A_A = \{(1-x)\epsilon_{AA}\bar{P}_{2A}^2 + x\epsilon_{AB}\bar{P}_{2A}\bar{P}_{2B}\}/2 - k_B T \ln Z_A \quad (4.22)$$

and that of component  $B$  is

$$A_B = \{x\epsilon_{BB}\bar{P}_{2B}^2 + (1-x)\epsilon_{AB}\bar{P}_{2A}\bar{P}_{2B}\}/2 - k_B T \ln Z_B. \quad (4.23)$$

The total orientational Helmholtz free energy of the mixture is then

$$A = (1-x)A_A + xA_B, \quad (4.24)$$

that is,

$$A = \{(1-x)^2\epsilon_{AA}\bar{P}_{2A}^2 + 2x(1-x)\epsilon_{AB}\bar{P}_{2A}\bar{P}_{2B} + x^2\epsilon_{BB}\bar{P}_{2B}^2\}/2 - (1-x)k_B T \ln Z_A - xk_B T \ln Z_B. \quad (4.25)$$

Thus we have three arbitrary parameters,  $\epsilon_{AA}$ ,  $\epsilon_{AB}$  and  $\epsilon_{BB}$ . One of these (say  $\epsilon_{AA}$ ) will be taken out as a common factor and used to scale the temperature to give the scaled temperature  $T^* = k_B T / \epsilon_{AA}$ . The other parameters then end up scaled by (in this case)  $\epsilon_{AA}$  and these ratios form the remaining input parameters. The Boltzmann factors are then constructed from the potentials of mean torque as

$$\begin{aligned} U_A(\beta)/k_B T &= -\frac{\epsilon_{AA}}{k_B T} \left\{ (1-x)\bar{P}_{2A} + x\frac{\epsilon_{AB}}{\epsilon_{AA}}\bar{P}_{2B} \right\} P_2(\cos\beta), \\ &= -\frac{1}{T^*} \left\{ (1-x)\bar{P}_{2A} + x\frac{\epsilon_{AB}}{\epsilon_{AA}}\bar{P}_{2B} \right\} P_2(\cos\beta) \end{aligned} \quad (4.26)$$

and

$$U_B(\beta)/k_B T = -\frac{\epsilon_{AA}}{k_B T} \left\{ x\frac{\epsilon_{BB}}{\epsilon_{AA}}\bar{P}_{2B} + (1-x)\frac{\epsilon_{AB}}{\epsilon_{AA}}\bar{P}_{2A} \right\} P_2(\cos\beta)$$

$$= -\frac{1}{T^*} \left\{ x \lambda \bar{P}_{2B} + (1-x) \frac{\epsilon_{AB}}{\epsilon_{AA}} \bar{P}_{2A} \right\} P_2(\cos \beta), \quad (4.27)$$

where  $T^*$  is the scaled temperature and  $\lambda$  is the ratio  $\epsilon_{BB}/\epsilon_{AA}$  which is equal to the ratio of the transition temperatures  $T_{NI}^B/T_{NI}^A$ . We now introduce the geometric mean approximation for  $\epsilon_{AB}$  in order to reduce the number of arbitrary parameters in the theory. In other words, we assume

$$\epsilon_{AB} = (\epsilon_{AA} \epsilon_{BB})^{1/2}, \quad (4.28)$$

so that there are only two independent parameters,  $\epsilon_{AA}$  and  $\epsilon_{BB}$ , one of these ( $\epsilon_{AA}$ ) being used to scale the temperature. The geometric mean approximation is exact for dispersive forces, so that it is correct to the extent that the intermolecular forces between particles of type  $A$  and  $B$  are dispersive or dispersive-like. This occurs because the anisotropic dispersion force between two identical molecules varies as the square of the anisotropy in the polarisability, that is

$$\epsilon_{AA} \sim U_{AA}^{\text{disp}} \sim \Delta\alpha_A^2 = \Delta\alpha_A \Delta\alpha_A. \quad (4.29)$$

If this is assumed to hold when the molecules are not identical then the strength parameter is given by

$$\epsilon_{AB} \sim U_{AB}^{\text{disp}} \sim \Delta\alpha_A \Delta\alpha_B \quad (4.30)$$

and so is equal to the geometric mean for the strength parameters of the pure components

$$(\Delta\alpha_A^2 \Delta\alpha_B^2)^{1/2} \sim (\epsilon_{AA} \epsilon_{BB})^{1/2}. \quad (4.31)$$

Within the geometric mean approximation the ratio  $\epsilon_{AB}/\epsilon_{AA}$  appearing in (4.26, 4.27) is

$$\epsilon_{AB}/\epsilon_{AA} = \left( \frac{\epsilon_{AA} \epsilon_{BB}}{\epsilon_{AA}^2} \right)^{1/2} = \lambda^{1/2}. \quad (4.32)$$

Equations (4.26, 4.27) then become

$$\frac{U_A(\beta)}{k_B T} = -\frac{1}{T^*} \left\{ (1-x) \bar{P}_{2A} + x \lambda^{1/2} \bar{P}_{2B} \right\} P_2(\cos \beta) \quad (4.33)$$



and

$$\frac{U_B(\beta)}{k_B T} = -\frac{1}{T^*} \{x \lambda \bar{P}_{2B} + (1-x) \lambda^{1/2} \bar{P}_{2A}\} P_2(\cos \beta). \quad (4.34)$$

We note that

$$\begin{aligned} \frac{U_B(\beta)}{k_B T} &= -\frac{\lambda^{1/2}}{T^*} \{x \lambda^{1/2} \bar{P}_{2B} + (1-x) \bar{P}_{2A}\} P_2(\cos \beta) \\ &= \lambda^{1/2} \frac{U_A(\beta)}{k_B T}, \end{aligned} \quad (4.35)$$

so that if we write

$$\begin{aligned} \frac{U_A(\beta)}{k_B T} &= -X_A^* P_2(\cos \beta), \\ \frac{U_B(\beta)}{k_B T} &= -X_B^* P_2(\cos \beta) \end{aligned} \quad (4.36)$$

then

$$\frac{U_B(\beta)}{k_B T} = -\lambda^{1/2} X_A^* P_2(\cos \beta). \quad (4.37)$$

Thus we see that within the geometric mean approximation the ratio  $X_B^*/X_A^* = \lambda^{1/2}$  is constant and that for a given value of  $\lambda$  everything is controlled by the single scaled strength parameter  $X_A^*$ . The scaled free energy is then written

$$\begin{aligned} \frac{A}{k_B T} &= \frac{1}{T^*} \{ (1-x)^2 \bar{P}_{2A}^2 + 2x(1-x) \lambda^{1/2} \bar{P}_{2A} \bar{P}_{2B} + x^2 \lambda \bar{P}_{2B}^2 \} / 2 \\ &\quad - (1-x) \ln Z_A - x \ln Z_B, \end{aligned} \quad (4.38)$$

with

$$\begin{aligned} Z_A &= \int \exp \left[ \frac{1}{T^*} \{ (1-x) \bar{P}_{2A} + x \lambda^{1/2} \bar{P}_{2B} \} P_2(\cos \beta) \right] \sin \beta d\beta, \\ Z_B &= \int \exp \left[ \frac{1}{T^*} \{ x \lambda \bar{P}_{2B} + (1-x) \lambda^{1/2} \bar{P}_{2A} \} P_2(\cos \beta) \right] \sin \beta d\beta. \end{aligned} \quad (4.39)$$

## 4.4 Methodology for Solving the Molecular Field Equations

The methodology of choice to obtain the order parameters would be minimisation of the equilibrium free energy (see Chapter 2). It would be natural and straightforward to assume that this minimisation should be performed with respect to the order parameters appearing in the potential of mean torque and hence using the free energy expression (4.25). Minimising the free energy in this way is not possible, however, because the free energy surface will not possess a minimum with respect to the two order parameters  $\bar{P}_2^A$  and  $\bar{P}_2^B$  when treated as independent variational parameters. This was confirmed by calculation, visual representation and inspection of a wide variety of free energy surfaces [3]. This situation obtains because these order parameters are not independent; only if the free energy is expressed as a function of the minimum number of independent degrees of freedom of the system can it possess a global minimum [4]. It turns out that within the geometric mean approximation for the mixed interaction parameter (which we are using) the free energy expression can be rewritten in terms of a single, composite order parameter [2]

$$P = (1 - x) \epsilon_{AA}^{1/2} \bar{P}_2^A + x \epsilon_{BB}^{1/2} \bar{P}_2^B, \quad (4.40)$$

this representing the single independent order parameter. We note that such a manipulation is not possible outside of the geometric mean approximation, which thus represents a special, limiting case. Indeed, outside of the geometric mean approximation attempts to minimise (4.25) using the standard methodology always yield solutions [3]. Using the composite order parameter, then, we write the free energy as

$$\begin{aligned} A &= \frac{P^2}{2} - (1 - x)k_B T \ln Z_A - xk_B T \ln Z_B, \\ Z_A &= \int \exp \left( \frac{\epsilon_{AA}^{1/2}}{k_B T} P P_2(\cos \beta) \right) \sin \beta d\beta, \\ Z_B &= \int \exp \left( \frac{\epsilon_{BB}^{1/2}}{k_B T} P P_2(\cos \beta) \right) \sin \beta d\beta. \end{aligned} \quad (4.41)$$

The question now arises as how best to scale the free energy for the purposes of computing the solutions. It is usual in molecular field calculations to scale the free energy with  $k_B T$ . Normally this manipulation would enable the quantity  $A/k_B T$  to be written in terms of  $k_B T$  divided by one of the molecular field coefficients (thus furnishing a scaled temperature), with the other molecular field coefficients being scaled by that coefficient. These scaled quantities are then the input parameters to the calculation. In this case we would have

$$\frac{A}{k_B T} = \frac{P^2}{2k_B T} - (1-x) \ln Z_A - x \ln Z_B, \quad (4.42)$$

which does not allow us to write the function to be minimised with the desired minimum number of input parameters due to the explicit appearance of  $k_B T$  in the molecular field correction to the free energy. However, if we write the composite order parameter as

$$P = \epsilon_{AA}^{1/2} \{(1-x)\bar{P}_2^A + x \lambda^{1/2} \bar{P}_2^B\} \quad (4.43)$$

the molecular field correction becomes

$$\frac{P^2}{2} = \frac{\epsilon_{AA}}{2} \{(1-x)^2 \bar{P}_2^{A2} + 2x(1-x) \lambda^{1/2} \bar{P}_2^A \bar{P}_2^B + x^2 \lambda \bar{P}_2^{B2}\}. \quad (4.44)$$

Then if we define a new composite order parameter

$$P_\epsilon = \frac{P}{\epsilon_{AA}^{1/2}} = \{(1-x)\bar{P}_2^A + x \lambda^{1/2} \bar{P}_2^B\} \quad (4.45)$$

so that

$$P_\epsilon^2 = \{(1-x)^2 \bar{P}_2^{A2} + 2x(1-x) \lambda^{1/2} \bar{P}_2^A \bar{P}_2^B + x^2 \lambda \bar{P}_2^{B2}\} \quad (4.46)$$

we may now scale the free energy with  $k_B T$  as

$$\frac{A}{k_B T} = \frac{P_\epsilon^2}{2T^*} - (1-x) \ln Z_A - x \ln Z_B. \quad (4.47)$$

The partition functions may be expressed explicitly in terms of the new composite order parameter, since the scaled potentials of mean torque (4.33, 4.34) may now be written

$$\frac{U_A(\beta)}{k_B T} = -\frac{1}{T^*} P_\epsilon P_2(\cos \beta),$$

$$\frac{U_B(\beta)}{k_B T} = -\frac{\lambda^{1/2}}{T^*} \{x \lambda^{1/2} \bar{P}_{2B} + (1-x) \bar{P}_{2A}\} P_2(\cos \beta),$$

$$\frac{U_B(\beta)}{k_B T} = -\frac{\lambda^{1/2}}{T^*} P_\epsilon P_2(\cos \beta). \quad (4.48)$$

There is also another possible scaling of the free energy using this new composite order parameter, and this is by scaling the free energy with respect to the coefficient  $\epsilon_{AA}$ . This gives

$$\frac{A}{\epsilon_{AA}} = \frac{P_\epsilon^2}{2} - (1-x)T^* \ln Z_A - xT^* \ln Z_B \quad (4.49)$$

with the partition functions as indicated previously, that is

$$Z_A = \int \exp\left(\frac{1}{T^*} P_\epsilon P_2(\cos \beta)\right) \sin \beta d\beta$$

$$Z_B = \int \exp\left(\frac{\lambda^{1/2}}{T^*} P_\epsilon P_2(\cos \beta)\right) \sin \beta d\beta. \quad (4.50)$$

The value of  $P_\epsilon$  for any given mixture is thus obtained by minimising the scaled free energy with respect to it for given values of the scaled temperature, mole fraction of dopant and the ratio  $\lambda$ . The scaled temperatures employed were calculated from consideration of the reduced temperature (with respect to the solvent) at which the experiments are normally performed. That is, the reduced temperature of the mixture is in the range 0.8 – 1.0 at most, more likely in practise 0.9 – 1.0. The free energy was therefore minimised at scaled temperatures corresponding to reduced temperatures  $T_r$  of 0.8, 0.9 and 0.95, for a range of compositions spanning the whole range and taking  $\lambda$  to be either 0.75 or 0.5. In addition, for comparison some very low reduced temperatures, far outside the experimentally accessible range, namely, 0.4, 0.45, 0.60 and 0.68, were also used to generate results. The values of  $\lambda$  ( $\equiv T_{NI}^B/T_{NI}^A$ ) employed span the likely range of anisotropies of the dopants relative to the solvent. The dopants are usually less anisotropic than the nematogenic solvent, so generally we expect  $\lambda < 1.0$ . The order parameters of the individual components were calculated from the corresponding

singlet orientational distribution functions once the composite order parameter had been determined as

$$\begin{aligned}\bar{P}_2^A &= Z_A^{-1} \int P_2(\cos \beta) \exp(P_\epsilon P_2(\cos \beta)/T^*) \sin \beta d\beta, \\ \bar{P}_2^B &= Z_B^{-1} \int P_2(\cos \beta) \exp(\lambda^{1/2} P_\epsilon P_2(\cos \beta)/T^*) \sin \beta d\beta.\end{aligned}\quad (4.51)$$

The order parameter of the mixture is then given by the mole fraction weighted average of those of the components,

$$\bar{P}_2^{\text{mixt}} = (1 - x)\bar{P}_2^A + x\bar{P}_2^B. \quad (4.52)$$

This is similar in form to  $P_\epsilon$  (see equation (4.45)), which in fact becomes equal to it in  $\lim x \rightarrow 0$ . In addition, in  $\lim x \rightarrow 1$ ,  $P_\epsilon = \lambda^{1/2} \bar{P}_2^B$ .

## 4.5 Results and Discussion

Figures (4.1)–(4.8) show the order parameters as a function of composition at various very low reduced temperatures (ie, much lower than is ever achieved experimentally) for two values of  $\lambda$ , namely 0.75 and 0.5.

In figure (4.1) we see a weak, linear dependence of the order parameters on the composition. This dependence is due to the very low temperature of the system and the relatively high anisotropy of the solute, which ensures that the order parameters are always high and near to the limiting values across the entire composition range. In the limit of low temperature the order parameters would be unity across the range and so there would be no dependence and the graphs would be perfectly linear. As we have seen, the order parameter  $P_\epsilon$  at  $x = 1$  is related to the order parameter of the additive by a factor of  $\lambda^{1/2}$ , so that in this case it is  $\sqrt{0.75} \sim 0.87$  times the value of  $\bar{P}_2^B$ .

Figure 4.1: Second rank orientational order parameters  $\overline{P}_2^{\text{mixt}}$  (—),  $\overline{P}_2^A$  (---),  $\overline{P}_2^B$  (- -) and  $P_\epsilon$  (....) as a function of composition at a reduced temperature of 0.40 with  $\lambda = 0.75$ .

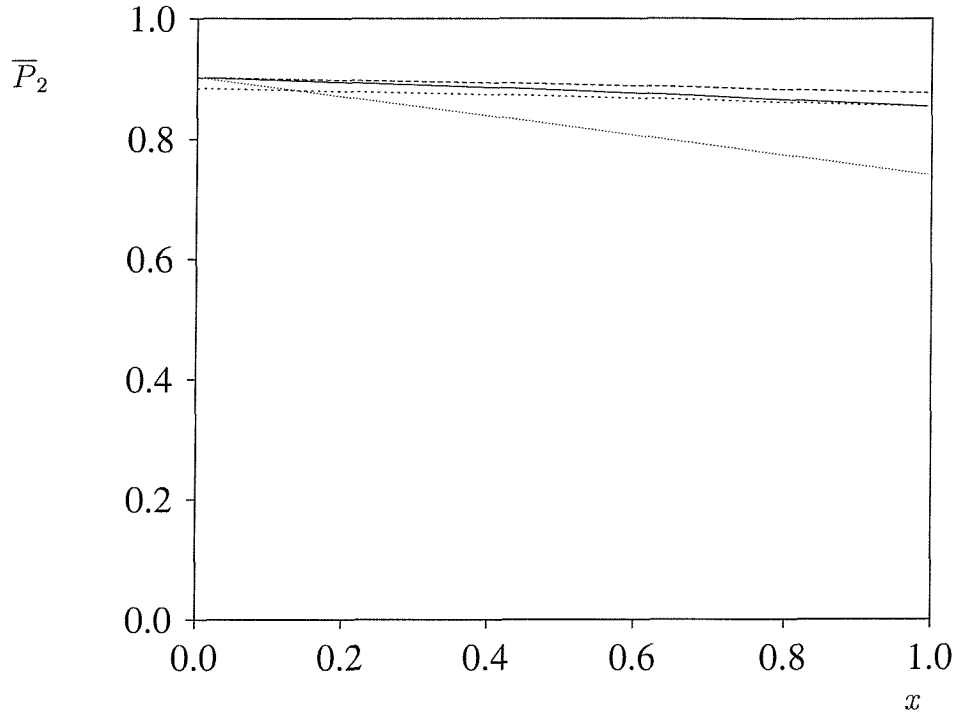
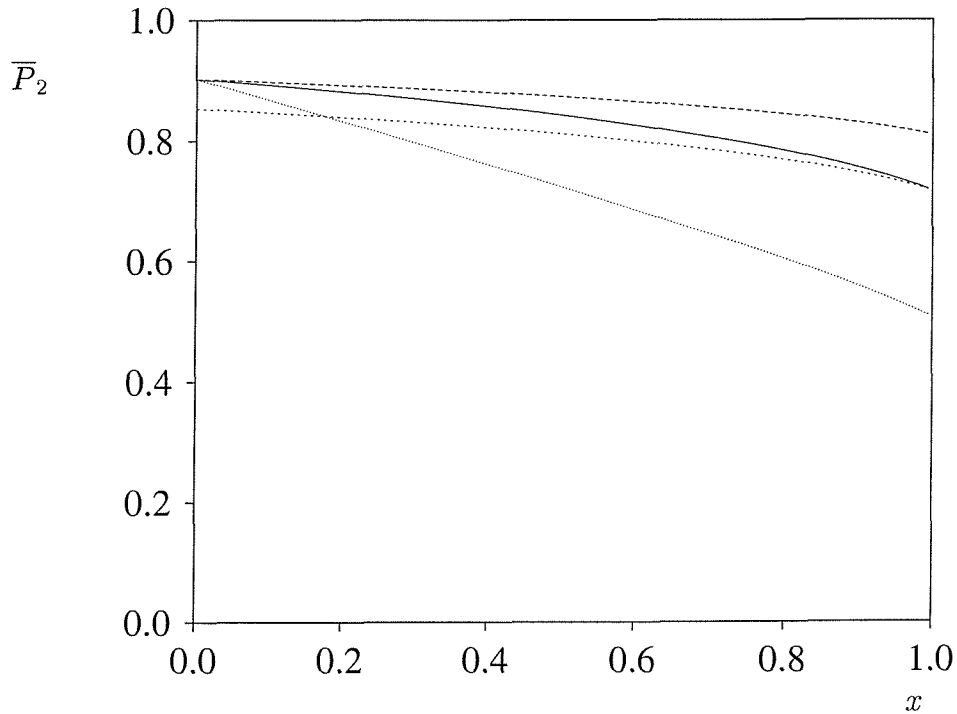


Figure 4.2: Second rank orientational order parameters  $\overline{P}_2^{\text{mixt}}$  (—),  $\overline{P}_2^A$  (---),  $\overline{P}_2^B$  (- -) and  $P_\epsilon$  (....) as a function of composition at a reduced temperature of 0.40 with  $\lambda = 0.5$ .



In figure (4.2) we have the same temperature but the anisotropy of the solute is considerably less and  $P_\epsilon = \sqrt{0.5} \bar{P}_2^B \sim 0.71 \bar{P}_2^B$ , so that the larger difference between  $P_\epsilon$  and  $\bar{P}_2^B$  is due to the smaller value of  $\lambda$ . We find that nevertheless, due to the temperature, the order parameters are still sufficiently high that the graphs of component and mixture order parameters are still quite linear.

In figures (4.3) and (4.4) we have the results for  $\lambda = 0.75, 0.5$  as before, but now at a slightly higher reduced temperature of 0.45. For  $\lambda = 0.75$  the high anisotropy of the solute ensures that even though the temperature is slightly higher, the order parameters of the pure components (ie, the order parameters at the extremes of the range) are still sufficiently high and similar that the dependence remains weak and linear. When we consider the graphs for  $\lambda = 0.5$ , however, we begin to see deviation of the order parameters from linearity and concomitantly a stronger dependence of the order parameters on the composition.

In figures (4.5) and (4.6) we have the same solutes but at a somewhat higher reduced temperature. For the more anisotropic solute the dependence is slightly stronger, but the order parameters are still essentially linear in the composition. This contrasts strongly with the other solute, however. At this temperature the less anisotropic solute is not liquid crystalline, so that somewhere between the pure solvent at  $x = 0$  and the pure dopant at  $x = 1$  there is a solvent-induced phase transition. The associated transitional order parameter of the mixture is about 0.43. This does not occur for  $\lambda = 0.75$  since the more anisotropic dopant is nematic at this temperature within the theory. We note that in the case of the solvotropic phase transition the order parameters of the components and the mixture do not come together to become equal at the transition. This is simply because within the ordered phase these order parameters can only become equal at  $x = 1$ . Therefore the inequality of the order parameters at the transition will always be observed where there is a solvent-induced transition.

Figure 4.3: Second rank orientational order parameters  $\overline{P}_2^{mixt}$  (—),  $\overline{P}_2^A$  (---),  $\overline{P}_2^B$  (- -) and  $P_e$  (....) as a function of composition at a reduced temperature of 0.45 with  $\lambda = 0.75$ .

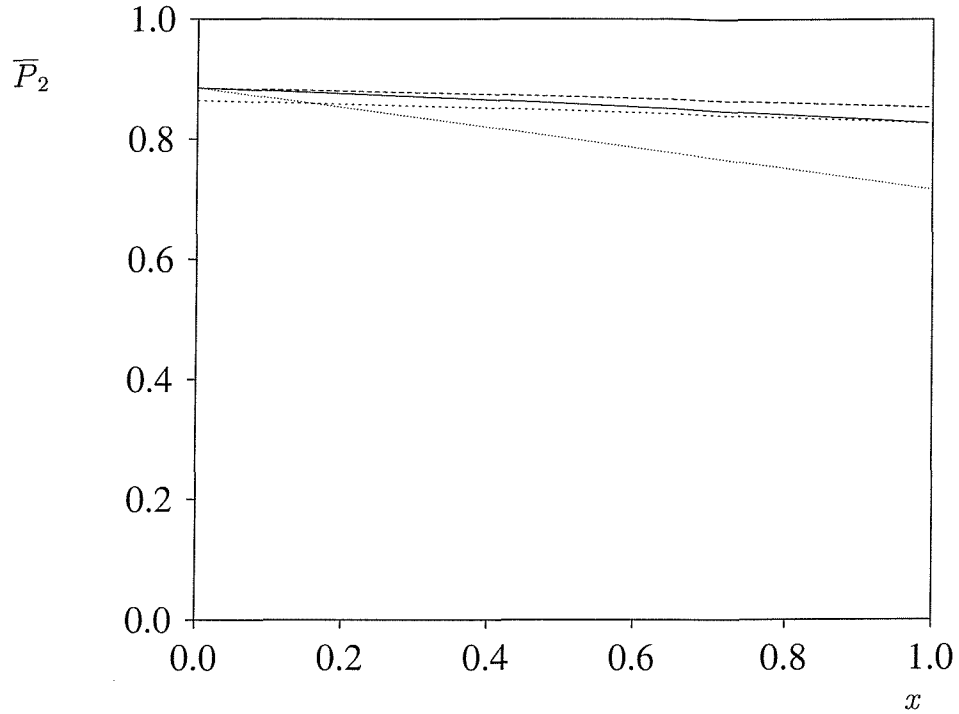


Figure 4.4: Second rank orientational order parameters  $\overline{P}_2^{mixt}$  (—),  $\overline{P}_2^A$  (---),  $\overline{P}_2^B$  (- -) and  $P_e$  (....) as a function of composition at a reduced temperature of 0.45 with  $\lambda = 0.5$ .

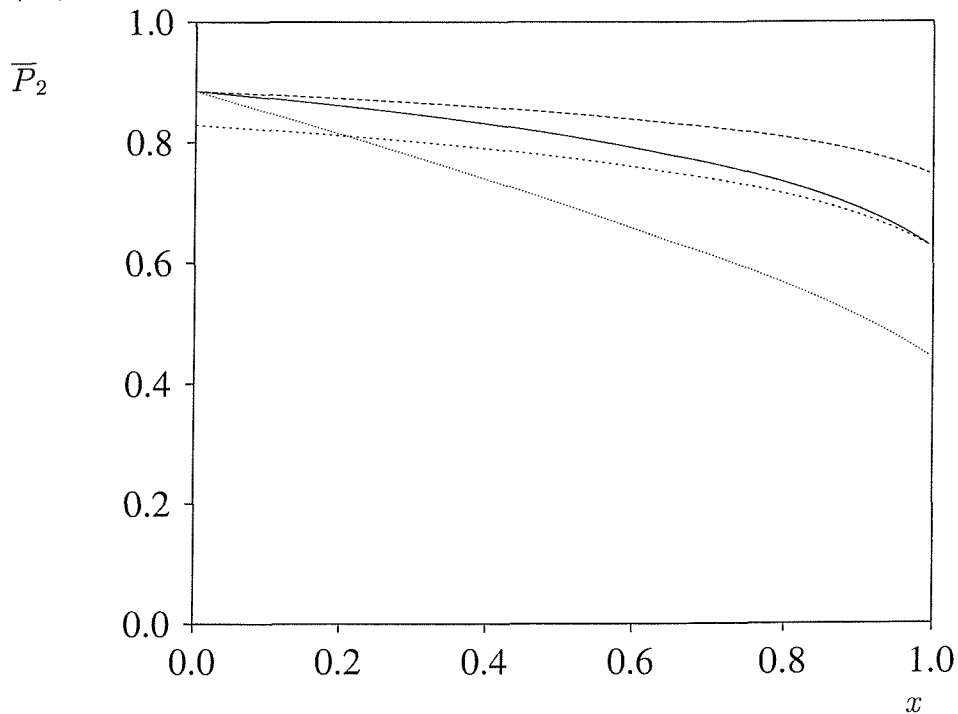




Figure 4.5: Second rank orientational order parameters  $\overline{P}_2^{\text{mixt}}$  (—),  $\overline{P}_2^A$  (---),  $\overline{P}_2^B$  (- -) and  $P_\epsilon$  (...) as a function of composition at a reduced temperature of 0.6 with  $\lambda = 0.75$ .

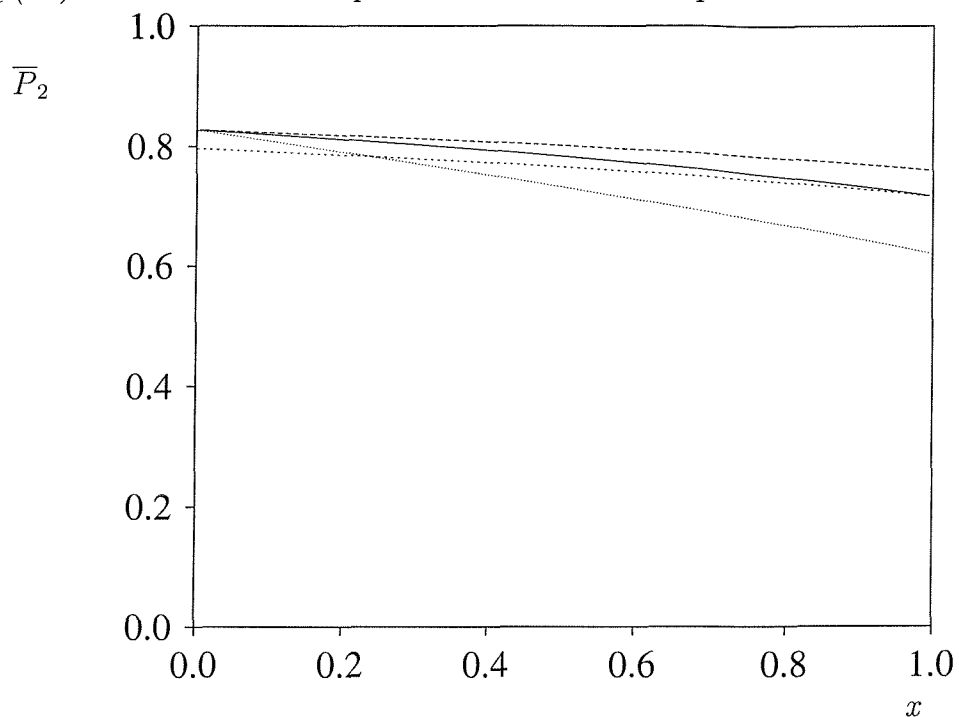


Figure 4.6: Second rank orientational order parameters  $\overline{P}_2^{\text{mixt}}$  (—),  $\overline{P}_2^A$  (---),  $\overline{P}_2^B$  (- -) and  $P_\epsilon$  (...) as a function of composition at a reduced temperature of 0.6 with  $\lambda = 0.5$ .

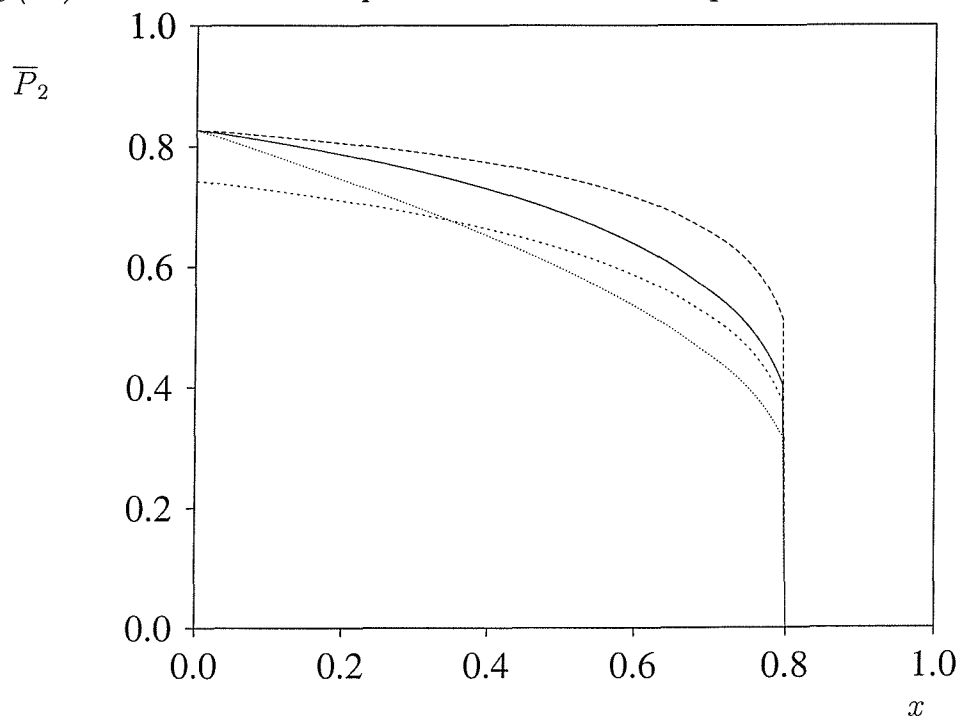
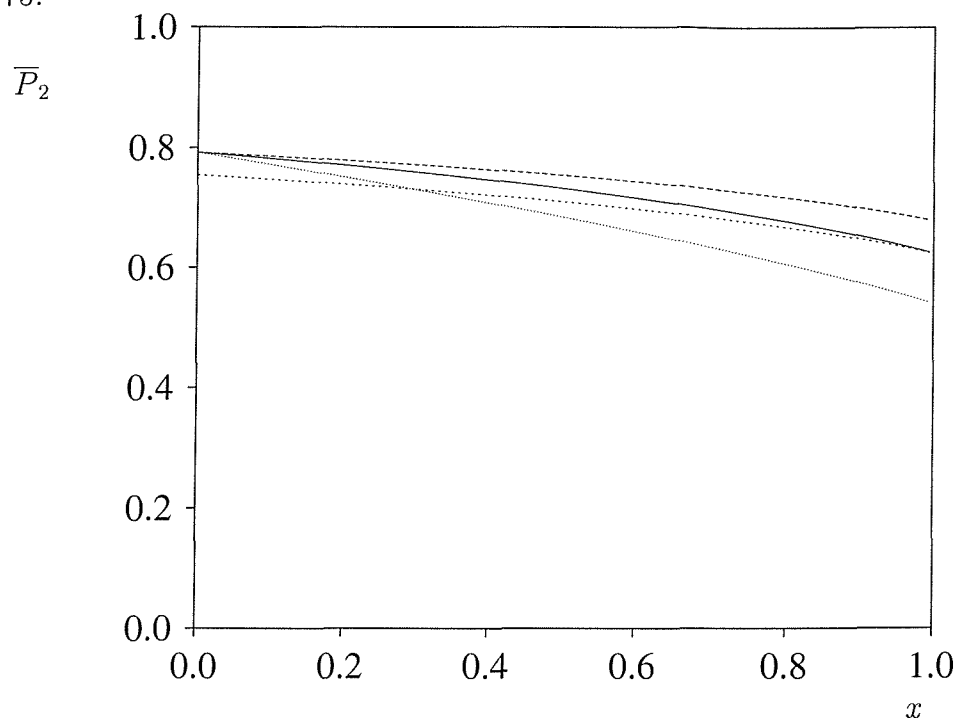
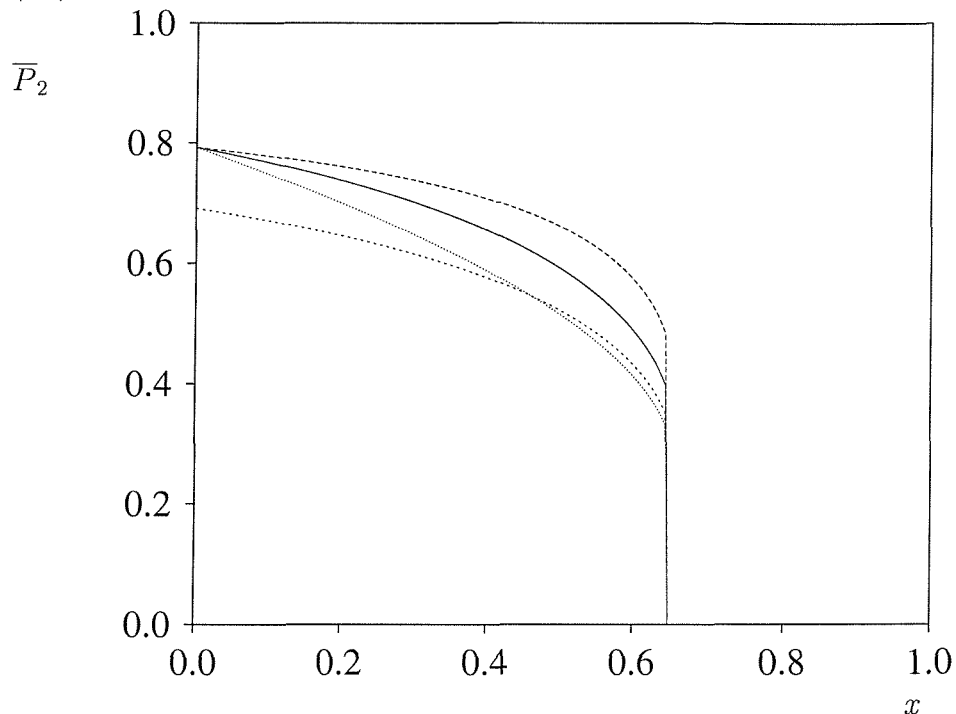


Figure 4.7: Second rank orientational order parameters  $\overline{P}_2^{mixt}$  (—),  $\overline{P}_2^A$  (---),  $\overline{P}_2^B$  (- -) and  $P_e$  (...) as a function of composition at a reduced temperature of 0.68 with  $\lambda = 0.75$ .



In figures (4.7) and (4.8) we see the results at a yet higher temperature still. In the case of  $\lambda = 0.75$  the order parameters are slightly lower and there is a slightly stronger mole fraction dependence, but still quite linear. In contrast, for  $\lambda = 0.5$  we again have a solvotropic transition. This time however, it is at lower mole fraction, since at higher temperature a greater proportion of the highly anisotropic solvent is required for the mixture to remain nematic. The transitional order parameter is again seen to be about 0.43.

Figure 4.8: Second rank orientational order parameters  $\overline{P}_2^{mixt}$  (—),  $\overline{P}_2^A$  (---),  $\overline{P}_2^B$  (- -) and  $P_c$  (....) as a function of composition at a reduced temperature of 0.68 with  $\lambda = 0.5$ .



Figures (4.9)–(4.14) show analogous results for reduced temperatures in the range 0.8 – 0.95 (ie, nearer that typically encountered in experiment). In figure (4.9) we see that now even with a highly anisotropic solute at a reduced temperature which for a real experiment is very low indeed, there is a solvotropic phase transition. The order parameters are now strongly temperature-dependent and deviate greatly from linearity. In figure (4.10) we have the same features, but more pronounced, with the transition occurring at an even lower mole fraction. This trend now continues for both  $\lambda = 0.75, 0.5$  with increasing temperature.

Figure 4.9: Second rank orientational order parameters  $\overline{P}_2^{\text{mixt}}$  (—),  $\overline{P}_2^A$  (---),  $\overline{P}_2^B$  (- -) and  $P_\epsilon$  (....) as a function of composition at a reduced temperature of 0.8 with  $\lambda = 0.75$ .

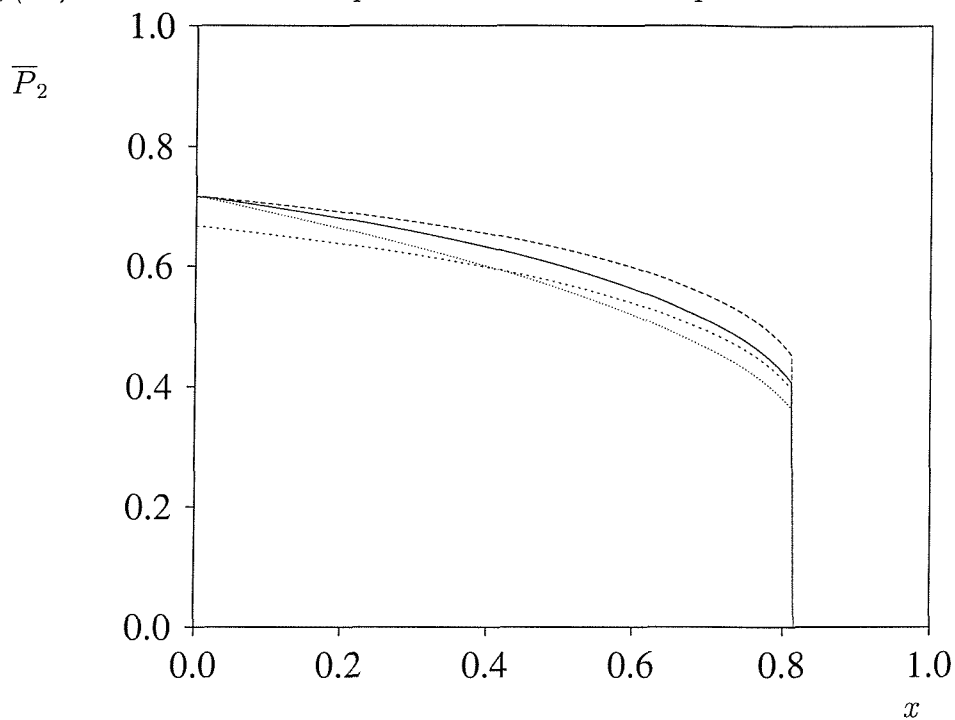


Figure 4.10: Second rank orientational order parameters  $\overline{P}_2^{\text{mixt}}$  (—),  $\overline{P}_2^A$  (---),  $\overline{P}_2^B$  (- -) and  $P_\epsilon$  (....) as a function of composition at a reduced temperature of 0.8 with  $\lambda = 0.5$ .

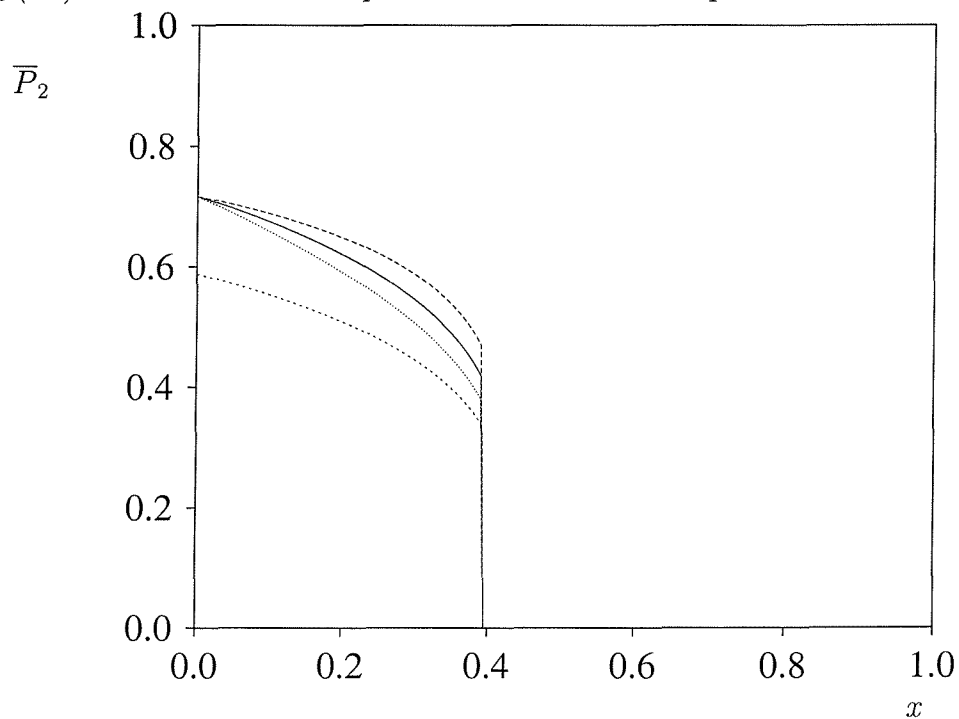
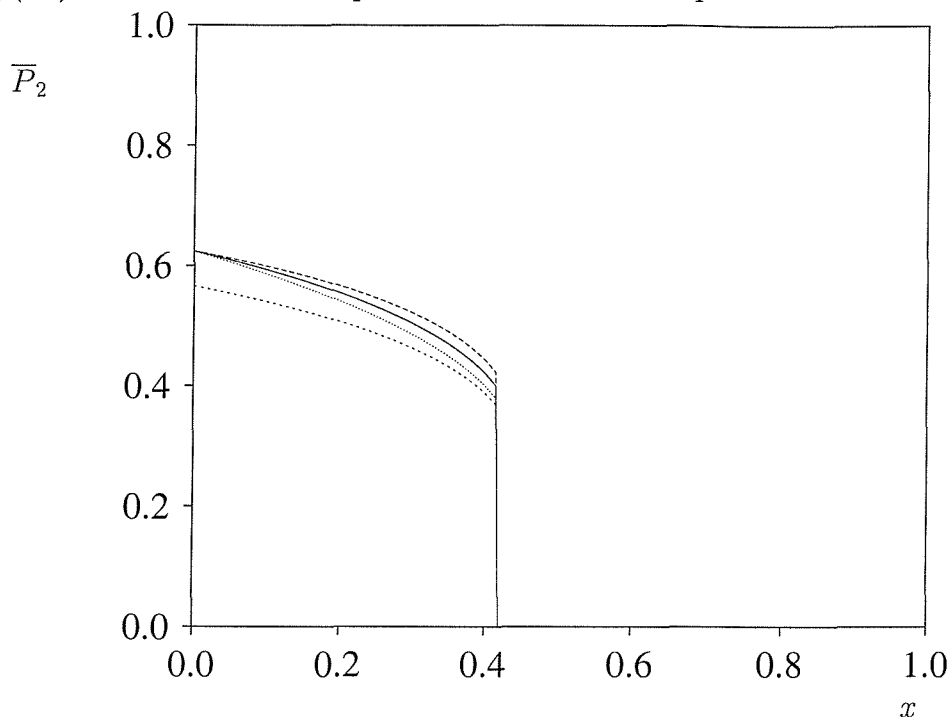
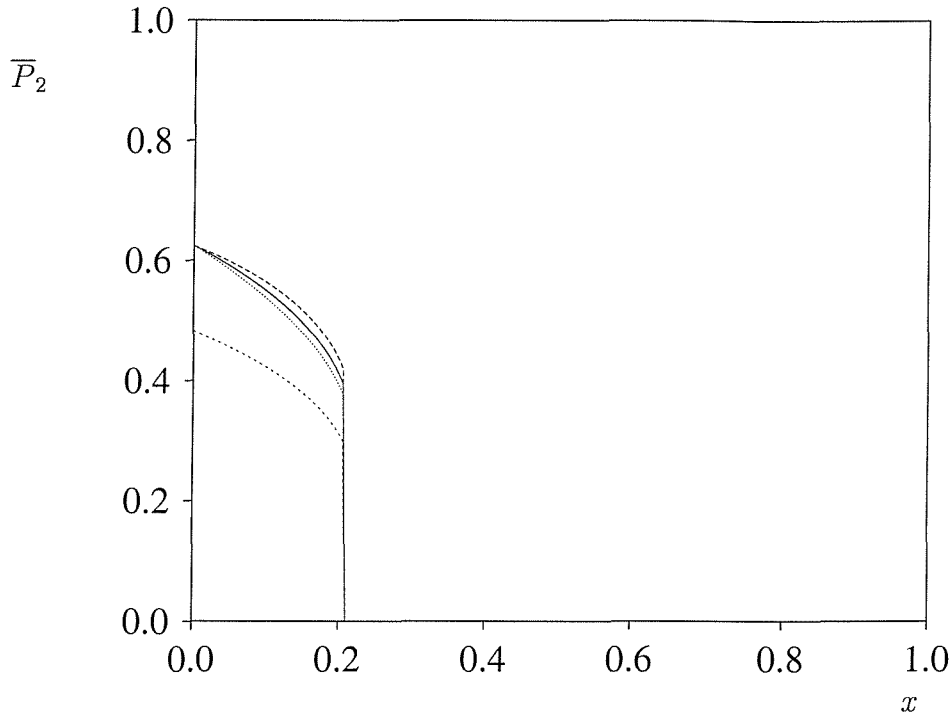


Figure 4.11: Second rank orientational order parameters  $\overline{P}_2^{mixt}$  (—),  $\overline{P}_2^A$  (---),  $\overline{P}_2^B$  (- -) and  $P_\epsilon$  (....) as a function of composition at a reduced temperature of 0.9 with  $\lambda = 0.75$ .



It is clear that whilst the order parameter of the mixture is initially linear as expected, significant deviations from linearity may occur at higher mole fractions of solute. It would seem that this deviation is due to the fact that  $T_{NI}$  for the mixture falls with increasing mole fraction,  $x$ , of solute, simply due to the size of the order parameters. If the mixture transition temperature falls to the temperature  $T_{expt}$  of the mixture within  $0 \leq x \leq 1$  then the order parameter of the mixture shows a first order transition to zero rendering the extrapolation unacceptable. Deviation from linearity is thus seen to occur if and when  $T_{NI}^{mixt}$  falls to anywhere near  $T_{expt}$  within the physically meaningful range of  $x$ . We note that this effect is more pronounced for small values of  $\lambda$  and at high reduced temperatures of the solvent.

Figure 4.12: Second rank orientational order parameters  $\overline{P}_2^{\text{mixt}}$  (—),  $\overline{P}_2^A$  (---),  $\overline{P}_2^B$  (- -) and  $P_\epsilon$  (....) as a function of composition at a reduced temperature of 0.9 with  $\lambda = 0.5$ .



At very low temperatures the  $\overline{P}_2^{\text{mixt}}$  line is almost linear for  $\lambda = 0.75$  up to a reduced temperature of a little under 0.60. Above  $T_r = \text{ca. } 0.60$ , however, we begin to see deviation. If  $\lambda$  is now decreased to 0.5 we begin to observe a deviation from linearity even at the lowest  $T_r$  investigated, namely 0.40. At more realistic temperatures the deviation from linearity is very great and the present experimental method of estimating solute birefringence power is thus manifestly unacceptable. The only circumstances under which the  $\overline{P}_2^{\text{mixt}}$  line is seen to be sufficiently linear even for values of  $\lambda$  at least as large as those encountered experimentally (ie,  $T_{NI}^A/T_{NI}^B \geq \text{ca. } 0.75$ ) is for values of  $T_r$  that are so low as to be well outside of the experimental regime (ie,  $T_r < \text{ca. } 0.6$ ).

Figure 4.13: Second rank orientational order parameters  $\overline{P}_2^{\text{mixt}}$  (—),  $\overline{P}_2^A$  (---),  $\overline{P}_2^B$  (- -) and  $P_\epsilon$  (....) as a function of composition at a reduced temperature of 0.95 with  $\lambda = 0.75$ .

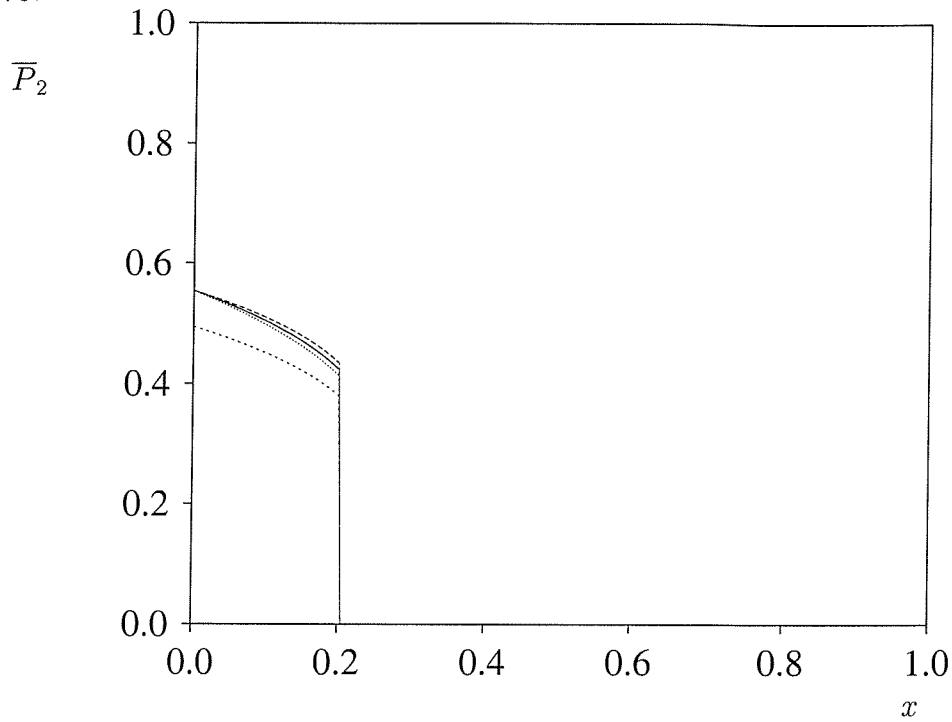
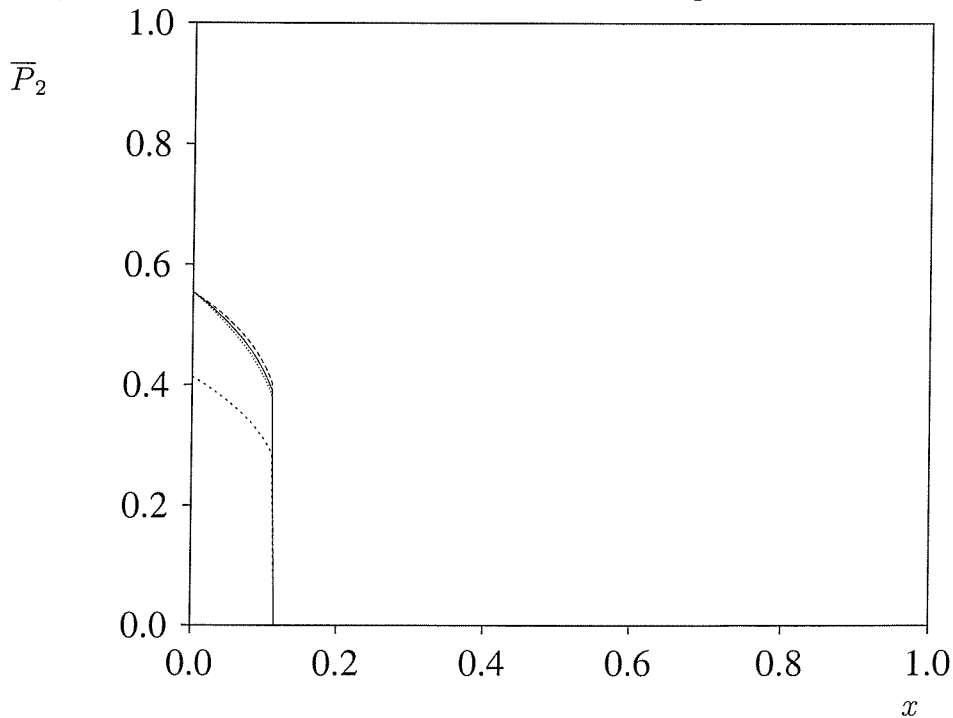


Figure 4.14: Second rank orientational order parameters  $\overline{P}_2^{\text{mixt}}$  (—),  $\overline{P}_2^A$  (---),  $\overline{P}_2^B$  (- -) and  $P_\epsilon$  (....) as a function of composition at a reduced temperature of 0.95 with  $\lambda = 0.5$ .



Given that the extrapolated value does not, within the reduced temperature regimes accessible to experiment, even remotely correspond to the extrapolated order parameter of the pure dopant, the question arises as to what this value corresponds in terms of the theory. To address this question we need to obtain the gradient of the curve  $\bar{P}_2^{\text{mixt}}(x)$  in the limit that  $x \rightarrow 0$ . Then from the equation of the straight line with this gradient through the known point (the intercept of  $P_2^{\text{mixt}}(x)$  on the ordinate) we have the equation of the extrapolation line. The value of the ordinate where this line intercepts the line  $x = 1$  can then be found. This is then the extrapolated hypothetical order parameter of the mixture.

#### 4.5.1 Analysis of the meaning of the extrapolated value for the order parameter of the dopant in the pure phase

First, we require an analytic expression for the gradient of  $\bar{P}_2^{\text{mixt}}(x)$  at  $x = 0$ . The order parameter of the mixture is

$$\bar{P}_2^{\text{mixt}} = (1 - x)\bar{P}_2^A + x\bar{P}_2^B. \quad (4.53)$$

The gradient of this with respect to the composition is then

$$\begin{aligned} \frac{d}{dx}\bar{P}_2^{\text{mixt}} &= \frac{d}{dx}\left((1 - x)\bar{P}_2^A\right) + \frac{d}{dx}\left(x\bar{P}_2^B\right) \\ &= \bar{P}_2^B - \bar{P}_2^A + (1 - x)\frac{d}{dx}\bar{P}_2^A + x\frac{d}{dx}\bar{P}_2^B. \end{aligned} \quad (4.54)$$

Hence the limiting gradient we require is

$$\left(\frac{d}{dx}\bar{P}_2^{\text{mixt}}\right)_{x=0} = (\bar{P}_2^B)_{x=0} - (\bar{P}_2^A)_{x=0} + \left(\frac{d}{dx}\bar{P}_2^A\right)_{x=0}. \quad (4.55)$$

The search for an analytic expression for  $(d\bar{P}_2^{\text{mixt}}/dx)_{x=0}$  then reduces to a search for an analytic expression for  $(d\bar{P}_2^A/dx)_{x=0}$ . The derivative of  $\bar{P}_2^A$  with respect to composition is, in general (ie, irrespective of making the geometric mean approximation)

$$\frac{d}{dx}\bar{P}_2^A = \frac{d}{dx}\left[Z_A^{-1} \int_{-1}^1 P_2(\cos \beta) \exp\left\{\left((1 - x)\epsilon_{AA}\bar{P}_2^A + x\epsilon_{AB}\bar{P}_2^B\right)P_2(\cos \beta)/k_B T\right\} d \cos \beta\right] \quad (4.56)$$



$$\begin{aligned}
&= -Z_A^{-2} \frac{dZ_A}{dx} \int P_2(\cos \beta) \exp(-U_A(\beta)/k_B T) d \cos \beta \\
&+ Z_A^{-1} \int \frac{d}{dx} \left[ P_2(\cos \beta) \exp \left\{ \left( (1-x) \epsilon_{AA} \bar{P}_2^A + x \epsilon_{AB} \bar{P}_2^B \right) P_2(\cos \beta) / k_B T \right\} \right] d \cos \beta
\end{aligned} \tag{4.57}$$

$$\begin{aligned}
&= -Z_A^{-2} \int P_2(\cos \beta) / k_B T \left[ \epsilon_{AA} \left( \frac{d\bar{P}_2^A}{dx} - \left( \bar{P}_2^A + x \frac{d\bar{P}_2^A}{dx} \right) \right) + \epsilon_{AB} \left( \bar{P}_2^B + \frac{d\bar{P}_2^B}{dx} \right) \right] \\
&\quad \times \exp(-U_A(\beta)/k_B T) d \cos \beta \int P_2(\cos \beta) \exp(-U_A(\beta)/k_B T) d \cos \beta \\
&+ Z_A^{-1} \int P_2(\cos \beta)^2 / k_B T \left[ \epsilon_{AA} \left( \frac{d\bar{P}_2^A}{dx} - \left( \bar{P}_2^A + x \frac{d\bar{P}_2^A}{dx} \right) \right) + \epsilon_{AB} \left( \bar{P}_2^B + \frac{d\bar{P}_2^B}{dx} \right) \right] \\
&\quad \times \exp(-U_A(\beta)/k_B T) d \cos \beta
\end{aligned} \tag{4.58}$$

The quantity

$$1/k_B T \left[ \epsilon_{AA} \left( \frac{d\bar{P}_2^A}{dx} - \left( \bar{P}_2^A + x \frac{d\bar{P}_2^A}{dx} \right) \right) + \epsilon_{AB} \left( \bar{P}_2^B + \frac{d\bar{P}_2^B}{dx} \right) \right]$$

appearing in both terms of (4.58) is not a function of the space of integration as it contains only constants and non-angular variables (quantities that are already integrated over the space). For the sake of convenience we call this quantity  $\Gamma$ . Then the derivative is

$$\begin{aligned}
\frac{d}{dx} \bar{P}_2^A &= -\Gamma \left\{ Z_A^{-2} \left[ \int P_2(\cos \beta) \exp(-U_A(\beta)/k_B T) d \cos \beta \right]^2 \right. \\
&\quad \left. - Z_A^{-1} \int P_2(\cos \beta)^2 \exp(-U_A(\beta)/k_B T) d \cos \beta \right\}.
\end{aligned} \tag{4.59}$$

But

$$Z_A^{-2} \left[ \int P_2(\cos \beta) \exp(-U_A(\beta)/k_B T) d \cos \beta \right]^2$$

$$= \left[ Z_A^{-1} \int P_2(\cos \beta) \exp(-U_A(\beta)/k_B T) d \cos \beta \right]^2 = \overline{P_2^{A^2}} \quad (4.60)$$

and

$$Z_A^{-1} \int P_2(\cos \beta)^2 \exp(-U_A(\beta)/k_B T) d \cos \beta = \overline{P_2^{A^2}} \quad (4.61)$$

so

$$\frac{d}{dx} \overline{P_2^A} = \Gamma \left( \overline{P_2^{A^2}} - \overline{P_2^A}^2 \right). \quad (4.62)$$

We note that the quantity  $\overline{P_2^{A^2}} - \overline{P_2^A}^2 = \overline{[P_2^A(\cos \beta) - \overline{P_2^A}]^2}$ , the fluctuation quantity in  $P_2(\cos \beta)$  for component  $A$ . We require the limit  $x \rightarrow 0$ , in other words

$$\lim_{x \rightarrow 0} \Gamma = \lim_{x \rightarrow 0} \left[ \frac{1}{k_B T} \left\{ \epsilon_{AA} \left( (1-x) \frac{d\overline{P_2^A}}{dx} - \overline{P_2^A} \right) + \epsilon_{AB} \left( \overline{P_2^B} + x \frac{d\overline{P_2^B}}{dx} \right) \right\} \right], \quad (4.63)$$

giving

$$\lim_{x \rightarrow 0} \Gamma = \frac{1}{k_B T} \left\{ \epsilon_{AA} \left( \frac{d\overline{P_2^A}}{dx} - \overline{P_2^A} \right) + \epsilon_{AB} \overline{P_2^B} \right\}, \quad (4.64)$$

where all the quantities involving the order parameters here are implicitly evaluated at  $x = 0$ . We can now collect the terms in  $d\overline{P_2^A}/dx$  and solve for the gradient. Multiplying out we obtain

$$\begin{aligned} \frac{d\overline{P_2^A}}{dx} &= \left( \frac{\epsilon_{AA}}{k_B T} \frac{d\overline{P_2^A}}{dx} - \frac{\epsilon_{AA}}{k_B T} \overline{P_2^A} + \frac{\epsilon_{AB}}{k_B T} \overline{P_2^B} \right) \left( \overline{P_2^{A^2}} - \overline{P_2^A}^2 \right) \\ &= \frac{\epsilon_{AA}}{k_B T} \frac{d\overline{P_2^A}}{dx} \left( \overline{P_2^{A^2}} - \overline{P_2^A}^2 \right) - \frac{1}{k_B T} \left[ \epsilon_{AA} \overline{P_2^A} - \epsilon_{AB} \overline{P_2^B} \right] \left( \overline{P_2^{A^2}} - \overline{P_2^A}^2 \right). \end{aligned} \quad (4.65)$$

Then

$$\begin{aligned} \frac{d\overline{P_2^A}}{dx} - \frac{\epsilon_{AA}}{k_B T} \frac{d\overline{P_2^A}}{dx} \left( \overline{P_2^{A^2}} - \overline{P_2^A}^2 \right) &= -\frac{1}{k_B T} \left[ \epsilon_{AA} \overline{P_2^A} - \epsilon_{AB} \overline{P_2^B} \right] \left( \overline{P_2^{A^2}} - \overline{P_2^A}^2 \right), \\ \frac{d\overline{P_2^A}}{dx} \left[ 1 - \frac{\epsilon_{AA}}{k_B T} \left( \overline{P_2^{A^2}} - \overline{P_2^A}^2 \right) \right] &= -\frac{1}{k_B T} \left[ \epsilon_{AA} \overline{P_2^A} - \epsilon_{AB} \overline{P_2^B} \right] \left( \overline{P_2^{A^2}} - \overline{P_2^A}^2 \right) \end{aligned} \quad (4.66)$$

and so

$$\frac{d\overline{P_2^A}}{dx} = \frac{(1/k_B T) (\epsilon_{AA} \overline{P_2^A} - \epsilon_{AB} \overline{P_2^B}) (\overline{P_2^{A^2}} - \overline{P_2^A}^2)}{1 + (\epsilon_{AA}/k_B T) (\overline{P_2^{A^2}} - \overline{P_2^A}^2)}. \quad (4.67)$$

We reiterate that here all of the orientationally-averaged quantities are implicitly evaluated at  $x = 0$ . Written in terms of the scaled quantities we would have

$$\begin{aligned} \frac{d\bar{P}_2^A}{dx} &= \frac{(\epsilon_{AA}/k_B T) \left( \bar{P}_2^A - (\epsilon_{AB}/\epsilon_{AA}) \bar{P}_2^B \right) \left( \bar{P}_2^{A^2} - \overline{P_2^{A^2}} \right)}{1 + (\epsilon_{AA}/k_B T) \left( \bar{P}_2^{A^2} - \overline{P_2^{A^2}} \right)}, \\ &= \frac{\left( \bar{P}_2^A - (\epsilon_{AB}/\epsilon_{AA}) \bar{P}_2^B \right) \left( \bar{P}_2^{A^2} - \overline{P_2^{A^2}} \right) / T^*}{1 + \left( \bar{P}_2^{A^2} - \overline{P_2^{A^2}} \right) / T^*}, \\ &= \frac{\left( \bar{P}_2^A - (\epsilon_{AB}/\epsilon_{AA}) \bar{P}_2^B \right) \left( \bar{P}_2^{A^2} - \overline{P_2^{A^2}} \right)}{T^* + \left( \bar{P}_2^{A^2} - \overline{P_2^{A^2}} \right)}. \end{aligned} \quad (4.68)$$

Within the geometric mean approximation for  $\epsilon_{AB}$  equation (4.68) becomes

$$\frac{d\bar{P}_2^A}{dx} = \frac{\left( \bar{P}_2^A - \lambda^{1/2} \bar{P}_2^B \right) \left( \bar{P}_2^{A^2} - \overline{P_2^{A^2}} \right)}{T^* + \left( \bar{P}_2^{A^2} - \overline{P_2^{A^2}} \right)}. \quad (4.69)$$

We note the unusual combination of different kinds of quantities (ie, the fluctuation quantities and order parameters on the one hand and the scaled temperature on the other), the physical interpretation of which is far from clear.

To calculate this gradient numerically we are clearly required to calculate the additional quantity  $\overline{P_2^{A^2}}$ , which is evaluated either as

$$\overline{P_2^{A^2}} = Z_A^{-1} \int P_2(\cos \beta)^2 \exp(-U_A(\beta)/k_B T) \sin \beta d\beta \quad (4.70)$$

or by noting that  $P_2(\cos \beta)^2$  can be written in terms of  $P_4(\cos \beta)$  and a Clebsch-Gordan coefficient and substituting this for  $P_2(\cos \beta)^2$  in (4.70).

The gradient of the order parameter of the mixture in the low concentration limit (see equation (4.55)) is then

$$\left( \frac{d}{dx} \bar{P}_2^{\text{mixt}} \right)_{x=0} = \left( \bar{P}_2^B \right)_{x=0} - \left( \bar{P}_2^A \right)_{x=0} - \left( \frac{\left( \bar{P}_2^A - \lambda^{1/2} \bar{P}_2^B \right) \left( \overline{P_2^{A^2}} - \bar{P}_2^{A^2} \right)}{T^* - \left( \bar{P}_2^{A^2} - \overline{P_2^{A^2}} \right)} \right)_{x=0}, \quad (4.71)$$

remembering that in general (ie, outside of the geometric mean approximation) the quantity  $\lambda^{1/2}$  can be replaced by  $(\epsilon_{AB}/\epsilon_{AA})$ . This gives us the equation of the straight line we require. In other words, if we write the equation of a straight line in the usual way as  $y = mx + c$  then the independent variable  $x$  is simply the composition  $x$  and the dependent variable  $y(x)$  is  $\overline{P}_2^{\text{mixt}}(x)$ . The gradient  $m$  is then clearly the gradient  $(d\overline{P}_2^{\text{mixt}}/dx)_{x=0}$  and the  $y$ -axis intercept  $c$  is  $\overline{P}_2^{\text{mixt}}(x=0)$ , which by (4.53) is equal to  $\overline{P}_2^A(x=0)$  and so

$$\overline{P}_2^{\text{mixt}}(x) = x \left( \frac{d}{dx} \overline{P}_2^{\text{mixt}} \right)_{x=0} + \overline{P}_2^A(0). \quad (4.72)$$

We are required to find *for this straight line*  $\overline{P}_2^{\text{mixt}}(x=1)$ . Thus the extrapolated point is  $(1, \overline{P}_2^{\text{mixt}}(1))$  where

$$\overline{P}_2^{\text{mixt}}(1) = \left( \overline{P}_2^B - \frac{(\overline{P}_2^A - \lambda^{1/2} \overline{P}_2^B)(\overline{P}_2^{A^2} - \overline{P}_2^{A^2})}{T^* - (\overline{P}_2^{A^2} - \overline{P}_2^{A^2})} \right)_{x=0}. \quad (4.73)$$

This expression is found to give complete agreement with the results of extrapolating the graphs by hand, as would be expected. It was thought that knowing what the data from the experimental studies represents might possibly provide a clue as to how to manipulate pre-existing results to provide a better way of comparing potential dopant compounds. However, the significance of the extrapolated point would still seem to be far from clear. In particular, the physical interpretation of the expression for the gradient (4.71) is not obvious, although we can look at some limiting cases.

We note that the gradient can be written in terms of the order parameter at the extrapolated point simply as

$$\left( \frac{d}{dx} \overline{P}_2^{\text{mixt}} \right)_{x=0} = \overline{P}_2^B(1) - \overline{P}_2^A(0), \quad (4.74)$$

where  $\overline{P}_2^B(1)$  is the hypothetical ordinate of the extrapolated point on the straight line. In the limit of high order we might be tempted to set the third term in (4.71) equal to zero and note that the resulting equation

$$\left( \frac{d}{dx} \overline{P}_2^{\text{mixt}} \right)_{x=0} = \overline{P}_2^B(0) - \overline{P}_2^A(0) \quad (4.75)$$

is similar to (4.74). This would imply that  $\overline{P}_2^B(1) = \overline{P}_2^B(0)$ , which seems initially strange. However, as the limit is approached the order parameters become increasingly linear and nearer to being equal to the same constant value (unity) over the composition range, so that it does in fact become a good approximation for highly ordered systems. This analysis of the limit may seem flawed because the high order limit occurs only in the limit of low temperature and it is not clear that the denominator in the third term of (4.71) does not render the limiting gradient indeterminate. However, we know that in the limit of high order the mixture order parameter is a constant, so that the gradient is zero; given that the first two terms cancel, the third must vanish.

The other limit we can explore is that  $\lambda \rightarrow 0$ , that is, the solute is spherical. In this limit the gradient is

$$\left(\frac{d}{dx}\overline{P}_2^{\text{mixt}}\right)_{x=0} = -\overline{P}_2^A(0) \left[ 1 + \frac{\delta P_2^A(\cos \beta)}{T^* - \delta P_2^A(\cos \beta)} \right], \quad (4.76)$$

where  $\delta P_2^A(\cos \beta)$  is the fluctuation in  $P_2(\cos \beta)$  for component  $A$ . We see that the gradient is now a function only of the order parameter and fluctuation for the solvent and the temperature, as expected.

This still does not seem to provide much enlightenment as to what physical meaning to attach to values obtained from the experimental extrapolations and what, if anything, can be gleaned from the pre-extant experimental data. The values obtained from experiment refer to a hypothetical pure nematic state beyond the experimental regime, but it turns out that this state does not, under most circumstances in these experiments, exist. The technique also assumes that by extrapolating to the pure solute we obtain a property that is intrinsic to the solute and independent of the solvent. However, the intercept obtained is clearly determined by (in this case) the order parameter of the pure solvent and the slope at infinite dilution, which also contains quantities pertaining to the solvent. The solvent dependence in each of these contributing factors does not disappear upon evaluation of the intercept at  $x = 1$  and so the order parameters obtained are manifestly related to the nature of the solvent—both its order parameter and the fluctuations in  $P_2(\cos \beta)$ . It has been suggested [5] that a better experimental

procedure would be to measure the birefringence as a function of composition, but always at the same reduced temperature with respect to the *mixture* rather than the solvent. The order parameter profile is then expected to remain linear in the composition across the entire range, thus enabling the concept of linear extrapolation to be retained in a manner that is valid, although clearly more difficult experimentally.

## References

- [1] M. J. Goulding, PhD thesis, University of Southampton (1995).
- [2] R. L. Humphries, P. G. James and G. R. Luckhurst, *Symp. Farad. Soc.*, **5**, 107 (1971).
- [3] T. H. Payne, unpublished notes.
- [4] C. Zannoni, personal communications.
- [5] G. R. Luckhurst, personal communications.

# Chapter 5: Liquid Crystals Formed from Highly Flexible Molecules

## 5.1 Introduction

In addition to the standard classes of mesogenic molecule (see Chapter 1), in recent years it has been found that highly flexible dendritic structures (dendrimers) are also capable of mesophase formation [1, 2, 3]. The first demonstration of this was by de Jeu [1]. Dendromesogens (see figures 5.1, 5.2, 5.3) as they are called thus form a new class of mesogenic compounds consisting of a central core attached to which are flexible chains, which may branch a number of times, terminated in rigid mesogenic units such as cyanobiphenyl moieties. These structures generally do not form nematics but only smectic phases. The molecules may exhibit several levels of branching, the number of branching levels being known as the generation number. A dendrimer with  $n$  branching levels is known as a  $G_n$  dendrimer. In addition, it is common to place the standard abbreviation for the mesogenic unit (with linking group) afterwards. Thus, a dendrimer with just a central core and chains which do not branch is a zeroth generation ( $G_0$ ) dendrimer, and if the mesogenic groups are ether-linked cyanobiphenyl groups (for instance) then we have a  $G_0OCB$  dendrimer. Zeroth generation dendrimers are also commonly called multipodes. In spite of the above generalisation about phase behaviour, some examples of multipodes do form a nematic phase, notably those with cyanobiphenyl groups attached laterally to the chains; the analogues with the groups attached terminally, however, form only smectic phases. The term ‘flexible’ here refers to the large range of conformational states the molecule may adopt.



Figure 5.1: Examples of the first liquid crystal dendrimers [1]

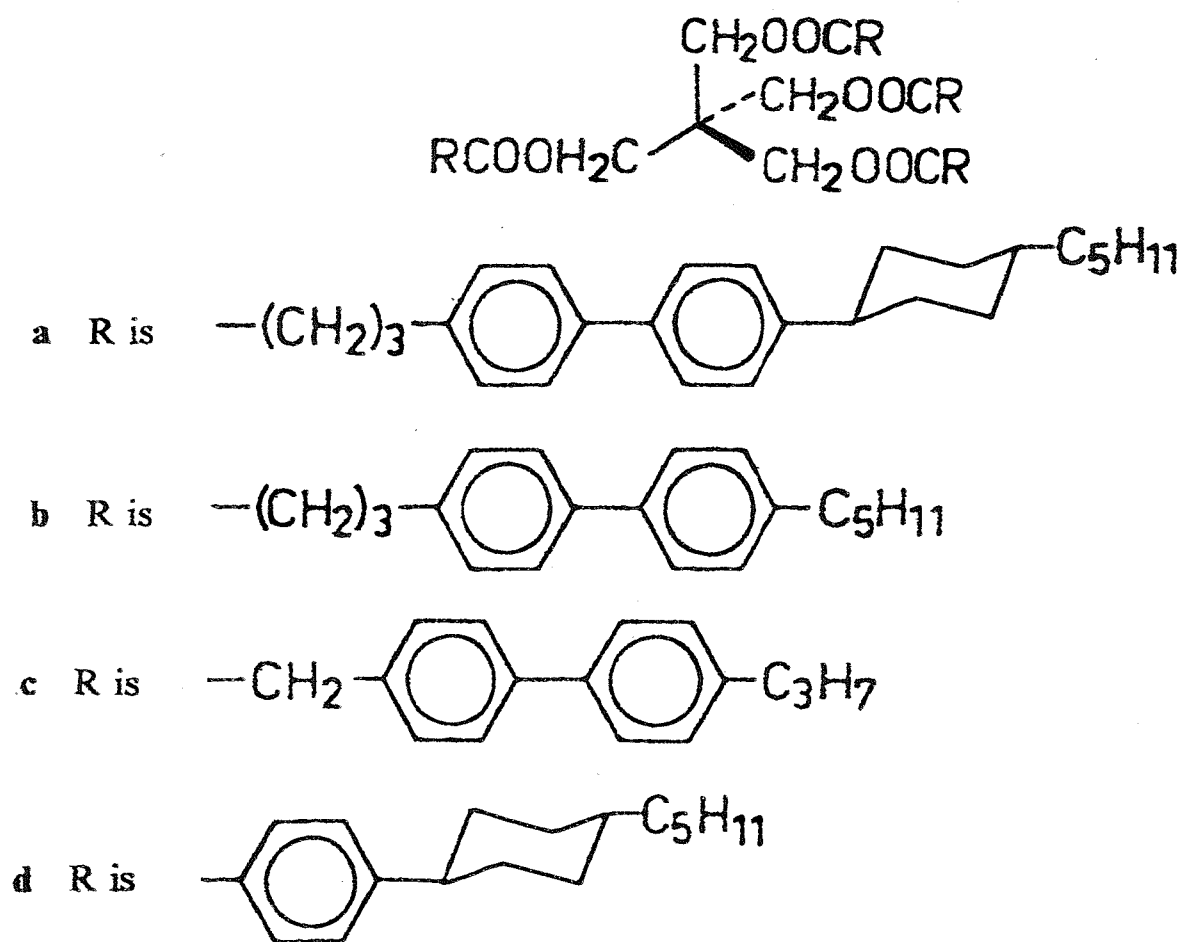


Figure 5.2: Another early example of a liquid crystal dendrimer [2]

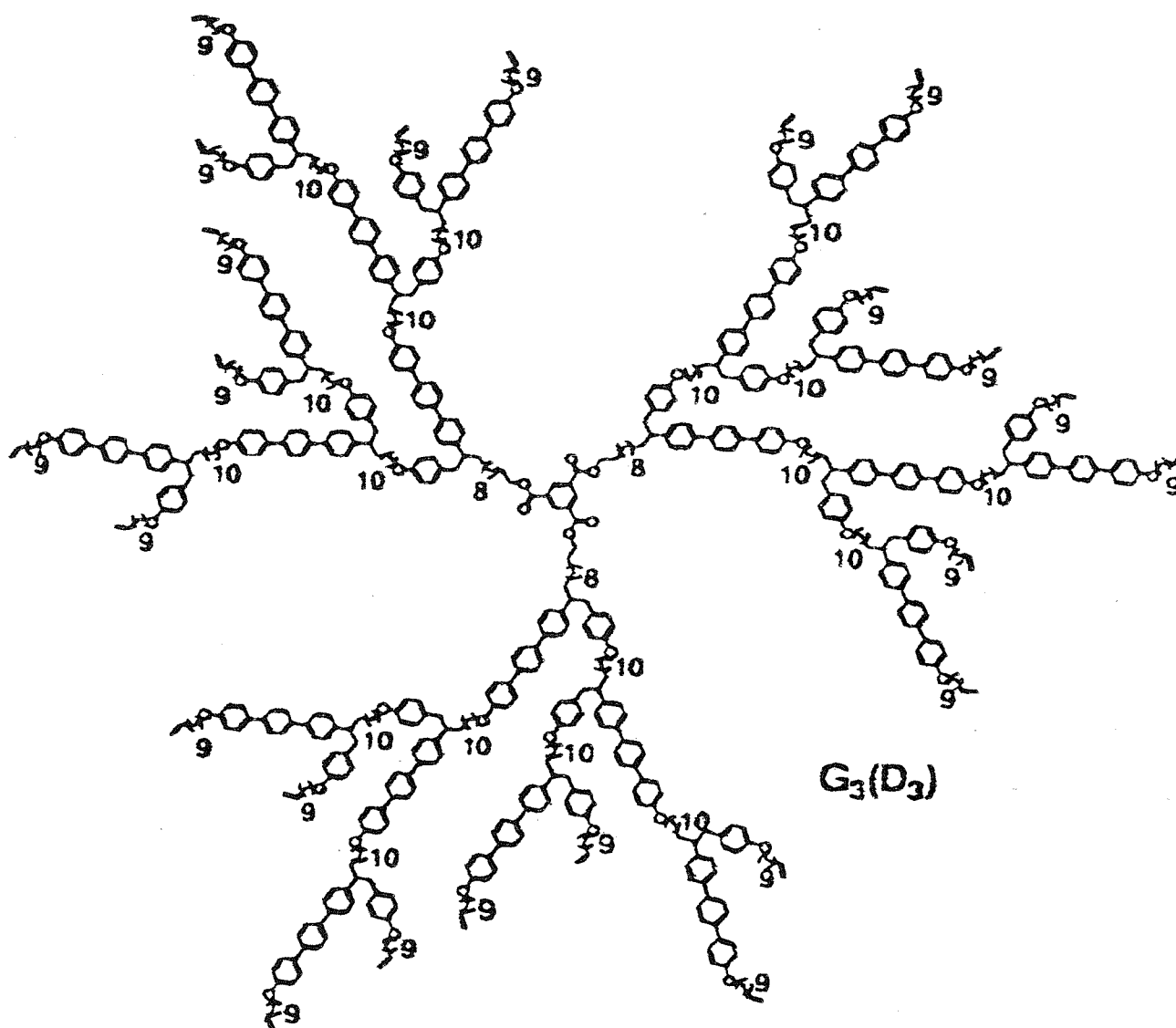
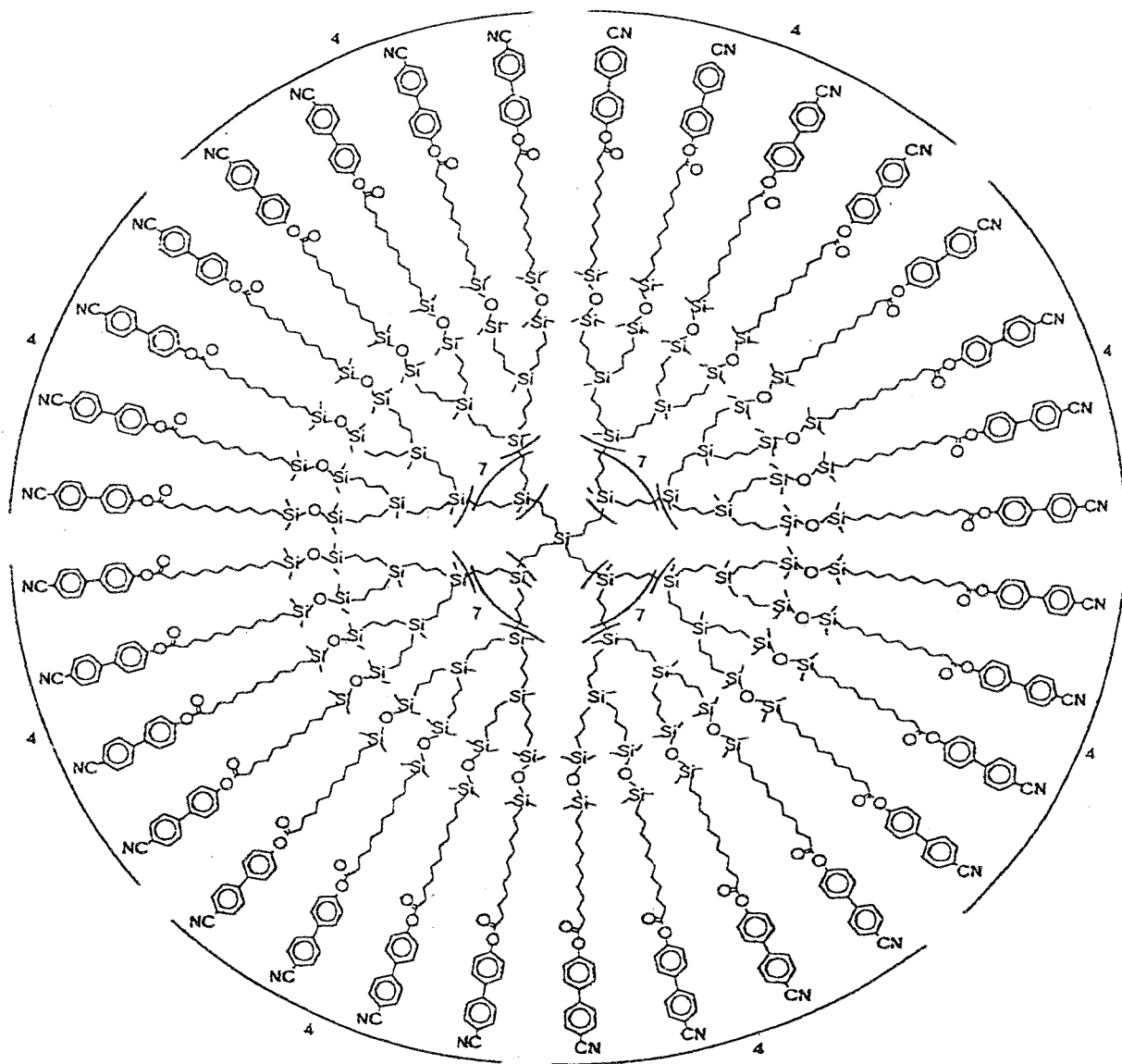


Figure 5.3: A more recent example: Structural formula of a fifth generation carbosilane dendrimer with 128 terminal cyanobiphenyl groups G-5(Und-CB) [Und = undecanoyl] [3]



In this chapter we describe a study which is a starting point for the theoretical modelling of liquid crystal dendrimers. For simplicity, we shall focus solely on zeroth generation dendrimers (multipodes) in which the central core is simply a quarternary carbon atom and the mesogenic groups are cyanobiphenyl moities. We shall consider the case where the cyanobiphenyl groups are attached terminally and also that where they are attached laterally to the chains via ether linkages (see figures 5.4 and 5.5). In accordance with the results of experimental studies (such as X-ray diffraction) on ether-linked flexible liquid crystal dimers, the torsional angle around the bond between the phenyl ring and the ether linkage is kept fixed at  $0^\circ$  in these calculations. Again, for simplicity, we shall focus just on nematic behaviour as a convenient starting point. Thus the calculations on the lateral multipodes allow contact with real systems which form nematic phases. Also, for comparison we have performed the calculations on flexible liquid crystal dimers, which are in a sense analogous to the terminal dendrimers, and also form nematic phases. The calculations have been performed on a homologous series for each type of molecule (flexible dimer, terminal and lateral dendrimers). This facilitates validation of the methodology using the dimer series (by comparison with experiment and previous application of the methodology to dimers [4]) and permits comparison between the different series to compare features of interest. There is then the possibility of finding in the multipodes odd-even effects analogous to those obtained for flexible dimers. In addition, we are able to explore the effect of conformational-orientational synergy on the transitional order parameter, an important phenomenon in flexible liquid crystal dimers.

Figure 5.4: Structure of a typical zeroth generation ether-linked cyanobiphenyl dimer, G-0OCB, as used in the theoretical calculations. Here, the cyanobiphenyl groups are attached to the chain terminally.

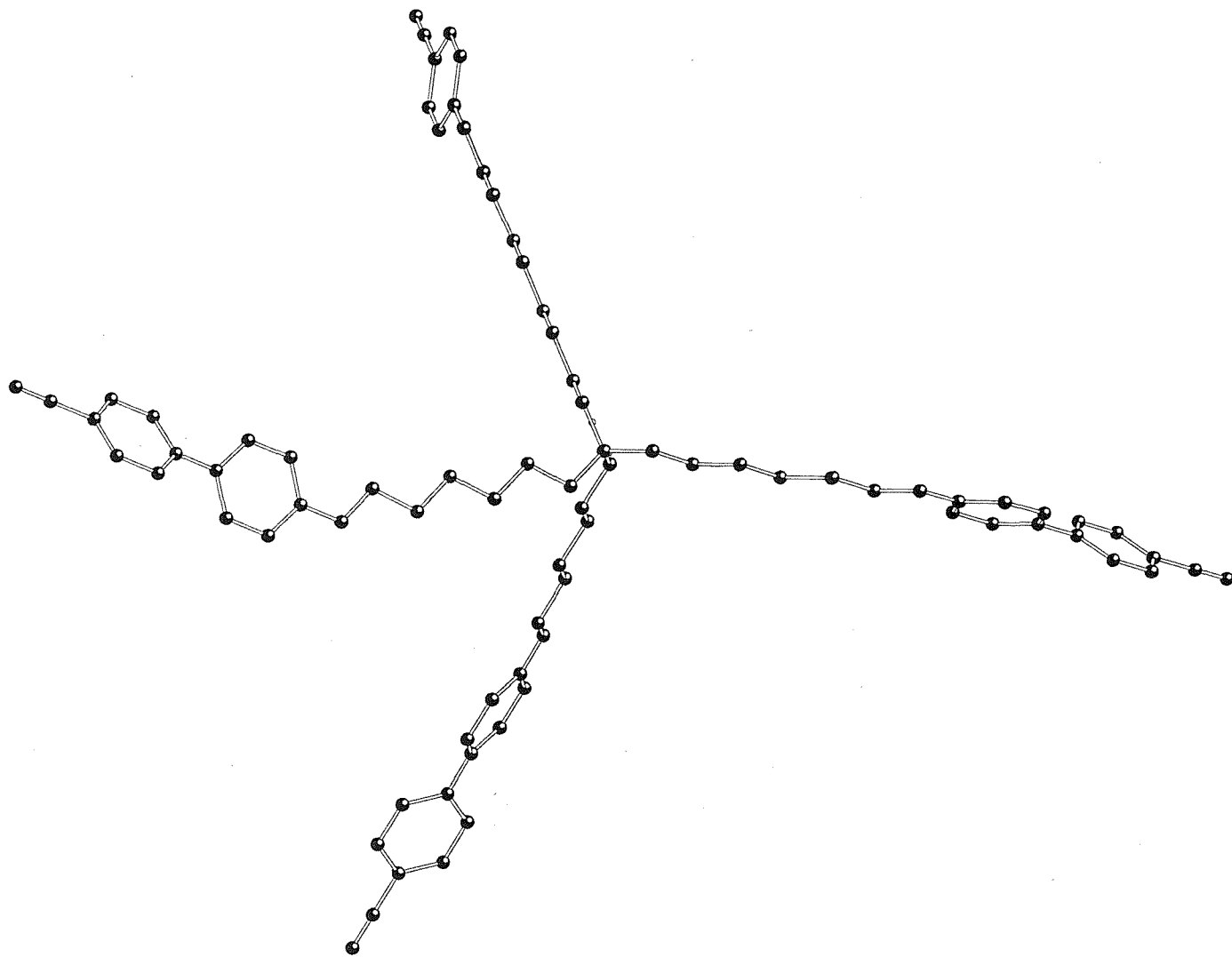
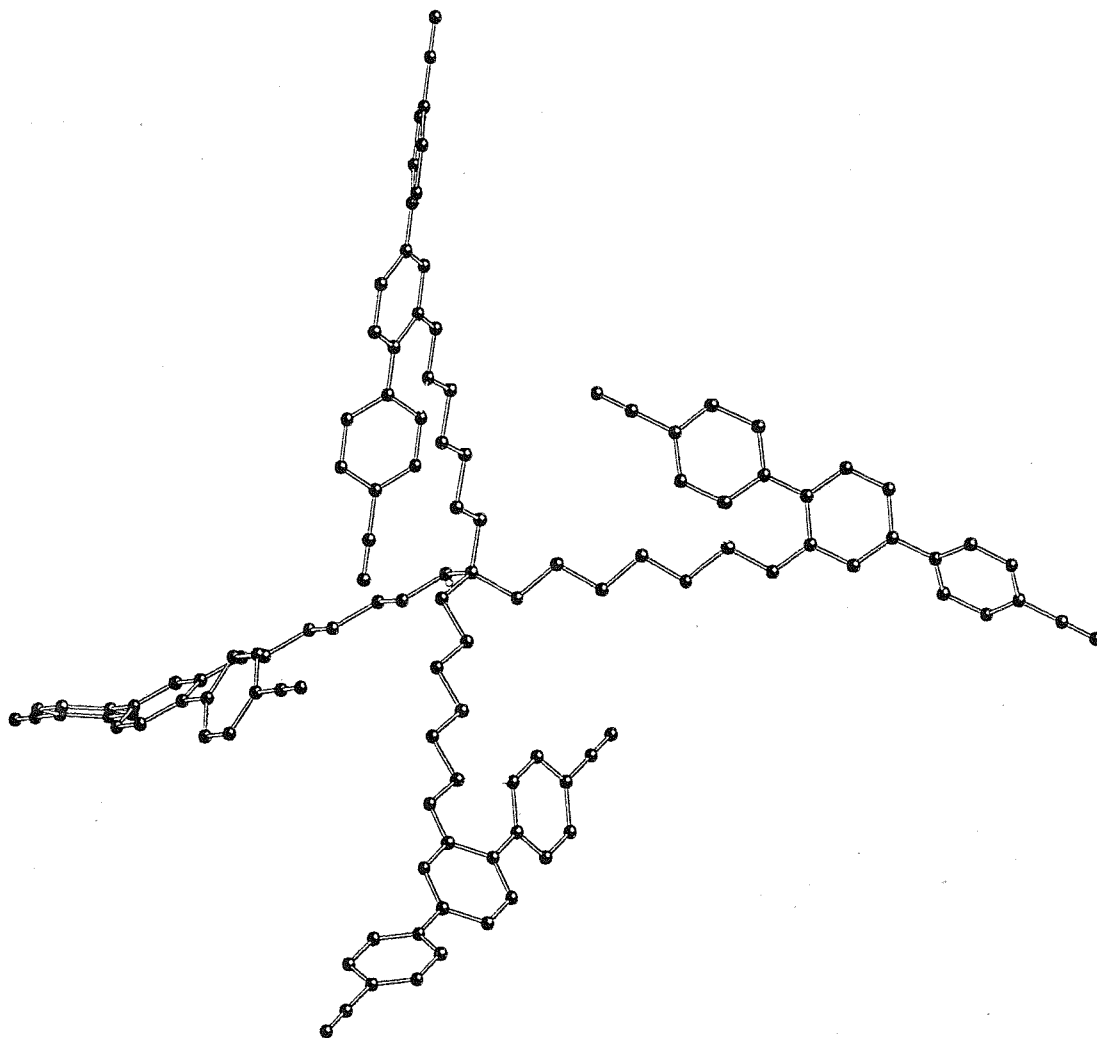


Figure 5.5: Structure of a typical zeroth generation ether-linked cyanobiphenyl dendrimer, G-0OCB, as used in the theoretical calculations. Here, the cyanobiphenyl groups are attached to the chain laterally.



## 5.2 Theoretical Background and Methodology

### 5.2.1 General introduction to the problem

We take as the starting point of the treatment the molecular field theory of liquid crystals composed of flexible molecules first proposed by Marcelja [5] and subsequently extended by Luckhurst [6]. The theory treats the conformations available to the molecule resulting from the chain flexibility using the rotameric isomeric state (RIS) model of alkanes proposed by Flory [7]. In the RIS model the only conformations that are deemed to exist are those corresponding to the torsional potential minima.

The main problem in applying the theory to molecules with a very high degree of conformational flexibility, such as dendrimers, is the inherently huge number of conformational states available to them. In the RIS model, there are  $3^{N-3}$  conformations for an alkyl chain containing  $N$  methylene units. The RIS-based theory generates all possible conformers (even if some are eventually rejected because overlaps of atoms occur), a task that in the case of dendrimers is beyond all possible developments in conventional computing power. For example, for the largest multipode we have studied (which is only a “zeroth generation” dendrimer) this gives something of the order of  $3^{41} \approx 3.6 \times 10^{19}$  conformers. If conformers were to be generated and dealt with at a rate of  $10^4$  per second the entire calculation (apart from final calculations at the end of the algorithm) would require over 100 159 728 years.

There is also another kind of problem, and that concerns the validity of the RIS model of the physical situation itself. In reality, at and around ambient temperature, flexible molecules librate in the well minima of the torsional potentials. This contrasts with the RIS model in which only the minima exist and so that in, say, a flexible liquid crystal dimer, the mesogenic group axes are always either collinear or at some fixed angle to each other and so are correlated. When there are fluctuations in the well minima, the extent of these correlations is reduced—to an extent that depends, for

a given temperature, on the length of the chain, since in longer chains the effect of these fluctuations accumulates until in the limit, all correlations between the mesogenic groups are lost. Thus in reality, in the limit of a long chain length, we effectively have orientationally isolated uncorrelated mesogenic groups in a sea of liquid alkyl chain, and we should recover the Maier-Saupe results. (Note: This is not strictly true if we decide to include within the theory anisotropic interactions coming from the chains.) The effect of removing the RIS restriction on the possible conformational states on the mesogenic orientational correlations is therefore expected to be relatively insignificant at short chain lengths but progressively more significant for increasing chain lengths. Thus we expect that the deviation of the RIS-based theory from experimental findings will increase as we consider more flexible systems with larger numbers of chains of greater length—precisely the sort of systems we are interested in, in fact. Indeed, application of the RIS model to flexible liquid crystal dimers and comparison of the results with those of experiment reveals this increasing discrepancy of the RIS-based theory as the chain length is increased, although this deficiency is partially ameliorated when conformers containing steric overlaps are excluded from the calculation [4]. Given the numbers and lengths of flexible chains present in the kinds of molecules we are hoping to study, this would seem to mitigate against invoking the RIS approximation and favour employing continuous torsional potentials instead. After all, this would be preferable in any case if it can be achieved with modern computing power, simply because it models much more closely the real physical situation.

Clearly then, we require a new methodology to deal with such systems, since there are no analytic or semi-analytic solutions (the required total integrals are numerical and of high dimensionality) and the RIS model-based theory is seen to be inadequate. We obviously need some kind of sampling scheme to generate discrete conformers within the conformational space. It would seem that the most appropriate strategy would be to adopt some kind of random (“stochastic”) sampling scheme. The most obvious candidate is that employed in stochastic-type computer simulations where points in phase space are sampled according to their importance based on the Boltzmann fac-



tors for their energies, namely the form of “Monte Carlo” sampling first suggested by Metropolis, Rosenbluth, Rosenbluth, Teller and Teller [8]. In addition, given that in principle we can just as easily apply the “Metropolis” sampling protocol to the whole conformational space as to the RIS subspace, it makes sense to apply the Metropolis sampling scheme to the whole space, which allows us to employ continuous torsional potentials. With this decided, the sampling protocol then becomes entirely equivalent to performing the requisite multi-dimensional integrations exactly (within, we should note, the tacit assumption that the multiple integral may be treated with the approximation that the total torsional energy may be represented as a sum of effective single-torsional energies).

We could use this approach to sample all of the variables whose values determine the classical Hamiltonian of the system—not only the conformational coordinates but also the orientational ones. The required integrations over orientational variables can, however, be performed exactly by a combination of analytic and simple numerical integration in just the same manner as in the previous RIS-based theory for flexible systems. (This is just the same as for the theory of uniaxial phases of biaxial rigid particles described in Chapter 2.) Sampling on the whole phase space would then seem unnecessary and computationally inefficient, and so we choose to perform Metropolis Monte Carlo sampling on the conformational variables only and obtain the usual orientational integrals exactly as in standard molecular field theory.

The subtlety here in applying the molecular field theory to the orientational part of the state space and the Monte Carlo procedure to the conformational part is in how we combine these two approaches when obtaining the ensemble averages over the simulation. As we shall see, it turns out that because conformers are accepted or rejected solely on the basis of their conformational potential energy, we have to include in each contribution to the average a weighting factor that reflects the orientational bias coming from the molecular field, that is, the fact that we are modelling an orientationally ordered fluid [9]. The weighting factor that we must build in for each accepted (or

reaccepted) conformer is its orientational partition function. In addition this accumulated quantity must be normalised at the end of the simulation by a factor which is just the sum of these partition functions. This corresponds essentially to the “umbrella sampling” technique (see section 5.2.2).

## 5.2.2 Formal Aspects of the Molecular Field Calculation

The starting point of the molecular field calculation is an effective single molecule potential energy. This energy is taken to be the sum of two contributions, an intramolecular contribution and an orientational contribution. The former is a function only of the internal coordinates of the single molecule and is in a sense exact within whatever approximate deconvolution is assumed for calculating it. Here we implicitly assume the validity of a Born-Oppenheimer-type deconvolution of the total energy into separate contributions associated exclusively with assumed independent degrees of internal freedom, these being bond lengths, bond angles and dihedral (torsional) angles. We then proceed to ignore the dependence upon bond lengths and angles and assume that the intramolecular potential energy may be faithfully represented simply by the torsional energy alone which is itself assumed to be a sum of effective single-torsion energies. The second contribution is the anisotropic part of the thermodynamic potential energy (the “potential of mean torque”) and is a function of both the conformation (internal degrees of freedom) of the molecule and its orientation defined by the orientational variables; these are denoted collectively by  $\omega(= \alpha, \beta)$ , the spherical polar angles of the nematic director in the molecular frame of reference. The potential of mean torque construction replaces the many body interactions with a single molecule interacting with an average (or “mean”) field, referred to as the “molecular field”, and is an effective single particle potential energy function, or strictly speaking, just the orientationally-varying part of it. We write

$$U_{tot}(\{\phi\}, \omega) = U_{int}(\{\phi\}) + U_{ext}(\{\phi\}, \omega), \quad (5.1)$$

where  $\{\phi\}$  denotes the collective set of torsional angles which define a given conformational state. The single molecule orientational potential energy is assumed to take the same form as that described in Chapter 2, namely,

$$U_{\text{ext}}(\{\phi\}, \omega) = - \sum_m (-)^m X_{2m}(\{\phi\}) C_{2-m}(\omega), \quad (5.2)$$

where  $m = -2, -1, \dots, 2$ ,  $X_{2m}$  is the molecular interaction tensor expressed as a second rank irreducible spherical tensor and  $C_{2m}(\omega)$  is a spherical harmonic. (See Appendix 1B for the functional form of the  $C_{2m}(\omega)$ .)

As in the previous theories for flexible molecules the molecular interaction tensor is taken to be a sum of segmental interaction tensors from whatever parts of the molecule are deemed to contribute. The strengths and weaknesses of this construction assumed for the molecular interaction tensor have been discussed elsewhere [10].

As in any simulation or theoretical calculation the main aim is to obtain the bulk thermodynamic averages of the system in the ensemble under consideration. Ultimately what is required is to be able to find the ensemble average of any property  $B$  of interest that we might choose, and this is defined formally by

$$\langle B \rangle_{\text{ens}} = \int_{\{X\}} B\{X\} P\{X\} d\{X\}, \quad (5.3)$$

where  $\{X\}$  denotes the collective set of degrees of freedom,  $x_1, x_2, \dots, x_N$ , of the system and  $P\{X\}$  is the total probability density distribution function of the system over all its degrees of freedom. This is defined by

$$P\{X\} = \exp(-U\{X\}/k_B T) \bigg/ \int_{\{X\}} \exp(-U\{X\}/k_B T) d\{X\}. \quad (5.4)$$

Within the theoretical framework of this present study, these equations become

$$\langle B \rangle_{\text{ens}} = \int_{\{\phi\}} \int_{\omega} B(\{\phi\}, \omega) P(\{\phi\}, \omega) d\omega d\{\phi\}, \quad (5.5)$$

with

$$P(\{\phi\}, \omega) = \exp(-U_{\text{tot}}(\{\phi\}, \omega)/k_B T) \bigg/ \int_{\{\phi\}} \int_{\omega} \exp(-U_{\text{tot}}(\{\phi\}, \omega)/k_B T) d\omega d\{\phi\}. \quad (5.6)$$

There is then the problem of how to perform the integrations. Given that we cannot expect to perform them analytically, we clearly need to invoke some kind of discretised approximation. Standard numerical integration techniques form a class of such approximations but are inadequate to deal with the very high dimensionality of the spaces we are considering, as we have already mentioned. The RIS model, where we assume that the only conformational states that exist are those corresponding to the torsional potential minima, could also be considered in this way but, as we have seen, is also inadequate to deal with the range of systems we wish to study. (If we view the RIS model as equivalent to numerical integration then the integrals are replaced by summations over the states of the model of the quantities represented by the integrands.) Alternatively, at the other extreme, we could sample discrete states from the total conformational space at random. If we sample stochastically from a uniform distribution then we retain the exact form of the integrands and the integrals are then replaced by summations giving us an expression exactly analogous to the RIS model-based one—except that this time the summations are over the stochastically-sampled states (ie, other kinds of conformational states are sampled). If we sample from a non-uniform distribution then we still have a summation over sampled states, but the integrands must be modified to take account of the fact that we have sampled from a biased distribution. More specifically they must be multiplied by the inverse of the distribution from which we are sampling. That is, if the quantity we require is in general

$$\langle B \rangle_{\text{ens}} = \int B\{X\} \exp(-U\{X\}/k_B T) d\{X\} \bigg/ \int \exp(-U\{X\}/k_B T) d\{X\} \quad (5.7)$$

then unbiased sampling gives  $\langle B \rangle_{\text{ens}}$  as the limit

$$\langle B \rangle_{\text{ens}} = \lim_{N \rightarrow \infty} \left\{ \sum_{i=1}^N B\{X_i\} \exp(-U\{X_i\}/k_B T) \bigg/ \sum_{i=1}^N \exp(-U\{X_i\}/k_B T) \right\}, \quad (5.8)$$

where  $N \rightarrow \infty$  is interpreted to mean that  $N$  can be as large as is necessary to obtain convergence of the quantity. If we now introduce stochastic sampling on the  $\{X\}$  from

the biased distribution  $P\{X\}$  given by (8.4) then this expression becomes modified as

$$\begin{aligned}
\langle B \rangle_{\text{ens}} &= \lim_{N \rightarrow \infty} \left\{ \frac{\sum_{i=1}^N B\{X_i\}}{\sum_{i=1}^N 1} \right\} \\
&= \lim_{N \rightarrow \infty} \left\{ \frac{\sum_{i=1}^N B\{X_i\} \exp(-U\{X_i\}/k_B T) [\exp(-U\{X_i\}/k_B T)/Q]^{-1}}{\sum_{i=1}^N \exp(-U\{X_i\}/k_B T) [\exp(-U\{X_i\}/k_B T)/Q]^{-1}} \right\} \\
&= \lim_{N \rightarrow \infty} \left\{ \frac{\sum_{i=1}^N B\{X_i\}}{N} \right\}, \tag{5.9}
\end{aligned}$$

where

$$Q = \int \exp(-U\{X\}/k_B T) d\{X\}. \tag{5.10}$$

Given that we have already rejected the RIS model in favour of allowing the torsional angles to vary continuously, the question that presents itself is whether it is more efficient (in terms of rate of convergence over iterations to the true value  $\langle B \rangle_{\text{ens}}$ ) to employ unbiased stochastic sampling or stochastic sampling from a non-uniform distribution. In the field of computer simulation of liquids it is generally asserted that direct evaluation of the thermodynamic averages via unbiased sampling is quite infeasible and that achieving convergence is beyond all possible developments in conventional computer power. This is because a very high proportion of states generated in a uniform random distribution will contain elements of the system (particles, non-bonded atoms) that are very close to each other, giving rise to a very high potential energy. This means that the Boltzmann factor for the energy will be vanishingly small, and so give a negligible Boltzmann weighting in the numerator of (5.8) for the corresponding value of the property in question. For the same reason the constant scaling factor in (5.8), which for the sample taken is just the sum of the Boltzmann factors (ie, the simulation estimate of the partition function) is also then composed almost entirely of very small contributions. The remainder of the space itself not sampled will also be overwhelmingly dominated (in number) by such contributions. Such a sampling scheme would be prohibitively inefficient, since almost all states sampled make virtually no contribution to the average being computed. Thus, straightforward random sampling from an

unbiased distribution is not usually regarded as a viable way in practise of obtaining ensemble averages.

One of the most important forms of Monte Carlo sampling is “importance” sampling, the most widely used of which is the sampling protocol devised by Metropolis et al. mentioned earlier, and it is this one which we have chosen to employ. The Metropolis protocol [8, 18] is as follows. A new configuration is generated (by changing on or more degrees of freedom by some random amount) and the change in energy  $\Delta E$  between the new and old configurations is calculated. If the energy of the system has decreased ( $\Delta E < 0$ ) then the move is accepted. If the energy has increased ( $\Delta E > 0$ ) then the move has a chance of being accepted, the probability being proportional to the Boltzmann factor for the energy difference. That is, a random number is generated uniformly on  $(0, 1)$ . If the random number is smaller than the Boltzmann factor  $\exp(-\Delta E/k_B T)$  then the move is accepted. If the random number is greater than the Boltzmann factor the move is rejected and we return to the old configuration which, we note, is to be reaccepted (ie, counted as the next configuration in the set over which averages are to be computed). Thus,  $\Delta E > 0$  moves are accepted with a probability proportional to the Boltzmann factors for the corresponding energy differences. The Metropolis sampling scheme ensures that the limiting distribution of the simulation over the variables  $\{X\}$  so sampled will be  $P\{X\}$ . This occurs because the algorithm sets up a Markov chain of states of the system in phase space and from the theory of random processes it can be shown that, with the Metropolis criteria for acceptance or rejection of trial moves, this chain has a limiting distribution  $\rho_{NVT}$  which is the  $P\{X\}$  encountered previously [18]. Thus we obtain the desired distribution over which we wish to average automatically and indirectly through the sampling mechanism itself. Then, bearing in mind our earlier comments about the modification of the calculation of averages required when sampling from a biased distribution, we obtain the ensemble average of a property from (5.9) with  $N$  being the total number of trials (ie, states included in the average).

The situation we are trying to deal with here, however, is somewhat more involved, because although we could apply the Metropolis Monte Carlo procedure to all the degrees of freedom, it is not necessary, as we have already stated. (Indeed, to do so would preclude location of the  $N-I$  phase transition.) Rewriting the formal expression for  $\langle B \rangle_{\text{ens}}$  in terms of semi-analytic integrations and leaving the conformational space for Monte Carlo sampling we obtain

$$\langle B \rangle_{\text{ens}} = \frac{\int_{\{\phi\}} \langle B\{\phi\} \rangle_{\omega} Q_{\text{ext}}\{\phi\} \exp(-U_{\text{int}}\{\phi\}/k_B T) d\{\phi\}}{\int_{\{\phi\}} \exp(-U_{\text{int}}\{\phi\}/k_B T) Q_{\text{ext}}\{\phi\} d\{\phi\}}, \quad (5.11)$$

where

$$\langle B \rangle_{\omega} = Q_{\text{ext}}^{-1} \int_{\omega} B(\omega, \{\phi\}) \exp(-U_{\text{ext}}(\omega, \{\phi\})/k_B T) d\omega \quad (5.12)$$

and

$$Q_{\text{ext}} = \int_{\omega} \exp(-U_{\text{ext}}(\omega, \{\phi\})/k_B T) d\omega. \quad (5.13)$$

Performing Metropolis sampling on the  $\{\phi\}$  ensures that the limiting distribution is

$$\begin{aligned} P\{\phi\} &= \exp(-U_{\text{int}}\{\phi\}/k_B T) \Big/ \int_{\{\phi\}} \exp(-U_{\text{int}}\{\phi\}/k_B T) d\{\phi\}, \\ &= Q_{\text{int}}^{-1} \exp(-U_{\text{int}}\{\phi\}/k_B T). \end{aligned} \quad (5.14)$$

Thus the simulation average is computed as

$$\begin{aligned} \langle B \rangle_{\text{ens}} &= \lim_{N \rightarrow \infty} \left\{ \frac{\sum_{i=1}^N B\{\phi_i\} Q_{\text{ext}}\{\phi_i\}}{\sum_{i=1}^N Q_{\text{ext}}\{\phi_i\}} \right\}, \\ &= \left\langle B\{\phi_i\} Q_{\text{ext}}\{\phi_i\} \right\rangle_{\text{trials}} \Big/ \left\langle Q_{\text{ext}}\{\phi_i\} \right\rangle_{\text{trials}}, \end{aligned} \quad (5.15)$$

where now  $B\{\phi_i\} = \langle B\{\phi_i\} \rangle_{\omega}$ .

### 5.2.3 Details of the Molecular Field Calculation

We shall now discuss in detail the form of the molecular field calculations. We begin by turning our attention to the total interaction tensor of the molecule. As already discussed (see Chapter 2) the potential of mean torque is assumed to be dominated by second rank tensorial quantities to the extent that it is appropriate to consider only these to obtain all the qualitative features and essential physics of nematic liquid crystalline systems. The quantitative aspects that one might think could be obtained by extending the theory to higher order are in any case unobtainable, a feature that results from the severity of the molecular field approximation itself, that is, the fact that we assume an effective single particle orientational potential. To obtain better than semi-quantitative information the first step we would have to take would be to look beyond the potential of mean torque concept itself. Thus the essential qualitative physics is taken to be completely encapsulated by a single molecular interaction tensor of second degree. The total interaction tensor,  $X_{2m}$ , (or its cartesian analogue) is taken to be the (tensorial) sum of individual tensors in some way related to various parts of the molecule that are assumed to contribute, although there are other possible schemes for constructing  $X_{2m}$  [19, 20].

Here we have assumed that only the highly anisometric mesogenic regions contribute and that their tensors are cylindrically symmetric about their long axes when referred to the principal frames of the mesogens (ie, their para axes, since the mesogenic groups are of the biphenyl or terphenyl type). The predominant driving force to form liquid crystalline phases, in terms of intermolecular interactions, is thus identified with the mesogenic groups and in this study we are neglecting the influence of the chains. This is not unreasonable, since the formation of the phase is dependent upon the presence of rigid, elongated units, which is indeed why they are referred to as “mesogenic”—mesophase-inducing.

The strength of the orienting molecular field is set by a parameter, the scalar strength



parameter,  $X$ . This input parameter determines the components of the cartesian interaction tensor for each mesogenic group in its own principal axis system as follows:

$$x_{ij}^{\text{meso}} = \begin{cases} -\frac{X}{2}\delta_{ij} & (i, j = 1, 2, 3 \text{ and } (i, j) \neq (3, 3)) \\ X & (i = j = 3), \end{cases} \quad (5.16)$$

where the local principal  $z$  axis is taken as the assumed cylindrical symmetry axis of the mesogenic group. The total cartesian interaction tensor is obtained by transforming the mesogenic interaction tensors into a common frame and taking the tensorial sum.

The irreducible analogue,  $X_{2m}$ , of the total interaction tensor is obtained by diagonalisation of the cartesian tensor matrix to obtain a principal axis system (represented as a set of eigenvectors) with only diagonal elements surviving as non-vanishing, these being the eigenvalues associated with their corresponding eigenvectors. The appropriate linear combinations of the principal components of the total cartesian interaction tensor are then taken to form the components of the irreducible spherical tensor analogue as

$$X_{20} = X_{zz}/\sqrt{6} \quad X_{2\pm 1} = 0 \quad X_{2\pm 2} = (X_{xx} - X_{yy})/2. \quad (5.17)$$

The rotational partition function for the accepted conformer  $\{\phi_i\}$  in question is then computed as

$$\begin{aligned} Q_{\text{ext}}\{\phi_i\} &= \int \exp(-U_{\text{ext}}(\omega, \{\phi_i\})/k_B T) d\omega \\ &= \int_{\alpha=0}^{2\pi} \int_{\beta=0}^{2\pi} \exp(-U_{\text{ext}}(\omega, \{\phi_i\})/k_B T) \sin\beta d\beta d\alpha, \end{aligned} \quad (5.18)$$

with  $U_{\text{ext}}(\omega, \{\phi\})$  given by (8.2) and  $X_{2m}\{\phi\}$  as obtained already. From  $X_{2m}$  (or hence equivalently  $U_{\text{ext}}(\omega, \{\phi\})$ , which gives the ‘‘external’’ partition function), all the other properties follow. Within the theoretical framework of the molecular field approximation, the molecular order parameters for this conformer  $\{\phi_i\}$  are given by

$$\bar{C}_{2m} = Q_{\text{ext}}^{-1} \int C_{2m}(\omega) \exp(-U_{\text{ext}}(\omega, \{\phi\})/k_B T) d\omega \quad \forall m (m = -2, -1, \dots, 2). \quad (5.19)$$

The averages  $\langle B \rangle_{\text{ens}}$  of quantities  $B(\omega, \{\phi\})$  may now be computed at the end of the simulation as

$$\langle B \rangle_{\text{ens}} = \langle \tilde{B}\{\phi_i\} \rangle_{\text{trials } i} / \langle Q_{\text{ext}}\{\phi_i\} \rangle_{\text{trials } i}, \quad (5.20)$$

where

$$\tilde{B}\{\phi_i\} = \int B(\omega, \{\phi_i\}) \exp(-U_{\text{ext}}(\omega, \{\phi_i\})/k_B T) d\omega. \quad (5.21)$$

(Note:

$$B\{\phi_i\} = Q_{\text{ext}}^{-1} \int B(\omega, \{\phi_i\}) \exp(-U_{\text{ext}}(\omega, \{\phi_i\})/k_B T) d\omega \quad (5.22)$$

so that

$$\begin{aligned} \tilde{B}\{\phi_i\} &= Q_{\text{ext}} Q_{\text{ext}}^{-1} \int B(\omega, \{\phi_i\}) \exp(-U_{\text{ext}}(\omega, \{\phi_i\})/k_B T) d\omega \\ &= Q_{\text{ext}}\{\phi\} B\{\phi_i\} \end{aligned} \quad (5.23)$$

and

$$\langle B \rangle_{\text{ens}} = \langle B\{\phi_i\} Q_{\text{ext}}\{\phi_i\} \rangle_{\text{trials}} / \langle Q_{\text{ext}}\{\phi_i\} \rangle_{\text{trials}}. \quad (5.24)$$

Quantities that we compute which are averages over the orientational space must be multiplied by the rotational partition function before accumulating—or rather, integrated with the Boltzmann factor in the orientational energy and not normalised by the partition function in the first place. Where a quantity is not a function of  $\omega$ , then it is accumulated without any need of integration, simply multiplication by the partition function. The simulation average is then simply this accumulator divided by the sum of the rotational partition functions, since the number of configurations pertaining to the averages in the ratio (see equations (5.20, 5.24)) is the same in each case.

### *Properties Calculated*

The average properties we wish to calculate in the simulation are the second rank orientational order parameters,  $\langle \overline{P}_2 \rangle$ , of the mesogenic groups, the scaled Helmholtz

free energy difference,  $\Delta A_{IN}/k_B T$ , between isotropic and nematic phases and the scaled entropy difference,  $\Delta S_{NI}/k_B$ , between the phases.

The order parameters of the mesogenic groups are calculated as follows. For each accepted conformer, the calculated irreducible spherical tensor order parameter of the molecule is used to form the Saupe ordering matrix in the principal axis system according to

$$S_{zz} = \bar{C}_{20} \quad S_{yy} = -\frac{1}{2} \left( \bar{C}_{20} + \frac{3}{2} \bar{C}_{22} \right) \quad S_{xx} = -(S_{yy} + S_{zz}) \quad S_{ij} = 0 \quad (i \neq j) \quad (5.25)$$

and this is then transformed back into the local frame of each mesogenic group in turn to obtain the corresponding second rank orientational order parameter. This requires a double reverse transformation.

We first transform back into the common BOSS frame by making use of the rotation matrix obtained from diagonalising the interaction tensor, since this specifies the forward transformation that takes the BOSS frame into the current, principal frame. The elements  $R_{ij}$  of the rotation matrix  $R$  in the transformation

$$T' = R T R^T \quad (5.26)$$

that takes the matrix  $T$  of cartesian tensor components in the BOSS frame into the corresponding matrix  $T'$  in the rotated (principal) frame are in fact the direction cosines  $a_{ij}$  that appear in the equivalent general transformation law for second order cartesian tensors under rotation of the axis system

$$T'_{jl} = \sum_{ik} a_{ij} a_{kl} T_{ik}, \quad (5.27)$$

where  $T_{ik}$  is a second order cartesian tensor in some arbitrary original frame (in this case the BOSS frame) and  $T'_{jl}$  is the tensor referred to some arbitrary rotated frame (in this case the principal frame). Since the above transformation law is completely general and the original and rotated frames to which it refers are arbitrary, we may write for the reverse transformation

$$T_{ik} = \sum_{jl} a_{ji} a_{lk} T'_{jl} = \sum_{jl} a_{ij} a_{kl} T'_{jl}. \quad (5.28)$$

We note that the sense of the rotation in either direction is contained not in the individual direction cosines themselves (which by definition can have no inherent directionality) but in the indices over which summation is taken in the transformation law. Since in this case we are transforming from a principal axis system (ie,  $S'_{jl} = 0 \forall j \neq l$  as we have already indicated) all terms for which  $j \neq l$  vanish so that the transformation simplifies to

$$S_{ik} = \sum_j a_{ji} a_{jk} S'_{jj} = \sum_j a_{ij} a_{kj} S'_{jj}, \quad (5.29)$$

giving a sum of just three terms for each  $S_{ik}$ .

The next step is to transform the Saupe ordering tensor in the BOSS frame back into the local frames of each of the mesogenic groups in turn. Since the local frame is by definition a principal frame and the mesogenic group is taken to be cylindrically symmetric, we only need calculate  $S_{zz}$  in the local principal frame to construct the entire Saupe ordering tensor in this frame. In fact we only require  $S_{zz}$  anyway, since we simply wish to find the order parameter  $\bar{P}_2$  of the assumed symmetry axis which is by definition  $S_{zz}$ . We write for the ordering tensor in a given local mesogenic frame

$$S'_{jl} = \sum_{ik} a_{ij} a_{kl} S_{ik}, \quad (5.30)$$

which, given that  $S_{jl} = 0 \forall j \neq l$ , simplifies to

$$S'_{jj} = \sum_{ik} a_{ij} a_{kj} S_{ik} \quad (5.31)$$

from which we require

$$S'_{33} = \sum_{ik} a_{i3} a_{k3} S_{ik} = \bar{P}_2^{\text{meso}}. \quad (5.32)$$

We have the  $S_{ik}$  and so only require direction cosines of the form  $a_{i3}$  for each mesogenic group, but these are simply the direction cosines between the mesogenic group z-axes and the axes of the BOSS frame—which we already have and indeed will have been used to transform the local interaction tensors into the BOSS frame at the very start of the molecular field calculations on the current accepted conformer.

To calculate the simulation averages of the order parameters of the mesogenic groups, the order parameter of each group is accumulated over the accepted conformers, having first been weighted by the rotational partition function, and the partition functions are also accumulated over accepted conformers. Then, at the end of the simulation, the ensemble averages are computed by taking the ratio of these accumulated quantities in accordance with equation 5.24, that is,

$$\langle \bar{P}_2^{\text{meso}} \rangle_{\text{ens}} = \sum_i \bar{P}_2^{\text{meso}i} Q_{\text{ext}}^i / \sum_i Q_{\text{ext}}^i. \quad (5.33)$$

The free energy difference,  $\Delta A_{IN}/RT$ , between isotropic and nematic phases is also calculated at the end of the simulation as

$$\begin{aligned} \Delta A_{IN}/RT &= -\frac{1}{2} \langle U_{\text{ext}}^*{}^i Q_{\text{ext}}^i \rangle / \langle Q_{\text{ext}}^i \rangle - \ln \left\{ \langle Q_{\text{ext}}^i \rangle / 4\pi \right\} \\ &= -\frac{1}{2} \sum_i U_{\text{ext}}^*{}^i Q_{\text{ext}}^i / \sum_i Q_{\text{ext}}^i - \ln \left\{ \frac{1}{N} \sum_{i=1}^N Q_{\text{ext}}^i / 4\pi \right\}, \end{aligned} \quad (5.34)$$

where the angle brackets  $\langle \rangle$  here denote a straightforward arithmetic mean.

We also, at this stage, calculate the  $N - I$  entropy difference at the phase transition, which is by definition (at constant volume)

$$\Delta S_{NI} = \frac{\Delta U_{NI}}{T} = \frac{\langle U \rangle_I - \langle U \rangle_N}{T}. \quad (5.35)$$

Now the (average) internal energies of each of the respective phases have two contributions, the intramolecular contribution,  $\langle U_{\text{int}} \rangle$ , and the intermolecular contribution,  $\langle U_{\text{ext}} \rangle$ , so that the quantity we require

$$\begin{aligned} \Delta S_{NI}/R &= \left[ (\langle U_{\text{int}} \rangle_I + \langle U_{\text{ext}} \rangle_I) - (\langle U_{\text{int}} \rangle_N + \langle U_{\text{ext}} \rangle_N) \right] / RT \\ &= \left[ (\langle U_{\text{int}} \rangle_I - \langle U_{\text{int}} \rangle_N) + (\langle U_{\text{ext}} \rangle_I - \langle U_{\text{ext}} \rangle_N) \right] / RT \\ &= \frac{\Delta U_{NI}^{\text{int}}}{RT} + \frac{\Delta U_{NI}^{\text{ext}}}{RT}. \end{aligned} \quad (5.36)$$

Thus we may write

$$\Delta S_{NI}/R = \Delta S_{NI}^{\text{conf}}/R + \Delta S_{NI}^{\text{or}}/R, \quad (5.37)$$

where

$$\Delta S_{NI}^{\text{conf}} = \Delta U_{NI}^{\text{int}}/T \quad (5.38)$$

is the conformational entropy change and

$$\Delta S_{NI}^{\text{or}} = \Delta U_{NI}^{\text{ext}}/T \quad (5.39)$$

is the orientational entropy change. The quantity  $\langle U_{\text{int}} \rangle_I$  in equation (5.36) is given by the unweighted average of the intramolecular potential energies

$$\langle U_{\text{int}} \rangle_I = \langle U_{\text{int}} \rangle = \sum_i U_{\text{int}}^i / N, \quad (5.40)$$

whereas  $\langle U_{\text{int}} \rangle_N$  is given by the orientational partition function weighted average

$$\langle U_{\text{int}} \rangle_N = \langle U_{\text{int}} Q_{\text{ext}} \rangle / \langle Q_{\text{ext}} \rangle = \sum_i U_{\text{int}}^i Q_{\text{ext}}^i / \sum_i Q_{\text{ext}}^i. \quad (5.41)$$

Thus

$$\Delta S_{NI}^{\text{conf}}/R = \frac{1}{RT} \left[ \sum_i U_{\text{int}}^i / N - \sum_i U_{\text{int}}^i Q_{\text{ext}}^i / \sum_i Q_{\text{ext}}^i \right], \quad (5.42)$$

where the value of  $T$  is the absolute temperature at which the BOSS Monte Carlo algorithm is sampling the conformational space. The orientational contribution to the total entropy change is similarly calculated from the averages in the isotropic and nematic phases of the orientational intermolecular energy, the main difference being that this energy is zero in the isotropic phase regardless of conformation, so there is no need to calculate the average. The other difference is that these energies are calculated already automatically scaled by  $RT$  so that

$$\langle U_{\text{ext}}^* \rangle_N = \sum_i U_{\text{ext}}^*{}^i Q_{\text{ext}}^i / \sum_i Q_{\text{ext}}^i \quad (5.43)$$

(with the asterisk denoting division by  $RT$ ) and so

$$\Delta S_{NI}^{\text{or}}/R = - \langle U_{\text{ext}}^* \rangle_N. \quad (5.44)$$

### 5.3 Computational Technique

Monte Carlo sampling of the conformational space of the single molecule is achieved using the program BOSS (Biochemical and Organic Simulation System) 3.8 [11], which has been suitably modified to obtain a model potential consistent with previous application of this methodology [4]. That is, the intramolecular potential energy is calculated as a sum of effective single-torsion energies for the various torsions present, these being modelled by a Ryckaert-Bellemans-type potential [12] suitably parameterised for each torsion type in question. The form of the Ryckaert-Bellemans potential used in the BOSS code is

$$V(\phi) = V_0 + \frac{V_1}{2}[1 + \cos(\phi + f_1)] + \frac{V_2}{2}[1 - \cos(2\phi + f_2)] + \frac{V_3}{2}[1 + \cos(3\phi + f_3)] \quad (5.45)$$

That is, it is in its most general form the expansion

$$V(\phi) = \sum_{n=0}^{\infty} V'_n [1 + (-1)^{n+1} \cos(n\phi + f_n)] \quad (5.46)$$

so that the  $V'_0$  term becomes

$$V'_0 [1 - \cos(0\phi + f_0)] = V'_0 [1 - \cos(f_0)] = V_0 \quad (5.47)$$

and is thus invariant with respect to  $\phi$ . The  $V'_1$  term is then

$$V'_1 [1 + \cos(\phi + f_1)] = \frac{V_1}{2} [1 + \cos(\phi + f_1)] \quad (5.48)$$

and so in general for all  $V'_n$  with  $n > 0$  the  $V'_n$  term is

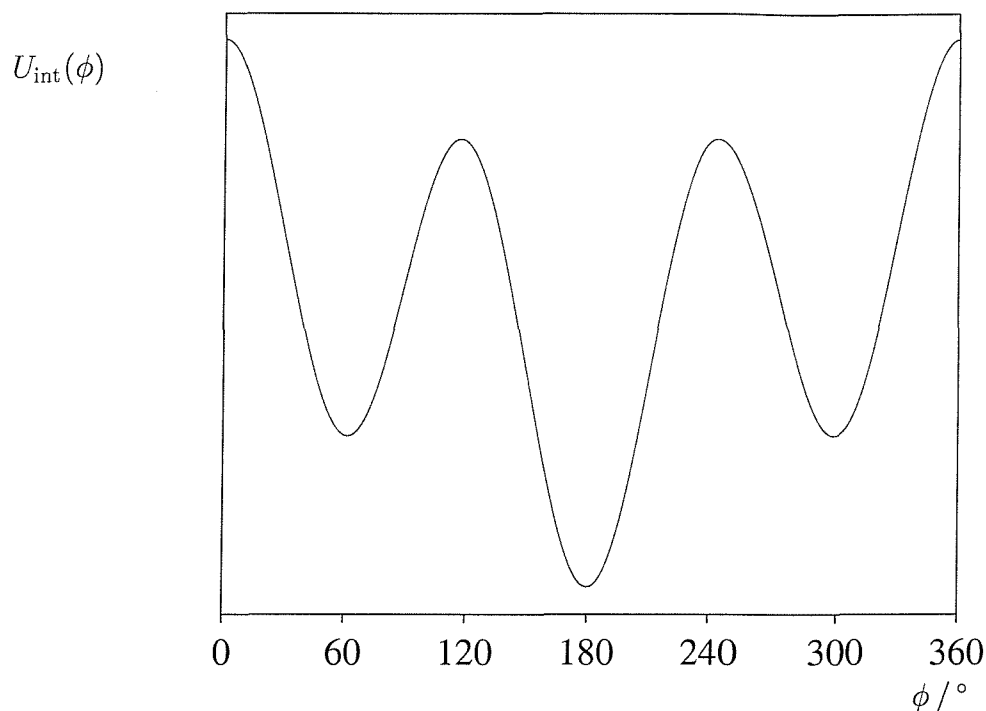
$$V'_n [1 + (-1)^{n+1} \cos(n\phi + f_n)] = \frac{V_n}{2} [1 + (-1)^{n+1} \cos(n\phi + f_n)] \quad (5.49)$$

with

$$V'_n = \frac{V_n}{2}. \quad (5.50)$$

The quantities  $f_n$  are phase shift angles and for our purposes they are all zero (except for  $f_0$ ). The expansion is taken upto third order as indicated in equation (5.45). The

Figure 5.6: The form of the Ryckaert-Bellemans potential employed in the BOSS united atom forcefield for the standard alkane torsion



parameters required to calculate expression (5.45) are from the united-atom version of the BOSS potential and are to be found in the BOSS file `oplsua.par`. The Ryckaert-Bellemans potential is illustrated in figure 5.6. As far as the non-bonded interactions are concerned, the atoms were modelled as hard spheres with diameters of  $2.6 \text{ \AA}$  so that moves that introduce steric clashes are always rejected. The value of  $2.6 \text{ \AA}$  was chosen as it is close to the “size” of the methylene combined atom (ie,  $\sigma$  in its Lennard-Jones potential) and is consistent with that used in previous applications of this methodology [4]. All attractive forces between non-bonded atoms have been removed, since the molecule will otherwise tend to fold up, which, while realistic for the environment in which it finds itself (effectively a vacuum), one would think physically unrealistic in the bulk isotropic liquid where it is surrounded by many other identical molecules. It is only the orienting tendency of the nematic environment that is being modelled by the molecular field, not the intermolecular interactions in the isotropic phase, so we should choose a potential model that is reasonable for the isotropic phase, given that we have



chosen to model only a single molecule explicitly. In addition to these modifications the molecular field calculations were also implemented in the BOSS code to simulate the anisotropic environment. The input to this part of the code consists of a set of scaled strength parameters,  $X^* = X/k_B T$ , that determine the strength of the nematic orienting field in comparison to the thermal energy of the system. These values are used to construct the tensors  $x_{ij}^*$  for the individual mesogenic groups having the same form as the  $x_{ij}^{\text{meso}}$  in equation (5.16), namely

$$x_{ij}^* = \begin{cases} -\frac{X^*}{2}\delta_{ij} & (i, j = 1, 2, 3 \text{ and } (i, j) \neq (3, 3)) \\ X^* & (i = j = 3). \end{cases} \quad (5.51)$$

These tensors are then transformed into the common molecular (BOSS) frame using the direction cosines of the mesogenic group axes in that frame:

$$x_{ab}^{*'} = X^*(3l_a l_b - \delta_{ab})/2, \quad (5.52)$$

where  $x_{ab}^{*'}$  are the components of the scaled mesogen interaction tensor in the molecular (ab) frame,  $X^*$  is the scaled strength parameter and  $l_a$  is the direction cosine between the mesogenic group long axis and the a axis of the molecular frame. The calculation continues as described in the previous section, but using these scaled quantities rather than the unscaled interaction parameter and tensor components directly.

This is standard technique in molecular field calculations, but within this particular hybrid methodology leads to subtlety not encountered in calculations that are solely molecular field or solely Monte Carlo in nature, and that concerns the concept of temperature. In the Monte Carlo part of the calculation, BOSS operates with a “real” (ie, unscaled) temperature, input to it in °C. The molecular field calculation, on the other hand, works with a scaled temperature, the value of which we do not actually know until the end of the simulation, since we do not actually input the scaled temperature directly, but rather the scaled strength parameter, which determines the values of the order parameters. The scaled temperature is the ratio of the order parameter (which in this case will be the arithmetic mean of the simulation averages of the order parameters of the mesogenic groups) to the scaled strength parameter. Thus we have two,

in general different, temperature scales. The question then arises as to how to ensure that the the temperatures operating in the two parts of the calculation are reasonably consistent, rather than widely disparate. The most straightforward way is by making use of prior knowledge and to set the BOSS temperature to a value which is our best estimate of that at which the  $N-I$  transition is likely to occur. The temperature scales will then be most closely consistent in precisely the molecular field scaled temperature regime that attracts our primary interest, namely the region in the neighbourhood of the transition. We know that for mesogenic systems in general, and for the systems most closely related to dendrimers for which we have experimental data in particular (ie, liquid crystal dimers), this temperature is in the region of 400 K. This suggests that we should employ this temperature within BOSS.

However, here we encounter another subtlety, and that relates to the fact that, for convenience, we have ignored contributions to the interaction tensor arising from the flexible chain regions of the molecule. In setting up the molecular field calculations we have included only the mesogenic group contributions explicitly as they are expected to be the dominant contribution. In the previous application of this methodology [4] and in molecular field theories where chain interactions are included explicitly [9] the relative strength of the contribution from a chain segment is a fraction of that associated with the mesogenic groups. The effect of this weaker interaction coming from each torsional segment is to create an additional contribution to the effective energy difference between the gauche and trans forms of each such segment. This could be equivalently conceptualised as a reduction in the effective temperature at which the torsional space is being sampled. This suggests that we may calculate the interaction energy coming from a single butane link in both gauche and trans forms and obtain the difference between the two in order to estimate the size of this effect. By equating the Boltzmann distribution between gauche and trans forms with this chain contribution to the gauche-trans energy difference at a real temperature of some 400 K with the distribution at some lower artificial temperature where the chain contribution is taken as zero, we can calculate this lower effective temperature at which the effect of

the chain interactions may be included implicitly. We performed the simulations using for convenience, by default, a BOSS temperature close to room temperature, namely 25 °C. It turns out [17] that, based on a transition temperature of 400 K and assuming a strength parameter of unity for each torsional segment, the effective temperature which models most closely the influence of the interactions arising from these segments is in the neighbourhood of 40 °C , which on an absolute scale, seen in reduced terms, is essentially the temperature we have employed.

It is also worth noting that since the conformers are accepted or rejected solely on the basis of the intramolecular energy, which is independent of the molecular field energy, it is inefficient to run the simulation multiple times, each time for a different scaled strength parameter, since the conformations sampled by Monte Carlo will be the same and so this part of the calculation would be repeated over and over again. Thus, the input to the molecular field part of the program consists of a set of (scaled) strength parameters. The molecular field calculations for the various values of  $X^*$  are performed together during the same run.

Every 500 conformations the instantaneous values and cumulative averages of the intramolecular potential energy and order parameters for the mesogens are written to file. At the end of the simulation the average quantities (for each value of  $X^*$ ) are computed and also written to file, these averages being the Helmholtz free energy and entropy differences between the isotropic and nematic phases and the order parameters for the mesogens. The entropy difference is composed of an orientational and a conformational contribution, both of which are also output.

The other inputs to the program are those required by BOSS itself and those that we have to concern ourselves with here are mainly the Z-matrix, which defines the starting conformation (ie, the molecule being modelled and its geometry) and the parameter file, which enables us to change the conformational temperature, the frequency with which the molecular coordinates are output to file and the maximum number of torsional angles altered in a Monte Carlo attempted move. A complete specification of the

various files required to run BOSS and their contents is given in the BOSS manual [11].

The starting conformation chosen for the molecules was the all-trans, as this has the lowest intramolecular energy, and ground state conformations are a standard starting point in Monte Carlo simulations of small numbers of flexible molecules at finite temperature. The sampling protocol was as follows. The maximum number of torsional angles altered in a single Monte Carlo attempted move was set to 5. The number of torsions moved is then an integer in the range 1 – 5, chosen randomly. This number of torsions are then altered, the actual torsional angles changed to make up this complement of moves themselves being selected at random. There are two types of move employed for any given torsional angle. One is the standard type and involves a move of up to a certain maximum displacement, the size of the move being chosen randomly with uniform probability over the allowed range specified. The maximum displacement we have chosen is  $20^\circ$ . The other type of move is a large move of exactly  $\pm 120^\circ$ ; this gives the system a chance of jumping between adjacent torsional minima. The probabilities of the different move types are chosen so that on average the standard moves occur 90 % of the time and the large moves the remaining 10 % of the time. This gives an acceptance rate of approaching 30 %. It is clear that the acceptance rate will be influenced by the kinds of moves that are attempted. If the proportion of large moves is increased or if for the standard-type moves the maximum displacement is increased, the acceptance rate will fall. We would obviously like to optimise the progress of the system in sampling phase space as a function of the number of attempted moves (or, more exactly, as a function of computer time). If we have a very high proportion of the large moves and also make the maximum displacements for the ordinary moves very large, then almost no moves will be accepted. At the other extreme, almost all the moves will be accepted, but they will be so small that the system will be essentially stationary. Somewhere between these extremes will be the optimum we seek, and it has become common to look upon a 50 % acceptance rate as being this optimum. It should be said, however, that the basis of this rule of thumb is certainly questionable; indeed, for some systems acceptance rates of considerably less than the “ideal” value

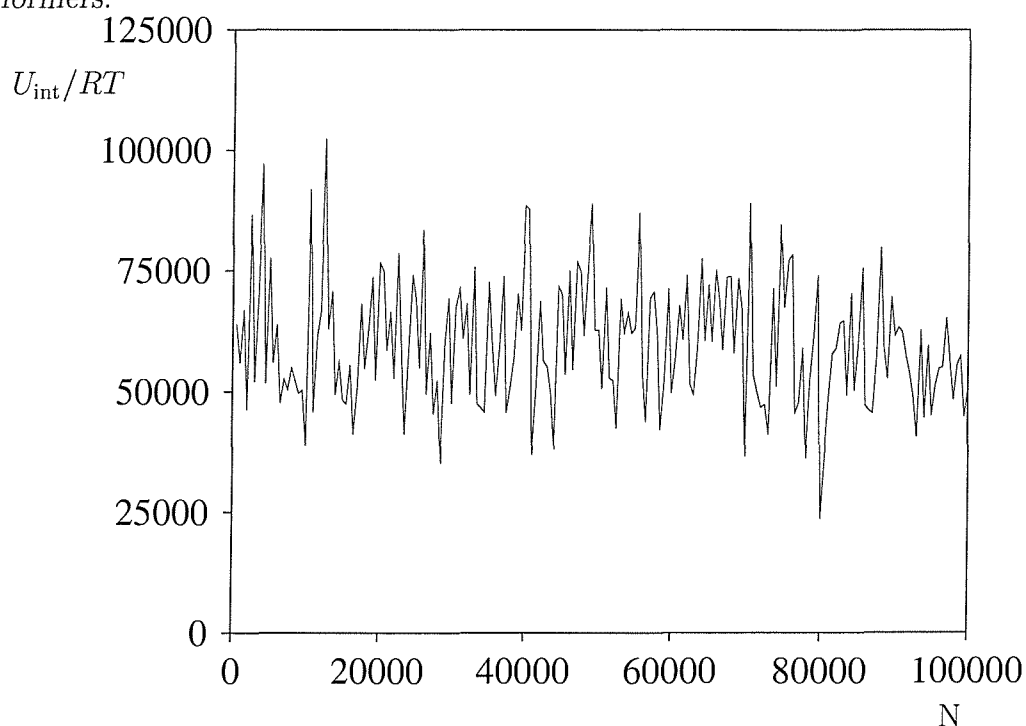
of 50 % (even as low as 10 %) have been shown to produce the greatest rate of progression through phase space, at least by the measures employed, suggesting that a small number of large moves is most cost effective [18, 21]. The protocol we have used may have an acceptance rate of somewhat less than 50 % (which could clearly be “improved” by reducing the proportion of large moves and the maximum displacement), but nevertheless seems to be fairly well-optimised.

It is customary in Monte Carlo simulations to divide the process into two distinct stages, namely an “equilibration” stage followed by a “production” stage. In the former, the system is allowed to evolve from the starting configuration and allowed to settle down so that the instantaneous properties oscillate about a mean value which does not show any further systematic variation with continued progress of the simulation. Then, from a point assumed to be representative of the state of the system at equilibrium, the simulation is continued and data to be used in calculating the bulk properties of the system are collected. This is the production stage, which is made as long as necessary such that the cumulative simulation estimates of the properties of interest have converged to constant values. Strictly speaking, of course, this two stage procedure is not actually necessary. All Monte Carlo simulations could in principle be started from any configuration and one could take the cumulative estimates of the properties after a sufficiently long “time” that the the distribution of states had reached the limiting distribution of the Markovian chain, regardless of the starting configuration. However, if the initial configuration is highly unrepresentative of the system at the state point in question (ie, its Boltzmann probability is very low), this could be a very, very long time indeed from a human perspective, since the simulation would have to generate a sufficiently large number of configurations that the appearance of the initial set of highly unrepresentative ones had become progressively less unrepresentative until ultimately they had occurred no more frequently than would be consistent with the Boltzmann distribution. The way around this, then, is to run the simulation until there is no longer any systematic trend in the fluctuations of the instantaneous properties when viewed on a “human” scale of, say, tens to hundreds of thousands of configurations,

so that what is observed is a Poisson distribution around a constant value. Then, the simulation can be restarted from the last accepted configuration from the initial, equilibration, stage, and a further simulation, the production stage, can be performed over which the bulk properties of the system are computed.

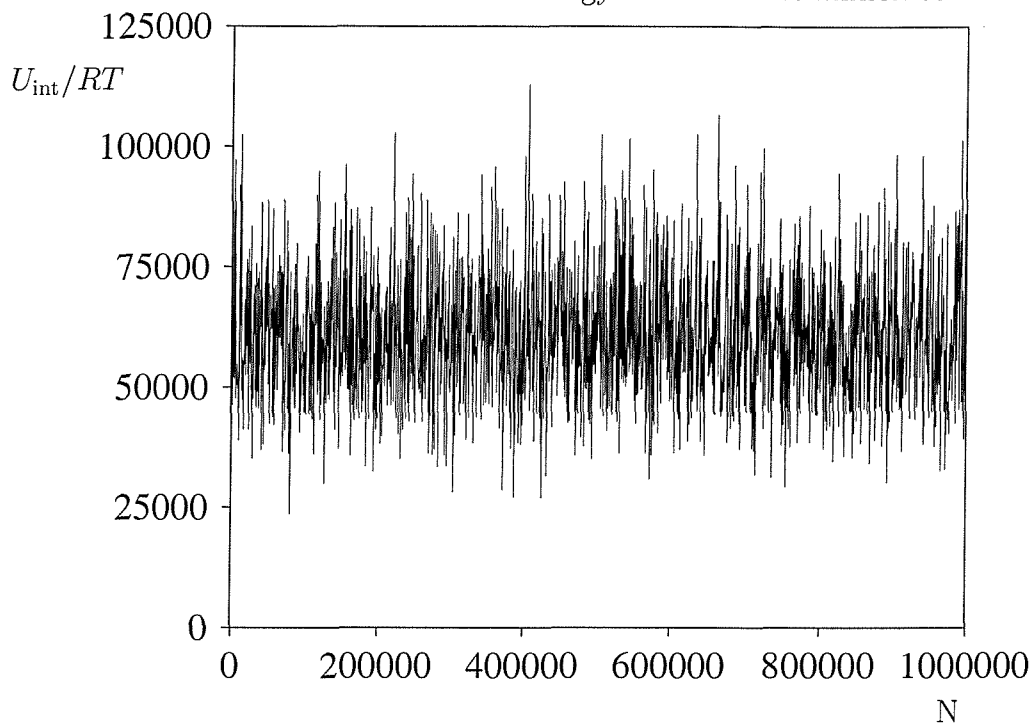
In the case of the simulations presented here, the equilibration stage is almost a mere formality, since we are just sampling the torsional degrees of freedom of a single molecule, and the starting conformation (the all-trans) is one whose conformational energy is sufficiently close to the mean value at equilibrium as to be within the range of the likely oscillation arising from Boltzmann sampling of states at the BOSS temperature employed (ie, room temperature). To illustrate this, figures 5.7 and 5.8 show the instantaneous values of the intramolecular potential energy as a function of the conformer number. It can be seen that from essentially the start of the simulation

*Figure 5.7: Instantaneous intramolecular energy over the first one hundred thousand conformers.*



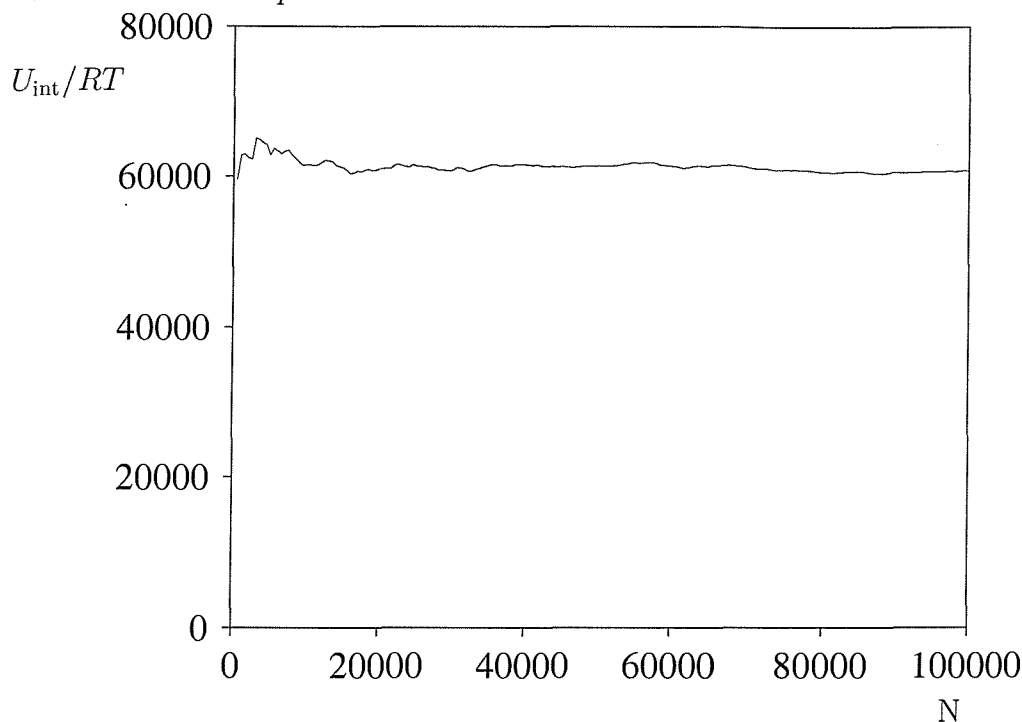
the energy oscillates about a constant mean value and that the energy of the initial

Figure 5.8: Instantaneous intramolecular energy over the first million conformers.



conformer is well within this oscillation, suggesting that the starting conformation is just as representative (on the length scale of practical simulations) as those accepted by the Boltzmann sampling scheme in the system at equilibrium. The properties of the system, which are all simulation averages of one form or another, are computed from the total number of conformations included in the averaging, which should clearly be performed over a sufficiently large number of them that the cumulatives as a function of the number of conformers have converged to constant values. In this study, convergence of the simulation averages was generally achieved after about one million conformations, as evidenced by the cumulative averages of the intramolecular potential energy (see figures 5.9 and 5.10) and the mesogenic group order parameters (see figures 5.11 and 5.12). We have an additional check of convergence in the case of the order parameters in that not only should each mesogenic group order parameter converge to a constant value, but it should also converge to the same constant value as that of all the others.

Figure 5.9: Cumulative average intramolecular energy during the first hundred thousand conformers of the production run.



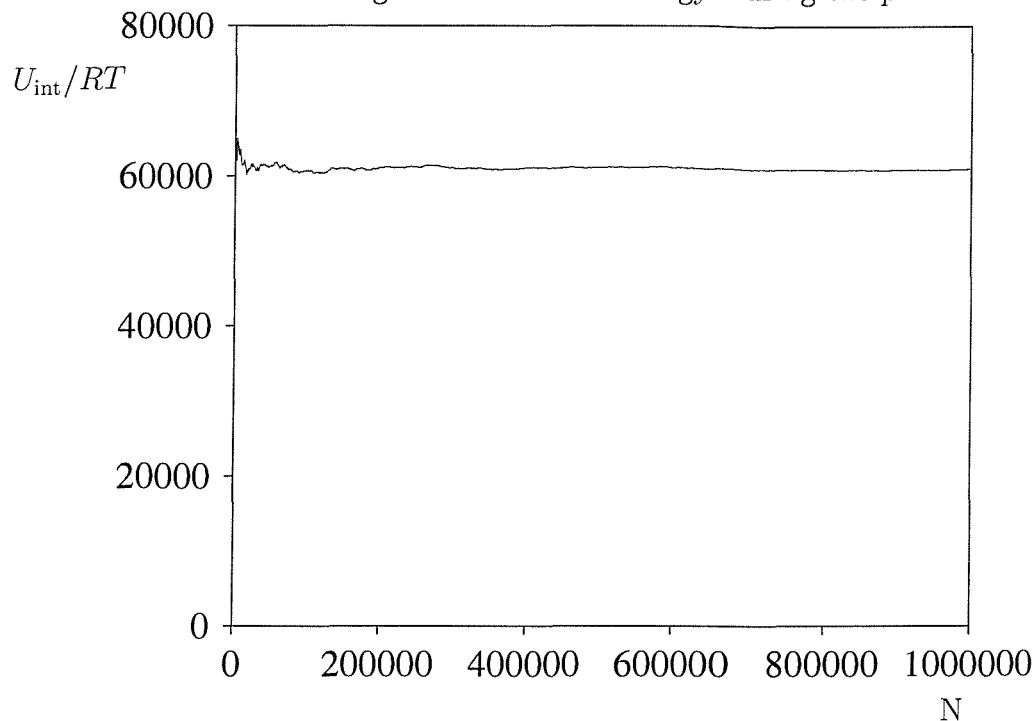
It can be seen that convergence of the order parameter (the quantity thought to be the most sensitive marker of convergence in these calculations) occurs within about one million attempted moves. The value of  $X^*$  corresponding to the  $N - I$  transition was located as the point where the graph of  $\Delta A_{IN}(X^*)/RT$  cuts the abscissa. The values of the simulation averages corresponding to this value of  $X^*$  are then the  $N - I$  transitional values. So from the range of  $X^*$  we have the temperature dependence of the properties (ie, part of the phase diagram) and from the value of  $X^*$  at the transition,  $X_{NI}^*$ , we have the transitional properties. These calculations were performed not only for the zeroth order dendrimer multipodes of various chain lengths, but also for the multipodes with laterally attached mesogenic groups.

#### *Treatment of Errors*

We should remember in performing these simulations that, in part, it is an idealised computer experiment, and that like an experiment, this aspect will be subject to er-



Figure 5.10: Cumulative average intramolecular energy during the production run.

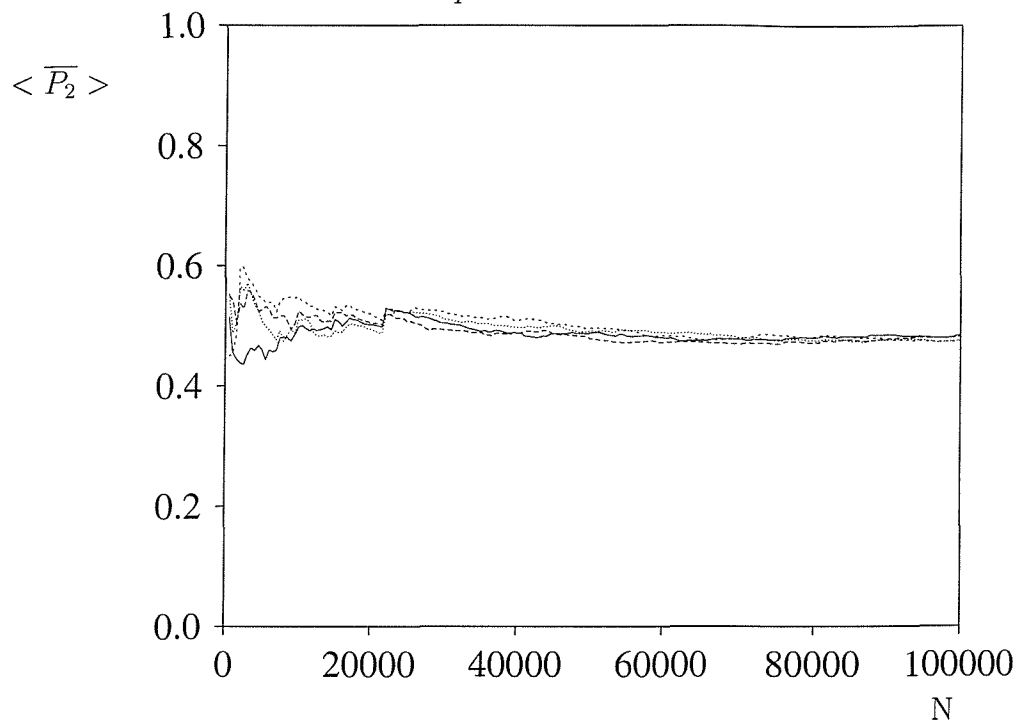


ror. The size of the statistical errors associated with the results may be estimated by means of performing a typical production run subdivided into a number of blocks. The simulation average quantities for each of these blocks is then obtained, in addition to the overall averages and this is used to provide information about the likely statistical error in the quantities. The number of blocks should be chosen such that the length of each block is short enough that there are a reasonable number of blocks available to yield sub-averages, but not so short that the averages within each block are highly correlated (ie, so they are statistically independent). These data are then analysed to give an indication of the likely errors in the following way. The standard deviation in the simulation-calculated value  $X$  of some property of the system, obtained in such a simulation run is given by [13]

$$\sigma(X) = \sqrt{\frac{1}{N(N-1)} \sum_i (X_i - X)^2}, \quad (5.53)$$

where  $N$  is the number of blocks and  $X_i$  is the value of the property obtained from block  $i$  alone. We have chosen to take  $N = 10$  so that we divide a typical production

Figure 5.11: Cumulative average order parameters of the four mesogens during the first hundred thousand conformers of the production run.



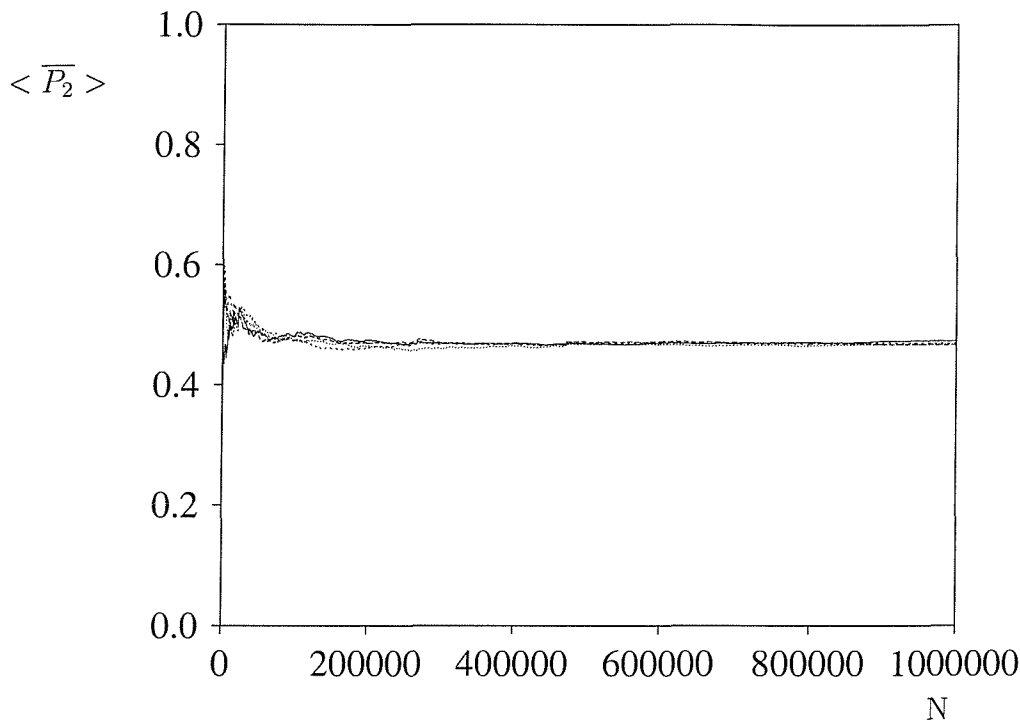
run of  $10^6$  configurations into ten blocks of  $10^5$  configurations each. In addition, the properties obtained as averages for each of the individual blocks may be analysed to see if there is any systematic drift in the values rather than a Poisson distribution of values about the overall average. The latter indicates the system is indeed at equilibrium, whereas the former implies the opposite.

## 5.4 Results and Discussion

### 5.4.1 Determination of the Transitional Properties

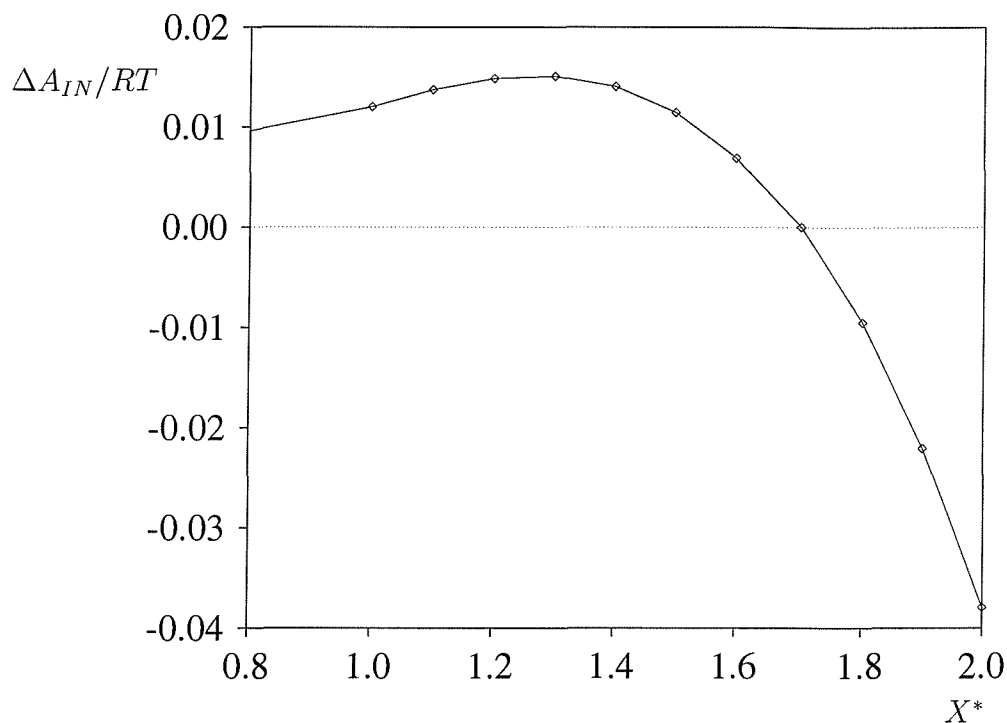
We have seen previously how we may calculate a variety of properties of interest for various strengths of the molecular field. We now turn our attention to the problem of how to locate the nematic-isotropic phase transition and thereby determine the  $N - I$

Figure 5.12: Cumulative average order parameters of the four mesogens during the production run.



transitional values of these properties. The  $N - I$  phase transition occurs, by definition, where the free energies of the  $N$  and  $I$  phases become equal, that is, when the difference in the free energies between the two phases vanishes. From the simulation we obtain the value of this difference,  $\Delta A_{IN}/RT$ , for each value of the scaled strength parameter for which the calculations are performed. Figures 5.13 and 5.14 show the quantity  $\Delta A_{IN}/RT$  as a function of the scaled strength parameter for a typical terminal dendrimer and a typical lateral dendrimer respectively. It can be seen that  $\Delta A_{IN}(X^*)/RT$  has the same form as in the standard Maier-Saupe theory, rising from zero, passing through a maximum and then decreasing and passing through zero at the transition to become negative in the nematic phase, with the region around the transition being approximately linear. To locate the  $N - I$  transition precisely, the simulations were restarted from the last accepted configuration and another production run performed using a smaller range of strength parameters centred around the approximate location of the transition (ie, the linear region). Then, the value of  $X^*$  at

Figure 5.13: The scaled free energy difference as a function of the scaled strength parameter for a medium sized terminal dendrimer



the transition,  $X_{NI}^*$ , is obtained by linear interpolation between the points most closely straddling the transition. That is, if we write the gradient of the straight line as

$$m = (y_2 - y_1)/(x_2 - x_1), \quad (5.54)$$

where  $(x_1, y_1)$  and  $(x_2, y_2)$  are the points either side of the transition, then the value of the scaled strength parameter for which the free energy difference is zero may be found by setting  $y = 0$  and solving for  $x$  in the equation of the straight line written as

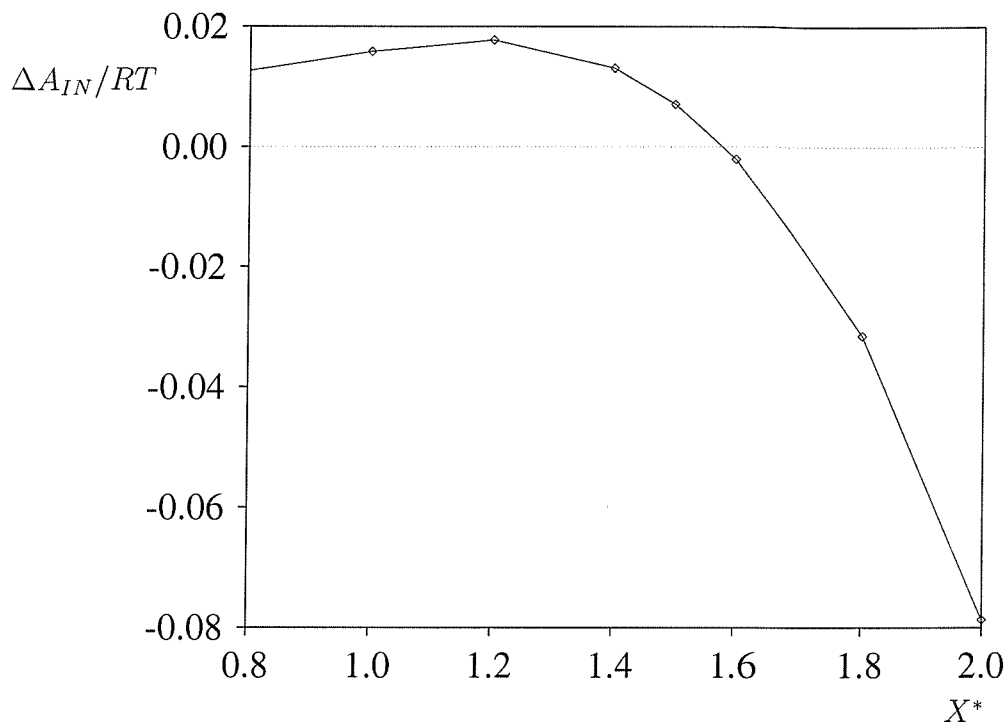
$$y - y_0 = m(x - x_0) \quad (5.55)$$

(where  $x_0, y_0$  are either  $x_1, y_1$  or  $x_2, y_2$ ) to yield

$$x = -y_0/m + x_0, \quad (5.56)$$

thus giving us  $X_{NI}^*$ .

Figure 5.14: The scaled free energy difference as a function of the scaled strength parameter for a medium sized lateral dendrimer



To obtain the properties corresponding to this value of  $X^*$  we perform a similar interpolation procedure on the graph of the property as a function of the scaled strength parameter. That is, we find the value of the ordinate of the point corresponding to  $X_{NI}^*$  on the straight line between the two points straddling the transition. Thus, using our previous notation, if the points either side of the transition are  $(x_1, y_1)$  and  $(x_2, y_2)$ , then the value of the property at the transition is

$$y = m(x - x_0) + y_0, \quad (5.57)$$

where  $x = X_{NI}^*$ .

Figures 5.15 and 5.16 show the average mesogenic group order parameters as a function of the scaled strength parameter for a typical terminal dendrimer. Figure 5.15 shows the order parameters over the same range of  $X^*$  as in the free energy curve 5.13. Within this range the order parameters are seen to be approximately linear in  $X^*$  and are well converged. Figure 5.16 shows the order parameters over a much greater range of the

scaled strength parameter, so as to encapsulate as near to the total range of the order parameters as possible. As expected, we obtain a curve similar to the Maier-Saupe result—a sigmoid curve beginning at zero, rising monotonically with an approximately linear central region and finally becoming shallower and forming a plateau as it rises near to its ultimate limiting value of unity, reached in the limit that  $X^* \rightarrow \infty$ .

Figure 5.15: The order parameter as a function of the scaled strength parameter in the transitional region for the terminal dendrimer of figure 5.13

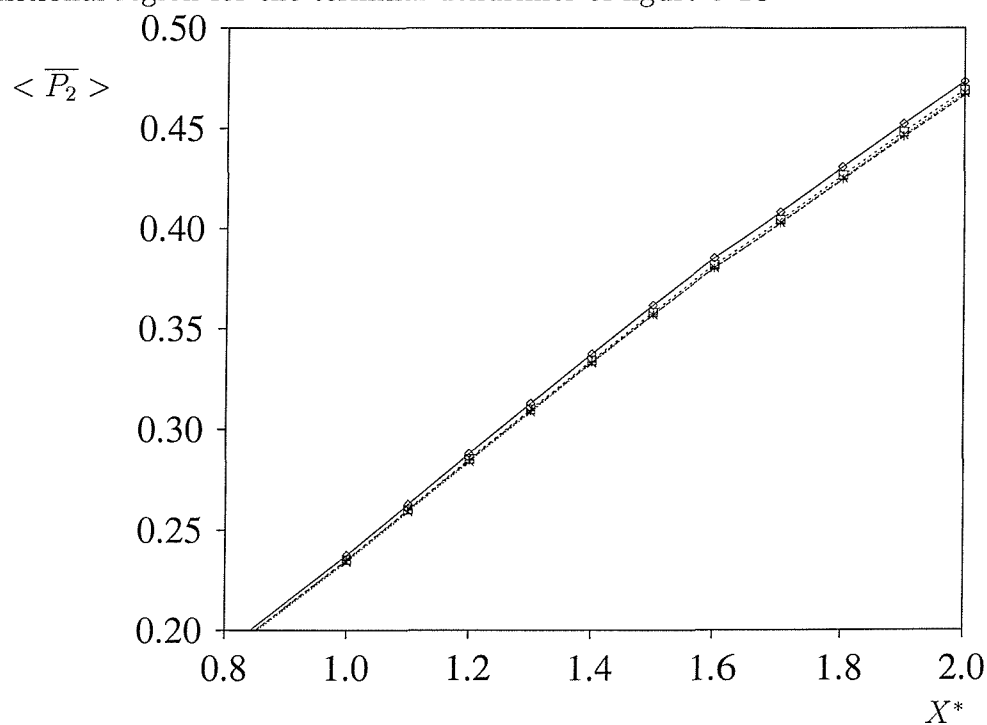
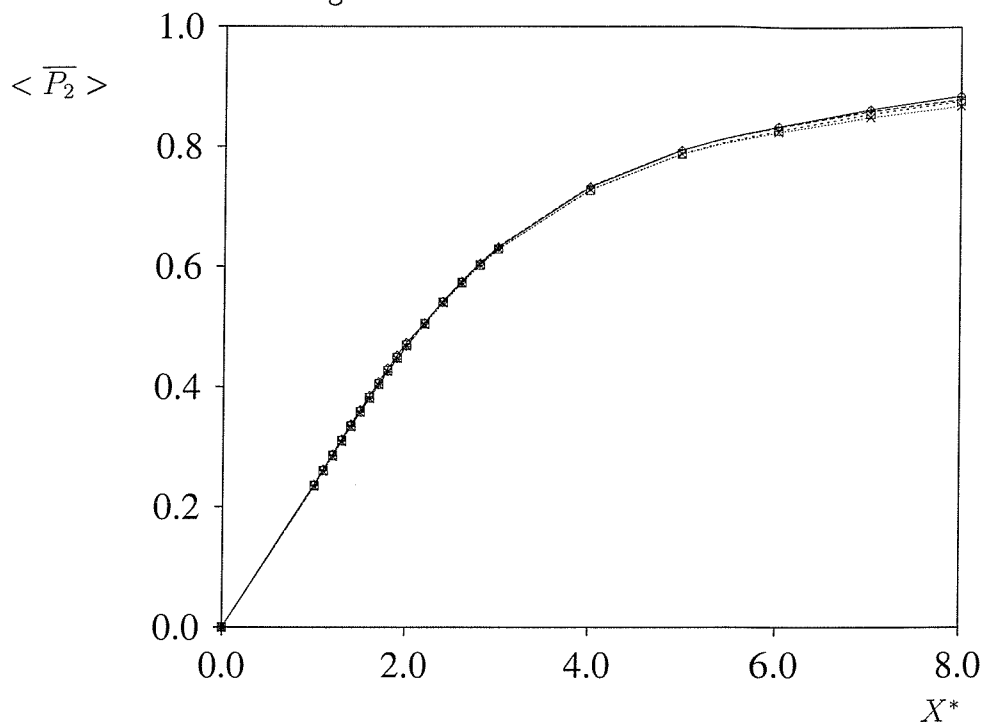


Figure 5.16: The order parameter as a function of the scaled strength parameter for the terminal dendrimer of figure 5.13



Figures 5.17 and 5.18 show the free energy difference  $\Delta A_{IN}/RT$  as a function of the scaled temperature  $T^* = \langle \bar{P}_2 \rangle / X^*$  for the terminal and lateral dendrimers featured in figures 5.13 and 5.14 respectively. We note that the form of the graphs is as expected for the curve  $\Delta A(T)/RT$  in general on passing through a weakly first order phase transition, and is very similar to the Maier-Saupe case encountered previously. That is, the curve rises from a negative value with a positive gradient, which is rapidly diminishing, and it looks as though it may join the line  $\Delta A/RT = 0$  smoothly without a sharp change in gradient, but instead it just cuts this line (so that passing to the line  $\Delta A/RT = 0$  would involve a discontinuity in gradient) and then changes its own gradient abruptly, turning back on itself to fall to zero smoothly and continuously from the right.

Figure 5.17: The scaled  $N - I$  free energy difference as a function of scaled temperature for the terminal dendrimer of figure 5.13

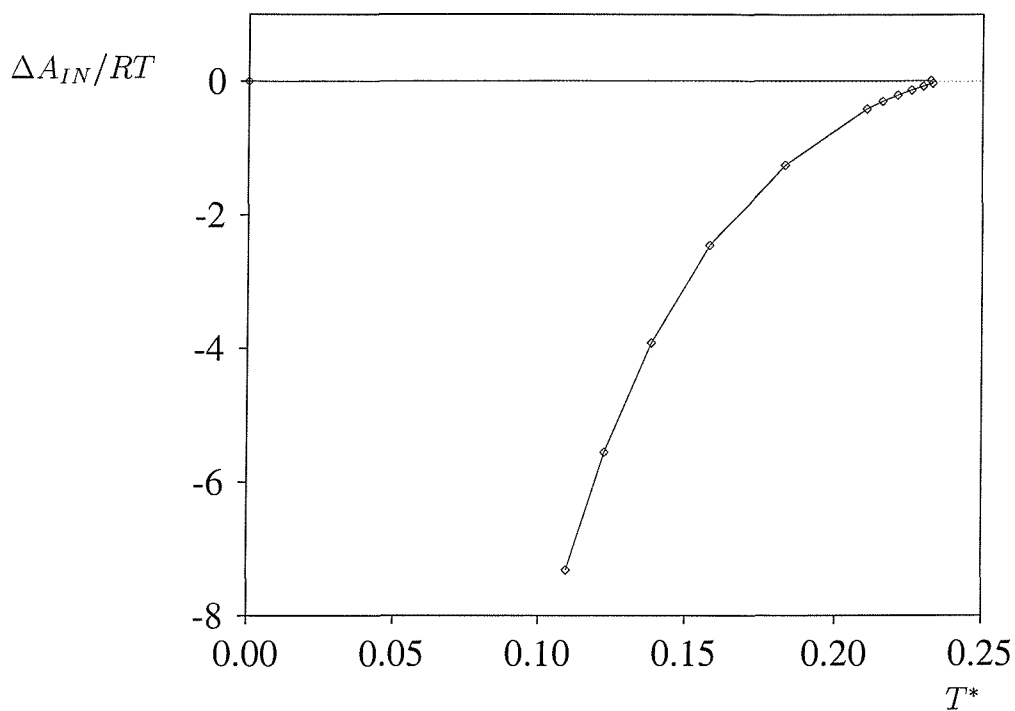
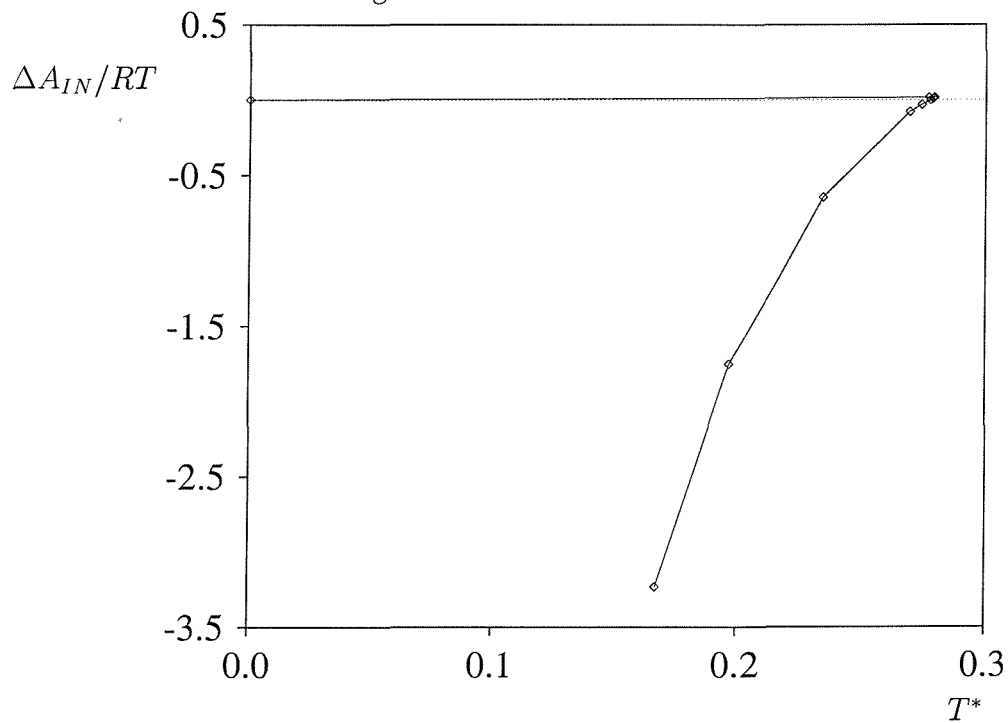


Figure 5.18: The scaled  $N - I$  free energy difference as a function of scaled temperature for the lateral dendrimer of figure 5.14





Figures 5.19 and 5.20 show the mesogenic group order parameters as a function of the scaled temperature for the terminal and lateral dendrimers featured in the free energy curves respectively. We note the Maier-Saupe-like form of  $\langle \overline{P}_2 \rangle (T)$ , in particular its multiple-valuedness in certain temperature regimes due to the order parameter curve bending back on itself, a feature we have already discussed in relation to the Maier-Saupe theory in Chapter 2.

Figure 5.19: Mesogenic group order parameters as a function of scaled temperature for the dendrimer of figure 5.13

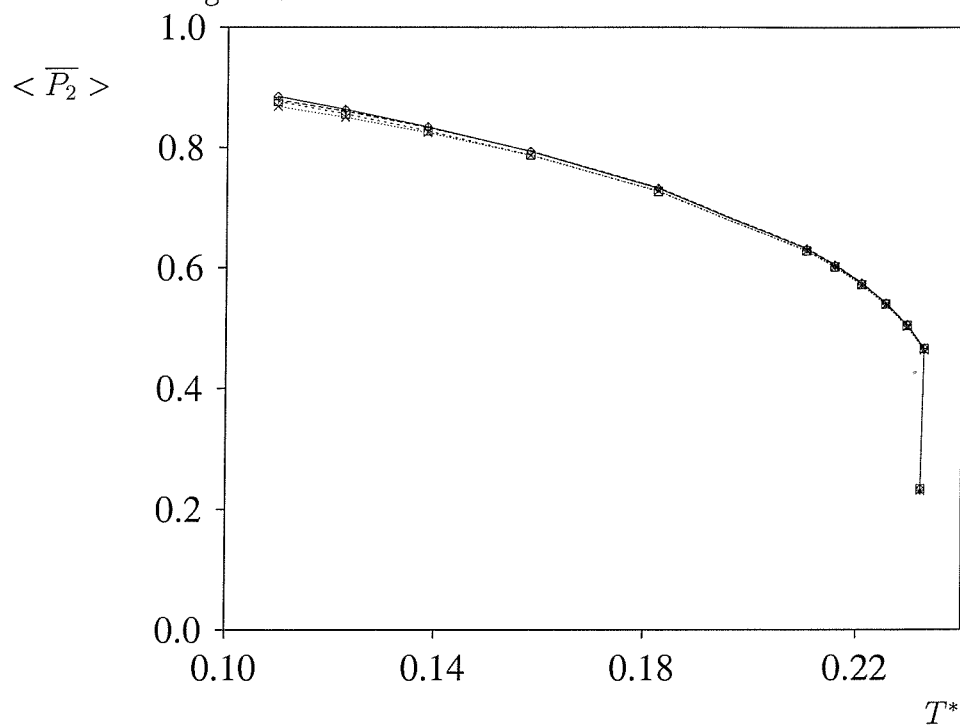
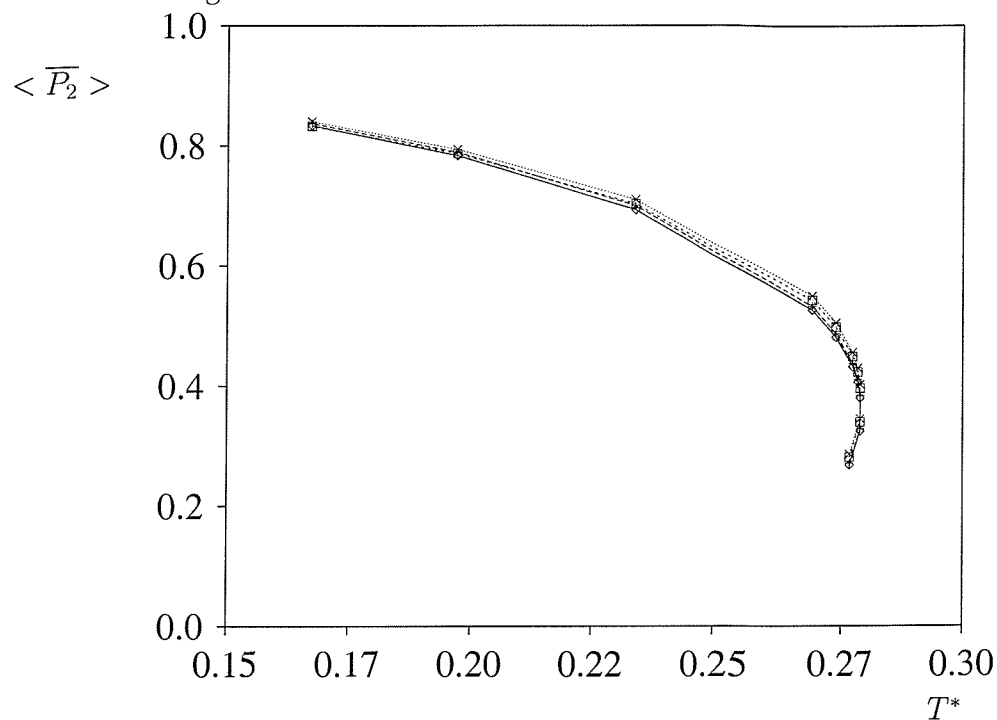


Figure 5.20: Mesogenic group order parameters as a function of scaled temperature for the dendrimer of figure 5.14



#### 5.4.2 Statistical Errors

The likely statistical errors in the various properties calculated in the simulation were obtained by the method already described (see section 5.3), taking a terminal dendrimer of intermediate size as being a typical system. The errors in the simulation averages were found to be as follows. The accuracy with which the  $N - I$  transition is located as a function of the scaled strength parameter was to within 1.5 %, the error in the transitional order parameter was 1.7 %, that in the scaled transition temperature is 0.39 % and that in the transitional entropy change was 4.1 %. Similarly the pre-extant results for the dimers had associated with them errors of 0.76 %, 0.62 %, 0.88 % and 2.6 % in the values of  $X_{NI}^*$ ,  $\langle \overline{P}_2 \rangle^{NI}$ ,  $T_{NI}^*$  and  $\Delta S_{NI}/R$  respectively.

It is clear that in the main the errors in the properties calculated are small. It will be noticed, however, that the statistical error in the entropy change is considerably greater than for the other properties. This clearly deserves some comment. We might tentatively hypothesise that the reason for this is that the statistical sampling of the  $N-I$  entropy difference is somehow poorer than for the other properties, this being due to the way it is calculated (see section 5.2.3) as a difference between two sampled quantities, such that this difference is small in comparison to the order of magnitude of the quantities. That is, whilst the orientational contribution to the entropy difference is essentially a single sampled quantity (the rotational partition function weighted average molecular field energy) since the isotropic orientational energy is zero, the conformational contribution is a difference between the non-weighted (isotropic) and rotational partition function weighted (nematic) averages of the intramolecular potential energies. In this case, we may be calculating a property that is a relatively small difference between the averages of two relatively large quantities—in which case one would expect the sampling to be relatively poor. In addition we might speculate that a significant contribution to the total difference could be coming from a relatively small number of very large contributions to this difference, the larger contributions being progressively more rarely sampled. To see this we might rewrite equation (5.36) as

$$T\Delta S_{NI}^{\text{conf}} = \sum_{i=1}^N U_{\text{int}}^i / N - \sum_{i=1}^N U_{\text{int}}^i Q_{\text{ext}}^i / \sum_{i=1}^N Q_{\text{ext}}^i \quad (5.58)$$

and then manipulate it as follows:

$$\begin{aligned} T\Delta S_{NI}^{\text{conf}} &= \frac{(\sum_i Q_{\text{ext}}^i)(\sum_i U_{\text{int}}^i) - N \sum_i U_{\text{int}}^i Q_{\text{ext}}^i}{N \sum_i Q_{\text{ext}}^i} \\ &= \sum_i U_{\text{int}}^i \left[ \left( \sum_i Q_{\text{ext}}^i \right) - N Q_{\text{ext}}^i \right] / N \sum_i Q_{\text{ext}}^i \\ &= \left\{ \sum_i U_{\text{int}}^i [ \langle Q_{\text{ext}} \rangle - Q_{\text{ext}}^i ] \right\} / \sum_i Q_{\text{ext}}^i. \end{aligned} \quad (5.59)$$

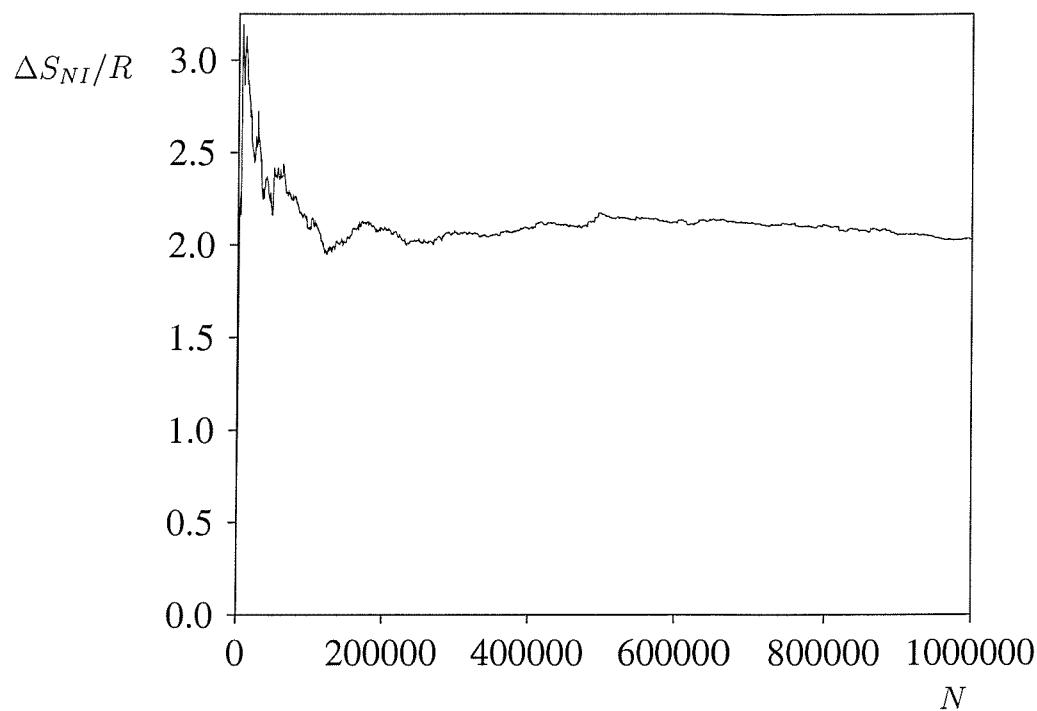
Thus we see that the conformational entropy difference is related to the sum of the differences between the mean rotational partition function and the rotational partition

function for the individual conformers, since the denominator is a constant. Obviously this is something of an oversimplification since the differences are also scaled by the intramolecular energies of the same conformers, and so the argument only holds if there is no simple systematic cancellation of effects. Even so, we do not know if rarely sampled, large contributions coming from very large partition functions are sufficiently large to be significant in relation to their frequency of occurrence to make them a significant contribution. It is in principle a subtle balance of effects.

The final clarification would be to calculate the simulation estimate of the total entropy difference as a function of the number of conformers to look at how quickly it converges so that we can compare its rate of convergence to that of other properties. This we have done (see figure 5.21) and it is clear that the total entropy change converges much more slowly than the order parameter (see figures 5.11, 5.12), which may at first seem surprising, since in molecular field theories the entropy change is normally thought of as being quadratically related to the order parameter. However, it is the orientational entropy difference that is related to the order parameter—not the conformational contribution. When we look at the total entropy change in relation to the convergence of its component contributions (see figure 5.22), the source of the effect becomes clear. The orientational entropy change converges very quickly in a manner that mirrors the order parameter, whereas the conformational contribution is quite poor, indeed we would say that it has not converged; it is this contribution, superimposed on the orientational part, that produces the poor convergence of the total. This confirms that it is primarily the sampling of the conformational entropy difference that is the root cause of the relatively large statistical error in the calculated transitional entropy change.

Indeed, the foregoing analysis is supported by the fact that for the dendrimers the statistical error in the conformational contribution to the total entropy change, is found to be much greater (17 %) than the orientational contribution (3.1 %), so even though the former is in general found to be a small contribution to the total (see later) it is subject to rather large statistical noise, thus significantly increasing the error in

Figure 5.21: Simulation estimate of the scaled  $N - I$  entropy difference as a function of the number of attempted moves



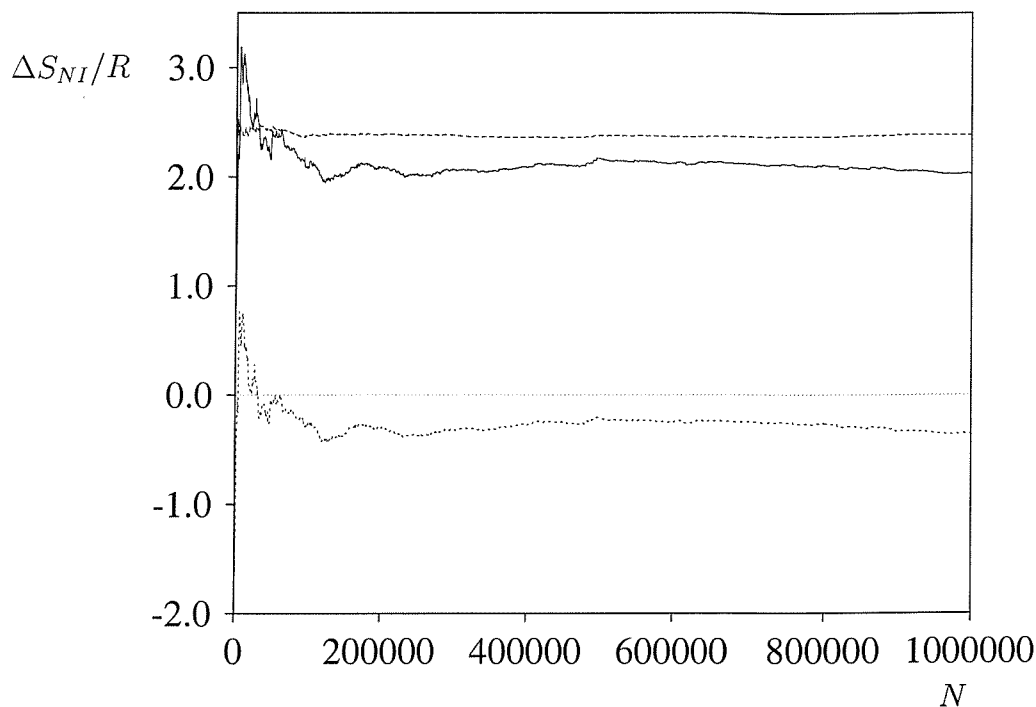
the total. The results for the dimers were similar with the error in the orientational contribution at 1.1 % and that in the conformational contribution at 36 %.

### 5.4.3 The Transitional Properties

We turn now to the predictions obtained from the production runs for the transitional properties of the multipodes and, for comparison, to results for liquid crystal dimers obtained using the same methodology.

First, we consider the variation of the scaled transition temperature,  $T_{NI}^*$ , the entropy change at the transition,  $\Delta S_{NI}/R$ , and the order parameter at the transition,  $\langle \overline{P}_2 \rangle^{NI}$ , for the analogous dimers as a function of the number of units,  $n$ , in the flexible spacer (including the linkage group) joining the two mesogenic groups. These data were generated using the same methodology and essentially the same model as

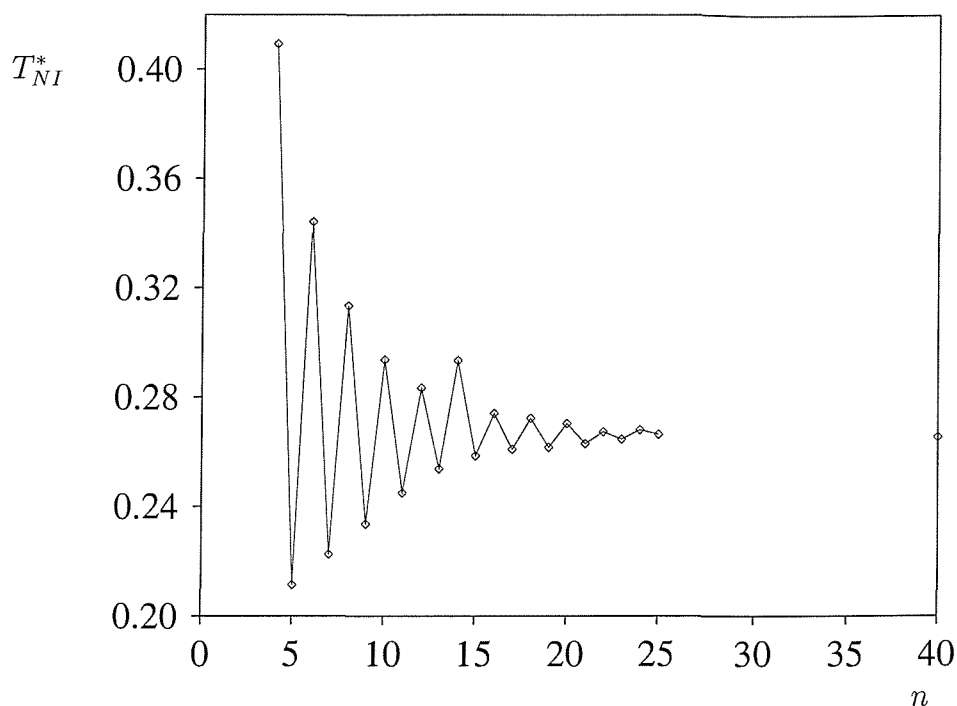
Figure 5.22: Scaled  $N - I$  entropy difference (—) and its orientational (--) and conformational (-.) contributions as a function of the number of attempted moves



the one we have employed so as to facilitate comparison with systems that, unlike the multipodes themselves, do in fact exhibit nematic phases.

Figure 5.23 shows the variation of  $T_{NI}^*$  with  $n$  for the ether-linked dimers. We note the marked odd-even effect, becoming rapidly attenuated as the spacer length increases, the odd members having lower values than the adjacent even members of the series. The values for the even members decrease across the series, whereas those for odd dimers increase, both sets eventually converging to a constant long chain limit approximately equal to the Maier-Saupe value, the even dimers approaching the limit from above, the odd ones from below. In the limit of short spacer length and complete correlation of the mutual orientations of the mesogens we would expect  $T_{NI}^*$  to take on a value equal to twice that of a system of Maier-Saupe rods, namely, 0.4406. We then expect to see a decrease towards the Maier-Saupe value in the limit of long spacer length. This is indeed what we observe for the even dimers. For the odd dimers there must

Figure 5.23: Scaled  $N - I$  transition temperature of ether-linked dimers as a function of spacer length



be some additional effect. The strong influence of the parity of the spacer is usually rationalised in the following way. Even dimers have a shape that on average is much more linear than odd dimers. This is because for the even dimers there is a much larger proportion of linear conformers with sufficiently low intramolecular energy to be thermally accessible than for the odd ones. (The only way an odd dimer can have a linear conformer within the RIS model is to have at least two gauche links.) That is, for odd dimers the vast majority of the conformers (in the RIS model) that are (in practise) available are bent (some 90 %), whereas only half the conformers of even dimers are bent. This depresses the scaled transition temperature of the odd dimers with respect to even ones of similar spacer length, giving rise to the characteristic odd-even alternation of flexible dimers. In the limit that the spacer is sufficiently long that all correlations between the orientations of the mesogenic groups are lost, the value of  $T_{NI}^*$  then becomes independent of the parity or length of the spacer and takes on approximately the Maier-Saupe value of 0.2203.

Another consideration in molecular field calculations as regards  $N - I$  transition temperatures is the volume of the system. It is possible to take into account the effect of the volume of the system on the transition temperature and here it is more pressing to do so because of the need to compare between systems with different molecular volumes. The manner in which this may be achieved has been given by Luckhurst [6, 22] and is consistent with the analysis of Cotter [23] who showed that for statistical mechanical consistency the volume dependence in a molecular field theory based (as it will be) on the canonical ensemble must be inverse linear. We write the molecular field strength parameter in this case as

$$X = n \epsilon \phi \nu^{-1} \bar{P}_2, \quad (5.60)$$

where  $n$  is the number of mesogenic groups,  $\nu$  is the volume of one mesogenic group and  $\phi$  is the volume fraction of one mesogenic group. This clearly simplifies to

$$X = \frac{n \epsilon \bar{P}_2}{V_{\text{mol}}}, \quad (5.61)$$

where  $V_{\text{mol}}$  is the total molecular volume. We take out a factor of  $n\nu$  from the denominator

$$X = \frac{n \epsilon \bar{P}_2}{n\nu(V_{\text{mol}}/n\nu)} = \frac{\epsilon \bar{P}_2}{\nu(V_{\text{mol}}/n\nu)} \quad (5.62)$$

so that

$$X^* = \frac{X}{k_B T} = \frac{(\epsilon/k_B T) \bar{P}_2}{\nu(V_{\text{mol}}/n\nu)}, \quad (5.63)$$

where  $\{\epsilon/k_B T\}^{-1} = T^{*'} is the scaled temperature. We rearrange this for the scaled temperature and put  $T^{*'} = T_{NI}^{*}'$  to obtain the scaled transition temperature as$

$$T_{NI}^{*}' = \frac{\bar{P}_2^{NI}/X_{NI}^*}{\nu(V_{\text{mol}}/n\nu)} = \frac{T_{NI}^*}{\nu(V_{\text{mol}}/n\nu)}, \quad (5.64)$$

where  $T_{NI}^* = \bar{P}_2^{NI}/X_{NI}^*$  is the scaled transition temperature without allowing for volume effects. The purpose of scaling the molecular volume as we have done is so that we may then rescale the new scaled transition temperature with the volume of the



mesogenic group so that the quantity we are calculating to compare to the real experimental values remain dimensionless for convenience. That is, the quantity we actually calculate is

$$T_{NI}^* \nu = \frac{T_{NI}^*}{V_{\text{mol}}/n\nu}. \quad (5.65)$$

For instance, in the case of the dimers we have the total volume of the molecule as

$$V_{\text{mol}} = n\nu + n_{\text{CH}_2}V_{\text{CH}_2} + 2V_{\text{O}} \quad (5.66)$$

and we factor out and scale with  $n\nu$  as

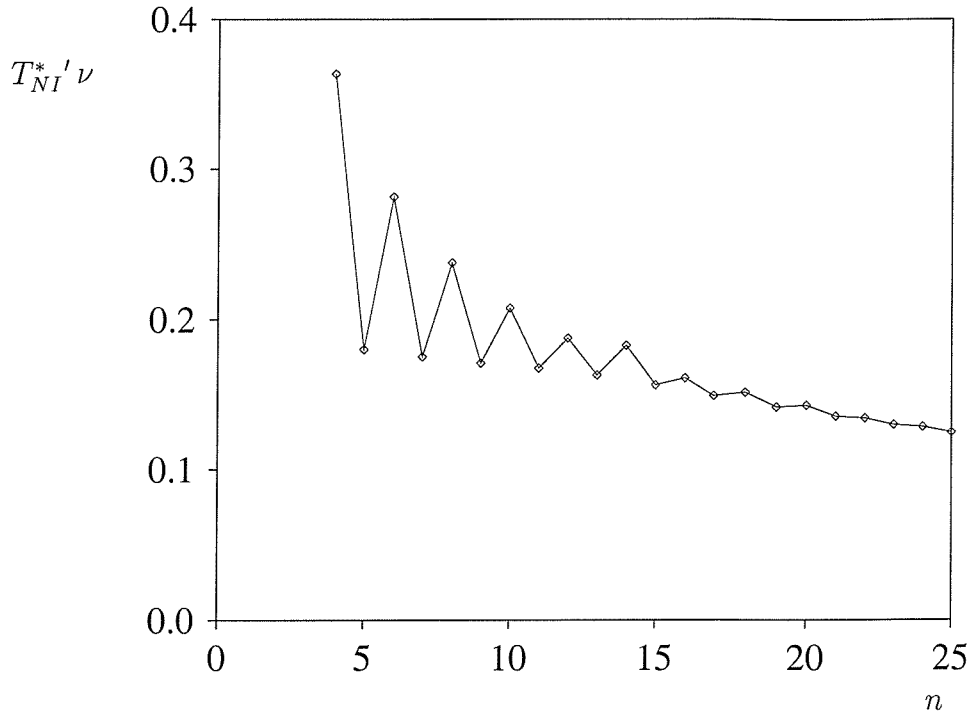
$$V_{\text{mol}}/n\nu = 1 + \frac{n_{\text{CH}_2}}{2\nu}V_{\text{CH}_2} + \frac{V_{\text{O}}}{\nu}, \quad (5.67)$$

leaving the denominator of (5.64), when itself scaled by the volume  $\nu$  of the mesogenic group as in (5.65), dimensionless. An analogous procedure was followed for the other molecule types in this study. The results of this process as applied to the ether-linked dimers are shown in figure 5.24 and we note the remarkable similarity to the qualitative form of the corresponding experimental results (see figure 5.25).

Figures 5.26 and 5.27 show the variation of  $\Delta S_{NI}/R$  and  $\langle \overline{P}_2 \rangle^{NI}$  with  $n$  respectively. Again we see a clear alternation with parity, with the even members having higher values than their adjacent odd member homologues. In the long spacer limit the values of the odd and even members begin to converge to a constant value, which in the case of  $\Delta S_{NI}/R$  would appear to be about twice the Maier-Saupe value of 0.417, namely about 0.8, and which in the case of  $\langle \overline{P}_2 \rangle^{NI}$  would appear to be approximately the Maier-Saupe value itself, namely about 0.4.

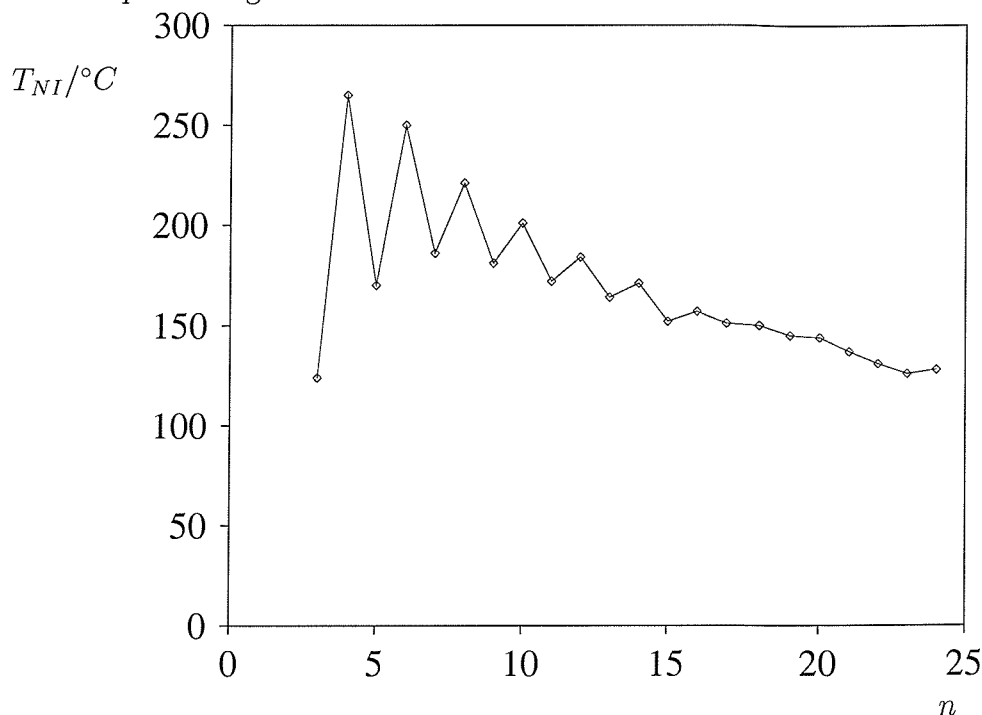
It is important to notice that, contrary to the intuitive assumption of many, the order parameter at the transition does not necessarily reflect the value of  $T_{NI}^*$ . In other words, one might have assumed that dimers with a relatively high  $T_{NI}^*$  also have a relatively high  $\langle \overline{P}_2 \rangle^{NI}$  and that these two transitional properties may be usefully thought of as directly related in some simple physical way. If this were the case, dimers that are on average more anisotropic would have a higher  $T_{NI}^*$  and this would be assumed

Figure 5.24: Scaled  $N - I$  transition temperature of ether-linked dimers as a function of spacer length, taking into account the effect of molecular volume



to lead physically by proxy in some way to a higher value of  $\langle \overline{P}_2 \rangle^{NI}$ . Indeed, this would seem to fit in well with the basic observation that  $T_{NI}^*$  and  $\langle \overline{P}_2 \rangle^{NI}$  appear to alternate in sympathy with each other, with the even members taking the higher values. However, if the presence of bent conformers depresses  $T_{NI}^*$  with respect to its upper limit (which occurs when the mesogenic groups are totally correlated at short chain lengths) of twice the Maier-Saupe value (thus corresponding to a rigid, linear molecule) then we would be lead to expect this to be reflected in order parameters of transition lower than the corresponding value in the same physical limit (ie, 0.429). This is clearly not necessarily the case, however, as evidenced by the even dimers which have a considerably higher value of  $\langle \overline{P}_2 \rangle^{NI}$  than this for spacer lengths significantly different from both the extremes (which correspond to the limits of completely correlated and completely uncorrelated mesogenic groups). To understand this intriguing phenomenon of transitional order parameters in excess of the Maier-Saupe value in the case of the even-spacer dimers, we consider the isotropic phase and what happens when on cooling

Figure 5.25: Experimental  $N - I$  transition temperature of ether-linked dimers as a function of spacer length



it undergoes a transition to the nematic phase. That is, there is a large proportion of bent conformers in the isotropic phase, which nevertheless have energetically low-lying linear conformations available, so that when the transition occurs to the nematic phase, linear conformers are considerably more favoured by the nematic environment and the energetic cost of converting bent conformers to linear ones is less than the energy reduction by virtue of being in the ordered phase. Thus the probability of occurrence of linear conformers rises and that of bent ones falls and so the preponderance of linear conformers increases to a higher value than it would otherwise be expected to be if there were no change in the conformational distribution. The phase can thus be considered to be at an effective temperature much less than its actual temperature—or alternatively that it has an effective transition temperature much higher than the actual temperature at which the order parameter increases discontinuously from zero. Thus the nematic phase at the transition temperature is behaving like a nematic at a much lower reduced temperature (ie, much further into the nematic on the phase

Figure 5.26: Scaled  $N - I$  entropy difference of ether-linked dimers ( $\diamond$ ) and its orientational (+) and conformational ( $\square$ ) contributions as a function of spacer length

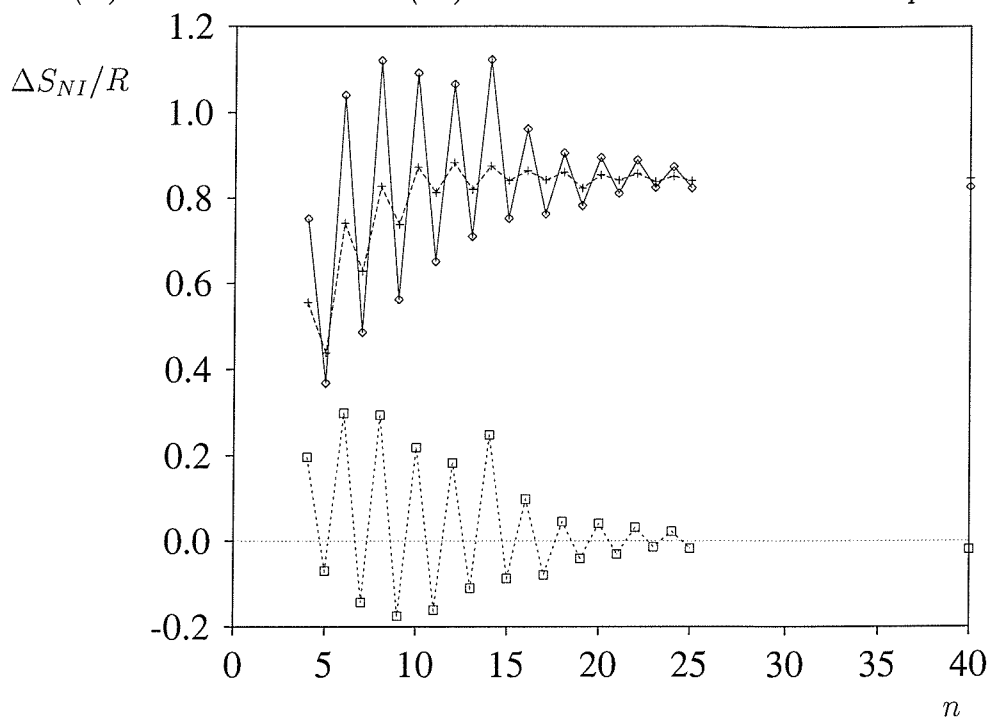
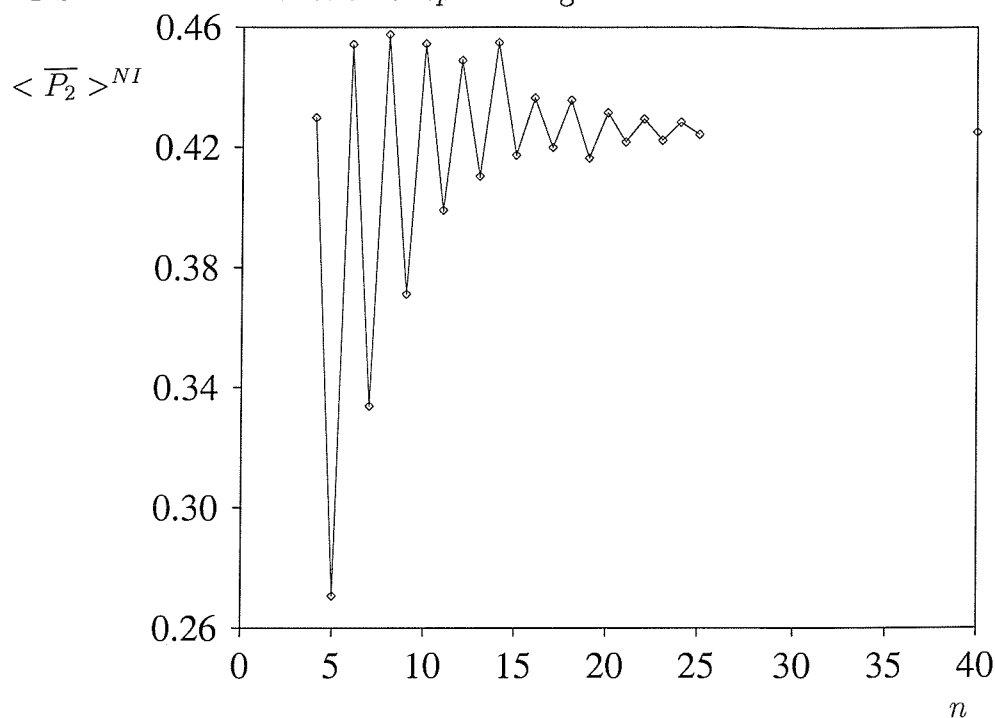


diagram). Hence the order parameter reflects this and is elevated above the Maier-Saupe value. In the case of the odd dimers this effect does not operate because the energy required to straighten out the odd dimers is so high that the proportion of conformers with a high anisotropy is essentially unchanged at the phase transition. In consequence there is no substantial change in the conformational distribution in going from the isotropic to the nematic phase. The foregoing analysis of the unusually high order parameters of the even dimers in contrast to the odd ones is based upon energetic arguments alone and is strictly speaking incomplete and non-rigorous, since it ignores entropic effects. The conformational distribution in the ordered phase compared to the isotropic phase is also determined by the relative entropies of the two phases, not only the conformational entropies, but also the orientational ones, since the orientational entropy is also affected by the conformational distribution (ie, if the conformational distribution changes, so does the orientational entropy).

Figure 5.27: Orientational order parameter of the mesogenic groups of dimers at the  $N - I$  transition as a function of spacer length



Similar arguments can be constructed to rationalise the variation of  $\Delta S_{NI}/R$  with spacer length. The entropy change at the transition is expected to correlate well with the order parameter, since the latter is a measure of the orientational order just before entering the isotropic phase. The higher the order parameter, the higher the associated entropy change is expected to be. The correlation will not be exact, since strictly the correlation will be with the change in orientational entropy rather than the total entropy change; however, the orientational contribution is, for the most part, predominant. In the limit of long spacers we expect  $\Delta S_{NI}/R$  to take on twice the Maier-Saupe value (since there are two mesogenic groups which act independently), namely 0.834, which is indeed approximately what we find. If the entropy change does indeed tally with the order parameter then in the absence of the conformational-orientational synergy discussed earlier we would have expected an odd-even effect, attenuated, but perhaps not as rapidly as that in  $T_{NI}^*$ , with the overall trend being one of rising to the long chain limit from below. However, this synergistic effect of

bent conformers being converted to linear ones in the nematic phase causes many of the even dimers (ie, ones other than those near the spacer length extremes) to have orientational order parameters and hence, entropies, higher than that found at the long spacer limit where the mesogenic groups are uncorrelated. Thus the higher than expected order parameters ultimately lead to higher than expected overall entropies of transition. In addition, one might have thought that we could obtain support for the concept of the operation or otherwise of this synergistic effect in different systems by looking to the change in conformational entropy as a proxy, since the conformational entropy in each phase is related to its conformational distribution. Thus we find that the magnitude of the conformational contribution is somewhat larger relative to the dominant orientational contribution for the even dimers than the odd ones. However, the conformational entropy change for the odd ones is still not insignificant, and we surmise that the straightening out of bent conformers is simply a contribution to this entropy change for some systems, and that the issue is somewhat more subtle than equating significant changes in conformational entropy with significant conformational-orientational synergy in the system. The conformational entropy change (on going from the nematic to the isotropic phase) in the case of the even dimers is positive, suggesting that the system becomes conformationally more disordered on passing into the isotropic phase, which is what we might intuitively expect. However, we note that in the case of the odd dimers this entropy change is not just smaller in magnitude, but negative, revealing that the system becomes more conformationally ordered on passing into the isotropic phase, which would seem counter-intuitive. It may be that for odd dimers, for whom the vast majority of available conformers are non-linear, the influence of orientational order in the nematic phase on the conformational distribution actually drives it to be more diverse and access a greater range of states (an odd dimer in the trans conformation requires at least two gauche links to become linear) to attempt to conform with the orientationally ordered environment and so the system has increased order in orientational degrees of freedom at the expense of that in the conformational degrees of freedom in the nematic compared to the isotropic phase. In any case, the

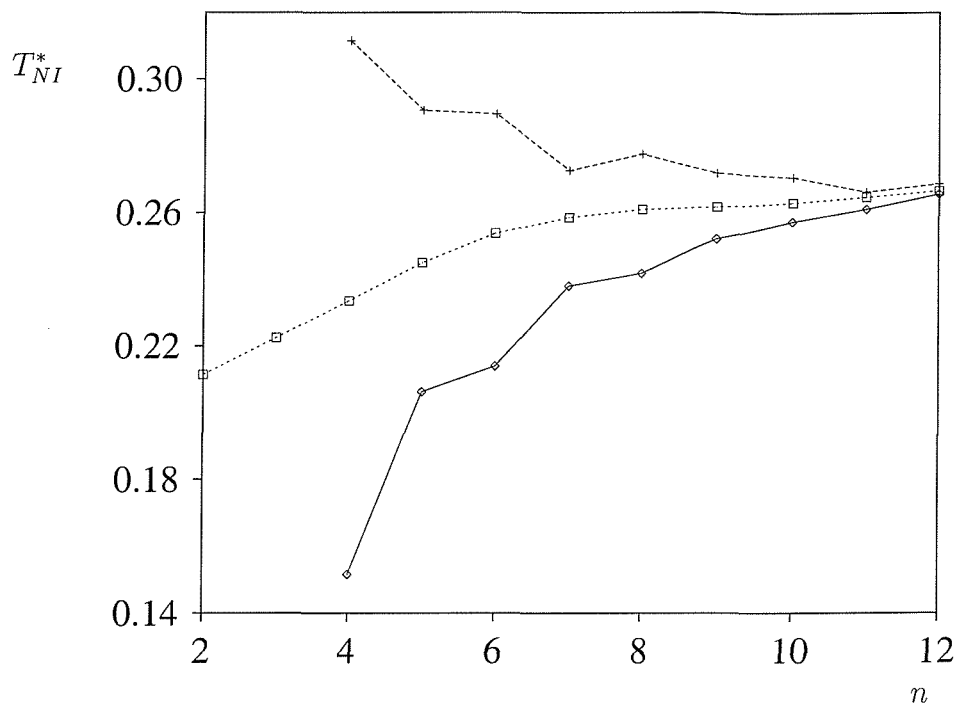
problem of finding simple ways of understanding the changes in the conformational distribution and relating these to the conformational entropy change may turn out to be far from straightforward, as we shall see later with regard to the multipodes.

We now turn our attention to the multipodes (zeroth generation dendrimers, G-0OCB) with terminal and lateral attachments and consider how their transitional properties vary with the lengths of the flexible chains. In the case of dimers the term “chain length” is clearly to be interpreted as the number of links in the flexible spacer connecting the two mesogenic groups. In the case of the multipodes we take the defining chain length,  $n$ , to be the number of units in the chain (including the linkage group) connecting the mesogenic group to the central quaternary carbon atom. The question then arises as to how comparison should be made between dimers and multipodes of various sizes. It would seem clear that the dimer most closely related to a given multipode would be the one whose spacer contained one more than twice the number of units in the dendrimer’s characteristic chain length. The multipodes, then, are envisaged as two dimers superimposed at the mid-point of the spacer. As a result, the dimer analogue of any given dendrimer will always have an odd spacer length.

Figure 5.28 shows the result of plotting  $T_{NI}^*$  against  $n$  (now the dendrimer chain length, not the dimer spacer length) for the terminal and lateral multipodes, with the analogous dimer results plotted on the same graph for sake of comparison.

As can be seen the dimer results when compared in this way no longer appear to exhibit an odd-even effect—an inevitable consequence of the fact that this comparison selects only the odd membered dimers for inclusion. The value of  $T_{NI}^*$  for the dimers rises with increasing chain length from a very small value to a limit close to that of the Maier-Saupe value of 0.2203. This suggests that for short spacers the molecule has a high biaxiality, but that as the spacer length grows, the additional flexibility in conjunction with the continuous torsional potentials, allows the mesogenic groups to mutually arrange themselves in a manner more in keeping with the liquid crystalline environment, and so the molecule becomes less biaxial and more anisotropic. In the

Figure 5.28: Scaled  $N - I$  transition temperatures of ether-linked terminal ( $\diamond$ ) and lateral (+) dendrimers and dimers ( $\square$ ) as a function of chain length



long chain limit we expect all orientational correlations between the mesogenic groups to be lost and so to obtain the Maier-Saupe result, as indeed we have found.

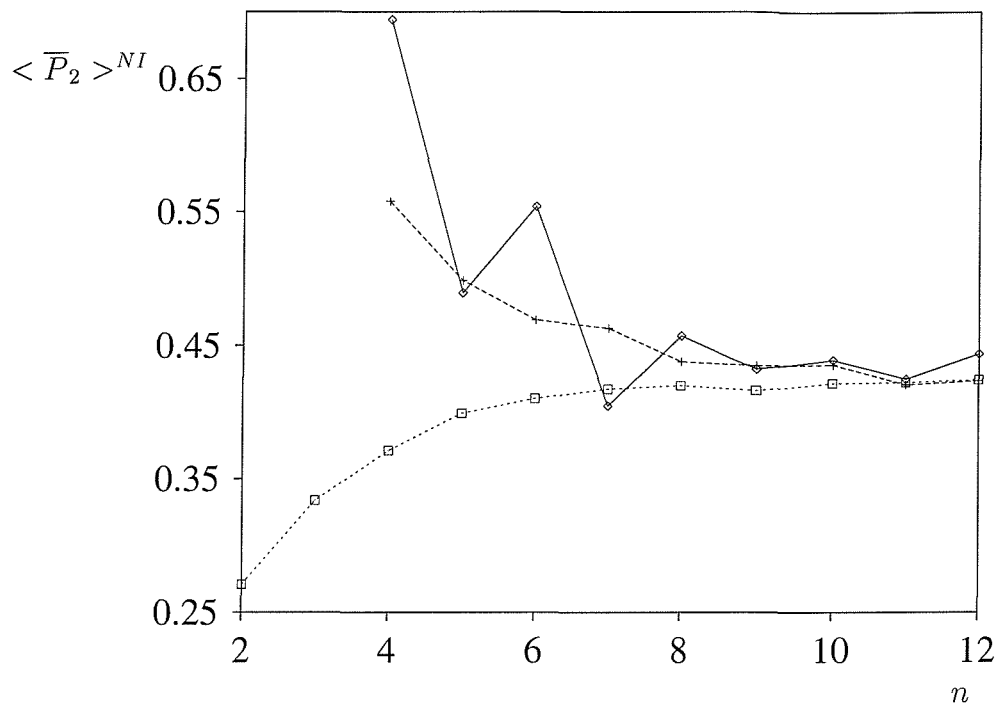
In the case of the terminal multipodes, there is clear evidence of some form of odd-even effect—even though the dimer analogues of these molecules all have odd spacers. The effect is rapidly attenuated along the series. In this case it is the odd members which have values higher than a curve fitted through the points, although the distinction between odd and even is in this case somewhat arbitrary, depending as it does on the definition of the chain length. The  $T_{NI}^*$  values rise from below the Maier-Saupe limit at the short chain extreme to a value close to this limit at the long chain extreme. We surmise that as the chains become longer the additional flexibility allows the mesogenic groups to align into more anisotropic mutual orientations, as a result of the mesogenic group orientations becoming less correlated, until in the limit, the system is Maier-Saupe-like. The lateral multipodes, by contrast, exhibit in many ways completely the



opposite behaviour—almost the mirror image of the terminal case. There is again an odd-even effect in  $T_{NI}^*$ , but here it is the even members that have higher than expected values. There is also an attenuation of the effect of similar rapidity, superimposed on an overall trend going towards the same, Maier-Saupe, limit—except that here the trend is a falling one, decreasing from values considerably higher than the Maier-Saupe value. In this case we have to speculate that the lateral multipodes with short chains are, on average inherently anisotropic, that is, that with very few flexible links they are constrained geometrically, to a semi-rigid, anisotropic shape. In the case of the dimers and terminal multipodes it was this effect that conferred an average geometry inherently low in anisometry, but that with increasing number of flexible links, the mesogenic groups became less correlated and the molecule less like a semi-rigid constrained low-anisometry object and able to adopt more anisotropic shapes in the presence of the orienting molecular field. Here we have the opposite situation; the short chain molecules are on average quite anisometric, but as we pass to higher chain lengths the orientational correlation of the mesogenic groups is gradually lost, so that the Maier-Saupe limit is approached from above rather than below. We also make the observation that, the dimers and the dendrimers reach the same long chain limit, as expected, but that for dendrimers the limit is reached at greater chain lengths. In addition, we note that the terminal dendrimers have lower values than the comparative dimers, so that even though both series reach the same limit from below, the dendrimer curve appears shifted to the right by comparison with the dimer curve. This implies that not only are the terminal dendrimers inherently less anisotropic than the lateral ones at chain lengths where the mesogens are correlated—they are also somewhat less anisotropic than the related dimers. This is taken to be due to the more tetrahedral shape of the terminal dendrimers in the short chain limit.

We now turn our attention to the variation of the transitional values of the second rank orientational order parameter with chain length, the results for which are shown in figure 5.29. We see, for the short chain dimers, a rapid increase with increasing chain length. The curves then become shallower fairly rapidly and finally reach a

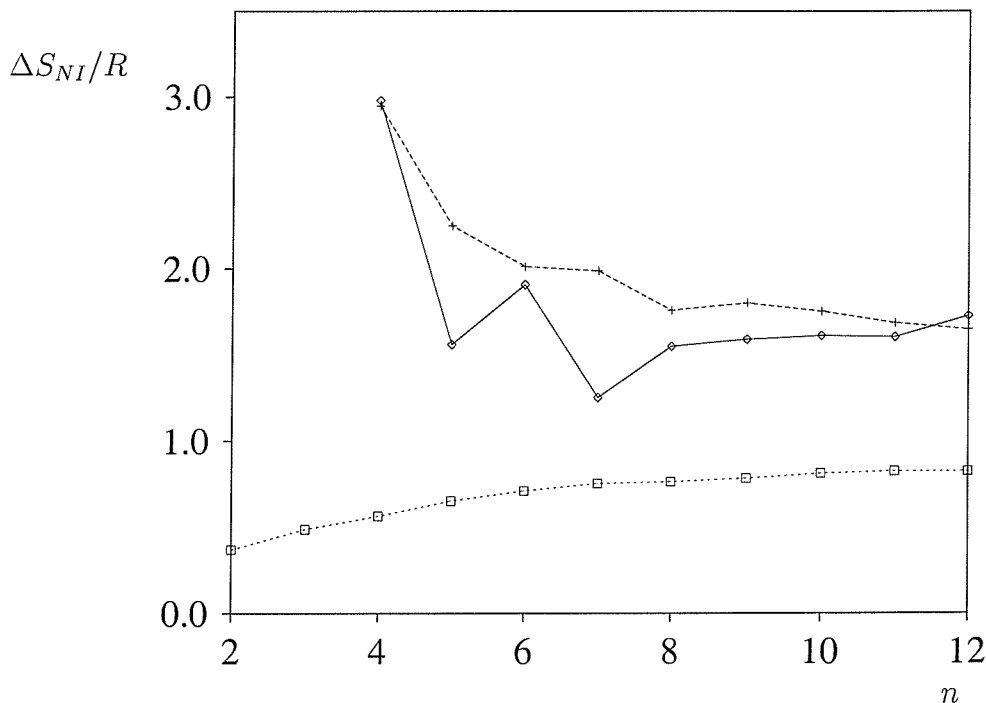
Figure 5.29:  $N - I$  transitional value of the mesogenic group orientational order parameters of ether-linked terminal ( $\diamond$ ) and lateral (+) dendrimers and dimers ( $\square$ ) as a function of chain length



plateau; the long chain limit would appear to be approximately the Maier-Saupe value of 0.429. For the terminal dendrimers we see a clear odd-even effect superimposed on a general trend that falls rapidly from a very high order parameter to about the Maier-Saupe value in the long chain limit, with the odd-even effect becoming rapidly attenuated as we pass along the series. The lateral dendrimers, on the other hand, do not exhibit an unambiguous odd-even effect (although there is just the hint of some kind of alternation with parity), but simply fall—again to approximately the Maier-Saupe value in the limit. This limit of  $\langle \overline{P}_2 \rangle^{NI}$  for the various molecule types results from the fact that in the limit of long chains there is sufficient overall molecular flexibility and freedom through the continuous nature of the torsional potentials that the mesogenic group orientations are completely uncorrelated. However, there is an additional feature, namely that the value of  $\langle \overline{P}_2 \rangle^{NI}$  for the multipodes starts at such a high value—higher than the Maier-Saupe value—at short chain lengths, and the Maier-Saupe limit

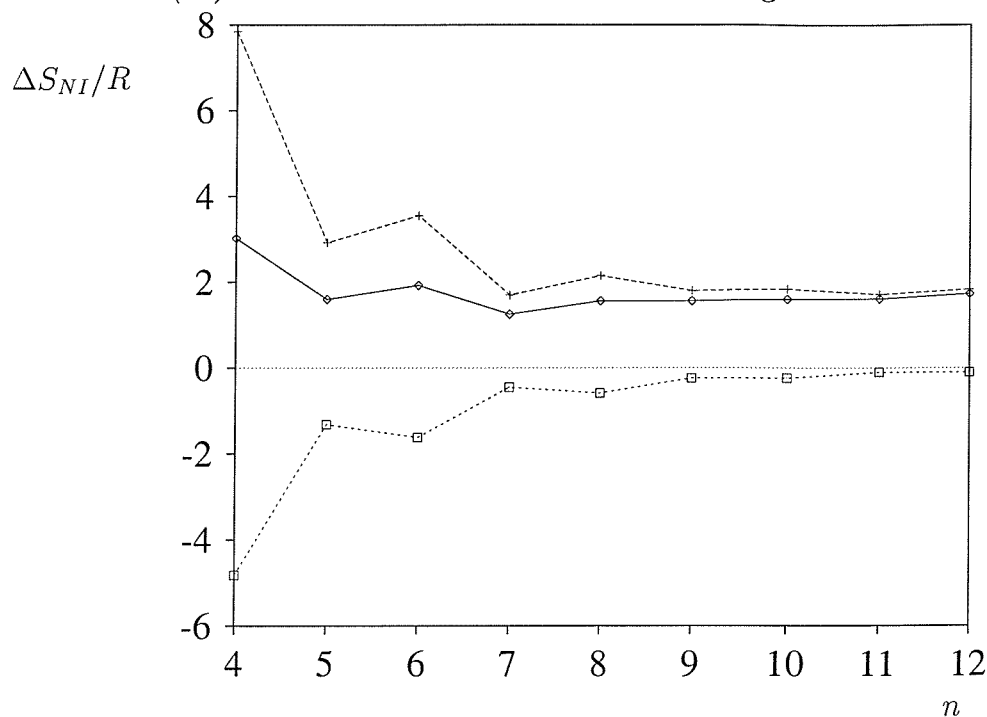
is reached from above for both “odd” and “even” multipodes. We might speculate that, in a manner somewhat analogous to the similar phenomenon seen in even spacer dimers, there is a significant proportion of anisotropic conformers that are low in energy. When the transition occurs to the nematic phase, however, a significant proportion of the conformers may then become converted to ones with a higher anisotropy, since this is now favoured by the orienting environment and outweighs the small energetic cost of undergoing the conversion. This confers on the nematic phase an effective temperature significantly less than the phase transition temperature, elevating the order parameter above the normal upper limit.

Figure 5.30: Scaled  $N - I$  transitional entropy change of ether-linked terminal ( $\diamond$ ) and lateral (+) dendrimers and dimers ( $\square$ ) as a function of chain length



We now turn our attention to the entropy change at the  $N - I$  transition (see figure 5.30). In the case of the (odd) dimers we see a curve rising from a very small value and reaching a plateau at about twice the Maier-Saupe value of 0.417, namely, ca. 0.8. In the case of the terminal multipodes, we see a clear odd-even effect su-

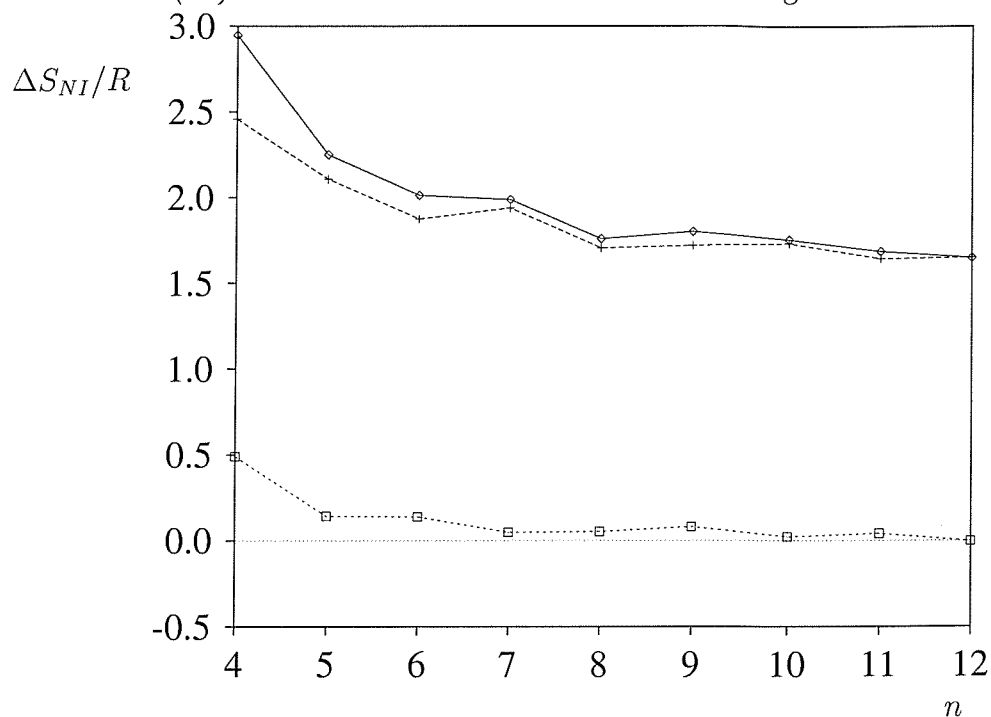
Figure 5.31: Scaled  $N - I$  transitional entropy change ( $\diamond$ ) and its orientational ( $+$ ) and conformational ( $\square$ ) contributions as a function of chain length for terminal dendrimers



perimposed on a falling trend which starts at a very high value (ca. eight times the Maier-Saupe value), passes through a minimum of ca. 1.3 at a chain length of seven and finally levels off at a limit for long chains of about twice that for dimers, that is, four times the Maier-Saupe limit or about 1.6. Here the even parity members take on the high values and the odd-even effect is rapidly attenuated. The lateral multipodes also show a falling trend, superimposed on a much more muted odd-even effect, from a similar very high value down to approximately the same limit of about four times the Maier-Saupe value.

The limits attained by the dimers and multipodes at long chain lengths are consistent with the increase in flexibility as the chain length is increased and the resulting loss of orientational correlations of the mesogenic groups. In the limit of complete decoupling we expect the value of  $\Delta S/R$  to be twice the Maier-Saupe value for the dimer series and four times the Maier-Saupe value for the dendrimers. This is in fact what we observe

Figure 5.32: Scaled  $N - I$  transitional entropy change ( $\diamond$ ) and its orientational ( $+$ ) and conformational ( $\square$ ) contributions as a function of chain length for lateral dendrimers



at the long chain extreme of the range studied. The general trends in the values can be explained on the basis that the transitional entropy change essentially reflects the order parameter at the transition. This can be understood intuitively in the sense that the transitional order parameter is obviously a measure of (orientational) order in the system just before it undergoes transition to the isotropic phase, where it takes on a fixed value. Thus, the higher the orientational order at the transition, the higher the associated entropy change is expected to be when the system becomes isotropic. We should note, however, that the associated entropy change is strictly the orientational contribution to the total. More precisely, the orientational entropy change is quadratic in the order parameter. Nevertheless, the orientational entropy change is the dominant contribution to the total and so to a first approximation we would expect a reasonable correlation, and this is indeed what we find.

So, given that the overall trend in the dendrimer entropy changes is from a very high

value twice that expected in the limit that the system is Maier-Saupe-like decreasing down to that limit, it seems logical to rationalise these results in the following way. The higher-than-limiting values of  $\Delta S/R$  of the multipodes are taken to be due to the synergy between the conformational distribution and orientational ordering (which we invoked to explain the similarly elevated transitional order parameters) and the decline of the values to the long chain limit we take to be a decorrelation effect.

In addition to these general trends there is an intriguing comparison to be made between the lateral and terminal multipodes with regard to the entropies of transition and their contributions. The lateral multipodes, for the most part, have the higher entropies of transition, especially for the odd members. This stems from the fact that the conformational contribution to the entropy change is positive, whereas for the terminal ones it is negative. Indeed, the dominant, orientational contribution to the total in the case of the lateral dendrimers is, for the most part, somewhat less than for the terminal dendrimers, however, the terminal dendrimers have a conformational entropy considerably larger in magnitude than the lateral ones, and also negative. Thus in the terminal case the overall entropy change is composed of a huge orientational entropy change, mitigated by a somewhat smaller, but still significant conformational entropy change. This is to be contrasted with the lateral case, where we have a negligible conformational contribution and so the total entropy change is composed essentially entirely of the orientational contribution, the size of which is comparable to the total change in the terminal case. This seems to indicate that while the overall values for both sets of dendrimers are roughly the same, the underlying reasons may be somewhat different.

In a similar manner to the case of the dimers we may try to relate the conformational entropy changes to orientational-conformational coupling in the systems. The terminal multipodes have a relatively large, conformational entropy change at the transition, which would seem to correlate with transitional order parameters in excess of the Maier-Saupe limit. The values are, however, opposite in sign to that in the case of the

even dimers, which also exhibit the synergistic coupling. In addition, they are then negative, which is counter-intuitive, since it shows that the nematic is conformationally disordered with respect to the isotropic liquid. Furthermore, the lateral dendrimers also must exploit this synergistic coupling, since their transitional order parameters (and total entropy changes) are of about the same magnitude (or greater) and yet their conformational entropy changes are very small, and positive. To add to the confusion, the odd dimers do not appear to exhibit this coupling and whilst their conformational entropy changes are smaller than the even ones in magnitude, they are larger than for the lateral dendrimers and also negative in sign. It would appear, then, that the conformational-orientational synergy that is the vehicle allowing the transitional order parameter to exceed the Maier-Saupe value does not necessarily impact on the conformational distribution in such a way as to cause a dramatic or even well-defined change in the conformational entropy.

It may be that, due to the enormous complexity of conformational states available to systems with this degree of molecular flexibility, there is no easy understanding of all the effects on the conformational distribution of passing into the orientationally ordered phase and how this relates to conformational-orientational coupling. Indeed we cannot even predict the sign of the change in systems in which we believe this effect to operate, let alone what its magnitude should be in relation to systems for which the effect is believed to be negligible. This is surely in part because it is far from clear what are the analogues of “linear” and “bent” as limiting conformation types in the case of the G-0OCB dendrimers (assuming such concepts could be defined at all) and to what extent the situation changes when we change the kind of dendrimer (eg, in this study, the mode of attachment of the mesogenic group and its size). It may be that the effect of the difference in this case is such that there is plenty of scope, energetically speaking, for conversion of conformers to more anisotropic forms on going into the nematic phase, but that this still occurs in some cases at the expense of decreasing order in conformational degrees of freedom. In addition it may also be that the intuitive notion of entropy as the degree of disorder is just too simplistic here,

bearing in mind the formal definition of entropy

$$S_{\text{conf}} = -k_B \int P\{\phi\} \ln(P\{\phi\}) d\{\phi\} \quad (5.68)$$

in terms of the distribution  $P\{\phi\}$  of states  $\{\phi\}$  and their considerable complexity in this case. These factors may all conspire to preclude any easy explanation or understanding of the effect of conformational-orientational coupling on the conformational distributions and entropy changes.

#### FURTHER VALIDATION

In addition to validating the methodology we may also seek to investigate the efficacy of the sampling of the conformational states by the BOSS Monte Carlo algorithm. This we can do by averaging the cartesian interaction tensor (ie, averaging its corresponding components) referred to the common molecular (BOSS) frame over the conformers sampled. Symmetry dictates that the components when averaged in a local frame should vanish. The extent to which they do so is a measure of how good is the sampling.

We note that this is not supposed to occur as a pragmatic consequence of accidental cancellation—it is a requirement of symmetry. Having said this, BOSS does not sample by sequentially and systematically generating sets of conformers whose interaction tensor components automatically cancel—it is a stochastic algorithm. So in practise cancellations are to that extent ‘accidental’. The extent to which these ‘accidental’ cancellations ultimately reproduce the non-accidental cancellation that must occur by symmetry constraints is a measure of how well BOSS is sampling the conformational space as regards our purposes in performing molecular field calculations.

To test this, we performed a simulation run of  $\sim 700\,000$  conformers on a medium-sized terminal dendrimer and averaged the cartesian interaction tensor components  $x_{ab}^*/X^* \equiv x_{ab}/X$  referred to the local frame over the conformers.



The result was

$$\begin{pmatrix} -0.022835 & -0.001792 & 0.005233 \\ -0.001792 & 0.018848 & 0.001430 \\ 0.005233 & 0.001430 & 0.003986 \end{pmatrix}.$$

Given that the components of the tensors take values of the order of unity it can be seen that they average to zero to within 1 – 2% (at worst), thus indicating that the BOSS sampling of the conformational space is indeed effective for our purposes.

#### AVERAGE SHAPES OF DENDRIMERS AND THEIR TRANSITION TEMPERATURES

It has become common to think of dendrimers as “being spherical” due to the tetrahedral symmetry (or some other cubic symmetry which is spherical at the level of second rank) of the core of the molecule to which the chains are attached. In addition this has been used as an argument that they should not exhibit liquid crystalline phases. The idea here is that having “a” shape of such low anisometry the transition temperature should be very low, and therefore so should the propensity of such materials to show orientationally ordered phases in practise. There then seems to be genuine surprise when it turns out that the materials are in fact mesogenic.

This state of affairs warrants some close scrutiny. The first, and rather obvious, point is that these molecules do not have “a” shape at all, but rather a huge range of shapes, so that clearly the concept being held in mind, if only tacitly, is that of some kind of average structure. Persisting with this concept of the average structure, then, we see from the calculation in the previous section that on average the molecule is indeed spherical (although, we should say, strictly at the second rank level). That is, to arrive at some kind of representation of an average structure we must average some tensorial quantity related to the molecular structure in a common molecular frame. Here, we have averaged the cartesian interaction tensors of the conformers in this fashion. These tensors are of second rank and therefore must average to zero by symmetry, and indeed, this is what we see. There is nothing surprising about this.

However, to focus on the average structure of a flexible molecule for the purpose of assessing its transition temperature (ie, its likelihood of being mesogenic) is misleading. The  $N-I$  transition temperature for some set of molecules (eg, conformers or molecular structures) is not determined by their “shape” (ie, average shape) but by the weighted average of the transition temperatures of the component structures of the set. To illustrate this we have calculated histograms of the  $X_{2m}^*/X^* \equiv X_{2m}/X$  ( $m = 0, 2$ ) for the same simulation run that produced the results for the average interaction tensors in the local frame in the previous section (see figures 5.33, 5.34). The  $X_{2m}$  are the quantities that go into the calculation of the liquid crystalline properties, not the tensor components referred to the local frame. The set of  $X_{2m}$  for each conformer is the equivalent of the  $x_{ab}$  but referred to its own principal frame. The histogram of  $X_{20}$  (which is a basic measure of the anisotropy of the conformers) does not, then, show a distribution centred on zero and rapidly falling off either side. Rather it shows a maximum at some non-zero positive value and a relatively broad, almost gaussian, distribution. It reveals that there is a high proportion of very anisotropic conformers contributing to elevating the transition temperature above that of a spherical rigid particle (ie, zero). It is therefore not at all surprising, then, that dendrimers readily form liquid crystals.

This reinforces the basic concept in statistical mechanics that the correct way to calculate the properties is to regard the fluid as a mixture of structures (conformers in this case) and to calculate the properties of the components. The weighted average of the properties of the components over the corresponding probability distribution then yields the properties of the fluid (mixture). This is in contrast to taking a distribution weighted average of some property reflecting the structure and computing the properties of the average structure. It shows that, contrary to popular wisdom, the shape that a flexible molecule has on average is fundamentally irrelevant in determining its transition temperature and its liquid crystalline behaviour.

Figure 5.33: Histogram of  $X_{20}$  for a medium-sized terminal dendrimer over  $\sim 700\,000$

BOSS-generated conformers

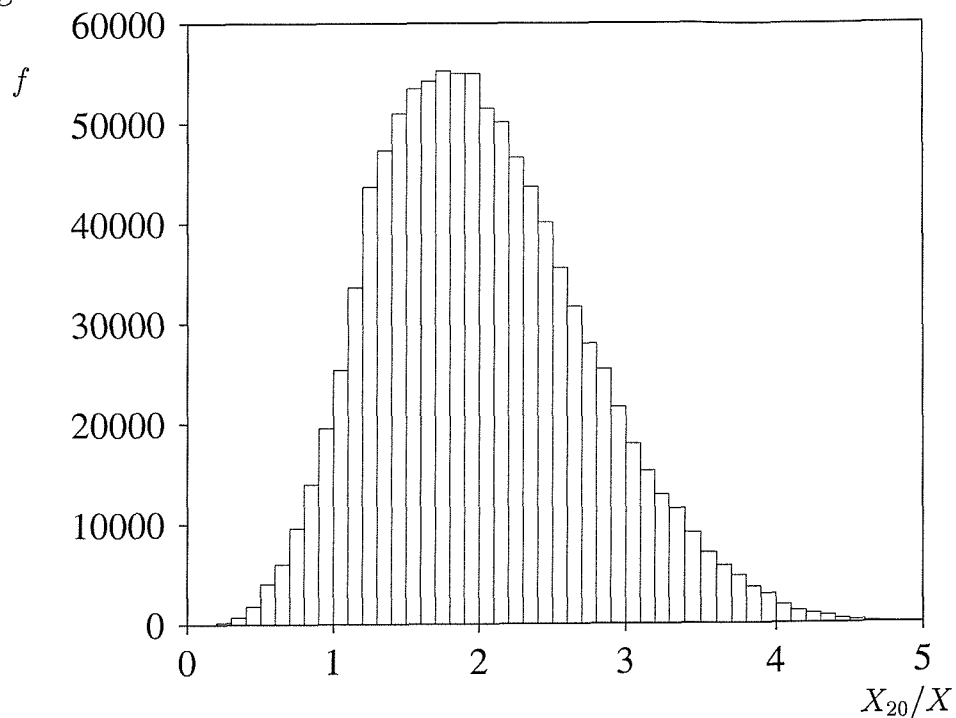
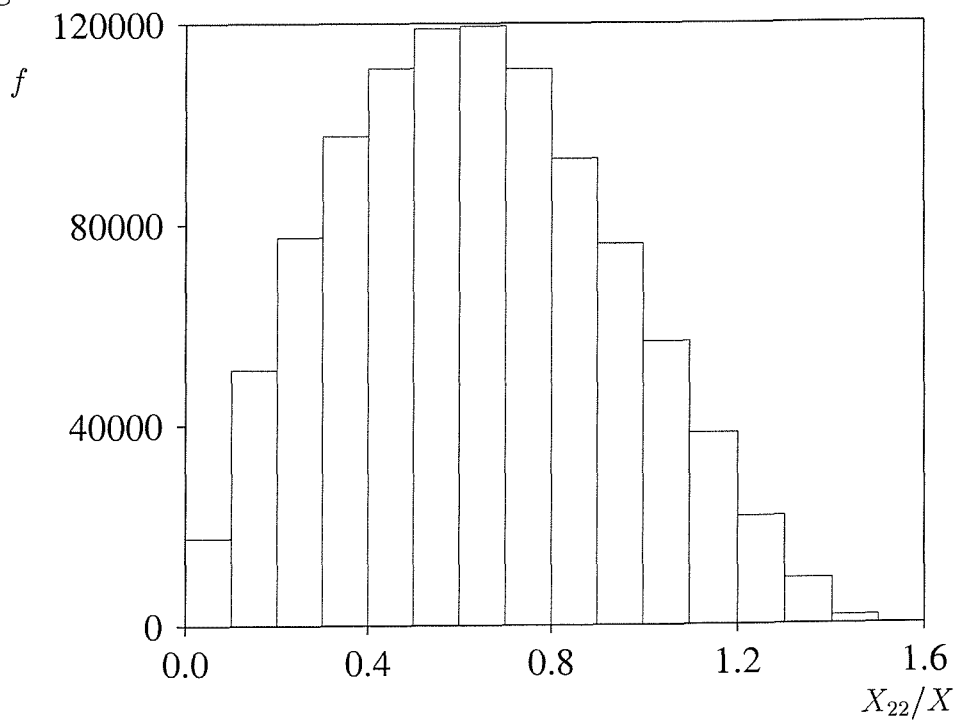


Figure 5.34: Histogram of  $X_{22}$  for a medium-sized terminal dendrimer over  $\sim 700\,000$

BOSS-generated conformers



## References

- [1] R. Eidenschink, F.-H. Kreuzer and W. H. de Jeu, *Liq. Cryst.*, **8**, 879 (1990).
- [2] V. Percec, P. Chu, G. Ungar and J. Zhou, *J. Am. Chem. Soc.*, **117**, 11 441 (1995).
- [3] R. M. Richardson, S. A. Ponomarenko, N. I. Boiko and V. P. Shibaev, *Liq. Cryst.*, **26**, 101 (1999).
- [4] A. Ferrarini, G. R. Luckhurst and P. L. Nordio, *Mol. Phys.*, **85**, 131 (1995).
- [5] S. Marcelja, *J. Chem. Phys.*, **60**, 3599 (1974).
- [6] G. R. Luckhurst in *Recent Advances in Liquid Crystalline Polymers*, Edited by L. L. Chapoy (Elsevier Applied Science, London, 1985), Chapter 7.
- [7] P. J. Flory, *The Statistical Mechanics of Chain Molecules*, Interscience (Wiley, New York, 1969).
- [8] N. Metropolis, A. W. Rosenbluth, M. N. Rosenbluth, A. H. Teller and E. Teller, *J. Chem. Phys.*, **21**, 1087 (1953).
- [9] J. W. Emsley and G. R. Luckhurst, *Mol. Phys.*, **41**, 19 (1980).
- [10] A. Ferrarini, G. R. Luckhurst, P. L. Nordio and S. J. Roskilly, *J. Chem. Phys.*, **100** 1460 (1994).
- [11] W. L. Jorgensen, *BOSS, Version 3.8*, Yale University, New Haven, CT (1997).
- [12] J. P. Ryckaert and A. Bellemans, *Chem. Phys. Lett.*, **30**, 123 (1975).
- [13] C. Zannoni in *The Molecular Physics of Liquid Crystals*, Edited by G. R. Luckhurst and G. W. Gray (Academic Press Inc. Ltd, London, 1979), Chapter 9.
- [14] P. G. de Gennes and J. Prost, *The Physics of Liquid Crystals*, second edition, Clarendon Press, Oxford (1993).

- [15] W. H. de Jeu, *Physical Properties of Liquid Crystalline Materials*, Gordon and Breach, New York (1980).
- [16] A. Ferrarini, private communications (1999).
- [17] T. H. Payne, unpublished notes.
- [18] M. P. Allen and D. J. Tildesley in *Computer Simulation of Liquids* (Clarendon Press, Oxford, 1987), Chapter 4.
- [19] S. Marcelja, *Biochem. Biophys. Acta*, **367**, 165 (1974).
- [20] D. J. Photinos, E. T. Samulski and H. Toriumi, *J. Phys. Chem.*, **94**, 4688 (1990);  
D. J. Photinos, E. T. Samulski and H. Toriumi, *Mol. Cryst. Liq. Cryst.*, **204**, 161 (1991).
- [21] W. W. Wood and J. D. Jacobson, *Proceedings of the Western Joint Computer Conference*, (San Francisco), 261 (1959).
- [22] A. Kloczkowski and G. R. Luckhurst, *Liq. Cryst.*, **3**, 95 (1988).
- [23] M. A. Cotter, *Mol. Cryst. Liq. Cryst.*, **39**, 173 (1977).